



SQUARK ANNIHILATION INTO A PAIR OF GLUONS IN THE MSSM

MASTER'S THESIS

Submitted by:

Luca Paolo Wiggering

University of Münster

Institute of Theoretical Physics

First examiner: Prof. Dr. Michael Klasen

Second examiner: PD Dr. Karol Kovařík

Münster, October 20, 2021

This version of the thesis differs only slightly from the version submitted to the Examinations Office.

Contents

1	Introduction	1
2	Supersymmetry and the MSSM	3
2.1	A supersymmetric toy model	3
2.2	The Minimal Supersymmetric Standard Model	6
2.3	Soft SUSY Breaking	7
2.4	The phenomenological MSSM	8
2.5	Squark and gaugino mixing pattern	9
2.5.1	Neutralino sector	9
2.5.2	Squark sector	10
3	Dark Matter: Evidence and Production Mechanism	13
3.1	Observational evidence for dark matter	13
3.2	The freeze-out mechanism	14
4	BRS-symmetry and polarization vectors	17
4.1	Classical Electrodynamics	17
4.2	Canonical quantization of Yang-Mills theories	19
4.2.1	BRS-transformations	20
4.2.2	Gauge fixing the theory	21
4.2.3	Covariant canonical quantization of the free fields	22
4.2.4	Slavnov-Taylor identities	23
5	The Catani-Seymour dipole formalism for massive initial states	25
5.1	Brief review of the dipole subtraction method	25
5.2	Final-state emitter and initial-state spectator	27
5.2.1	Dipole kinematics and phase space factorization	28
5.2.2	The dipole splitting functions	31
5.2.3	The integrated dipole functions	33
5.3	Initial-state emitter and final-state spectator	38
5.3.1	Kinematics and phase space factorization	38
5.3.2	The dipole splitting functions	38
5.3.3	The integrated dipole functions	39
5.4	Initial-state emitter and initial-state spectator	41
5.4.1	Kinematics and phase space factorization	41
5.4.2	The dipole splitting function	43
5.4.3	The integrated dipole functions	43
5.5	Final-state emitter and final-state spectator	44
5.6	Comparison with the phase space slicing method	44
5.6.1	Processes with a Higgs boson in the final state	45
5.6.2	Processes with a gluon in the final state	48

6	Colour bases	53
6.1	Group and representation theory essentials	53
6.2	Colour space	56
6.3	Trace bases	57
6.4	Orthogonal multiplet bases	57
6.4.1	Construction of the bases	57
6.4.2	Calculation of Clebsch-Gordan coefficients	58
7	Phenomenology of squark annihilation	63
7.1	Squark annihilation into gluons at leading order	63
7.2	Selection of scenarios in the pMSSM	68
7.3	Numerical analysis	70
8	Computation of the next-to-leading order corrections	73
8.1	Regularization and one-loop integrals	73
8.1.1	Dimensional regularization	74
8.1.2	Scalar n -point functions and Passarino-Veltman reduction	74
8.1.3	Variants of dimensional regularization and dimensional reduction	77
8.2	Renormalization in <code>DM@NLO</code>	80
8.2.1	Gluon sector	81
8.2.2	Squark sector	83
8.2.3	Ghost sector	85
8.2.4	Renormalization of α_s	86
8.3	The virtual corrections	86
8.3.1	The propagator corrections	87
8.3.2	The vertex corrections	88
8.3.2.1	The four-gluon-squark vertex correction	88
8.3.2.2	The triple-gluon vertex correction	89
8.3.2.3	The squark-gluon vertex correction	91
8.3.3	Ghost corrections	93
8.3.4	The counterterms	95
8.4	The real corrections	96
8.4.1	Kinematics and phase space integration	96
8.4.2	Real emission processes	98
8.4.3	Treatment of soft and collinear divergences	105
8.4.3.1	Three gluons in the final state	105
8.4.3.2	A quark-antiquark pair in the final state	106
8.5	Preliminary results and discussion	107
9	Conclusion and outlook	109
A	Useful formula and relations	111
A.1	Useful functions within dimensional regularization	111
A.1.1	Gamma and Beta function	111
A.1.2	Spence function	111
A.1.3	Gaussian hypergeometric function	112
A.1.4	Integrals related to the dipole subtraction method	113
A.2	Useful relations for the $SU(N_c)$ generators	114

B	Feynman rules	117
B.1	Propagators	117
B.2	Couplings	117
B.3	Counterterms	119
C	Vertex corrections	121
C.1	Four-gluon-squark vertex	121
C.1.1	Bubbles	121
C.1.2	Triangles	123
C.1.3	Boxes	130
C.2	Triple-gluon vertex	135
C.3	Squark-gluon vertex	143
C.4	Ghost-gluon vertex	146
C.5	Further ghost boxes and triangles	147
C.6	Mathematica codes for the Passarino-Veltman reduction	149
C.6.1	Boxes	149
C.6.2	Triple-gluon vertex	150
C.6.3	Squark-gluon vertex	151
	Bibliography	153
D	Acknowledgments	159

1 Introduction

Compelling evidence for dark matter and neutrino masses apart from the fact that there is no unified description of the four fundamental forces indicate the need for physics beyond the Standard Model. The R -parity conserving Minimal Supersymmetric Standard Model (MSSM) is one of the most appealing top-down approaches for the extension of the Standard Model as it expands the Poincaré group as one of the main building blocks of the Standard Model in the only possible non-trivial way. The quest for more symmetry has often proven successful in the past. The invariance under general coordinate transformations led to general relativity and the principle of gauge symmetry allowed the description of the electroweak and the strong force. In this sense, supersymmetry provides with the lightest neutralino a candidate for cold dark matter, a possible solution for the hierarchy problem and furthermore allows for the unification of gauge couplings at the GUT scale.

Having a well-motivated dark matter candidate on the one hand and a very precise measurement of the present amount of dark matter in the universe through the cosmic microwave background on the other hand, justifies the inclusion of higher-order corrections to relic density calculations such that the theoretical precision matches the experimental one. For this purpose, the `DM@NLO` project aims at providing next-to-leading order (NLO) corrections for a broad range of (co)-annihilation processes in the MSSM which in turn allow to constrain the MSSM parameter space from cosmological observations. It turns out that for parameter regions where the masses of the scalar top and the lightest neutralino are nearly degenerate, the annihilation of a squark-antisquark pair can contribute in a sizeable manner to the relic density. For this reason, the subject of this thesis is to provide a NLO correction for the annihilation of squarks into two gluons within the `DM@NLO` codebase.

The second chapter gives a short introduction into supersymmetry with the main focus to provide an overview of the particle content of the MSSM as well as the mixing patterns in the squark and gaugino sector that emerge from soft supersymmetry breaking. The problem of dark matter is introduced in the third chapter along with the freeze-out mechanism which is a model for the production of dark matter in the early universe that allows to compute the present relic density. In chapter four, Ward-Takahashi identities are introduced in the context of BRS-symmetry and polarizations sums. These allow to derive how ghost processes have to be included. The fifth chapter deals with the development of the Catani-Seymour dipole subtraction method for massive initial states which represents a continuation of the work started in [1]. The following chapter deals with colour bases that are a necessary ingredient for resummation and allow a more efficient calculation of scattering amplitudes in (SUSY)-QCD. Chapters seven and eight are devoted to the calculation of the cross section for squark-antisquark annihilation into two gluons. The computation of the tree level cross section and the virtual corrections is shown in detail. The real emission processes that are needed to achieve an infrared finite result are included as well.

Notation and conventions

The Einstein summation convention is employed throughout this thesis unless denoted otherwise. The complex conjugate is indicated via an asterisk $*$ whereas a bar $\bar{}$ on a four-component spinor ψ represents the Dirac adjoint $\bar{\psi} = \psi^\dagger \gamma^0$. In the case of a two-component Weyl fermion ξ the bar is used as a shorthand for $\bar{\xi} = \xi^\dagger$ instead. The Minkowski metric $g^{\mu\nu}$ follows the mostly plus convention $g = \text{diag}(+, -, -, -)$. The spatial components of a four-vector p are denoted with an arrow \vec{p} . The "Feynman slash notation" $\not{p} = \gamma_\mu p^\mu$ is used as a shorthand for the inner product between a four-vector p and the Dirac gamma matrices γ^μ . The Dirac algebra is chosen to be $\{\gamma^\mu, \gamma^\nu\} = 2g^{\mu\nu}$. Divergent loop integrals are regularized in $D = 4 - 2\epsilon$ dimensions. Physical quantities are expressed in natural units, i.e. $c = 1$ and $\hbar = 1$.

2 Supersymmetry and the MSSM

With the success of gauge and relativistic quantum field theories to describe elementary particles in the 1950s, the idea came up whether it would be possible to combine the external space-time symmetries given by the Poincaré group and internal symmetries into some sort of a higher symmetry group. This pursuit led to the "no-go" theorem by Coleman and Mandula who found that a combination of these two types of symmetries besides their trivial direct product results in an overconstrained S -matrix and is therefore not possible [2]. In 1974 Wess and Zumino discovered a new type of transformation which is not parameterized by an ordinary commuting number, but by an object that transforms like a spinor under the Lorentz group and converts bosonic into fermionic fields [3]. They originally called these transformations supergauge transformations but they spread under the name of supersymmetry (SUSY). As a follow-up it became apparent that the Coleman-Mandula theorem takes only commuting generators into account and can, consequently, be bypassed by expanding the concept of a Lie algebra to include anticommuting generators. This idea ultimately resulted in a theorem by Haag, Lopuszanski und Sohnius in 1975 stating that the most general continuous symmetry of the S -matrix is achieved by including supersymmetry as a non-trivial expansion of the Poincaré algebra [4].

The application of supersymmetry to the Standard Model led to the MSSM which is a possible supersymmetric extension of the Standard Model. As a full understanding of supersymmetry and especially the superfield formalism is not necessary to be able to give phenomenological predictions for a given final supersymmetric theory, the reader is referred to [5, 6, 7] for more information on supersymmetry and the MSSM. However, to grab the quintessence the path of Wess and Zumino of constructing a simple toy model is adopted here followed by a brief summary of the particle content of the MSSM. In addition, the parameter space of a variant of the MSSM is introduced which takes into account phenomenological observations and is the so-called pMSSM-19.

2.1 A supersymmetric toy model

As a supersymmetric toy model we consider a theory with only massless and non-interacting fields with the Lagrangian density

$$\mathcal{L} = \mathcal{L}_{\text{scalar}} + \mathcal{L}_{\text{fermion}} = \partial_\mu \phi^* \partial^\mu \phi + i \bar{\psi} \bar{\sigma}^\mu \partial_\mu \psi \quad (2.1)$$

which consists of a single chiral supermultiplet, i.e. a complex scalar field ϕ as well as left-handed Weyl fermion with components ψ_α . A simple approach to relate the boson to the fermion is the *global* supersymmetry transformation

$$\delta_\epsilon \phi = \sqrt{2} \epsilon \psi \quad (2.2)$$

$$\delta_\epsilon \phi^* = \sqrt{2} (\epsilon^\alpha)^* (\psi_\alpha)^* = \sqrt{2} \bar{\epsilon}_{\dot{\alpha}} \bar{\psi}^{\dot{\alpha}} = \sqrt{2} \bar{\epsilon} \bar{\psi} \quad (2.3)$$

where the infinitesimal transformation parameter ϵ is not an ordinary commuting number but a two-component Weyl spinor which anticommutes with itself and has mass dimension $[\text{mass}]^{-1/2}$. In order to counteract the variation of the scalar part under this transformation

$$\delta_\epsilon \mathcal{L}_{\text{scalar}} = \sqrt{2} \bar{\epsilon}_{\dot{\alpha}} \partial_\mu \bar{\psi}^{\dot{\alpha}} \partial^\mu \phi + \sqrt{2} \epsilon^\alpha \partial_\mu \phi^* \partial^\mu \psi_\alpha \quad (2.4)$$

one can deduce that the Weyl fermion must transform as

$$\delta_\epsilon \psi_\alpha = -i\sqrt{2} (\sigma^\mu \bar{\epsilon})_\alpha \partial_\mu \phi \quad (2.5)$$

$$\delta_\epsilon \bar{\psi}_{\dot{\alpha}} = i\sqrt{2} (\epsilon \sigma^\mu)_{\dot{\alpha}} \partial_\mu \phi^* \quad (2.6)$$

such that the variation of the fermionic part becomes

$$\delta_\epsilon \mathcal{L}_{\text{fermion}} = -\sqrt{2} (\epsilon \sigma^\nu \bar{\sigma}^\mu)^\alpha \partial_\nu \phi^* \partial_\mu \psi_\alpha + \sqrt{2} \bar{\psi} \bar{\sigma}^\mu \sigma^\nu \bar{\epsilon} \partial_\mu \partial_\nu \phi. \quad (2.7)$$

In order to match the right hand side to $\delta \mathcal{L}_{\text{scalar}}$, we can employ the Pauli matrix identity

$$\sigma^\mu \bar{\sigma}^\nu + \sigma^\nu \bar{\sigma}^\mu = 2g^{\mu\nu} \quad (2.8)$$

and the fact that partial derivatives commute to perform the simplifications

$$(\epsilon \sigma^\nu \bar{\sigma}^\mu)^\alpha \partial_\nu \phi^* \partial_\mu \psi_\alpha = \partial_\mu ((\epsilon \sigma^\nu \bar{\sigma}^\mu)^\alpha \partial_\nu \phi^* \psi_\alpha + \epsilon^\alpha \partial^\mu \phi^* \psi_\alpha) + \epsilon^\alpha \partial_\mu \phi^* \partial^\mu \psi_\alpha \quad (2.9)$$

$$\bar{\psi} \bar{\sigma}^\mu \sigma^\nu \bar{\epsilon} \partial_\mu \partial_\nu \phi = \bar{\psi} \bar{\epsilon} \partial^2 \phi = -\bar{\epsilon}_{\dot{\alpha}} \partial_\mu \bar{\psi}^{\dot{\alpha}} \partial^\mu \phi + \partial_\mu (\bar{\psi} \bar{\epsilon} \partial^\mu \phi) \quad (2.10)$$

so that when we combine both transformations the Lagrangian remains unchanged up to a surface term

$$\delta_\epsilon \mathcal{L} = \partial_\mu ((\epsilon \sigma^\nu \bar{\sigma}^\mu)^\alpha \partial_\nu \phi^* \psi_\alpha - \epsilon^\alpha \partial^\mu \phi^* \psi_\alpha - \bar{\epsilon} \bar{\psi} \partial^\mu \phi) \quad (2.11)$$

which has no effect on the action $\delta_\epsilon S = 0$. We can now derive the supersymmetry algebra. For two supersymmetry transformations parameterized by ϵ and η , we obtain for the commutator acting on the scalar

$$[\delta_\epsilon, \delta_\eta] \phi = -2i (\eta \sigma^\mu \bar{\epsilon} - \epsilon \sigma^\mu \bar{\eta}) \partial_\mu \phi \quad (2.12)$$

whereas we have for the Weyl fermion

$$[\delta_\epsilon, \delta_\eta] \psi_\alpha = -2i (\sigma^\mu \bar{\eta})_\alpha \epsilon \partial_\mu \psi - i (\sigma^\mu \bar{\epsilon})_\alpha \eta \partial_\mu \psi \quad (2.13)$$

which can be recast into a more useful form by applying the Fierz identity

$$\chi_\alpha (\xi \eta) = -\xi_\alpha (\eta \chi) - \eta_\alpha (\chi \xi) \quad (2.14)$$

involving three Weyl spinors χ , ξ , η which yields

$$[\delta_\epsilon, \delta_\eta] \psi_\alpha = -2i (\eta \sigma^\mu \bar{\epsilon} - \epsilon \sigma^\mu \bar{\eta}) \partial_\mu \psi_\alpha - 2i \eta_\alpha \bar{\epsilon} \bar{\sigma}^\mu \partial_\mu \psi + 2i \epsilon_\alpha \bar{\eta} \bar{\sigma}^\mu \partial_\mu \psi. \quad (2.15)$$

If ψ is on-shell, its equation of motion implies $\bar{\sigma}^\mu \partial_\mu \psi = 0$ and we can conclude that the commutator takes the general form

$$[\delta_\epsilon, \delta_\eta] = -2i (\eta \sigma^\mu \bar{\epsilon} - \epsilon \sigma^\mu \bar{\eta}) \partial_\mu. \quad (2.16)$$

As $P_\mu = -i\partial_\mu$ is the generator of space-time translations, the commutator gives the insight that supersymmetry is indeed a symmetry of space-time. In order to ensure that supersymmetry also holds off-shell, one can use a trick and introduce an auxiliary complex scalar field F with a Lagrangian density

$$\mathcal{L}_{\text{auxiliary}} = F^* F \quad (2.17)$$

and mass dimension $[\text{mass}]^2$. This new field can now be used to compensate the terms in eq. (2.15) which do not vanish for an off-shell fermion. A simple guess is that F transforms into a multiple of the equation of motion for ψ :

$$\delta_\epsilon F = -\sqrt{2}i\bar{\epsilon}\bar{\sigma}^\mu\partial_\mu\psi \quad (2.18)$$

$$\delta_\epsilon F^* = \sqrt{2}i\partial_\mu\bar{\psi}\bar{\sigma}^\mu\epsilon. \quad (2.19)$$

Then the auxiliary part in the Lagrangian transforms as

$$\delta_\epsilon \mathcal{L}_{\text{auxiliary}} = \sqrt{2}i\partial_\mu\bar{\psi}\bar{\sigma}^\mu\epsilon F + \sqrt{2}i\bar{\epsilon}\bar{\sigma}^\mu\partial_\mu\psi F^*. \quad (2.20)$$

A small modification of the transformation rule of ψ which is

$$\delta_\epsilon \psi_\alpha = -\sqrt{2}i(\sigma^\mu\bar{\epsilon})_\alpha\partial_\mu\psi + \sqrt{2}\epsilon_\alpha F \quad (2.21)$$

$$\delta_\epsilon \bar{\psi}_{\dot{\alpha}} = \sqrt{2}i(\epsilon\sigma^\mu)_{\dot{\alpha}}\partial_\mu\psi^* + \sqrt{2}\bar{\epsilon}_{\dot{\alpha}} F^* \quad (2.22)$$

suffices to ensure that the extra term in $\delta_\epsilon \mathcal{L}_{\text{fermion}}$ cancels $\delta_\epsilon \mathcal{L}_{\text{auxiliary}}$ up to a surface term. With that

$$\mathcal{L} = \mathcal{L}_{\text{scalar}} + \mathcal{L}_{\text{fermion}} + \mathcal{L}_{\text{auxiliary}} \quad (2.23)$$

is invariant under supersymmetry and eq. (2.16) holds also off-shell. The generators Q_α and $\bar{Q}_{\dot{\alpha}}$ of supersymmetry transformations are themselves two-component Weyl spinors and are defined through the requirement

$$\delta_\epsilon X = (\epsilon Q + \bar{\epsilon}\bar{Q}) X \quad (2.24)$$

for any field X that transforms under supersymmetry. Consistency of the generators with eq. (2.16) requires

$$\begin{aligned} [\delta_\epsilon, \delta_\eta] &= [\epsilon Q + \bar{\epsilon}\bar{Q}, \eta Q + \bar{\eta}\bar{Q}] = [\epsilon Q, \bar{\eta}\bar{Q}] + [\bar{\epsilon}\bar{Q}, \eta Q] \\ &= (\eta_\alpha \bar{\epsilon}^{\dot{\alpha}} - \epsilon^\alpha \bar{\eta}_{\dot{\alpha}}) \{Q_\alpha, \bar{Q}^{\dot{\alpha}}\} \stackrel{!}{=} -2i(\eta\sigma^\mu\bar{\epsilon} - \epsilon\sigma^\mu\bar{\eta})\partial_\mu. \end{aligned} \quad (2.25)$$

Comparing the last two expressions yields

$$\{Q_\alpha, \bar{Q}_{\dot{\alpha}}\} = 2(\sigma^\mu)_{\alpha\dot{\alpha}} P_\mu. \quad (2.26)$$

From

$$[\delta_\epsilon, a^\mu\partial_\mu] = 0 \quad (2.27)$$

for any four-vector a^μ , one can deduce that the generators Q_α commute with translations

$$[Q_\alpha, P^\mu] = [\bar{Q}_{\dot{\alpha}}, P^\mu] = 0. \quad (2.28)$$

Next to a chiral supermultiplet we could also have a vector supermultiplet which consists of a massless gauge field A_a^μ and a massless two-component Majorana fermion λ_a . The gauge transformations for these two fields are

$$A_a^\mu \rightarrow A_a^\mu + \frac{1}{g} \partial^\mu \alpha_a + f^{abc} A_b^\mu \alpha_c \quad (2.29)$$

$$\lambda_a \rightarrow f^{abc} \lambda_b \alpha_c \quad (2.30)$$

where α_a parameterize the transformation, g is the gauge coupling and f^{abc} are the totally antisymmetric structure constants. Whereas the degrees of freedom of A_a^μ and λ_a match on-shell, the gauge boson has off-shell three real degrees of freedom and the gaugino as a complex object with two components has four degrees. In order to ensure that supersymmetry also holds off-shell, we can again introduce an auxiliary field D^a . The Lagrangian density

$$\mathcal{L}_{\text{gauge}} = -\frac{1}{4} F_\mu^a F_a^{\mu\nu} + i \bar{\lambda} \sigma^\mu D_\mu \lambda_a + \frac{1}{2} D_a D_a \quad (2.31)$$

with the field strength tensor

$$F_a^{\mu\nu} = \partial^\mu A_a^\nu - \partial^\nu A_a^\mu + g f^{abc} A_b^\mu A_c^\nu \quad (2.32)$$

and the covariant derivative

$$D^\mu \lambda_a = \partial^\mu \lambda_a + g f^{abc} A_b^\mu \lambda_c \quad (2.33)$$

is then invariant under supersymmetry. In order to get further insights into the construction of supersymmetric theories with the help of the superfield formalism and the inclusion of interactions the reader is referred to [6].

2.2 The Minimal Supersymmetric Standard Model

The R -parity conserving Minimal Supersymmetric Standard Model (MSSM) is the supersymmetric extension of the Standard Model with one set of SUSY generators $\mathcal{N} = 1$ and an additional discrete \mathbb{Z}_2 symmetry called R -parity whose corresponding conserved multiplicative quantum number is defined as

$$P_R = (-1)^{3(B-L)+2s} \quad (2.34)$$

with baryon number B , lepton number L and spin s . The concept of R -parity was initially introduced to forbid lepton and baryon number violating processes which would be in principle allowed by the requirements of supersymmetry, gauge invariance and renormalizability but undergo very stringent experimental limits. As a very important phenomenological side effect each Standard Model particle receives R -parity $+1$ and each supersymmetric particle (sparticle) -1 which forbids the decay of a sparticle into Standard Model particles alone, thus, offering the possibility for a stable dark matter candidate.

Within the MSSM, each helicity state of a fermion receives a scalar superpartner, which, apart from the spin, does not differ from its Standard Model equivalent. In a similar way, each gauge boson receives a Majorana fermion as superpartner. Concerning nomenclature, each scalar superpartner is prefixed with "s" and each superpartner of a boson is suffixed with "ino". In addition, all sparticles are distinguished by a tilde. For example, the partner of a quark q is then called a "squark" labelled as \tilde{q} and the partner of a gluon is referred to as a "gluino" \tilde{g} . In contrast to the Standard Model, its supersymmetric version does not

only contain one Higgs doublet but is a so-called Two-Higgs-Doublet model. Otherwise the theory would become inconsistent on quantum level through gauge anomalies appearing in the electroweak sector. Consequently, the Higgs with hypercharge $Y = +1/2$ gives mass to the "up-type" quarks and the other one with $Y = -1/2$ gives mass to the "down-type" quarks and the charged leptons. The corresponding fermionic superpartners are called Higgsinos.

The whole particle content of the MSSM is displayed in tables 2.1 and 2.2 and given in terms of supermultiplets which are in fact elements of the representation space of irreducible representations of the supersymmetry algebra and combine the Standard Model particles with their superpartners.

Names		spin 0	spin 1/2	$SU(3)_C, SU(2)_L, U(1)_Y$
squarks, quarks ($\times 3$ families)	Q	$(\tilde{u}_L \ \tilde{d}_L)$	$(u_L \ d_L)$	$(\mathbf{3}, \mathbf{2}, \frac{1}{6})$
	\bar{u}	\tilde{u}_R^*	u_R^\dagger	$(\bar{\mathbf{3}}, \mathbf{1}, -\frac{2}{3})$
	\bar{d}	\tilde{d}_R^*	d_R^\dagger	$(\bar{\mathbf{3}}, \mathbf{1}, \frac{1}{3})$
sleptons, leptons ($\times 3$ families)	L	$(\tilde{\nu} \ \tilde{e}_L)$	$(\nu \ e_L)$	$(\mathbf{1}, \mathbf{2}, -\frac{1}{2})$
	\bar{e}	\tilde{e}_R^*	e_R^\dagger	$(\mathbf{1}, \mathbf{1}, 1)$
Higgs, higgsinos	H_u	$(H_u^+ \ H_u^0)$	$(\tilde{H}_u^+ \ \tilde{H}_u^0)$	$(\mathbf{1}, \mathbf{2}, +\frac{1}{2})$
	H_d	$(H_d^0 \ H_d^-)$	$(\tilde{H}_d^0 \ \tilde{H}_d^-)$	$(\mathbf{1}, \mathbf{2}, -\frac{1}{2})$

Table 2.1: Chiral supermultiplets in the MSSM. Table taken from [6].

Names	spin 1/2	spin 1	$SU(3)_C, SU(2)_L, U(1)_Y$
gluino, gluon	\tilde{g}	g	$(\mathbf{8}, \mathbf{1}, 0)$
winos, W bosons	$\tilde{W}^\pm \ \tilde{W}^0$	$W^\pm \ W^0$	$(\mathbf{1}, \mathbf{3}, 0)$
bino, B boson	\tilde{B}^0	B^0	$(\mathbf{1}, \mathbf{1}, 0)$

Table 2.2: Gauge supermultiplets in the MSSM. Table taken from [6].

2.3 Soft SUSY Breaking

The commutation relation $[P^2, Q_\alpha] = 0$ indicates that particles within one supermultiplet must possess the same mass. However, in experiments no superpartners have been observed so far which in turn requires that SUSY must be broken. There is no agreement on how SUSY should be broken but the general idea is that SUSY breaking takes place in a hidden sector which is transferred to the visible sector via a messenger which could be gravity or a gauge force. From a practical point of view the simplest way to break SUSY is to introduce additional terms in the effective MSSM Lagrangian which break SUSY explicitly. These terms should be "soft" in the sense that the fermionic and bosonic loop corrections to the Higgs

mass still cancel. With the Supersymmetry Parameter Analysis (SPA) convention [8] one agreed on the following form of the soft SUSY breaking Lagrangian ¹

$$\begin{aligned}
-\mathcal{L}_{\text{soft}} = & \frac{1}{2} \left(M_1 \tilde{B} \tilde{B} + M_2 \tilde{W} \tilde{W} + M_3 \tilde{g} \tilde{g} + \text{h.c.} \right) + \tilde{Q}_{iL}^* \left(m_{\tilde{Q}}^2 \right)_{ij} \tilde{Q}_{jL} + \tilde{L}_{iL}^* \left(m_{\tilde{L}}^2 \right)_{ij} \tilde{L}_{jL} \\
& + \tilde{u}_{iR}^* \left(m_{\tilde{u}}^2 \right)_{ij} \tilde{u}_{jR} + \tilde{d}_{iR}^* \left(m_{\tilde{d}}^2 \right)_{ij} \tilde{d}_{jR} + \tilde{e}_{iR}^* \left(m_{\tilde{e}}^2 \right)_{ij} \tilde{e}_{jR} \\
& + m_{H_d}^2 |H_d|^2 + m_{H_u}^2 |H_u|^2 - (B\mu H_d \cdot H_u + \text{h.c.}) \\
& + \left[(T_u)_{ij} H_u \cdot \tilde{Q}_{iL} \tilde{u}_{jR}^* + (T_d)_{ij} H_d \cdot \tilde{Q}_{iL} \tilde{d}_{jR}^* + (T_e)_{ij} H_d \cdot \tilde{L}_{iL} \tilde{e}_{jR}^* + \text{h.c.} \right] \quad (2.35)
\end{aligned}$$

where the T matrices are defined as the product of Yukawa couplings Y and the soft supersymmetry breaking trilinear couplings A

$$T_{ij} = A_{ij} Y_{ij} \text{ (no summation)}. \quad (2.36)$$

In eq. (2.35) only generation indices are explicitly given whereas all other are implicitly summed over. In contrast to unbroken SUSY where only the supersymmetric higgsino mass term μ appears as an additional parameter, the soft breaking of SUSY introduces in total 105 new free parameters.

2.4 The phenomenological MSSM

The large number of 105 additional parameters in the MSSM make it impossible to explore the parameter space in full generality. For this reason, simplified models such as the phenomenological MSSM (pMSSM) have evolved which constrain the MSSM based on strong experimental evidence. The pMSSM-19 takes into account the following three assumptions [10]:

- **No Flavour Changing Neutral Currents (FCNC)**

The appearance of FCNC is strongly constrained by experimental observations. Therefore, all sfermion mixing matrices and T matrices are assumed to be diagonal in flavour space.

- **No new source of CP-violation**

Experimental limits in the K -meson system as well as on the electric moments of the electron and neutron indicate no new sources of CP-violation. The simplest way to include this observation is to set all complex phases to zero.

- **First and Second Generation Universality**

The Yukawa couplings of the first two generations are small compared to the third generation. Hence, the associated trilinear couplings are less important and can be set to zero. In addition, $K^0 - \bar{K}^0$ mixing indicates a small mass splitting between first and second generation squarks, unless their masses exceed 1 TeV significantly. This justifies the assumption of identical soft-SUSY breaking scalar mass terms for the first two generations.

These assumptions leave 19 free parameters:

¹Note that the Lagrangian given in [9] used by the first version of **SPheno** differs from eq. (2.35), but **SPheno** supports the SPA conventions starting with version 2.2.2.

$\tan(\beta)$	ratio of the vevs of the two-Higgs doublet fields
M_1, M_2, M_3	gaugino mass parameters
A_t, A_b, A_τ	third generation trilinear couplings
μ	higgsino mass parameter
m_{A^0}	mass of the pseudoscalar Higgs boson
$M_{\tilde{l}_L}, M_{\tilde{\tau}_L}, M_{\tilde{l}_R}, M_{\tilde{\tau}_R}$	soft slepton masses
$M_{\tilde{q}_L}, M_{\tilde{u}_R}, M_{\tilde{d}_R}$	soft first/second generation squark masses
$M_{\tilde{q}_{3L}}, M_{\tilde{t}_R}, M_{\tilde{b}_R}$	soft third generation squark masses.

2.5 Squark and gaugino mixing pattern

So far, the Lagrangian of the MSSM is expressed through gauge (or interaction) eigenstates. However, as known from the Standard Model one has to distinguish between gauge and mass eigenstates where the latter ones are defined as those states that diagonalize the mass terms and are related through a change of basis to the gauge eigenstates. As the mass eigenstates correspond to freely propagating particles with fixed mass that are measured in experiments, calculations are usually performed in the mass basis. In the following, the connection between mass and gauge eigenstates for the sectors that are most important for this work are highlighted.

2.5.1 Neutralino sector

After electroweak symmetry breaking the mass terms for the uncharged higgsinos (\tilde{H}_d^0 and \tilde{H}_u^0), wino \tilde{W}^0 and bino \tilde{B} can be combined into the overall mass term

$$-\mathcal{L}_{\text{mass}}^{\tilde{\chi}^0} = \frac{1}{2} (\psi^0)^T \mathcal{M}_{\chi^0} \psi^0 \quad (2.37)$$

with all gauge-eigenstates being combined into the vector

$$(\psi^0)^T = (\tilde{B} \ \tilde{W}^0 \ \tilde{H}_d^0 \ \tilde{H}_u^0) \quad (2.38)$$

and with the mass matrix

$$\mathcal{M}_{\chi^0} = \begin{pmatrix} M_1 & 0 & -m_{Z^0} c_\beta s_W & m_{Z^0} s_\beta s_W \\ 0 & M_2 & m_{Z^0} c_\beta c_W & -m_{Z^0} s_\beta c_W \\ -m_{Z^0} c_\beta s_W & m_{Z^0} c_\beta c_W & 0 & -\mu \\ m_{Z^0} s_\beta s_W & -m_{Z^0} s_\beta c_W & -\mu & 0 \end{pmatrix} \quad (2.39)$$

where the Weinberg angle θ_W and the angle β enter through $c_\beta = \cos \beta$, $s_\beta = \sin \beta$, $s_W = \sin \theta_W$, $c_W = \cos \theta_W$. The wino and bino mass parameters M_1 and M_2 in \mathcal{M}_{χ^0} come directly from the soft-breaking Lagrangian whereas $-\mu$ is the supersymmetric higgsino mass term. As \mathcal{M}_{χ^0} is self-adjoint, it can be diagonalized through a unitary 4×4 matrix N whose rows are the eigenvectors of the mass matrix

$$N^* \mathcal{M}_{\chi^0} N^\dagger = \text{diag} (m_{\tilde{\chi}_1^0}, m_{\tilde{\chi}_2^0}, m_{\tilde{\chi}_3^0}, m_{\tilde{\chi}_4^0}) \quad (2.40)$$

where the order of the eigenvalues (masses) is conventionally chosen as $m_{\tilde{\chi}_1^0} \leq \dots \leq m_{\tilde{\chi}_4^0}$. The fields χ_i^0 that emerge from the change of basis

$$\chi_i^0 = N_{ij} \psi_j^0 \quad (2.41)$$

are the so-called neutralinos. It is possible that there arise imaginary or negative masses in the diagonalization procedure which can be turned into physical masses $m_{\tilde{\chi}_i^0} > 0$ by performing chiral rotations on the components of ψ_0 . As the neutralinos couple only to electroweak interactions, the lightest neutralino χ_1^0 is usually assumed to be the standard candidate for non-baryonic dark matter unless there exists a lighter gravitino which is the superpartner of the graviton.

2.5.2 Squark sector

As we work within the pMSSM, all non-diagonal terms in flavour space are neglected and for that reason only mixing between the superpartners \tilde{q}_L and \tilde{q}_R related to the two chirality parts of a quark takes place. All squark mass terms can be summarised under

$$-\mathcal{L}_{\text{squark mass}} = \sum_{\tilde{q}} (\tilde{q}_L^* \ \tilde{q}_R^*) \mathcal{M}_{\tilde{q}}^2 \begin{pmatrix} \tilde{q}_L \\ \tilde{q}_R \end{pmatrix} \quad (2.42)$$

where $\mathcal{M}_{\tilde{q}}^2$ is a 2×2 Hermitian matrix in chirality space

$$\mathcal{M}_{\tilde{q}}^2 = \begin{pmatrix} \mathcal{M}_{\tilde{q}LL}^2 & \mathcal{M}_{\tilde{q}LR}^2 \\ \mathcal{M}_{\tilde{q}LR}^{2*} & \mathcal{M}_{\tilde{q}RR}^2 \end{pmatrix} \quad (2.43)$$

with the diagonal

$$\mathcal{M}_{\tilde{q}LL}^2 = m_{\tilde{Q}}^2 + m_{Z^0}^2 \left(T_{3L}^{\tilde{q}} - Q_q \sin^2 \theta_W \right) \cos 2\beta + m_q^2 \quad (2.44)$$

$$\mathcal{M}_{\tilde{q}RR}^2 = m_{\tilde{u},\tilde{d}}^2 + Q_q m_{Z^0}^2 \cos 2\beta \sin^2 \theta_W + m_q^2 \quad (2.45)$$

and off-diagonal elements

$$\mathcal{M}_{\tilde{q}LR}^2 = -m_q X_q \quad (2.46)$$

where X_q is defined as $X_q = A_q^* + \mu (\tan \beta)^{-2 T_{3L}^{\tilde{q}}}$, $T_{3L}^{\tilde{q}}$ as the third component of the weak isospin and Q_q as the electric charge of the quark q in units of e . Furthermore, $m_{\tilde{Q}}$ is the soft SUSY breaking mass for "left-handed" squarks and $m_{\tilde{u},\tilde{d}}$ for "right-handed" up- and down-type squarks respectively. The eigenvalues of a 2×2 matrix can be conveniently expressed in terms of its trace and determinant

$$m_{\tilde{q}1,2}^2 = \frac{1}{2} \left(\text{Tr } \mathcal{M}_{\tilde{q}}^2 \pm \sqrt{\text{Tr}^2 \mathcal{M}_{\tilde{q}}^2 - 4 \det \mathcal{M}_{\tilde{q}}^2} \right) \quad (2.47)$$

such that the off-diagonal matrix elements enter the square root with a positive sign through the determinant. For the stop sector, this can induce a large mass splitting between \tilde{t}_1 and \tilde{t}_2 due to the large mass of the top quark which elevates \tilde{t}_1 to a potential candidate for the

next-to-lightest supersymmetric particle (NLSP). The gauge eigenstates are transformed to mass eigenstates through the orthogonal 2×2 matrix $R^{\tilde{q}}$:

$$\begin{pmatrix} \tilde{q}_1 \\ \tilde{q}_2 \end{pmatrix} = \begin{pmatrix} R_L^{\tilde{q}} & R_R^{\tilde{q}} \end{pmatrix} \begin{pmatrix} \tilde{q}_L \\ \tilde{q}_R \end{pmatrix}. \quad (2.48)$$

3 Dark Matter: Evidence and Production Mechanism

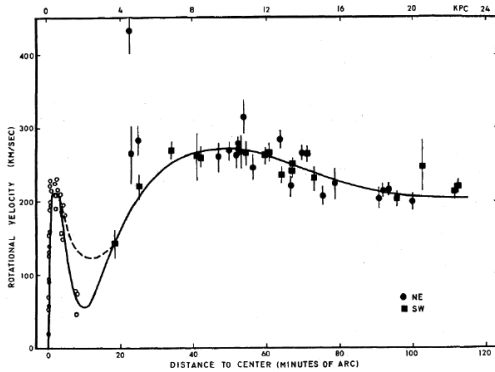
3.1 Observational evidence for dark matter

The question of dark matter dates back to the 1930s when the astronomer Fritz Zwicky provided the first renowned measurements of the velocity dispersion of the Coma cluster through the redshift. He found that in order to explain the observed velocities in the Coma cluster, its mean mass density would have to be four hundred times larger than what the amount of luminous matter indicates [11]. This "missing mass problem" was studied systematically in the 1970s by Vera Rubin and Kent Ford who investigated the rotation curve of the Andromeda Nebula (also called Messier 31 or M31) meaning the dependence of the circular speed v_c on the distance r from the center of the galaxy [12].

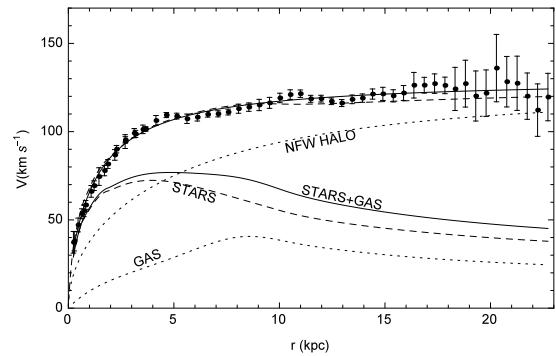
According to Newtonian gravity and under the assumption of circular orbits, one would expect objects far from the center to rotate with a velocity

$$v_c(r) = \sqrt{\frac{GM(r)}{r}} \quad (3.1)$$

where $M(r)$ denotes the mass enclosed within r and G the gravitational constant. Since the largest amount of matter must be located near the center of the galaxy, $M(r)$ remains roughly constant for large distances and thus v_c is expected to decrease as $1/\sqrt{r}$ with increasing radial distance. However, their measurements showed a completely different picture - the rotation



(a) Rotation curve of M31 from Rubin and Ford [12].



(b) Rotation curve of M33 [13].

Figure 3.1: Rotation curves for the galaxies M31 and M33 (black dots with error bars).

curves remain almost constant ("flatten") in outer regions of the disk as shown in fig. 3.1a. Since then, the rotation curves of many more spiral galaxies have been investigated, further confirming the problem of missing mass. In some cases like the M33 galaxy v_c even increases as shown in fig. 3.1b.

The accidental discovery of the cosmic microwave background (CMB) in 1965 led to a series of space missions including the COBE, WMAP and Planck satellites that allowed to measure the CMB with increasing precision which made it possible not only to give qualitative hints towards the existence of dark matter, but also to provide quantitative information on the dark matter content of the universe [14]. It turned out that this background radiation is not isotropic but contains small temperature fluctuations of the order of parts per million. These anisotropies in the spectrum are related to small density fluctuations in the early universe which allowed dark matter to accumulate within these over dense regions whereas the attraction of baryonic matter was counteracted by radiative pressure. The resulting oscillations are what we observe nowadays as the temperature fluctuations in the CMB and allow to deduce the relic density of cold dark matter with an astonishing precision

$$\Omega_{\text{CDM}}h^2 = 0.1200(12) \quad (3.2)$$

where the "little h " gives the present value of the Hubble expansion parameter H_0 in units of $100 \text{ km s}^{-1} \text{ Mpc}^{-1}$ and the uncertainty corresponds to the 68 % confidence level [15]. The increasing accuracy of the relic density measurement can be visualized by comparing the temperature variations as measured first by the COBE and then by the Planck satellite. The skymap of both temperature variations is displayed in fig. 3.2.

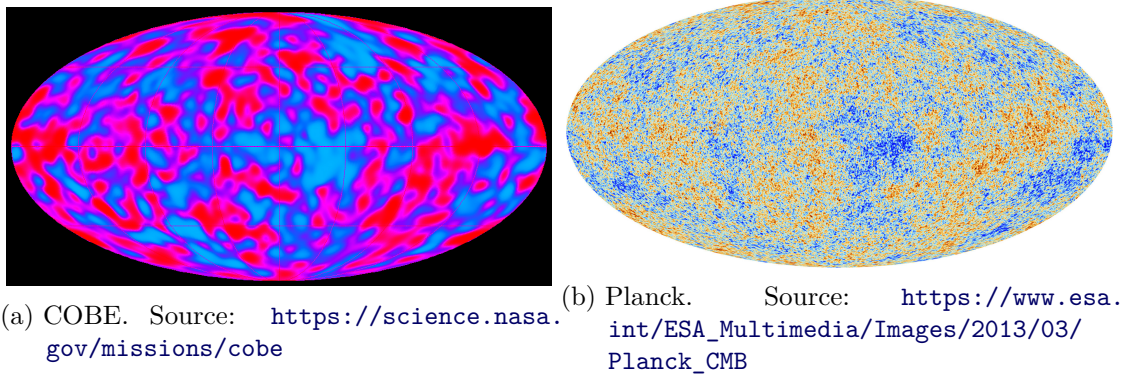


Figure 3.2: Skymap of the temperature variations in the cosmic microwave background as measured by the COBE and Planck satellites. (both pictures were retrieved on the 2021-10-02)

3.2 The freeze-out mechanism

The standard paradigm to explain dark matter is that it could consist of *weakly interacting massive particles* (WIMPs) which were in thermal equilibrium with the rest of the particle content of the universe shortly after the Big Bang. As the universe cooled down, the temperature must have dropped below their production threshold at one point and annihilation took over until the point where the expansion of the universe dominated the annihilation rate and the dark matter particles "froze-out". This so-called *freeze-out mechanism* leads under the assumptions of WIMPs naturally to the right relic density which is referred to as WIMP miracle. As we assume that dark matter consists of neutralinos, we describe the three different regimes more precisely directly on the example of the MSSM as in [16]. Therefore consider a set of N supersymmetric particles χ_i which eventually all decay to the dark matter candidate

χ . The evolution of the number density n_i of a particle i over time t is then described by a set of N coupled nonlinear ordinary differential equations

$$\frac{1}{a^3} \frac{d}{dt} (n_i a^3) = - \sum_{j=1}^N \langle \sigma_{ij} v_{ij} \rangle (n_i n_j - n_i^{\text{eq}} n_j^{\text{eq}}) \quad (3.3)$$

$$- \sum_X \sum_{j \neq i} \left[\langle \sigma'_{Xij} v_{Xi} \rangle (n_X n_i - n_X^{\text{eq}} n_i^{\text{eq}}) - \langle \sigma'_{Xji} v_{Xj} \rangle (n_X n_j - n_X^{\text{eq}} n_j^{\text{eq}}) \right] \quad (3.4)$$

$$- \sum_{j \neq i} \left[\Gamma_{ij} (n_i - n_i^{\text{eq}}) - \Gamma_{ji} (n_j - n_j^{\text{eq}}) \right], \text{ for } 1 \leq i \leq N \quad (3.5)$$

where X and Y are labels for all SM particles that could appear in the scattering or decay process, $\langle \sigma v \rangle$ denotes the thermal average of a cross section σ with a velocity distribution v and $a(t)$ the scale factor of the universe which is related to the Hubble expansion rate via $H(t) = \frac{\dot{a}(t)}{a(t)}$. The left-hand side of this equations corresponds to the change of the total number of particles $n_i a^3$ of the species i in time which is caused through different scattering processes described by the right-hand side where the differences between the number densities and equilibrium number densities ensure that no change occurs in thermal equilibrium. The first term accounts for annihilation

$$\sigma_{ij} = \sum_X \sigma (\chi_i \chi_j \rightarrow X), \quad (3.6)$$

the second accounts for the conversion of a supersymmetric particle through scattering with a SM particle

$$\sigma'_{Xij} = \sum_Y \sigma (X \chi_i \rightarrow \chi_j) \quad (3.7)$$

and the last one χ_i decays

$$\Gamma_{ij} = \sum_X (\chi_i \rightarrow \chi_j X). \quad (3.8)$$

As every sparticle must eventually decay to the LSP, all particle densities can be combined to

$$n = \sum_{i=1}^N n_i \quad (3.9)$$

which corresponds to the density of the neutralino for infinite times. Therefore, the set of equations above greatly simplifies to one equation

$$\frac{1}{a^3} \frac{d}{dt} (n a^3) = - \sum_{i,j=1}^N \langle \sigma_{ij} v_{ij} \rangle (n_i n_j - n_i^{\text{eq}} n_j^{\text{eq}}). \quad (3.10)$$

To express the right hand side of eq. (3.10) also through n , we can make the assumption that all supersymmetric particles remain in thermal equilibrium by scattering with the much lighter Standard Model particles

$$\frac{n_i}{n} \simeq \frac{n_i^{\text{eq}}}{n^{\text{eq}}}. \quad (3.11)$$

Inserting this approximation into eq. (3.10) results in the Boltzmann equation

$$\dot{n} = -3Hn - \langle \sigma_{\text{eff}} v \rangle (n^2 - n_{\text{eq}}^2) \quad (3.12)$$

where the whole particle physics information now resides in the effective cross section

$$\langle \sigma_{\text{eff}} v \rangle = \sum_{i,j=1}^N \langle \sigma_{ij} v_{ij} \rangle \frac{n_i^{\text{eq}}}{n^{\text{eq}}} \frac{n_j^{\text{eq}}}{n^{\text{eq}}}. \quad (3.13)$$

As the number density n_{nr} of a non-relativistic particle species with mass m scales as [17]

$$n_{\text{nr}} \sim \exp\left(-\frac{m}{T}\right) \quad (3.14)$$

at a temperature T , the ratios of the equilibrium number densities are proportional to

$$\frac{n_i^{\text{eq}}}{n^{\text{eq}}} \sim \exp\left(-\frac{m_i - m_\chi}{T}\right). \quad (3.15)$$

From this relation, one can deduce that the contribution of annihilations involving particles which are much heavier than the neutralino are suppressed whereas co-annihilation becomes important if the mass difference between the next-to-lightest supersymmetric particle (NLSP) and the LSP is small. If the NLSP and the LSP are nearly mass degenerate, even pair-annihilation of the NLSP can contribute in a sizeable manner which is the subject of this thesis.

4 BRS-symmetry and polarization vectors

An important aspect of calculations of scattering amplitudes in quantum field theories with massless gauge bosons is the treatment of polarization sums. It is well covered in the literature that ghosts can appear as internal lines [18, 19], but it is also possible to have them as external lines depending on the treatment of unphysical polarizations. The only common example for the latter case in the literature are processes with two gluons in either the initial or final state with only heuristic explanations as to why the ghosts processes have to be included that way. As a means to construct such processes for an arbitrary number of gluons BRS-symmetry as the quantum version of gauge symmetry and Slavnov-Taylor identities are introduced in this chapter. The applications follows in chapters 7 and 8.

4.1 Classical Electrodynamics

For the discussion of the relationship between gauge invariance and polarization states of massless gauge bosons we start with classical electrodynamics. Let's consider the homogeneous Maxwell equation in covariant form

$$\partial_\mu F^{\mu\nu} = 0. \quad (4.1)$$

All information about the gauge field A_μ is contained inside the field strength tensor

$$F_{\mu\nu} = \partial_\mu A_\nu - \partial_\nu A_\mu. \quad (4.2)$$

If we now tried to solve the equations of motion for the field A_μ , we would recognize that the solutions are not uniquely determined since Maxwell's equations are invariant under a gauge transformation

$$A_\mu(x) \rightarrow A_\mu(x) + \partial_\mu \alpha(x) \quad (4.3)$$

where α is an arbitrary scalar field that depends on space-time x . Thus, it is necessary to fix the gauge by imposing further constraints on A_μ . The Lorenz condition

$$\partial_\mu A^\mu(x) = 0 \quad (4.4)$$

is a common choice for this since it leaves the theory covariant and therefore belongs to the class of *covariant gauges*. Imposing this constraint reduces eq. (4.1) to the wave equation

$$\square A_\mu(x) = 0 \quad (4.5)$$

whose solution is given by a plane wave

$$A_\mu(x) = \epsilon_\mu(k) e^{ikx} + \epsilon_\mu^*(k) e^{-ikx} \quad (4.6)$$

if the four-momentum k is lightlike $k^2 = 0$. The next step is to determine the polarization vector $\epsilon_\mu(k)$ which has for now four degrees of freedom related to its four entries. In momentum space

the Lorenz condition becomes $k_\mu A^\mu = 0$, so that the polarization vector must be transverse to the momentum k

$$k \cdot \epsilon(k) = 0 \quad (4.7)$$

which reduces the number of degrees of freedom to three. However, there still remains some gauge freedom. As long as the scalar field α satisfies $\square\alpha = 0$, it is still possible to add an additional term to the field A_μ without changing the physics. The function

$$\alpha(x) = -i\eta e^{ikx} + i\eta e^{-ikx} \quad (4.8)$$

with an arbitrary real number η fulfills this condition since the momentum k is already defined to be lightlike $k^2 = 0$. Inserting α into the gauge transformation gives

$$A_\mu \rightarrow (\epsilon_\mu(k) + \eta k_\mu) e^{ikx} + (\epsilon_\mu(k) + \eta k_\mu)^* e^{-ikx} \quad (4.9)$$

which means that two polarization vectors that differ by a momentum k_μ are physically equivalent $\epsilon_\mu(k) \sim \epsilon_\mu(k) + k_\mu$ and define an equivalence class. This brings us to a total of two degrees of freedom which we already know from experiments as linear or circular polarized light (or from Wigner's theorem which states that every unitary irreducible representation of the Poincaré group for a massless particle contains two states independent of the particle's spin [20]). For the explicit construction of the polarization vectors

$$\epsilon_\mu = (\varepsilon_0, \varepsilon_1, \varepsilon_2, \varepsilon_3)^T \quad (4.10)$$

consider a momentum \vec{k} parallel to the z -axis

$$k_\mu = (k_0, 0, 0, k_0)^T. \quad (4.11)$$

The transversality condition in eq. (4.7) gives $\varepsilon_0 = \varepsilon_3$ and then η can be chosen as $\eta = -\frac{\varepsilon_0}{k_0}$ so that only the components ε_1 and ε_2 remain which we can use to build a basis for the two physical polarizations. Two possible bases for the transverse polarizations are

$$\epsilon_1^\mu(k) = \begin{pmatrix} 0 \\ 1 \\ 0 \\ 0 \end{pmatrix} \quad \epsilon_2^\mu(k) = \begin{pmatrix} 0 \\ 0 \\ 1 \\ 0 \end{pmatrix} \quad \text{or} \quad \epsilon_R^\mu(k) = \frac{1}{\sqrt{2}} \begin{pmatrix} 0 \\ 1 \\ i \\ 0 \end{pmatrix} \quad \epsilon_L^\mu(k) = \frac{1}{\sqrt{2}} \begin{pmatrix} 0 \\ 1 \\ -i \\ 0 \end{pmatrix} \quad (4.12)$$

where the first choice corresponds to linear polarized light and the second one to circularly polarized light. In order to ensure that all polarization vectors form a complete basis of Minkowski space, it is common to also define the unphysical polarization vectors. One possible definition is

$$\epsilon_+^\mu(k) = \begin{pmatrix} |\vec{k}| \\ \vec{k} \end{pmatrix} = k^\mu \quad \epsilon_-^\mu(k) = \frac{1}{2|\vec{k}|^2} \begin{pmatrix} |\vec{k}| \\ -\vec{k} \end{pmatrix} = \frac{1}{2|\vec{k}|^2} \bar{k}^\mu \quad (4.13)$$

where the notation

$$\bar{k}^\mu = \begin{pmatrix} k_0 \\ -\vec{k} \end{pmatrix} \quad (4.14)$$

for a parity transformed four-vector is used. These two vectors are called the forward and backward lightlike polarization vectors. The forward lightlike polarization cannot be normalized but the other vectors are normalized to -1 . Another choice is

$$\epsilon_0^\mu(k) = \begin{pmatrix} 1 \\ 0 \\ 0 \\ 0 \end{pmatrix} \quad \epsilon_3^\mu(k) = \begin{pmatrix} 0 \\ 0 \\ 0 \\ 1 \end{pmatrix} \quad (4.15)$$

where ϵ_0^μ is called the timelike polarization and ϵ_3^μ the longitudinal polarization. One convenient aspect of the latter choice is that $\epsilon_0, \dots, \epsilon_3$ form a canonical basis of Minkowski space and satisfy $\epsilon_\lambda^\mu(k) \epsilon_{\lambda', \mu}(k) = g_{\lambda\lambda'}$. So far, we have only considered the Lorenz gauge $\partial_\mu A^\mu = 0$. A different approach are axial gauges which fix an axis n^μ such that $n_\mu A^\mu = 0$. Special cases are the lightcone gauge where n^μ is lightlike $n^2 = 0$ or the Coulomb gauge $\vec{\nabla} \cdot \vec{A}$ (in momentum space $\vec{k} \cdot \vec{A} = 0$). A similar discussion of the polarization vectors for a massless gauge field for the Coulomb gauge instead of the Lorenz gauge is available in [18].

In order to perform sums over the two physical (transverse) polarizations with the transverse lightlike direction k^μ without relying on any particular basis we need to specify any other direction n^μ with $n \cdot k \neq 0$ and $\epsilon(\lambda, k) \cdot n = 0$ for $\lambda = 1, 2$ to form a complete basis. This is the idea behind the axial gauge. Then, we can make the covariant ansatz

$$d^{\mu\nu}(k, n) = \sum_{\lambda=1,2} \epsilon^{\mu*}(\lambda, k) \epsilon^\nu(\lambda, k) = A_1 g^{\mu\nu} + A_2 k^\mu k^\nu + A_3 n^\mu k^\nu + A_4 n^\nu k^\mu + A_5 n^\mu n^\nu \quad (4.16)$$

with coefficients A_i . The transversality conditions of the polarization vectors

$$k_\mu d^{\mu\nu} = k_\nu d^{\mu\nu} = n_\mu d^{\mu\nu} = n_\nu d^{\mu\nu} = 0 \quad (4.17)$$

show that A_5 must be zero and provide the constraints

$$A_1 + A_3 k \cdot n = A_1 + A_4 k \cdot n = A_2 k \cdot n + A_4 n^2 = 0 \quad (4.18)$$

which give

$$A_3 = A_4 = -\frac{A_1}{k \cdot n} \quad A_2 = A_1 \frac{n^2}{(k \cdot n)^2}. \quad (4.19)$$

Thus, $d^{\mu\nu}$ can be completely parameterized in terms of A_1 . If we now contract $d^{\mu\nu}$ with $g_{\mu\nu}$ and use the normalization of the transverse polarizations $\epsilon^*(\lambda, k) \cdot \epsilon(\lambda, k) = -1$ we get $A_1 = -1$ and the final expression for the *polarization tensor* is

$$d^{\mu\nu}(k, n) = -g^{\mu\nu} + \frac{k^\mu n^\nu + k^\nu n^\mu}{n \cdot k} - n^2 \frac{k^\mu k^\nu}{(n \cdot k)^2}. \quad (4.20)$$

4.2 Canonical quantization of Yang-Mills theories

The standard canonical quantization method following the work of Dirac, which can be carried out successfully in the case of abelian theories, becomes extremely difficult for non-abelian theories and ultimately fails because of the complexity [21]. However, after Faddeev and Popov found a path integral formulation of non-abelian gauge theories in covariant gauge [22], Becchi, Rouet and Stora discovered a transformation which leaves the associated Lagrangian density

invariant including the gauge fixing terms [23]. This symmetry is called BRS-symmetry after its discoverers. This symmetry allows the canonical quantization of Yang-Mills field theories and thus offers the possibility to determine the Hilbert space of physical states which is not possible within the path integral formulation. Instead of going the historical route of the path integral, we postulate BRS-symmetry as quantum version of gauge symmetry and derive a gauge fixing term from it allowing to proceed with the quantization following the work of Kugo and Ojima [24, 25].

4.2.1 BRS-transformations

As a first step we fermionize the gauge transformations of the gauge field A_a^μ and the matter field Φ_i by replacing the transformation parameter $\alpha(x)$ with a Grassmann number $\theta(x)$ multiplied with the ghost field $c(x)$. The field Φ_i is just a placeholder for any matter field that could appear in the gauge invariant Lagrangian $\mathcal{L}(A, \Phi)$. The infinitesimal gauge transformations then take the form

$$\delta_B A_a^\mu(x) = \frac{1}{g_s} \theta D^\mu c_a(x) \quad (4.21)$$

$$\delta_B \Phi_i(x) = i\theta c_a(x) T_{ij}^a \Phi_j(x) \quad (4.22)$$

with the covariant derivative $D^\mu c_a = \partial^\mu c_a + g_s f_{abc} A_b^\mu c_c$ and where the generators T_{ij}^a of some semi-simple compact Lie group are in the representation of Φ_i . We arrive at the BRS-transformation δ_B by removing the Grassmann valued constant θ from the transformation $\delta_B = \theta \delta_B$. The operator δ_B is now itself Grassmann valued which means that one has to pay attention to the Grassmann parity of the fields within the product rule

$$\delta_B(FG) = (\delta_B F)G + (-)^{|F|} \delta_B FG \quad (4.23)$$

where the statistical index $|F|$ takes the value zero if F is a bosonic field and one if F is fermionic. The operator δ_B which is sometimes referred to as *Slavnov operator* has the property of being nilpotent $\delta_B^2 = 0$ as a consequence of its Grassmannian nature. The antighost field \bar{c}_a is *defined* to transform under the BRS-symmetry into the Nakanishi-Lautrup field B_a which is for now just an auxiliary field that later enforces the gauge fixing condition as a Lagrange multiplier

$$\delta_B \bar{c}_a(x) = \frac{1}{g_s} B_a(x). \quad (4.24)$$

From the nilpotency of δ_B follows directly the transformation rule of the Nakanishi-Lautrup field

$$\delta_B B_a(x) = 0. \quad (4.25)$$

The transformation of the ghost field $c_a(x)$ is derived from the requirement that the Slavnov operator is nilpotent

$$\begin{aligned} 0 &= \delta_B(\delta_B \Phi_i) = iT_{ij}^a \delta_B(c_a \Phi_j) = iT_{ij}^a [(\delta_B c_a) \Phi_j - c_a \delta_B \Phi_j] \\ &= i \left[(\delta_B c_a) T_{ij}^a \Phi_j - \frac{i}{2} c_a c_b \left(\frac{1}{N} d_{abc} + i f_{abc} \right) T_{ij}^c \Phi_j \right]. \end{aligned} \quad (4.26)$$

The symmetric term d_{abc} drops out due to the anticommuting nature of the ghosts which means that the ghost field must transform as

$$\delta_B c_a = -\frac{1}{2} f_{abc} c_b c_c \quad (4.27)$$

in order for the whole expression to vanish. In summary, the BRS-transformations are as follows

$$\delta_B \Phi_i = i c_a T_{ij}^a \Phi_j \quad (4.28)$$

$$\delta_B A_a^\mu = \frac{1}{g_s} \partial^\mu c_a + f_{abc} A_b^\mu c_c \quad (4.29)$$

$$\delta_B \bar{c}_a = \frac{1}{g_s} B_a \quad (4.30)$$

$$\delta_B c_a = -\frac{1}{2} f_{abc} c_b c_c. \quad (4.31)$$

4.2.2 Gauge fixing the theory

With the tool of BRS symmetry it is now possible to add a gauge fixing \mathcal{L}_{GF} and Faddeev and Popov term \mathcal{L}_{FP} to the classical Lagrangian density $\mathcal{L}(A, \Phi)$. For this, we select a gauge fixing function $F^a(A, \Phi, c, \bar{c}, B)$ which must contain the same number of ghosts and antighosts and write

$$\mathcal{L}_{\text{GF+FP}} = g_s \delta_B (\bar{c}_a F^a) \quad (4.32)$$

such that global BRS invariance of the gauge fixed Lagrangian

$$\tilde{\mathcal{L}}(A, \Phi, c, \bar{c}, B) = \mathcal{L}(A, \Phi) + \mathcal{L}_{\text{GF+FP}}(A, \Phi, c, \bar{c}, B) \quad (4.33)$$

is guaranteed through the nilpotency of δ_B independently of the explicit choice for F^a . Note that \mathcal{L} is *locally* BRS invariant by construction but on the level of $\tilde{\mathcal{L}}$ only *global* BRS invariance holds. Applying the BRS transformation allows the separation of the ghost and the gauge fixing term

$$\mathcal{L}_{\text{GF}} = B_a F^a \quad (4.34)$$

$$\mathcal{L}_{\text{FP}} = -g_s \bar{c}_a \delta_B F^a. \quad (4.35)$$

There are two main classes of gauge fixing conditions. The class of covariant and renormalizable R_ξ -gauges

$$F_a = \partial_\mu A_a^\mu + \frac{1}{2} \xi B_a \quad (4.36)$$

as well as the class of axial gauges

$$F_a = n_\mu A_a^\mu + \frac{1}{2} \lambda B_a. \quad (4.37)$$

where λ and ξ are gauge parameters and n^μ an arbitrary non-zero four-vector. As we want the theory to be covariant and the commutation relations to be as simple as possible, the Feynman gauge $\xi = 1$ turns out to be a good choice.

4.2.3 Covariant canonical quantization of the free fields

In the case of Yang-Mills theories, the problem arises that the theory is intrinsically interacting, which is why there exists no free-field mode expansion for the Heisenberg operators. We are in this work only interested in computing elements of the S -matrix where it is according to the LSZ reduction formula sufficient to know the asymptotic in- and out-fields. These are in turn described by the free Lagrangian density

$$\tilde{\mathcal{L}}_0 = -\frac{1}{4}F_a^{\mu\nu}F_{\mu\nu}^a + B_a\partial_\mu A_a^\mu + \frac{1}{2}B_a^2 + \partial_\mu \bar{c}_a\partial^\mu c_a \quad (4.38)$$

which originates from eq. (4.32) upon using Feynman gauge with all interaction terms turned off ($g_s = 0$) and matter fields suppressed. From eq. (4.38) we obtain the canonically conjugate fields

$$\pi_a^\mu = \frac{\partial \tilde{\mathcal{L}}_0}{\partial \dot{A}_a^\mu} = F_a^{\mu 0} + B_a g^{\mu 0} \quad \pi_B = \frac{\partial \tilde{\mathcal{L}}_0}{\partial \dot{B}_a} = 0 \quad (4.39)$$

$$\pi_c^a = \frac{\partial \tilde{\mathcal{L}}_0}{\partial \dot{c}^a} = -\dot{\bar{c}}^a \quad \pi_{\bar{c}}^a = \frac{\partial \tilde{\mathcal{L}}_0}{\partial \dot{\bar{c}}^a} = \dot{c}^a \quad (4.40)$$

and the equation of motions

$$B_a + \partial_\mu A^\mu = 0 \quad (4.41)$$

$$\square \bar{c}_a = \square c_a = 0 \quad (4.42)$$

$$\square A^\mu - \partial^\mu \partial_\nu A^\nu + \partial^\mu B_a = 0 \quad (4.43)$$

where it is important to recall the rule for differentiating Grassmann valued fields. The temporal component of π_a^μ is now non-zero thanks to the gauge fixing condition which allows to perform the quantization by writing down the canonical equal time (anti)-commutation relations

$$[A_a^\mu(t, \vec{x}), \pi_b^\nu(t, \vec{y})] = i\delta_{ab}g^{\mu\nu}\delta^{(3)}(\vec{x} - \vec{y}) \quad (4.44)$$

$$[A_a^\mu(t, \vec{x}), A_b^\nu(t, \vec{y})] = [\pi_a^\mu(t, \vec{x}), \pi_b^\nu(t, \vec{y})] = 0 \quad (4.45)$$

$$\{c^a(t, \vec{x}), \pi_c^b(t, \vec{y})\} = \{\bar{c}^a(t, \vec{x}), \pi_{\bar{c}}^b(t, \vec{y})\} = i\delta^{ab}\delta^{(3)}(\vec{x} - \vec{y}) \quad (4.46)$$

$$\{\bar{c}^a(t, \vec{x}), \bar{c}^b(t, \vec{y})\} = \{c^a(t, \vec{x}), c^b(t, \vec{y})\} = 0 \quad (4.47)$$

$$\{c^a(t, \vec{x}), c^b(t, \vec{y})\} = \{\pi_c^a(t, \vec{x}), \pi_{\bar{c}}^b(t, \vec{y})\} = 0 \quad (4.48)$$

$$\{c^a(t, \vec{x}), \bar{c}^b(t, \vec{y})\} = 0. \quad (4.49)$$

Note that eq. (4.49) is consistent with eq. (4.46) due to the minus sign in $\pi_{\bar{c}}^a$. Moreover, the field B_a can be integrated out by replacing it with its equation of motion $B_a = -\partial_\mu A^\mu$ which yields the canonical momenta

$$\pi_a^0 = -\partial_\mu A_a^\mu \quad (4.50)$$

$$\pi_a^i = \partial^i A_a^0 - \partial^0 A_a^i \quad (4.51)$$

so that one obtains for the commutation relation of the gauge field

$$[A_a^\mu(t, \vec{x}), \dot{A}_b^\nu(t, \vec{y})] = -i\delta_{ab}g^{\mu\nu}\delta^{(3)}(\vec{x} - \vec{y}). \quad (4.52)$$

Now we can proceed with the mode expansion of the fields. Combining eq. (4.41) and eq. (4.43) yields the equation

$$\square A_a^\mu = 0 \quad (4.53)$$

which means that the gauge field enjoys the simple expansion into Fourier modes

$$A_a^\mu(x) = \int \frac{d^3k}{(2\pi)^3} \frac{1}{\sqrt{2k_0}} \sum_{\lambda=\pm,1,2} \left[\epsilon^\mu(\lambda, k) a_a(\lambda, \vec{k}) e^{-ikx} + \epsilon^{\mu*}(\lambda, k) a_a^\dagger(\lambda, \vec{k}) e^{ikx} \right] \quad (4.54)$$

where the polarization vectors are chosen to form an orthogonal basis

$$\epsilon(k, \lambda) \cdot \epsilon(k, \lambda') = g_{\lambda\lambda'}. \quad (4.55)$$

The mode expansion of the free ghost fields is more peculiar. In order to ensure that $\tilde{\mathcal{L}}_0$ is hermitian $\tilde{\mathcal{L}}_0 = \tilde{\mathcal{L}}_0^\dagger$ such that time-evolution is described by a unitary operator and energy is an observable quantity, the anti-ghost field has to be anti-hermitian $\bar{c}_a^\dagger = -\bar{c}_a$ whereas the ghost field is taken to be hermitian $c_a^\dagger = c_a$ ¹ such that

$$(\partial_\mu \bar{c}_a \partial^\mu c_a)^\dagger = \partial_\mu c_a^\dagger \partial^\mu \bar{c}_a^\dagger = -\partial_\mu c_a \partial^\mu \bar{c}_a = \partial_\mu \bar{c}_a \partial^\mu c_a. \quad (4.56)$$

As a consequence, the expansion of the anti-ghost field must contain a relative minus sign

$$\begin{pmatrix} c_a(x) \\ \bar{c}_a(x) \end{pmatrix} = \int \frac{d^3k}{(2\pi)^3} \frac{1}{\sqrt{2k_0}} \left[\begin{pmatrix} c_a(\vec{k}) \\ -\bar{c}_a(\vec{k}) \end{pmatrix} e^{-ikx} + \begin{pmatrix} c_a^\dagger(\vec{k}) \\ \bar{c}_a^\dagger(\vec{k}) \end{pmatrix} e^{ikx} \right]. \quad (4.57)$$

Based on these free-field expansions and the postulated commutation relations, the creation and annihilation operators fulfill

$$\left[a_a(\lambda, \vec{k}), a_b^\dagger(\lambda', \vec{p}) \right] = g_{\lambda\lambda'} \delta_{ab} (2\pi)^3 \delta^{(3)}(\vec{k} - \vec{p}) \quad (4.58)$$

$$\left\{ c_a(\vec{k}), \bar{c}_b^\dagger(\vec{p}) \right\} = \left\{ \bar{c}_a(\vec{k}), c_b^\dagger(\vec{p}) \right\} = \delta_{ab} (2\pi)^3 \delta^{(3)}(\vec{k} - \vec{p}). \quad (4.59)$$

The relative minus sign also allows to properly close the contour of the time ordered product

$$\langle 0 | T \{ c(x) \bar{c}(y) \} | 0 \rangle = \theta(x_0 - y_0) \langle 0 | c(x) \bar{c}(y) | 0 \rangle - \theta(y_0 - x_0) \langle 0 | \bar{c}(y) c(x) | 0 \rangle \quad (4.60)$$

to obtain the Feynman propagator

$$\langle 0 | T \{ c(x) \bar{c}(y) \} | 0 \rangle = D_F(x - y) \quad (4.61)$$

as for the scalar field.

4.2.4 Slavnov-Taylor identities

In general, global symmetries of a theory allow to derive relationships between different Green's functions. Such identities are called *Ward-Takahashi* identities or *Slavnov-Taylor* identities in

¹Kugo and Ojima define an additional factor $-i$ into the ghost part of the Lagrangian $\tilde{\mathcal{L}}_0 \supset -i\partial_\mu \bar{c}_a \partial^\mu c_a$ which allows to define ghost and anti-ghost as hermitian. However, this leads to different signs in the Feynman rules for the ghost propagator and ghost-gluon vertex than the ones provided in appendix B.

the non-abelian case. For BRS-symmetry these identities emerge from the application of the BRS-operator δ_B on time-ordered products [25]

$$0 = \sum_{k=1}^n (-1)^{s_k} \langle 0 | T \{ \mathcal{O}_1(x_1) \dots \mathcal{O}_{k-1}(x_{k-1}) (\delta_B \mathcal{O}_k(x_k)) \mathcal{O}_{k+1}(x_{k+1}) \dots \mathcal{O}_n(x_n) \} | 0 \rangle . \quad (4.62)$$

The index $s_k = \sum_{i=1}^{k-1} |i|$ counts the number of bosonic and fermionic fields before \mathcal{O}_k where $|i|$ gives the Grassmann parity of \mathcal{O}_i , i.e. i takes the value zero for bosonic and 1 for fermionic fields.

5 The Catani-Seymour dipole formalism for massive initial states

The main goal of this chapter is to work out the integrated dipoles, which make it possible to transfer analytically the infrared poles from the real corrections to the virtual ones. This represents a continuation of the work started in [1] where the necessary splitting functions are "derived" by showing that they obey the desired asymptotic behaviour and where the factorization of the different phase spaces is performed. In order to be able to use the new results for the completely massive case in conjunction with those of Catani and Seymour, the structure of this chapter and the notation follow the style of [26] to a large extent. We begin with a brief review of the dipole subtraction method and end with a comparison of the new results with the phase space slicing method which is an alternative approach for the treatment of infrared divergences.

5.1 Brief review of the dipole subtraction method

A generic cross section σ^{NLO} describing the production of m particles at NLO accuracy in (SUSY)-QCD is composed as

$$\sigma^{\text{NLO}} = \sigma^{\text{Tree}} + \Delta\sigma^{\text{NLO}} \quad (5.1)$$

where the NLO part $\Delta\sigma^{\text{NLO}}$ receives contributions from virtual corrections $d\sigma^{\text{V}}$ as well as from real emission $d\sigma^{\text{R}}$ of massless particles

$$\Delta\sigma^{\text{NLO}} = \int_m d\sigma^{\text{V}} + \int_{m+1} d\sigma^{\text{R}} \quad (5.2)$$

where the subscript on the integrals refers to the number of particles in the final state. After successful renormalization the virtual part is ultraviolet (UV) finite but still contains another type of divergence: the infrared (IR) divergence which appears when the loop momentum of a massless virtual particle becomes almost zero or collinear to the direction of another particle. Therefore, one distinguishes between soft, collinear and soft-collinear infrared divergences where in the latter case the massless particle is soft and collinear at the same time.

The same kind of infrared behaviour occurs within the real contribution. According to the Kinoshita-Lee-Nauenberg theorem every unitary quantum field theory such as the Standard Model or its supersymmetric extension the MSSM is infrared finite as a whole [27]. As a consequence, the IR divergences from the phase space integration cancel the ones coming from the loop integrals on the right hand side of eq. (5.2). In practice, the divergences have to be extracted in terms of some regulator which could be an artificial mass. However, the only known regularization procedure which preserves gauge and Lorentz invariance (as well as supersymmetry) is dimensional regularization (dimensional reduction). Within these procedures, the number of space-time dimensions is continued analytically from four to $D = 4 - 2\varepsilon$. In this regularization scheme, soft and collinear divergences take the form of simple $1/\varepsilon$ poles whereas soft-collinear divergences appear as double poles $1/\varepsilon^2$. Due to the

large number of terms that enter during the standard Feynman-diagrammatic calculation of (SUSY)-QCD matrix elements, it is often impossible to perform the integration over the $m + 1$ particle phase space in eq. (5.2) analytically in D dimensions except for the very simplest processes or by exploiting special symmetries in the scattering amplitudes. In order to make a numerical evaluation possible, Catani and Seymour developed the dipole subtraction method [28]. The basic idea is to construct an auxiliary cross section $d\sigma^A$ which converges pointwise to $d\sigma^R$ in the singular region in D dimensions, so that $d\sigma^R - d\sigma^A$ is finite over the whole region of phase space and can be integrated in $D = 4$ dimensions. At the same time it must be possible to integrate $d\sigma^R$ analytically in D dimensions over the one-particle phase space of the radiated massless particle giving rise to the divergence. This allows to add back the subtraction term and to cancel those divergences appearing in the virtual contribution which are present in the form of poles in $1/\epsilon$. The computation of the NLO correction can then be summarized as

$$\Delta\sigma^{\text{NLO}} = \int_{m+1} \left[d\sigma_{\epsilon=0}^R - d\sigma_{\epsilon=0}^A \right] + \int_m \left[d\sigma^V + \int_1 d\sigma^A \right]_{\epsilon=0}. \quad (5.3)$$

The counterterm $d\sigma^A$ is constructed from the knowledge that QCD amplitudes factorize in the soft and collinear limit in the process dependent Born level cross section $d\sigma^B$ convoluted with a universal splitting kernel dV_{dipole} which reflects the singular behaviour. From another point of view, the factorization can be thought of as a two-step process. In the first step, m final state particles are produced through the Born level cross section $d\sigma^B$. In the second step, the final $(m + 1)$ -particle configuration is reached through the decay of one of the m partons - *the emitter* - into two partons. This last step is described by the splitting function dV_{dipole} . The information about colour and spin correlations are accounted for by referencing an additional parton - *the spectator*. The final expression for $d\sigma^A$ is obtained by summing over all possible emitter-spectator pairs

$$d\sigma^A = \sum_{\text{dipoles}} d\sigma^B \otimes d\mathbf{V}_{\text{dipole}}. \quad (5.4)$$

The fact that the underlying structure of this factorization is formed by these pairs coined the name dipoles. However, as this factorization holds only in the strict soft and collinear limit and it is desirable that $d\sigma^A$ approximates $d\sigma^R$ also in a small region around the singularity to render the subtraction procedure numerically stable, one has to introduce the so-called *dipole momenta* to ensure that the factorization does not violate momentum conservation. These obey momentum conservation in the whole $m + 1$ -particle phase space and are defined through a smooth map from the $m + 3$ real emission momenta to the $m + 2$ dipole momenta. The fact that this map is smooth has the important consequence that soft and soft-collinear divergences do not undergo double counting.

In order to implement the aforementioned colour and spin correlations into the factorization formula, the splitting functions $\mathbf{V}_{\text{dipole}}$ are realized as operators in colour and spin space. For this purpose, Catani and Seymour introduce in [28, 26] a certain set of conventions as well as a special notation for matrix elements. That is, coloured particles in the initial state are labelled by a, b, \dots and partons¹ in the final state by i, j, k, \dots . Since non-coloured particles are irrelevant for the subtraction procedure, they are suppressed in the notation. Scattering

¹In this context a parton stands for a coloured particle and not necessarily a constituent of the proton.

amplitudes are considered as objects in an abstract vector space spanned by the spins s_a, s_i and colours c_a, c_i of all coloured particles involved in the process

$$|\{i, a\}\rangle_m = \frac{1}{\prod_b \sqrt{n_c(b)}} \mathcal{M}_m^{\{c_i, s_i; c_a, s_a\}}(\{p_i; p_a\}) (|\{c_i; c_a\}\rangle \otimes |\{s_i; s_a\}\rangle) \quad (5.5)$$

where $\prod_b \sqrt{n_c(b)}$ fixes the normalization by averaging over the $n_c(b)$ colour degrees of freedom for each initial parton b . The kets $|\{c_i; c_a\}\rangle$ and $|\{s_i; s_a\}\rangle$ constitute formally an orthogonal basis of the colour and spin space respectively. The colour charge operators \mathbf{T}_i or \mathbf{T}_a reflect the emission of a gluon (or another massless coloured particle) from a parton i or a . Their action on colour space is defined as

$$\begin{aligned} {}_m\langle\{i, a\}|\mathbf{T}_j \cdot \mathbf{T}_k|\{i, a\}\rangle_m &= \frac{1}{\prod_b n_c(b)} \left[\mathcal{M}_m^{c_1, \dots, c_j, \dots, c_k, \dots, c_m; \{a\}}(\{p_i; p_a\}) \right]^* \\ &\quad \times T_{c_j d_j}^e T_{c_k d_k}^e \mathcal{M}_m^{d_1, \dots, d_j, \dots, d_k, \dots, d_m; \{a\}}(\{p_i; p_a\}) \end{aligned} \quad (5.6)$$

and analogously if j or k are initial state partons. For a final state parton j the colour-charge matrix T_{cd}^e is defined as $T_{cd}^e = -i f_{cde}$ if j is in the adjoint representation of $\mathfrak{su}(3)_c$, as $T_{st}^e = t_{st}^e$ if j is in the fundamental representation of $\mathfrak{su}(3)_c$ and $T_{st}^e = -t_{ts}^e$ if j is in the anti-fundamental representation of $\mathfrak{su}(3)_c$ where the $t^a = \frac{\lambda^a}{2}$ are the usual Gell-Mann matrices. The colour charge operator \mathbf{T}_a of an initial parton a obeys the same action defined in eq. (5.6). However, by crossing symmetry the colour charge matrix in this case is defined as $T_{st}^e = -t_{ts}^e$ if a is in the fundamental representation and as $T_{st}^e = t_{st}^e$ if a transforms in the anti-fundamental. Since every (SUSY)-QCD interaction preserves colour, it follows directly from construction that each state $|\{i, a\}\rangle_m$ must be a colour singlet

$$\left(\sum_j \mathbf{T}_j + \sum_b \mathbf{T}_b \right) |\{i, a\}\rangle_m = 0. \quad (5.7)$$

The final dipole factorization formula that defines the auxiliary matrix element related to $d\sigma^A$ is

$$\left| \mathcal{M}_{m+1}^A \right|^2 = \sum_{i,j} \sum_{k \neq i,j} \mathcal{D}_{ij,k} + \sum_{i,j} \sum_a \mathcal{D}_{ij}^a + \sum_{a,i} \sum_{j \neq i} \mathcal{D}_j^{ai} + \sum_{a,i} \sum_{b \neq a} \mathcal{D}^{ai,b} \quad (5.8)$$

where one has to distinguish between four different dipoles for the four different initial/final state combinations of emitter and spectator which are shown in fig. 5.1. The precise definition of the dipoles $\mathcal{D}_{ij,k}$, \mathcal{D}_{ij}^a , \mathcal{D}_j^{ai} and $\mathcal{D}^{ai,b}$ will be given in the following sections.

5.2 Final-state emitter and initial-state spectator

The dipole contribution \mathcal{D}_{ij}^a in eq. (5.8) is defined as

$$\mathcal{D}_{ij}^a = \frac{1}{-2p_i \cdot p_j} \frac{1}{x_{ij,a}} {}_{m,a}\langle \dots, (\tilde{i}\tilde{j}), \dots, \tilde{a}, \dots | \frac{\mathbf{T}_a \cdot \mathbf{T}_{ij}}{\mathbf{T}_{ij}^2} \mathbf{V}_{ij}^a | \dots, (\tilde{i}\tilde{j}), \dots, \tilde{a}, \dots \rangle_{m,a} \quad (5.9)$$

where the tree matrix element with m -final state particles is obtained by discarding the external leg of the radiated particle i and replacing the momenta p_a and p_j in the real emission $(m+1)$ -particle matrix element with their dipole momenta \tilde{p}_a and \tilde{p}_{ij} . The function \mathbf{V}_{ij}^a describes the splitting process $\tilde{i}\tilde{j} \rightarrow i + j$. The mass of the emitter $\tilde{i}\tilde{j}$ is denoted as m_{ij} and

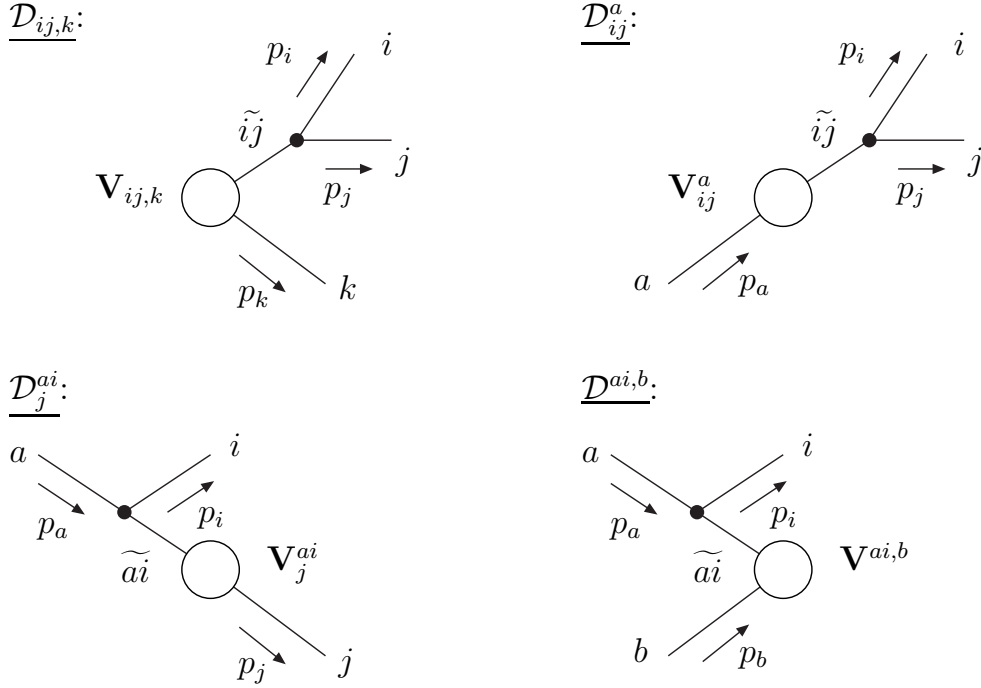


Figure 5.1: Effective diagrams for different emitter-spectator pairs. Figure taken from [26].

will be defined for each splitting process separately.

Since a treatment of massless initial partons with massless [28] and massive final states [26] is already available in the literature, the initial parton a will be treated as massive throughout this section.

5.2.1 Dipole kinematics and phase space factorization

The phase space factorization in dimensional regularization for the fully massive case was worked out in [1] where the kinematics of Dittmaier's work [29] were adopted with a slightly different notation. However, Dittmaier uses a small photon mass as IR regulator which is common in electroweak physics so that the crucial part lied in the generalisation of the phase space parametrization from four to D dimensions. In the following, the kinematic variables as well as the end result for the factorized phase space are summarized.

The two main quantities are the square of the total outgoing momentum of the dipole phase space

$$P^2 = (p_i + p_j)^2, \quad P = p_i + p_j \quad (5.10)$$

and the total transferred momentum

$$Q = P - p_a = p_b - p_k \quad (5.11)$$

$$\bar{Q}^2 = Q^2 - m_a^2 - m_j^2 \quad (5.12)$$

where p_k denotes the sum of the momenta of all other $(m - 1)$ -final state particles besides p_i and p_j . The dipole splitting functions are formulated in terms of the momentum fractions

$$z_j = \frac{p_a \cdot p_j}{P \cdot p_a} \quad (5.13)$$

$$z_i = \frac{p_a \cdot p_i}{P \cdot p_a} \quad (5.14)$$

$$x_{ij,a} = \frac{P \cdot p_a - p_i \cdot p_j}{P \cdot p_a} \quad (5.15)$$

which take by definition only values between zero and one. They can be expressed in terms of the future integration variables P^2 , Q^2 and z_i through the relations

$$P^2 = \frac{-\bar{Q}^2}{x_{ij,a}} + Q^2 - m_a^2 \quad (5.16)$$

$$P \cdot p_a = \frac{-\bar{Q}^2}{2x_{ij,a}} \quad (5.17)$$

$$z_j = 1 - z_i. \quad (5.18)$$

It is worth noting that since the product $P \cdot p_a$ is always positive and $x_{ij,a}$ can only take values between zero and one, the quantity \bar{Q}^2 is always negative such that $\sqrt{\bar{Q}^4} = -\bar{Q}^2$ where $\bar{Q}^4 = (\bar{Q}^2)^2$ to be precise. The auxiliary variables

$$\lambda_{aj} = \lambda(Q^2, m_j^2, m_a^2) = \bar{Q}^4 - 4m_a^2 m_j^2 \quad (5.19)$$

$$R_{aj} = \sqrt{\frac{(\bar{Q}^2 + 2m_a^2 x_{ij,a})^2 - 4m_a^2 Q^2 x_{ij,a}^2}{\lambda_{aj}}} = \frac{-\bar{Q}^2}{P^2 - Q^2 + m_a^2} \sqrt{\frac{(P^2 - Q^2 - m_a^2)^2 - 4m_a^2 Q^2}{\lambda_{aj}}} \quad (5.20)$$

with the Källén function

$$\lambda(x, y, z) = x^2 + y^2 + z^2 - 2xy - 2yz - 2zx \quad (5.21)$$

are introduced for later convenience. It is straightforward to check that z_i , z_j , $x_{ij,a}$, P^2 and R_{aj} behave in the soft $p_i^\mu \rightarrow 0$ and collinear limit $p_a \cdot p_i \rightarrow 0$ as

$$z_i \rightarrow 0 \quad z_j \rightarrow 1 \quad x_{ij,a} \rightarrow 1 \quad P^2 \rightarrow m_j^2 \quad R_{aj} \rightarrow 1. \quad (5.22)$$

The dipole momenta of the emitter and spectator

$$\tilde{p}_{ij}^\mu = \frac{x_{ij,a}}{R_{aj}} p_a^\mu + \left(\frac{1}{R_{aj}} \frac{\bar{Q}^2 + 2m_a^2 x_{ij,a}}{2Q^2} - \frac{Q^2 + m_a^2 - m_j^2}{2Q^2} + 1 \right) Q^\mu \quad (5.23)$$

$$\tilde{p}_a^\mu = \tilde{p}_{ij}^\mu - Q^\mu \quad (5.24)$$

are constructed from the requirement to fulfill the on-shell conditions $\tilde{p}_a^2 = m_a^2$, $\tilde{p}_{ij}^2 = m_{ij}^2$ and momentum conservation $\tilde{p}_a + p_b = \tilde{p}_{ij} + p_k$. The factorization of the three-particle phase space $d\Phi_3(p_i, p_j, p_k; p_a + p_b)$ into the two-particle phase space $d\Phi_2(P^2, Q^2)$ and the dipole phase space $dp_i(Q^2, P^2, z_i)$ involves a convolution over P^2

$$\int d\Phi_3(p_i, p_j, p_k; p_a + p_b) = \int_{m_j^2}^{P_+^2} \frac{dP^2}{2\pi} \int d\Phi_2(P^2, Q^2) \int [dp_i(Q^2, P^2, z_i)] \quad (5.25)$$

which corresponds to the integration of the boost parameter P^2 between the CM frame of $p_i + p_j$ and the CM frame of $p_a + p_b$. The integration of the splitting function over the one-particle phase space

$$\int [dp_i(Q^2, P^2, z_i)] = \frac{2\pi}{(4\pi)^{2-\varepsilon}} \frac{(P^2)^{-\varepsilon}}{\Gamma(1-\varepsilon)} \left(\frac{R_{aj}\sqrt{\lambda_{aj}}}{-\bar{Q}^2} \right)^{2\varepsilon-1} \int_{z_-}^{z_+} dz_i [(z_i - z_-)(z_+ - z_i)]^{-\varepsilon} \quad (5.26)$$

yields the singular behaviour parameterized by $D = 4 - 2\varepsilon$ dimensions where the integration limits read

$$z_{\pm} = \frac{1-x}{2} \frac{-\bar{Q}^2 \pm \sqrt{\lambda_{aj}} R_{aj}}{xm_j^2 - \bar{Q}^2(1-x)}. \quad (5.27)$$

In the case of a $2 \rightarrow 2$ process, the remaining m -particle phase space is just the usual two-particle phase space with outgoing momenta p_k and P

$$\int d\Phi_2(P^2, Q^2) = \frac{1}{\sqrt{\lambda(s, m_a^2, m_b^2)}} \int_{Q_-^2(P^2)}^{Q_+^2(P^2)} \frac{dQ^2}{8\pi} \quad (5.28)$$

where the "particle" that corresponds to P is off-shell. As Q^2 is a Lorentz invariant quantity the integration limits can be derived in any frame. Therefore, it is convenient to choose the center-of-mass frame of the initial particles with the well-known kinematics [30, 31]

$$E_b = \frac{s + m_b^2 - m_a^2}{2\sqrt{s}} \quad E_k = \frac{s + m_k^2 - P^2}{2\sqrt{s}} \quad (5.29)$$

$$|\vec{p}_b| = \frac{\sqrt{\lambda(s, m_a^2, m_b^2)}}{2\sqrt{s}} \quad |\vec{p}_k| = \frac{\sqrt{\lambda(s, m_k^2, P^2)}}{2\sqrt{s}}. \quad (5.30)$$

which were also derived again in [1] directly in the context of the phase space factorization. If we expand Q^2 into its components

$$Q^2 = m_b^2 + m_k^2 - 2E_b E_k + 2|\vec{p}_b||\vec{p}_k| \cos \theta \quad (5.31)$$

and use the knowledge that $-1 \leq \cos \theta \leq 1$, we obtain the integration limits

$$Q_{\pm}^2(P^2) = m_b^2 + m_k^2 - \frac{(s + m_b^2 - m_a^2)(s + m_k^2 - P^2)}{2s} \pm \frac{\sqrt{\lambda(s, m_a^2, m_b^2)}\sqrt{\lambda(s, m_k^2, P^2)}}{2s} \quad (5.32)$$

where it is important to realize that the integration limits of Q^2 depend on P^2 . For $P^2 = m_j^2$ the integration over Q^2 reduces to the usual two-particle phase space involving the integration over the scattering angle ϑ

$$\frac{1}{\sqrt{\lambda(s, m_a^2, m_b^2)}} \int_{Q_-^2(m_j^2)}^{Q_+^2(m_j^2)} \frac{dQ^2}{8\pi} = \frac{1}{16\pi s} \sqrt{\lambda(s, m_k^2, m_j^2)} \int_{-1}^1 d\cos \vartheta. \quad (5.33)$$

As the integrand of the remaining m -particle phase space is IR finite the integration can be performed for $\varepsilon = 0$. In order to deduce the integration limits for P^2 , we can take into account the soft limit

$$P^2 = m_j^2 + 2p_i \cdot p_j \xrightarrow{p_i^\mu \rightarrow 0} m_j^2 \quad (5.34)$$

which gives the lower limit $P_-^2 = m_j^2$. The upper limit can be obtained by minimizing

$$P^2 = s - m_k^2 - 2P \cdot p_k. \quad (5.35)$$

By working in the CMS of p_a and p_b and using energy $\sqrt{s} = \sqrt{m_i^2 + |\vec{p}_i|^2} + \sqrt{m_k^2 + |\vec{p}_k|^2} + |\vec{p}_j|$ and momentum conservation $|\vec{P}| = |\vec{p}_k|$, the product $P \cdot p_k$ can be parameterized through $|\vec{P}|$ as

$$p_k \cdot P = \left(\sqrt{s} - \sqrt{|\vec{P}|^2 + m_k^2} \right) \sqrt{|\vec{P}|^2 + m_k^2} + |\vec{P}|^2 \quad (5.36)$$

which becomes minimal for $|\vec{P}| = 0$. Therefore, we arrive at the upper limit

$$P_+^2 = (\sqrt{s} - m_k)^2. \quad (5.37)$$

In the massless case $m_j = 0$ the integration limits related to z_i simplify to

$$z_{\pm} = \frac{1}{2} (1 \pm R_{aj}). \quad (5.38)$$

Furthermore, an additional auxiliary parameter x_0 with $0 \leq x_0 < 1$ is introduced as a lower limit on $x_{ij,a}$ for which the splitting functions are applied. This lower limit on x_0 is provided by the constraint that the argument of the square root in eq. (5.20) remains positive for all possible values of Q^2 which translates to the condition

$$\frac{-\bar{Q}}{2m_a(m_a - \sqrt{Q^2})} < x_0 < 1. \quad (5.39)$$

Since the singular behaviour occurs for $x_{ij,a} \rightarrow 1$, applying the splitting function \mathbf{V}_{ij}^a for $x_0 < x_{ij,a} < 1$ still cancels the divergences. In addition, the independence of $\Delta\sigma^{\text{NLO}}$ on the choice of x_0 serves as a non-trivial check for the correct implementation of the subtraction procedure.

5.2.2 The dipole splitting functions

The functions \mathbf{V}_{ij}^a in eq. (5.9) for the three QCD splitting processes

- $Q \rightarrow g(p_i) + Q(p_j) : m_i = 0 \text{ and } m_{ij} = m_j = m_Q$
- $g \rightarrow g(p_i) + g(p_j) : m_{ij} = m_i = m_j = 0$
- $g \rightarrow Q(p_i) + \bar{Q}(p_j) : m_i = m_j = m_Q \text{ and } m_{ij} = 0$

were worked out for the fully massive case in [1]. The associated CPT -conjugated splitting processes are formally identical to those given here and are therefore not listed separately.

Explicitly, the dipole functions read

$$\langle s | \mathbf{V}_{gq}^a | s' \rangle = 2g_s^2 \mu^{2\varepsilon} C_F \left(\frac{2}{2 - x_{ij,a} - z_j} - 2 + (1 - \varepsilon) z_i - \frac{m_j^2}{p_i \cdot p_j} \right) \delta_{ss'} = \langle \mathbf{V}_{gq}^a \rangle \delta_{ss'} \quad (5.40)$$

$$\langle \mu | \mathbf{V}_{gg}^a | \nu \rangle = 4g_s^2 \mu^{2\varepsilon} C_A \left[-g^{\mu\nu} \left(\frac{1}{1 + z_i - x_{ij,a}} + \frac{1}{2 - z_i - x_{ij,a}} - 2 \right) + \frac{1 - \varepsilon}{p_i \cdot p_j} C^{\mu\nu} \right] \quad (5.41)$$

$$\langle \mathbf{V}_{gg}^a \rangle = 4g_s^2 \mu^{2\varepsilon} C_A \left[\frac{1}{1 + z_i - x_{ij,a}} + \frac{1}{2 - z_i - x_{ij,a}} - 2 + (z_+ - z_i)(z_i - z_-) \right] \quad (5.42)$$

$$\langle \mu | \mathbf{V}_{Q\bar{Q}}^a | \nu \rangle = 2g_s^2 \mu^{2\varepsilon} T_F \left(-g^{\mu\nu} - \frac{2}{p_i \cdot p_j} C^{\mu\nu} \right) \quad (5.43)$$

$$\langle \mathbf{V}_{Q\bar{Q}}^a \rangle = 2g_s^2 \mu^{2\varepsilon} T_F \left(1 - \frac{2}{1 - \varepsilon} (z_+ - z_i)(z_i - z_-) \right) \quad (5.44)$$

where z_{\pm} correspond to the integration limits in eq. (5.27). The spin correlation tensor

$$C^{\mu\nu} = \left(z_i^{(m)} p_i^\mu - z_j^{(m)} p_j^\mu \right) \left(z_i^{(m)} p_i^\nu - z_j^{(m)} p_j^\nu \right) \quad (5.45)$$

depending on the new variables

$$z_i^{(m)} = z_i - z_- = z_i - \frac{1}{2} (1 - R_{aj}) \quad z_j^{(m)} = z_j - z_- = z_j - \frac{1}{2} (1 - R_{aj}) \quad (5.46)$$

is constructed such that it is orthogonal to the direction of the emitter

$$\tilde{p}_{ij}^\mu \mathcal{C}_{\mu\nu} = \tilde{p}_{ij}^\nu \mathcal{C}_{\mu\nu} = 0. \quad (5.47)$$

By Lorentz invariance the integral over the one-particle phase space of a splitting function with a gluon emitter can only take the form

$$\int [dp_i (Q^2, P^2, z_i)] \langle \mu | \mathbf{V}_{ij}^a | \nu \rangle = -A_1 g^{\mu\nu} + A_2 \frac{\tilde{p}_{ij}^\mu \tilde{p}_a^\nu + \tilde{p}_{ij}^\nu \tilde{p}_a^\mu}{\tilde{p}_{ij} \cdot \tilde{p}_a} - A_3 \frac{m_a^2 \tilde{p}_{ij}^\mu \tilde{p}_{ij}^\nu}{(\tilde{p}_{ij} \cdot \tilde{p}_a)^2} + A_4 \frac{\tilde{p}_a^\mu \tilde{p}_a^\nu}{m_a^2}. \quad (5.48)$$

Due to the transversality condition on $\mathcal{C}_{\mu\nu}$ in eq. (5.47) the term A_4 is zero. The coefficients A_2 and A_3 can be chosen arbitrarily by the virtue of Slavnov-Taylor identities. However, in order to include the correct number of physical polarizations, we can think of A_2 and A_3 as being equal to A_1 such that A_1 can be disentangled by averaging over the $D - 2$ transverse polarizations of the emitter

$$A_1 = \int [dp_i (Q^2, P^2, z_i)] \langle \mathbf{V}_{ij}^a \rangle \quad (5.49)$$

with the averaged splitting function

$$\langle \mathbf{V}_{ij}^a \rangle = \frac{1}{D - 2} d_{\mu\nu} (\tilde{p}_{ij}, \tilde{p}_a) \langle \mu | \mathbf{V}_{ij}^a | \nu \rangle. \quad (5.50)$$

The polarization tensor

$$d^{\mu\nu} (\tilde{p}_{ij}, \tilde{p}_a) = -g^{\mu\nu} + \frac{\tilde{p}_{ij}^\mu \tilde{p}_a^\nu + \tilde{p}_{ij}^\nu \tilde{p}_a^\mu}{\tilde{p}_{ij} \cdot \tilde{p}_a} - \frac{m_a^2 \tilde{p}_{ij}^\mu \tilde{p}_{ij}^\nu}{(\tilde{p}_{ij} \cdot \tilde{p}_a)^2} \quad (5.51)$$

was introduced in eq. (4.20) and fulfills in D dimensions $d^{\mu\nu}d_{\mu\nu} = D - 2$.

5.2.3 The integrated dipole functions

The integral of the spin-averaged dipole function $\langle \mathbf{V}_{ij}^a \rangle$ over the dipole phase space is defined as

$$\frac{g_s^2}{2\pi} \frac{(4\pi)^\varepsilon}{\Gamma(1-\varepsilon)} I_{ij}^a(P^2, Q^2; \varepsilon) = \int [dp_i(Q^2, P^2, z_i)] \frac{1}{2p_i \cdot p_j} \frac{1}{x_{ij,a}} \langle \mathbf{V}_{ij}^a \rangle \quad (5.52)$$

where I_{ij}^a depends on the auxiliary variables P^2 and Q^2 . By writing the single-parton phase space in eq. (5.26) in the form

$$\int_{z_-}^{z_+} dz_i [(z_i - z_-)(z_+ - z_i)]^{-\varepsilon} = (z_+ - z_-)^{1-2\varepsilon} \int_0^1 dt [(1-t)t]^{-\varepsilon} \quad (5.53)$$

through the substitution $t = \frac{z_i - z_-}{z_+ - z_-}$, the integration of the splitting function becomes straightforward in terms of the beta and Gaussian hypergeometric function listed in appendix A.1 giving

$$\begin{aligned} I_{gQ}^a(P^2, Q^2; \varepsilon) &= \frac{C_F}{\sqrt{\lambda_{aj}} R_{aj}} \frac{(m_a^2 + P^2 - Q^2)^{1+2\varepsilon}}{(P^2 - m_j^2)^{1+2\varepsilon}} \left(\frac{m_j^2 x_{ij,a} + \bar{Q}^2(x_{ij,a} - 1)}{-\bar{Q}^2} \right)^{2\varepsilon} \left(\frac{\mu^2}{P^2} \right)^\varepsilon \\ &\times \left(\frac{\sqrt{\lambda_{aj}} R_{aj}}{\bar{Q}^2} \left(1 + \frac{\bar{Q}^4(x_{ij,a} - 1)^2}{4(m_j^2 x_{ij,a} + \bar{Q}^2(x_{ij,a} - 1))^2} (\varepsilon - 1) \right) \beta(1 - \varepsilon, 1 - \varepsilon) - I_1(-A; \varepsilon) \right) \end{aligned} \quad (5.54)$$

$$\begin{aligned} I_{gg}^a(P^2, Q^2; \varepsilon) &= \frac{C_A \mu^{2\varepsilon}}{R_{aj} (P^2)^{1+\varepsilon}} \frac{P^2 - \bar{Q}^2}{\bar{Q}^2} \left(I_1(-A; \varepsilon) - I_1(\tilde{A}; \varepsilon) \right. \\ &\quad \left. - R_{aj}^3 \beta(2 - \varepsilon, 2 - \varepsilon) + 2R_{aj} \beta(1 - \varepsilon, 1 - \varepsilon) \right) \end{aligned} \quad (5.55)$$

$$I_{Q\bar{Q}}^a(P^2, Q^2; \varepsilon) = \frac{T_F \mu^{2\varepsilon}}{2(P^2)^{1+\varepsilon}} \frac{\bar{Q}^2 - P^2}{\bar{Q}^2} \left(\beta(1 - \varepsilon, 1 - \varepsilon) - \frac{2}{1 - \varepsilon} R_{aj}^2 \beta(2 - \varepsilon, 2 - \varepsilon) \right) \quad (5.56)$$

where the variables A and \tilde{A} are defined as

$$A = \frac{z_+ - z_-}{1 - x + z_-} \quad \tilde{A} = \frac{z_+ - z_-}{2 - x - z_-}. \quad (5.57)$$

The ε -expansion of the hypergeometric function hidden in the new function

$$I_1(z; \varepsilon) = z \int_0^1 dt \frac{((1-t)t)^{-\varepsilon}}{1 - zt} = z \beta(1 - \varepsilon, 1 - \varepsilon) {}_2F_1(1, 1 - \varepsilon, 2 - 2\varepsilon; z) \quad (5.58)$$

$$= -\ln(1 - z) + \varepsilon \left(2 \text{Li}_2(z) + \frac{1}{2} \ln^2(1 - z) \right) + \mathcal{O}(\varepsilon^2) \quad (5.59)$$

is calculated in appendix A.1.3. The expansion is valid as long as the argument z remains bounded between one and negative infinity $-\infty < z < 1$ which is always fulfilled for a massive

emitter as in eq. (5.54). Following the Pfaff transformation of the hypergeometric function given in eq. (A.11), the function $I_1(z; \varepsilon)$ obeys the relation

$$I_1(z; \varepsilon) = -I_1\left(\frac{z}{z-1}; \varepsilon\right). \quad (5.60)$$

In the massless case $m_j = 0$ as in eq. (5.55), A and \tilde{A} take a similar form

$$A = \frac{2\sqrt{1-w^2}}{1-\sqrt{1-w^2}}, \quad 0 \leq A \quad (5.61)$$

$$\tilde{A} = \frac{2\sqrt{1-w^2}}{1+\sqrt{1-w^2}}, \quad 0 \leq \tilde{A} \leq 1 \quad (5.62)$$

when being expressed through the quantity

$$w = \frac{\sqrt{4P^2(m_a^2 + 2P^2 - \bar{Q}^2)}}{3P^2 - \bar{Q}^2}, \quad 0 \leq w \leq 1. \quad (5.63)$$

Writing A and \tilde{A} in this manner makes the relation

$$\frac{\tilde{A}}{\tilde{A}-1} = -A \quad (5.64)$$

apparent which allows to simplify the difference of the I_1 functions in eq. (5.55)

$$I_1(-A; \varepsilon) - I_1(\tilde{A}; \varepsilon) = 2I_1(-A; \varepsilon) \quad (5.65)$$

by employing the identity in eq. (5.60). Recall that eqs. (5.61) and (5.62) are only valid for $m_j = 0$. In the massive case A reads

$$A = \frac{-2\sqrt{\lambda_{aj}}R_{aj}}{-2x(\bar{Q}^2 + m_j^2) + 3\bar{Q}^2 + \sqrt{\lambda_{aj}}R_{aj}}. \quad (5.66)$$

For $\varepsilon = 0$ the functions I_{ij}^a become singular at the endpoint $P^2 \rightarrow m_j^2$ giving the infrared divergence. Therefore, the integration of the I_{ij}^a over P^2 and Q^2 can not be handled numerically yet. To allow for the extraction of the divergence in terms of ε while being able to perform the integration of the product $I_{ij}^a |\mathcal{M}|^2$ involving the tree matrix element squared numerically, the $[\dots]^+$ -distribution² defined as

$$g(x) = [g(x)]_{[a,b]}^+ + \delta(x-a) \int_a^b dy g(y) \quad (5.67)$$

provides a way around and serves as an artificially inserted zero to render the endpoint contribution finite. The endpoint part is then further decomposed into a finite $J_{ij}^{a;\text{NS}}$ and singular $J_{ij}^{a;\text{S}}$ piece where the latter contains the infrared poles in ε . This approach of making the convolution over P^2 numerically accessible for $\varepsilon = 0$ and the treatment of interdependent

²The $[\dots]^+$ -distribution defined in [1, 26, 29] involves the upper instead of the lower limit.

integration limits in the context of the $[\dots]^+$ -distribution is best illustrated for the case of $Q \rightarrow gQ$ splitting:

$$\begin{aligned}
& \int_{m_j^2}^{P_+^2} \frac{dP^2}{2\pi} \int_{Q_-^2(P^2)}^{Q_+^2(P^2)} \frac{dQ^2}{2\sqrt{\lambda(s, m_a^2, m_b^2)}} I_{gQ}^a(P^2, Q^2; \varepsilon) |\mathcal{M}(P^2, Q^2)|^2 \\
&= \sqrt{\lambda(s, m_k^2, m_j^2)} \int_{-1}^1 d\cos\vartheta \left(J_{gQ}^{a;S}(Q^2; \varepsilon) + J_{gQ}^{a;NS}(Q^2) \right) |\mathcal{M}|^2 \\
&+ \int_{m_j^2}^{P_+^2} \frac{dP^2}{2\pi} \int_{Q_-^2(m_j^2)}^{Q_+^2(m_j^2)} dQ^2 \left[\frac{1}{P^2 - m_j^2} \right]_{[m_j^2, P_0^2]}^+ \Delta Q^2 \tilde{I}_{gQ}^a(P^2, \tilde{Q}^2; 0) |\mathcal{M}(P^2, \tilde{Q}^2)|^2. \quad (5.68)
\end{aligned}$$

On the left hand side appears the integral we want to evaluate numerically but which is singular for $\varepsilon = 0$. Notice that the integration limits of Q^2 depend on P^2 . The first term on the right hand side corresponds to the integral proportional to the Dirac delta distribution in eq. (5.67). It was used that the integral over Q^2 reduces to the usual integration over the scattering angle $\cos\vartheta$ in the limit $P^2 \rightarrow m_j^2$ (cf. eq. (5.33)). The pieces $J_{gQ}^{a;S}$ and $J_{gQ}^{a;NS}$ arise from the integration of the singular factor $\frac{1}{P^2 - m_j^2}$ in eq. (5.54) which is placed inside the "plus"-distribution

$$\begin{aligned}
J_{gQ}^{a;S}(Q^2; \varepsilon) + J_{gQ}^{a;NS}(Q^2) &= \tilde{I}_{gQ}^a(m_j^2, Q^2; \varepsilon) \int_{m_j^2}^{P_0^2} \frac{dP^2}{2\pi} \frac{1}{(P^2 - m_j^2)^{1+2\varepsilon}} \\
&= \frac{1}{2\pi} \left(-\frac{1}{2\varepsilon} + \ln(P_0^2 - m_j^2) \right) \tilde{I}_{gQ}^a(m_j^2, Q^2; \varepsilon) + \mathcal{O}(\varepsilon). \quad (5.69)
\end{aligned}$$

One can take any value for the integration limit P_0^2 as long as $m_j^2 < P_0^2 \leq P_+^2$ since this choice must cancel out which can be seen by inserting the definition of the $[\dots]^+$ -distribution back into eq. (5.68). Checking the final result for P_0^2 independence is a further non-trivial check for the correct implementation of the "plus"-distribution. The factor $\tilde{I}_{gQ}^a(P^2, \tilde{Q}^2; 0)$ in the second term on the right hand side of eq. (5.68) is defined through everything of the integrated dipole $I_{gQ}^a(P^2, Q^2; \varepsilon)$ which is not inside the "plus"-distribution. The integration limits of Q^2 in this part were shifted through the substitution

$$Q^2 \mapsto \tilde{Q}^2 = \Delta Q^2 (Q^2 - Q_-^2(m_j^2)) + Q_-^2(P^2) \quad (5.70)$$

with

$$\Delta Q^2 = \frac{Q_+^2(P^2) - Q_-^2(P^2)}{Q_+^2(m_j^2) - Q_-^2(m_j^2)} \quad (5.71)$$

to guarantee a consistent numerical evaluation. From now on Q^2 represents the integration variable associated with the limits $Q_-^2(m_j^2)$ and $Q_+^2(m_j^2)$, whereas the transformed variable \tilde{Q}^2 is associated with the integration limits $Q_-^2(P^2)$ and $Q_+^2(P^2)$. The explicit expressions for the singular terms $J_{gQ}^{a;S}$ and $J_{gQ}^{a;NS}$ are provided at the end of this subsection. The lengthy integral form of decomposing the integrated dipole used in eq. (5.68) served only the purpose to illustrate the idea of the "plus"-distribution and to highlight the dependent integration

limits. It is more convenient to perform the decomposition by transforming the I_{ij}^a functions to distributions. So, an alternative to eq. (5.68) is:

$$I_{gQ}^a(P^2, Q^2; \varepsilon) = [J_{gQ}^a(P^2, Q^2)]_+ + 2\pi\delta(P^2 - m_j^2) \left(J_{gQ}^{a;S}(Q^2; \varepsilon) + J_{gQ}^{a;NS}(Q^2) \right) + \mathcal{O}(\varepsilon) \quad (5.72)$$

where $[J_{gQ}^a(P^2, Q^2)]_+$ is given by

$$[J_{gQ}^a(P^2, Q^2)]_+ = C_F \Delta Q^2 \frac{m_a^2 + P^2 - \tilde{Q}^2}{\sqrt{\lambda_{aj}} R_{aj}} \left[\frac{1}{P^2 - m_j^2} \right]_{[m_j^2, P_0^2]} \left(\frac{\sqrt{\lambda_{aj}} R_{aj}}{\tilde{Q}^2} \right. \\ \left. \times \left(1 - \frac{\tilde{Q}^4 (x-1)^2}{4(m_j^2 x + \tilde{Q}^2 (x-1))^2} \right) + \ln(1+A) \right). \quad (5.73)$$

Note that the notation in eq. (5.73) is purely symbolic: $[J_{gQ}^a(P^2, Q^2)]_+$ is not a "plus"-distribution itself but contains all the plus distributions.

We can now move on to the integrated dipole I_{gg}^a . Disentangling the infrared poles in this case of $g \rightarrow gg$ splitting is more involved due to the fact that besides the factor $\frac{1}{(P^2)^{1+\varepsilon}}$ in eq. (5.54) the function $I_1(-A; \varepsilon)$ diverges as well for $P^2 \rightarrow 0$. Since the expansion in ε of $I_1(-A; \varepsilon)$ is not analytic for $P^2 = 0$, the hypergeometric function itself has to be placed inside the $[\dots]^+$ -distribution. Since the entire content of the "plus"-distribution has to be integrated over P^2 analytically, it makes sense to choose the associated expression as minimal as possible, in the sense that the integration becomes as simple as possible. This is achieved by introducing the argument of the hypergeometric function as new integration variable

$$y_A = \frac{1}{A} = P^2 \mathcal{A}(P^2, \tilde{Q}^2) \quad (5.74)$$

which behaves analogously to P^2 in the singular region. This factorization is achieved by expanding the denominator and numerator of A as given in eq. (5.61) with $1 + \sqrt{1-w^2}$ leading to

$$\mathcal{A}(P^2, \tilde{Q}^2) = 2(m_a^2 + 2P^2 - \tilde{Q}^2) \left[(\rho + 3P^2 - \tilde{Q}^2) \rho \right]^{-1} \quad (5.75)$$

with

$$\rho = \sqrt{(P^2 - \tilde{Q}^2)^2 - 4m_a^2 P^2}. \quad (5.76)$$

In this new variable y_A only the integral

$$\mathcal{I}_1(y_0; \varepsilon) = \int_0^{y_0} dy \frac{1}{y^{1+\varepsilon}} I_1\left(-\frac{1}{y}, \varepsilon\right) = -\frac{1}{2\varepsilon^2} + \frac{\pi^2}{12} - \text{Li}_2\left(-\frac{1}{y_0}\right) + \mathcal{O}(\varepsilon) \quad (5.77)$$

has to be computed analytically. The associated steps are outlined in appendix A.1.4. When the numerical integration of the $[\dots]^+$ -distribution is still performed in terms of P^2 (which is advised in order to avoid separate integration routines), the derivative

$$y'_A = \frac{dy_A}{dP^2} = -\frac{1}{\rho^3} \left(3m_a^2 P^2 - \tilde{Q}^4 + \frac{d\tilde{Q}^2}{dP^2} P^2 (\tilde{Q}^2 - 2m_a^2 - P^2) + \tilde{Q}^2 (m_a^2 + P^2) \right) \quad (5.78)$$

has to be included inside the "plus"-distribution. In fact, it is not necessary to compute the derivative $\frac{d\tilde{Q}^2}{dP^2}$ when we make the replacement $\tilde{Q}^2 \rightarrow Q^2$ within the parts of the plus-distribution that are proportional to the Dirac delta distribution. As long as this replacement is made consistently for the integral that results in the singular pieces and the counterpart in the plus-distribution itself, this choice must cancel out. For the special case $P^2 = 0$ the derivative y'_A simply evaluates to

$$y'_A \Big|_{P^2=0} = \mathcal{A}(0, Q^2) = \frac{m_a^2 - \bar{Q}^2}{Q^4}. \quad (5.79)$$

The integrated dipole I_{gg}^a can now be expressed as a distribution itself

$$I_{gg}^a(P^2, Q^2; \varepsilon) = [J_{gg}^a(P^2, Q^2)]_+ + 2\pi\delta(P^2) \left(J_{gg}^{a;S}(Q^2; \varepsilon) + J_{gg}^{a;NS}(Q^2) \right) + \mathcal{O}(\varepsilon) \quad (5.80)$$

with

$$[J_{gg}^a(P^2, Q^2)]_+ = C_A \Delta Q^2 \frac{P^2 - \bar{Q}^2}{\bar{Q}^2} \left(\frac{1}{6} \left[\frac{1}{P^2} \right]_{[0, P_0^2]}^+ (12 - R_{aj}^2) - [y'_A A \ln(1 + A)]_{[0, P_0^2]}^+ \frac{2A}{y'_A R_{aj}} \right). \quad (5.81)$$

The singular $J_{gg}^{a;S}$ and non-singular term $J_{gg}^{a;NS}$ arise from the expansion

$$J_{gg}^{a;S}(Q^2; \varepsilon) + J_{gg}^{a;NS}(Q^2) = \frac{C_A}{2\pi} \left(\frac{1}{\varepsilon} \left(\frac{\mu^2}{P_0^2} \right)^\varepsilon (2\beta(1 - \varepsilon, 1 - \varepsilon) - \beta(2 - \varepsilon, 2 - \varepsilon)) - 2\mu^{2\varepsilon} \mathcal{A}(0, Q^2)^\varepsilon \mathcal{I}_1(y_A^{\max}; \varepsilon) \right) + \mathcal{O}(\varepsilon) \quad (5.82)$$

with

$$y_A^{\max} = P_0^2 \mathcal{B}(P_0^2, Q^2). \quad (5.83)$$

The extraction of the collinear divergence for the case of a gluon splitting into a massless quark-antiquark pair proceeds as in the case of $Q \rightarrow gQ$ splitting

$$I_{Q\bar{Q}}^a(P^2, Q^2; \varepsilon) = [J_{Q\bar{Q}}^a(P^2, Q^2)]_+ + 2\pi\delta(P^2) \left(J_{Q\bar{Q}}^{a;S}(\varepsilon) + J_{Q\bar{Q}}^{a;NS} \right) \quad (5.84)$$

with

$$[J_{Q\bar{Q}}^a(P^2, Q^2)]_+ = \Delta Q^2 \frac{T_F}{2} \left[\frac{1}{P^2} \right]_{[0, P_0^2]}^+ \frac{\bar{Q}^2 - P^2}{\bar{Q}^2} \left(1 - \frac{1}{3} R_{aj}^2 \right). \quad (5.85)$$

In summary, the three different singular and non-singular contributions are

$$J_{gQ}^{a;S}(Q^2; \varepsilon) = \frac{C_F}{4\pi\varepsilon} \left(1 - \frac{1}{v} \ln(A + 1) \right) \quad (5.86)$$

$$J_{gQ}^{a;NS}(Q^2) = \frac{C_F}{2\pi} \frac{1}{v} \left((v - \ln(A + 1)) \ln \left(\frac{\mu m_j}{P_0^2 - m_j^2} \right) + v + \frac{1}{4} \ln^2(1 + A) + \text{Li}_2(-A) \right) \quad (5.87)$$

$$J_{gg}^{a;S}(Q^2; \varepsilon) = \frac{C_A}{2\pi} \left(\frac{1}{\varepsilon^2} + \frac{1}{6\varepsilon} \left(6 \ln \left(\frac{\mu^2(m_a^2 - \bar{Q}^2)}{\bar{Q}^4} \right) + 11 \right) \right) \quad (5.88)$$

$$J_{gg}^{a;NS}(Q^2) = \frac{C_A}{36\pi} \left(9 \ln^2 \left(\frac{\mu^2(m_a^2 - \bar{Q}^2)}{\bar{Q}^4} \right) + 33 \ln \left(\frac{\mu^2}{P_0^2} \right) + 36 \text{Li}_2 \left(-\frac{1}{y_A^{\max}} \right) + 67 - 3\pi^2 \right) \quad (5.89)$$

$$J_{Q\bar{Q}}^{a;S}(\varepsilon) = -\frac{T_F}{6\pi\varepsilon} \quad (5.90)$$

$$J_{Q\bar{Q}}^{a;NS} = -\frac{T_F}{18\pi} \left(5 + 3 \ln \left(\frac{\mu^2}{P_0^2} \right) \right) \quad (5.91)$$

with $v = \frac{\sqrt{\lambda_{aj}}}{-\bar{Q}^2}$. Recall that A is evaluated in eqs. (5.86) and (5.87) at $P^2 = m_j^2$ giving

$$A = \frac{2\sqrt{\lambda_{aj}}}{2m_j^2 - \bar{Q}^2 - \sqrt{\lambda_{aj}}}. \quad (5.92)$$

The same poles given in eq. (5.88) are found in [32] after translating the different dipole variables.

5.3 Initial-state emitter and final-state spectator

The dipole \mathcal{D}_j^{ai} is defined as

$$\mathcal{D}_j^{ai} = -\frac{1}{2p_a \cdot p_i} \frac{1}{x_{ij,a}} \left\langle \dots, \tilde{j}, \dots; \tilde{ai}, \dots \left| \frac{\mathbf{T}_j \cdot \mathbf{T}_i}{\mathbf{T}_{ai}^2} \mathbf{V}_j^{ai} \right| \dots, \tilde{j}, \dots; \tilde{ai}, \dots \right\rangle_{m, \tilde{ai}} \quad (5.93)$$

where \mathbf{V}_j^{ai} describes the splitting process $\tilde{ai} \rightarrow a + i$. The momentum of parton a in the tree level matrix element is replaced by the dipole momentum \tilde{p}_{ai} and the momentum of j is replaced by \tilde{p}_j . Throughout this section the initial parton a is treated as massive since the case $m_a = 0$ is already worked out in [28, 26].

5.3.1 Kinematics and phase space factorization

The case of an initial-state emitter and final-state spectator is kinematically identical to the case of a final-state emitter and an initial-state spectator after switching the roles played by \tilde{j} and a . Particle j takes over the role of the spectator and the associated dipole momenta are relabelled accordingly as $\tilde{p}_{ij} \rightarrow \tilde{p}_j$ and $\tilde{p}_a \rightarrow \tilde{p}_{ai}$. Therefore, the kinematics from section 5.2.1 can be adopted completely.

5.3.2 The dipole splitting functions

The function \mathbf{V}_j^{ai} in eq. (5.93) for the SUSY-QCD splitting process

- $\tilde{q} \rightarrow g(p_i) + \tilde{q}(p_a) : m_i = 0$ and $m_a = m_{\tilde{q}}$

in presence of a massive emitter \tilde{ai} was postulated in [1] and reads

$$\langle s | \mathbf{V}_j^{\tilde{q}g} | s' \rangle = 2g_s^2 C_F \mu^{2\varepsilon} \left(\frac{2}{2 - x_{ij,a} - z_j} - 2 - \frac{m_a^2 x_{ij,a}}{p_a \cdot p_i} \right) \delta_{ss'} = \langle \mathbf{V}_j^{\tilde{q}g} \rangle \delta_{ss'}. \quad (5.94)$$

5.3.3 The integrated dipole functions

The integral of the spin-averaged dipole function $\langle \mathbf{V}_j^{ai} \rangle$ over the dipole phase space is defined as

$$\frac{g_s^2}{2\pi} \frac{(4\pi)^\varepsilon}{\Gamma(1-\varepsilon)} I_j^{ai}(P^2, Q^2; \varepsilon) = \int [dp_i(Q^2, P^2, z_i)] \frac{1}{2p_a \cdot p_i} \frac{1}{x_{ij,a}} \langle \mathbf{V}_j^{ai} \rangle. \quad (5.95)$$

The cases of a massive spectator $m_j \neq 0$ and a massless spectator $m_j = 0$ have to be treated separately due to different kinds of singular behaviour. The integrated dipole for $m_j = 0$ is marked with a hat to distinguish it from the massive case. The integral in eq. (5.95) can be performed in straightforward manner through the hypergeometric and beta function given in appendix A.1

$$\begin{aligned} I_j^{\bar{q}g}(P^2, Q^2; \varepsilon) &= \frac{C_F}{\sqrt{\lambda_{aj}} R_{aj}} \frac{(m_a^2 + P^2 - Q^2)^{1+2\varepsilon}}{(P^2 - m_j^2)^{1+2\varepsilon}} \left(\frac{m_j^2 x_{ij,a} + \bar{Q}^2(x-1)}{-\bar{Q}^2} \right)^{2\varepsilon} \left(\frac{\mu^2}{P^2} \right)^\varepsilon \\ &\times \left(I_1(-A; \varepsilon) - x I_1(-B; \varepsilon) + 4m_a^2 x_{ij,a}^2 \frac{m_j^2 x_{ij,a} + \bar{Q}^2(x_{ij,a} - 1)}{\bar{Q}^4 - \lambda_{aj} R_{aj}^2} \left(\frac{\sqrt{\lambda_{aj}} R_{aj}}{\bar{Q}^2} - \varepsilon \ln(1+B) \right) \right) \end{aligned} \quad (5.96)$$

$$\hat{I}_j^{\bar{q}g}(P^2, Q^2; \varepsilon) = -\frac{C_F}{R_{aj}} \frac{\mu^{2\varepsilon}}{(P^2)^{1+\varepsilon}} \left(I_1(-B; \varepsilon) + \frac{P^2 - \bar{Q}^2}{\bar{Q}^2} I_1(-A; \varepsilon) - \frac{1}{2}(R_{aj} + 1) I_2(-B; \varepsilon) \right) \quad (5.97)$$

where the variable B is defined as

$$B = \frac{z_+ - z_-}{z_-} = \frac{-2\sqrt{\lambda_{aj}} R_{aj}}{\bar{Q}^2 + \sqrt{\lambda_{aj}} R_{aj}}. \quad (5.98)$$

In the massless case it can be written as

$$B = \frac{2\sqrt{1-u^2}}{1-\sqrt{1-u^2}} \quad (5.99)$$

with

$$u = \frac{2m_a \sqrt{P^2}}{P^2 - Q^2 + m_a^2}. \quad (5.100)$$

The variable A as well as the function $I_1(z; \varepsilon)$ were introduced in section 5.2.3. The functions $I_1(-A; \varepsilon)$ and $I_1(-B; \varepsilon)$ in eq. (5.96) have to be understood in terms of their expansion in ε since this explicit form was used to simplify the end result. The function

$$I_2(z; \varepsilon) = z \int_0^1 dt \frac{((1-t)t)^{-\varepsilon}}{(1-zt)^2} = z\beta(1-\varepsilon, 1-\varepsilon) {}_2F_1(2, 1-\varepsilon; 2-2\varepsilon; z) \quad (5.101)$$

$$= \frac{z}{1-z} + \varepsilon \frac{2-z}{z-1} \ln(1-z) + \mathcal{O}(\varepsilon^2) \quad (5.102)$$

is defined similarly to $I_1(z; \varepsilon)$ but with a different argument set of the hypergeometric function and the associated expansion is derived in appendix A.1.3. The extraction of the divergences in the massless case is as peculiar as in the case of the gluon splitting function. However,

it is possible to proceed in the same way. In fact, the divergent piece given by $I_1(-A; \varepsilon)$ in eq. (5.97) leads to the same integral $\mathcal{I}_1(y_A^{\max}; \varepsilon)$ already worked out in section 5.2.3. The poles that arise through $I_1(-B; \varepsilon)$ and $I_2(-B; \varepsilon)$ can now be disentangled in a very similar manner by introducing the variable

$$y_B = \frac{1}{B} = P^2 \mathcal{B}(P^2, Q^2) \quad (5.103)$$

as new integration variable. This factorization is achieved as in the case of A by expanding B written as in eq. (5.99) with $1 + \sqrt{1 - u^2}$ which yields

$$\mathcal{B}(P^2, Q^2) = \frac{2m_a^2}{(P^2 - \bar{Q}^2)\rho + \rho^2} \quad (5.104)$$

where ρ was defined in eq. (5.76). For the integration of the function $I_2(-B; \varepsilon)$ the integral

$$\mathcal{I}_2(y_0; \varepsilon) = \int_0^{y_0} dy \frac{1}{y^{1+\varepsilon}} I_2\left(-\frac{1}{y}; \varepsilon\right) = \frac{1}{2\varepsilon} + \ln\left(1 + \frac{1}{y_0}\right) + \mathcal{O}(\varepsilon) \quad (5.105)$$

is calculated in appendix A.1.4. Connected to the substitution from P^2 to y_B the derivative

$$y'_B = \frac{dy_B}{dP^2} = \frac{2m_a^2(P^2 + \bar{Q}^2)(2m_a^2 P^2 + (\bar{Q}^2 - P^2)(P^2 + \rho - \bar{Q}^2))}{\rho((P^2 - \bar{Q}^2)(P^2 + \rho - \bar{Q}^2) - 4m_a^2 P^2)^2} \quad (5.106)$$

is needed which simply evaluates to

$$\left. \frac{dy_B}{dP^2} \right|_{P^2=0} = \mathcal{B}(0, Q^2) = \frac{m_a^2}{Q^4} \quad (5.107)$$

for $P^2 = 0$. With the knowledge of the integrals \mathcal{I}_1 and \mathcal{I}_2 , the poles result from the expansion

$$\begin{aligned} \hat{J}_j^{\tilde{q}g;S}(Q^2; \varepsilon) + \hat{J}_j^{\tilde{q}g;NS}(Q^2) = & -\frac{C_F \mu^{2\varepsilon}}{2\pi} (\mathcal{B}(0, Q^2)^\varepsilon (\mathcal{I}_1(y_B^{\max}; \varepsilon) - \mathcal{I}_2(y_B^{\max}; \varepsilon)) \\ & - \mathcal{A}(0, Q^2)^\varepsilon \mathcal{I}_1(y_A^{\max}; \varepsilon)) + \mathcal{O}(\varepsilon). \end{aligned} \quad (5.108)$$

Now, we can shift the integration limits for Q^2 through the linear transformation $Q^2 \rightarrow \tilde{Q}^2$ as discussed in section 5.2.3 and perform the decomposition in terms of the "plus"-distribution

$$I_j^{\tilde{q}g}(P^2, Q^2; \varepsilon) = \left[J_j^{\tilde{q}g}(P^2, Q^2) \right]_+ + 2\pi\delta(P^2 - m_j^2) \left(J_j^{\tilde{q}g;S}(Q^2; \varepsilon) + J_j^{\tilde{q}g;NS}(Q^2) \right) + \mathcal{O}(\varepsilon) \quad (5.109)$$

$$\begin{aligned} \left[J_j^{\tilde{q}g}(P^2, Q^2) \right]_+ = & C_F \Delta Q^2 \left[\frac{1}{P^2 - m_j^2} \right]_{[m_j^2, P_0^2]}^+ \frac{m_a^2 + P^2 - \tilde{Q}^2}{\sqrt{\lambda_{aj}} R_{aj}} (x_{ij,a} \ln(1 + B) - \ln(1 + A)) \\ & + 4m_a^2 x_{ij,a}^2 \frac{m_j^2 x_{ij,a} + \tilde{Q}^2 (x_{ij,a} - 1)}{\tilde{Q}^4 - \lambda_{aj} R_{aj}^2} \frac{\sqrt{\lambda_{aj}} R_{aj}}{\tilde{Q}^2} \end{aligned} \quad (5.110)$$

$$\hat{I}_j^{\tilde{q}g}(P^2, Q^2; \varepsilon) = \left[\hat{J}_j^{\tilde{q}g}(P^2, Q^2) \right]_+ + 2\pi\delta(P^2) \left(\hat{J}_j^{\tilde{q}g;S}(Q^2; \varepsilon) + \hat{J}_j^{\tilde{q}g;NS}(Q^2) \right) \quad (5.111)$$

$$\begin{aligned} \left[\hat{J}_j^{\bar{q}g}(P^2, Q^2) \right]_+ = C_F \frac{\Delta Q^2}{R_{aj}} & \left(\left[y'_B B \ln(1+B) \right]_{[0, P_0^2]}^+ \frac{\mathcal{B}}{y'_B} + \left[y'_A A \ln(1+A) \right]_{[0, P_0^2]}^+ \mathcal{A} \frac{P^2 - \bar{Q}^2}{y'_A \bar{Q}^2} \right. \\ & \left. - \left[y'_B \frac{B^2}{1+B} \right]_{[0, P_0^2]}^+ \frac{\mathcal{B}}{2y'_B} (1 + R_{aj}) \right). \end{aligned} \quad (5.112)$$

The singular and non-singular contributions in the massive and massless case read

$$J_j^{\bar{q}g;S}(Q^2; \varepsilon) = \frac{C_F}{4\pi\varepsilon} \left(1 - \frac{1}{v} \ln \left(\frac{1+B}{1+A} \right) \right) \quad (5.113)$$

$$J_j^{\bar{q}g;NS}(Q^2) = \frac{C_F}{2\pi} \frac{1}{v} \left(\left(v + \ln \left(\frac{1+A}{1+B} \right) \right) \ln \left(\frac{\mu m_j}{P_0^2 - m_j^2} \right) + \frac{1}{2} \ln(1+B) \right) \quad (5.114)$$

$$+ \frac{1}{4} [\ln^2(1+B) - \ln^2(1+A)] + \text{Li}_2(-B) - \text{Li}_2(-A) \quad (5.115)$$

$$\hat{J}_j^{\bar{q}g;S}(Q^2; \varepsilon) = \frac{C_F}{4\pi\varepsilon} \left(1 - \ln \left(\frac{m_a^2 - \bar{Q}^2}{m_a^2} \right) \right) \quad (5.116)$$

$$\hat{J}_j^{\bar{q}g;NS}(Q^2) = \frac{C_F}{2\pi} \left(\frac{1}{4} \ln^2 \left(\frac{\mu^2 m_a^2}{\bar{Q}^4} \right) + \ln \left(-\frac{\mu m_a}{\bar{Q}^2} \right) - \frac{1}{4} \ln^2 \left(\frac{\mu^2 (m_a^2 - \bar{Q}^2)}{\bar{Q}^4} \right) \right) \quad (5.117)$$

$$- \text{Li}_2 \left(-\frac{1}{y_A^{\max}} \right) + \text{Li}_2 \left(-\frac{1}{y_B^{\max}} \right) + \ln \left(1 + \frac{1}{y_B^{\max}} \right) \quad (5.118)$$

with the maximum value

$$y_B^{\max} = P_0^2 \mathcal{B}(P_0^2, Q^2). \quad (5.119)$$

5.4 Initial-state emitter and initial-state spectator

The dipole for emitter and spectator both from the initial state is defined as

$$\mathcal{D}^{ai,b} = \frac{1}{-2p_a \cdot p_i} \frac{1}{x_{i,ab}} \left\langle \tilde{1}, \dots, \widetilde{m+1}; \tilde{ai}, b \left| \frac{\mathbf{T}_b \cdot \mathbf{T}_{ai}}{\mathbf{T}_{ai}^2} \mathbf{V}^{ai,b} \right| \tilde{1}, \dots, \widetilde{m+1}; \tilde{ai}, b \right\rangle_{m,ab}. \quad (5.120)$$

The m -particle matrix element is obtained by discarding the parton i in the $(m+1)$ -parton element and replacing all other partons except for the spectator b .

5.4.1 Kinematics and phase space factorization

For the description of the dipole kinematics the same quantities as in [29] are used. The divergences are parameterized in terms of the variables

$$x_{i,ab} = \frac{p_a \cdot p_b - p_i \cdot p_a - p_i \cdot p_b}{p_a \cdot p_b} \quad (5.121)$$

$$y_{ab} = \frac{p_a \cdot p_i}{p_a \cdot p_b} \quad (5.122)$$

which behave in the soft limit $p_i^\mu \rightarrow 0$ as

$$x_{i,ab} \rightarrow 1, \quad y_{ab} \rightarrow 0. \quad (5.123)$$

The sum of all outgoing momenta p_k except for the soft gluon is denoted as

$$P_{ab} = p_a + p_b - p_i = \sum_k p_k. \quad (5.124)$$

Furthermore, it is convenient to define the auxiliary variables

$$\lambda_{ab} = \lambda(s, m_a^2, m_b^2) = \bar{s}^2 - 4m_a^2 m_b^2 \quad (5.125)$$

$$\bar{s} = s - m_a^2 - m_b^2. \quad (5.126)$$

The construction of the dipole momenta is different from the previous two cases. Instead of modifying only the momenta of emitter and spectator, the momentum of the spectator p_b remains unchanged whereas all other momenta are modified. The new momenta

$$\tilde{p}_{ai}^\mu = \sqrt{\frac{\lambda(P_{ab}^2, m_a^2, m_b^2)}{\lambda_{ab}}} p_a^\mu + \left(\frac{P_{ab}^2 - m_a^2 - m_b^2}{2m_b^2} - \frac{p_a \cdot p_b}{m_b^2} \sqrt{\frac{\lambda(P_{ab}^2, m_a^2, m_b^2)}{\lambda_{ab}}} \right) p_b^\mu \quad (5.127)$$

$$\tilde{P}_{ab}^\mu = \tilde{p}_{ai}^\mu + p_b^\mu \quad (5.128)$$

are build from the requirement to retain the mass-shell relations $\tilde{p}_a^2 = m_a^2$ and $\tilde{P}_{ab}^2 = P_{ab}^2$. The outgoing momenta p_k except for p_i are modified by a Lorentz transformation

$$\tilde{p}_k^\mu = \Lambda^\mu{}_\nu p_k^\nu \quad (5.129)$$

with

$$\Lambda^\mu{}_\nu = g^\mu{}_\nu - \frac{(P_{ab} + \tilde{P}_{ab})^\mu (P_{ab} + \tilde{P}_{ab})_\nu}{P_{ab}^2 + P_{ab} \cdot \tilde{P}_{ab}} + \frac{2\tilde{P}_{ab}^\mu P_{ab,\nu}}{P_{ab}^2}. \quad (5.130)$$

It follows from direct calculation that $\Lambda^\mu{}_\nu$ indeed leaves the Minkowski metric invariant $\Lambda_\rho{}^\mu \Lambda^{\rho\nu} = g^{\mu\nu}$ such that it can be verified easily that the new momenta \tilde{p}_k obey the on-shell condition $\tilde{p}_k^2 = m_k^2$. In order to ensure that $\lambda(P_{ab}^2, m_a^2, m_b^2)$ remains positive, so that the dipole momenta take only real values, the kinematical lower bound

$$x_{i,ab} > x_0 \geq \hat{x} = \frac{2m_a m_b}{\bar{s}} \quad (5.131)$$

has to be enforced. For values of $x_{i,ab}$ below \hat{x} the splitting functions $\mathbf{V}^{ai,b}$ are set to zero. The dependence on the lower bound x_0 must cancel out and can therefore be chosen arbitrarily which offers the possibility to check whether the implementation of the subtraction procedure is correct. Following again the work of Dittmaier [29] where a photon mass is used as regulator, the phase space factorization is performed in dimensional regularization in [1]. For $D = 4 - 2\varepsilon$ dimensions the dipole phase space then becomes

$$\int [dp_i(s, x, y_{ab})] = \frac{\bar{s}^{2-2\varepsilon}}{(4\pi)^{2-\varepsilon} \Gamma(1-\varepsilon)} \frac{s^{-\varepsilon}}{\sqrt{\lambda_{ab}}^{1-2\varepsilon}} \int_{y_-}^{y_+} dy_{ab} [(y_{ab} - y_-)(y_+ - y_{ab})]^{-\varepsilon} \quad (5.132)$$

with the integration boundaries

$$y_\pm = \frac{1-x}{2s} \left(\bar{s} + 2m_a^2 \pm \sqrt{\lambda_{ab}} \right). \quad (5.133)$$

5.4.2 The dipole splitting function

The dipole function $\mathbf{V}^{ai,b}$ in eq. (5.120) for the SUSY-QCD process

- $\tilde{q} \rightarrow \tilde{q}(p_a) + g(p_i) : m_i = 0 \text{ and } m_{ai} = m_a = m_{\tilde{q}}$

was derived in [1] and reads explicitly

$$\langle \mathbf{V}^{\tilde{q}g,b} \rangle = 2g_s^2 \mu^{2\varepsilon} C_F \left(\frac{2}{1 - x_{i,ab}} - 2 - \frac{x_{i,ab} m_a^2}{p_a \cdot p_i} \right). \quad (5.134)$$

The same splitting function holds if the squark is replaced by an antisquark which is why the associated conjugated process is not listed separately.

5.4.3 The integrated dipole functions

In complete analogy to previous cases, the integrated dipole for the case of emitter and spectator both from the initial state is defined as

$$\frac{g_s^2}{2\pi} \frac{(4\pi)^\varepsilon}{\Gamma(1-\varepsilon)} I^{ai,b}(x; \varepsilon) = \int [dp_i(s, x, y_{ab})] \frac{1}{2p_a \cdot p_i} \frac{1}{x_{i,ab}} \langle \mathbf{V}^{ai,b} \rangle \quad (5.135)$$

and the factorized phase space of the gluon can be turned into the convenient form

$$\int_{y_-}^{y_+} dy_{ab} [(y_{ab} - y_-)(y_+ - y_{ab})]^{-\varepsilon} = (y_+ - y_-)^{1-2\varepsilon} \int_0^1 dt [(1-t)t]^{-\varepsilon} \quad (5.136)$$

via the substitution $t = \frac{y_{ab} - y_-}{y_+ - y_-}$. By expressing the denominator in the dipole as $p_a \cdot p_i = y_{ab} \bar{s}/2$ and with the help of the already known integrals $I_1(z; \varepsilon)$ and $I_2(z; \varepsilon)$ defined in eq. (5.59) and eq. (5.102), the integration of the splitting function in eq. (5.134) is straightforward

$$I^{\tilde{q}g,b}(x; \varepsilon) = \frac{C_F}{2\pi} \frac{1}{\sqrt{\lambda_{ab}}} \frac{1}{(1-x)^{1+2\varepsilon}} \left(\frac{\mu^2 s}{\bar{s}^2} \right)^\varepsilon \left(\bar{s} I_1(-C; \varepsilon) - \frac{2m_a^2 s}{d_1} I_2(-C; \varepsilon) \right) \quad (5.137)$$

where the new auxiliary variables d_1 and C are defined as

$$C = \frac{y_+ - y_-}{y_-} = \frac{2\sqrt{\lambda_{ab}}}{d_1} \quad (5.138)$$

$$d_1 = \bar{s} + 2m_a^2 - \sqrt{\lambda_{ab}}. \quad (5.139)$$

Since only massive initial states are considered, the argument C of the hypergeometric functions hidden inside I_1 and I_2 does not diverge and we are allowed to use their associated expansions in ε . As it should be familiar now from section 5.2.3, the soft divergence can be disentangled with the help of the $[\dots]^+$ -prescription

$$I^{\tilde{q}g,b}(x; \varepsilon) = \left[J^{\tilde{q}g,b}(x) \right]_+ + \delta(1-x) \left[J^{\tilde{q}g,b;S}(\varepsilon) + J^{\tilde{q}g,b;NS} \right] + \mathcal{O}(\varepsilon). \quad (5.140)$$

The finite part that contains the "plus"-distribution is then given by

$$\left[J^{\tilde{q}g,b}(x) \right]_+ = \frac{C_F}{2\pi} \left[\frac{1}{1-x} \right]_{[1,x_0]}^+ (1 - d_2 \ln(1+C)) \quad (5.141)$$

and the singular terms originate from the expansion

$$\begin{aligned} J^{\tilde{q}g,b;S}(\varepsilon) + J^{\tilde{q}g,b;NS} &= \tilde{I}^{\tilde{q}g,b}(1;\varepsilon) \int_{x_0}^1 dx \frac{1}{(1-x)^{1+2\varepsilon}} \\ &= \left(-\frac{1}{2\varepsilon} + \ln(1-x_0) \right) \tilde{I}^{\tilde{q}g,b}(1;\varepsilon) + \mathcal{O}(\varepsilon) \end{aligned} \quad (5.142)$$

with $(1-x)^{-1-2\varepsilon} \tilde{I}^{\tilde{q}g,b}(x;\varepsilon) = I^{\tilde{q}g,b}(x;\varepsilon)$ which gives

$$J^{\tilde{q}g,b;S}(\varepsilon) = \frac{C_F}{4\pi\varepsilon} (1 - d_2 \ln(1+C)) \quad (5.143)$$

$$J^{\tilde{q}g,b;NS} = \frac{C_F}{4\pi} \left(\frac{1}{C} \ln(1+C) (C+2) + \frac{d_2}{2} (4 \text{Li}_2(-C) + \ln^2(1+C)) \right. \quad (5.144)$$

$$\left. + (1 - d_2 \ln(1+C)) \ln \left(\frac{\mu^2 s}{\bar{s}^2 (1-x_0)^2} \right) \right) \quad (5.145)$$

with

$$d_2 = \frac{\bar{s}}{\sqrt{\lambda_{ab}}}. \quad (5.146)$$

5.5 Final-state emitter and final-state spectator

Since the mass of the initial particles does not influence the splitting behaviour, the case of emitter and spectator both from the final state is already fully covered for the massless and massive case in works by Catani and Seymour [28, 26].

5.6 Comparison with the phase space slicing method

In an earlier DM@NLO work [33, 34] the NLO corrections to neutralino-stop coannihilation processes were performed where the phase space slicing method was used to render the cross section σ^{NLO} IR finite. The presence of this alternative method for the infrared treatment offers the possibility to compare the newly worked out dipole subtraction method for massive initial states against the results from phase space slicing.

Within the phase space slicing approach the three particle phase space is split into a hard and a soft part by imposing a cutoff δ_s on the energy of the radiated gluon

$$\sigma^{\text{R}} = \sigma^{\text{hard}}(\delta_s) + \sigma^{\text{soft}}(\delta_s) \quad (5.147)$$

such that the real emission cross section σ^{R} is split into a finite part $\sigma^{\text{hard}}(\delta_s)$ which is safe for numerical evaluation in $D = 4$ dimensions and a divergent piece $\sigma^{\text{soft}}(\delta_s)$ which has to be integrated analytically in $D = 4 - 2\varepsilon$ dimensions to isolate the infrared poles in ε . The latter is made possible by usage of the eikonal (or soft) approximation. If the process contains another massless particle, there can also occur collinear divergences. In this case the two cutoff method was employed which introduces an additional collinear cutoff δ_c on the angle between the two massless particles so that the hard phase space region is split further into a hard and collinear and a hard and non-collinear part

$$\sigma^{\text{R}} = \sigma_{\text{coll}}^{\text{hard}}(\delta_s, \delta_c) + \sigma_{\text{non-coll}}^{\text{hard}}(\delta_s, \delta_c) + \sigma^{\text{soft}}(\delta_s). \quad (5.148)$$

The dipole subtraction method is implemented on top of the existing code for neutralino-stop coannihilation `NeuQ2qx`. The processes $\tilde{\chi}_1^0 \tilde{t}_1 \rightarrow th/H$ as well as $\tilde{\chi}_1^0 \tilde{t}_1 \rightarrow tg$ are chosen for the comparison. The first case is simpler since it involves only two dipoles where both the emitter and spectator are massive whereas the latter requires twelve dipoles in total and in addition features the more complicated case of a gluon as emitter.

$\tan \beta$	μ	m_A	M_1	M_2	M_3	$M_{\tilde{q}_{1,2}}$	$M_{\tilde{g}_3}$	$M_{\tilde{u}_3}$	$M_{\tilde{\ell}}$	A_t
5.8	2925.8	948.8	335.0	1954.1	1945.6	3215.1	1578.0	609.2	3263.9	3033.7

Table 5.1: Parameters for the example scenario in the pMSSM examined in [34]. All quantities except $\tan \beta$ are given in GeV.

$m_{\tilde{\chi}_1^0}$	338.3 GeV
$m_{\tilde{t}_1}$	375.6 GeV
m_{h^0}	122.0 GeV
m_{H^0}	942.7 GeV

Table 5.2: Physical neutralino, stop, and Higgs masses computed with `SPheno 3.2.3` [9].

For the numerical study the example scenario in the pMSSM shown in table 5.1 is used. The associated physical mass spectrum is computed with `SPheno 3.2.3` [9] and the masses relevant for the examined processes are displayed in table 5.2. All parameters that go into the calculation are defined at the scale $\mu_R = Q_{\text{SUSY}} = 1 \text{ TeV}$. The cutoffs $p_2^0, p_3^0 \geq \delta_s = 3.0 \cdot 10^{-4} \sqrt{s}$ and $2p_2 \cdot p_3 \geq \delta_c = 3.0 \cdot 10^{-5} s$ are chosen as in [34] where \sqrt{s} denotes the center-of-mass energy. More details on the implementation of the dipole method for the selected processes as well as the results of the comparison are provided in the next two subsections devoted to respective processes.

5.6.1 Processes with a Higgs boson in the final state

A generic real emission diagram for the coannihilation process with a light CP -even Higgs h^0 or a heavy Higgs H^0 is shown in fig. 5.2.

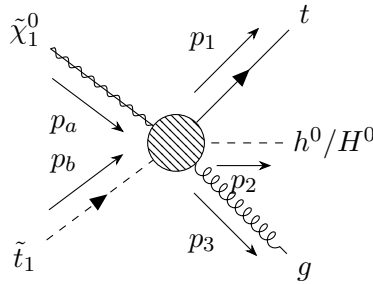


Figure 5.2: Generic real emission diagram for the processes $\tilde{\chi}_1^0 \tilde{t}_1 \rightarrow th$ and $\tilde{\chi}_1^0 \tilde{t}_1 \rightarrow tH$. The four-momenta are explicitly labelled.

According to the dipole factorization formula, the integral over the three particle phase space is rendered finite by constructing the auxiliary cross section from the two dipoles \mathcal{D}_{31}^b and \mathcal{D}_1^{b3} . For a process with two coloured particles, the identity

$$\mathbf{T}_1 \cdot \mathbf{T}_2 |1, 2\rangle = -\mathbf{T}_1^2 |1, 2\rangle = -\mathbf{T}_2^2 |1, 2\rangle \quad (5.149)$$

follows from colour conservation and makes the colour algebra trivial in this case. The expressions for the dipoles read

$$\mathcal{D}_{31}^b = \frac{1}{2p_1 \cdot p_3} \frac{1}{x_{31,b}} \langle \mathbf{V}_{g_3 t_1}^b \rangle |\mathcal{M}_2(\tilde{p}_b, \tilde{p}_{31})|^2 \quad (5.150)$$

$$\mathcal{D}_1^{b3} = \frac{1}{2p_b \cdot p_3} \frac{1}{x_{31,b}} \langle \mathbf{V}_1^{\tilde{t}_1, b g_3} \rangle |\mathcal{M}_2(\tilde{p}_{b3}, \tilde{p}_1)|^2 \quad (5.151)$$

where the Mandelstam variables s , t and u in the existing LO matrix element $|\mathcal{M}_2(p_{\tilde{t}_1}, p_t)|^2$ are replaced by the "dipole Mandelstam invariants"

$$\tilde{s} = (p_a + \tilde{p}_b)^2 \quad (5.152)$$

$$\tilde{t} = (\tilde{p}_b - p_2)^2 \quad (5.153)$$

$$\tilde{u} = (p_a - p_2)^2. \quad (5.154)$$

The explicit expression for $d\sigma^A$ is given by

$$\int_3 d\sigma^A = \frac{1}{2N_c F} \int d\Phi_3 \left(\mathcal{D}_{31}^b + \mathcal{D}_1^{b3} \right) \theta(x - x_0) \quad (5.155)$$

with the averaging factor $2N_c$ for initial colours and spins. The Heaviside function ensures that the auxiliary variable x is greater than x_0 where in this case the subscripts on x were dropped since both dipoles defined in eq. (5.150) and eq. (5.151) share the same kinematic quantities. The IR divergences appearing in the virtual corrections are cancelled by

$$\begin{aligned} \int_3 d\sigma^A &= \frac{1}{2N_c F} \int d\Phi_2 \left(\frac{g_s^2}{2\pi} |\mathcal{M}_2|^2 \left(J_{gt}^{\tilde{t}_1;S}(u; \varepsilon) + J_{gt}^{\tilde{t}_1;NS}(u) + J_t^{\tilde{t}_1 g;S}(u; \varepsilon) + J_t^{\tilde{t}_1 g;NS}(u) \right) \right. \\ &\quad + \frac{g_s^2}{4\pi N_c F} \int_{m_t^2}^{(\sqrt{s} - m_h/H)^2} \frac{dP^2}{2\pi} \int d\Phi_2(P^2, Q^2) \left[\frac{1}{P^2 - m_t^2} \right]_{[m_t^2, P_0^2]}^+ \Delta Q^2 \theta(x - x_0) \\ &\quad \times \left(\tilde{I}_{gt}^{\tilde{t}_1}(P^2, \tilde{Q}^2; 0) + \tilde{I}_t^{\tilde{t}_1 g}(P^2, \tilde{Q}^2; 0) \right) \left| \mathcal{M}_2(P^2, \tilde{Q}^2) \right|^2 \end{aligned} \quad (5.156)$$

where ΔQ^2 and \tilde{Q}^2 were introduced in eqs. (5.70) and (5.71). At this point it is appropriate to highlight the limits

$$\lim_{P^2 \rightarrow m_t^2} \Delta Q^2 = 1 \quad \lim_{P^2 \rightarrow m_t^2} \tilde{Q}^2 = Q^2 \quad \lim_{P^2 \rightarrow m_t^2} \left| \mathcal{M}_2(P^2, \tilde{Q}^2) \right|^2 = |\mathcal{M}_2|^2 \quad (5.157)$$

which are relevant for the implementation of the "plus"-distribution. In eq. (5.156) $|\mathcal{M}_2|^2$ denotes the ordinary LO matrix element depending on s , t and u . The dependence of P^2 and \tilde{Q}^2 in the tree matrix element $\left| \mathcal{M}_2(P^2, \tilde{Q}^2) \right|^2$ enters through the dipole momenta \tilde{p}_b and \tilde{p}_{13} .

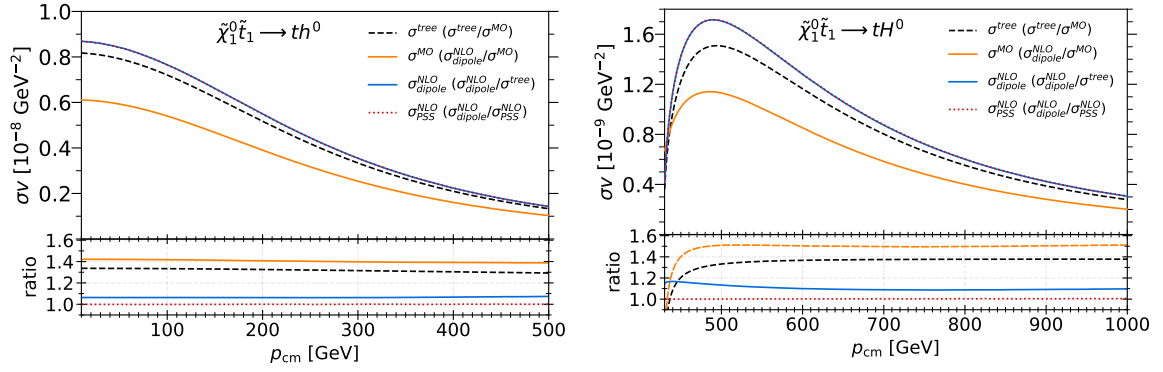


Figure 5.3: Tree-level cross section (black dashed line), full one-loop cross section obtained with phase space slicing (red dotted line) and with the dipole method (blue solid line) as well as the **micrOMEGAs** cross section (orange solid line) for the coannihilation processes with a Higgs in the final state. The upper part of each plot shows the absolute value of σv , whereas the lower part compares the different cross sections (second item in the legend).

Figure 5.3 shows the tree level cross section computed with **DM@NLO** and **CalcHEP** through **micrOMEGAs** as well as the NLO corrected cross section obtained with both methods - phase space slicing and the dipole subtraction method. The two free parameters x_0 and P_0^2 introduced in the dipole method are chosen to be $x_0 = 0.9$ and $P_0^2 = (\sqrt{s} - m_{h/H})^2$ where it was sufficiently checked that the final result is independent of these two values. The relative difference between the two methods is less than 1% and, thus, the dipole method verifies the cutoff choice made in [34] and the results for the cross section with a Higgs in the final state. The relative small difference of around 10% between the **DM@NLO** result and the tree cross section provided by **micrOMEGAs** is due to the fact that **DM@NLO** uses the on-shell mass $m_t^{\text{OS}} = 173.3 \text{ GeV}$ of the top quark, whereas **micrOMEGAs** takes the $\overline{\text{DR}}$ -mass $m_t^{\overline{\text{DR}}} = 161.6 \text{ GeV}$ in account. In table 5.3 some values for $\Delta\sigma^{\text{NLO}}$ obtained with the phase space slicing and dipole method are shown. The difference between the two methods is in the same order of

	$v\Delta\sigma^{\text{NLO}} [10^{-8} \text{ GeV}^{-2}]$		
$p_{\text{cm}} [\text{GeV}]$	dipole method	phase space slicing	$(\Delta\sigma_{\text{dipole}}^{\text{NLO}} - \Delta\sigma_{\text{PSS}}^{\text{NLO}})/\Delta\sigma_{\text{PSS}}^{\text{NLO}} [\%]$
10	0.05186	0.05096	1.8
100	0.04543	0.04446	2.2
250	0.02594	0.02569	1.0
500	0.00977	0.00985	-0.8

Table 5.3: Comparison of the $\mathcal{O}(\alpha_s)$ QCD corrections to the process $\tilde{\chi}_1^0 \tilde{t}_1 \rightarrow t h^0$ between the dipole and the phase space slicing (PSS) method.

magnitude as in [29].

5.6.2 Processes with a gluon in the final state

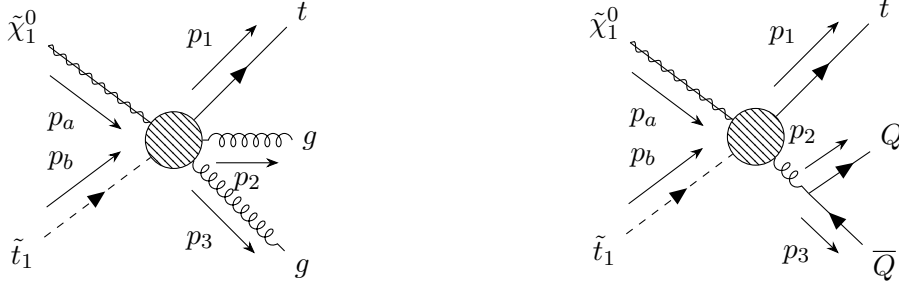


Figure 5.4: Generic real emission diagrams for the process $\tilde{\chi}_0^1 \tilde{t}_1 \rightarrow tg$.

At NLO the two real emission processes shown in fig. 5.4 contribute to $\tilde{\chi}_0^1 \tilde{t}_1 \rightarrow tg$. Besides the emission of another gluon also the decay of gluon into a pair of massless quarks leads to additional collinear divergences which cancel those singularities that appear through massless quarks running in a loop within the virtual corrections. In **DM@NLO** the first four quark flavours $N_f = 4$ are considered massless to avoid quasi-collinear divergences (large logarithms) which compromise the numerical stability.

For a process involving three coloured particles the different colour projections fully factorize in terms of the associated Casimirs and it is not necessary to calculate any colour-correlated tree amplitude thanks to the relation

$$2\mathbf{T}_2 \cdot \mathbf{T}_3 |1, 2, 3\rangle = (\mathbf{T}_1^2 - \mathbf{T}_2^2 - \mathbf{T}_3^2) |1, 2, 3\rangle \quad (5.158)$$

which holds analogously for $\mathbf{T}_1 \cdot \mathbf{T}_3$ and $\mathbf{T}_1 \cdot \mathbf{T}_2$. The factorization formula yields a total of ten dipoles to compensate all infrared divergences in the three-particle phase space

$$\mathcal{D}_{31,2} = \frac{1}{2p_1 \cdot p_3} \frac{C_A}{2C_F} \langle \mathbf{V}_{g_3 t_1, 2} \rangle |\mathcal{M}_2(p_b, \tilde{p}_{31}, \tilde{p}_2)|^2 \quad (5.159)$$

$$\mathcal{D}_{21,3} = \frac{1}{2p_1 \cdot p_2} \frac{C_A}{2C_F} \langle \mathbf{V}_{g_2 t_1, 3} \rangle |\mathcal{M}_2(p_b, \tilde{p}_{21}, \tilde{p}_3)|^2 \quad (5.160)$$

$$\mathcal{D}_{23,1} = \frac{1}{2p_2 \cdot p_3} \frac{1}{2} \langle \mu | \mathbf{V}_{g_2 g_3, 1} | \nu \rangle \mathcal{T}_{\mu\nu}(p_b, \tilde{p}_1, \tilde{p}_{23}) \quad (5.161)$$

$$\mathcal{D}_{23}^b = \frac{1}{2p_2 \cdot p_3} \frac{1}{x_{23,b}} \frac{1}{2} \langle \mu | \mathbf{V}_{g_2 g_3}^b | \nu \rangle \mathcal{T}_{\mu\nu}(\tilde{p}_b, p_1, \tilde{p}_{23}) \quad (5.162)$$

$$\mathcal{D}_{31}^b = \frac{1}{2p_1 \cdot p_3} \frac{1}{x_{31,b}} \left(1 - \frac{C_A}{2C_F}\right) \langle \mathbf{V}_{g_3 t_1}^b \rangle |\mathcal{M}_2(\tilde{p}_b, \tilde{p}_{31}, p_2)|^2 \quad (5.163)$$

$$\mathcal{D}_{21}^b = \frac{1}{2p_1 \cdot p_2} \frac{1}{x_{21,b}} \left(1 - \frac{C_A}{2C_F}\right) \langle \mathbf{V}_{g_2 t_1}^b \rangle |\mathcal{M}_2(\tilde{p}_b, \tilde{p}_{21}, p_3)|^2 \quad (5.164)$$

$$\mathcal{D}_2^{b3} = \frac{1}{2p_b \cdot p_3} \frac{1}{x_{32,b}} \frac{C_A}{2C_F} \langle \mathbf{V}_2^{\tilde{t}_1, b g_3} \rangle |\mathcal{M}_2(\tilde{p}_{b3}, p_1, \tilde{p}_2)|^2 \quad (5.165)$$

$$\mathcal{D}_3^{b2} = \frac{1}{2p_b \cdot p_2} \frac{1}{x_{23,b}} \frac{C_A}{2C_F} \langle \mathbf{V}_3^{\tilde{t}_1, b g_2} \rangle |\mathcal{M}_2(\tilde{p}_{b2}, p_1, \tilde{p}_3)|^2 \quad (5.166)$$

$$\mathcal{D}_1^{b3} = \frac{1}{2p_b \cdot p_3} \frac{1}{x_{31,b}} \left(1 - \frac{C_A}{2C_F}\right) \langle \mathbf{V}_1^{\tilde{t}_1, b g_3} \rangle |\mathcal{M}_2(\tilde{p}_{b3}, \tilde{p}_1, p_2)|^2 \quad (5.167)$$

$$\mathcal{D}_1^{b2} = \frac{1}{2p_b \cdot p_2} \frac{1}{x_{21,b}} \left(1 - \frac{C_A}{2C_F}\right) \langle \mathbf{V}_1^{\tilde{t}_1, b g_2} \rangle |\mathcal{M}_2(\tilde{p}_{b2}, \tilde{p}_1, p_3)|^2 \quad (5.168)$$

with the tree level matrix element $|\mathcal{M}_2(p_{\tilde{t}_1}, p_t, p_g)|^2$. The tensor $\mathcal{T}_{\mu\nu}$ corresponds to the LO squared amplitude where the polarization vector $\epsilon_\lambda^\mu(\tilde{p}_{ij})$ of the emitter gluon has been amputated. To cancel the collinear divergences from the production of N_f massless quark-antiquark pairs the dipoles

$$\mathcal{D}_{23,1} = \frac{1}{2p_2 \cdot p_3} \frac{1}{2} \langle \mu | \mathbf{V}_{Q_2 \bar{Q}_3,1} | \nu \rangle \mathcal{T}_{\mu\nu}(p_b, \tilde{p}_{23}, \tilde{p}_1) \quad (5.169)$$

$$\mathcal{D}_{23}^b = \frac{1}{2p_2 \cdot p_3} \frac{1}{x_{23,b}} \frac{1}{2} \langle \mu | \mathbf{V}_{Q_2 \bar{Q}_3}^b | \nu \rangle \mathcal{T}_{\mu\nu}(\tilde{p}_b, p_1, \tilde{p}_{23}) \quad (5.170)$$

are needed. Due to different kinematics it is no longer possible to give a single set of "dipole Mandelstams" for all dipoles compared to $\tilde{\chi}_0^1 \tilde{t}_1 \rightarrow th^0$. However, one can group together dipoles with the same kinematics and form the associated invariants \tilde{s} , \tilde{t} and \tilde{u} which is done in table 5.4.

$\mathcal{D}_{21}^b, \mathcal{D}_1^{b2}$	$\mathcal{D}_{31}^b, \mathcal{D}_1^{b3}$	$\mathcal{D}_{23}^b, \mathcal{D}_3^{b2}, \mathcal{D}_2^{b3}$
$\tilde{s} = (\tilde{p}_b + p_a)^2$	$\tilde{s} = (\tilde{p}_b + p_a)^2$	$\tilde{s} = (\tilde{p}_b + p_a)^2$
$\tilde{t} = (\tilde{p}_b - p_3)^2$	$\tilde{t} = (\tilde{p}_b - p_2)^2$	$\tilde{t} = (p_a - p_1)^2$
$\tilde{u} = (p_a - p_3)^2$	$\tilde{u} = (p_a - p_2)^2$	$\tilde{u} = (\tilde{p}_b - p_1)^2$
$\mathcal{D}_{31,2}$	$\mathcal{D}_{21,3}$	$\mathcal{D}_{23,1}$
$\tilde{s} = (p_a + p_b)^2$	$\tilde{s} = (p_a + p_b)^2$	$\tilde{s} = (p_a + p_b)^2$
$\tilde{t} = (p_b - \tilde{p}_2)^2$	$\tilde{t} = (p_b - \tilde{p}_3)^2$	$\tilde{t} = (p_a - \tilde{p}_1)^2$
$\tilde{u} = (p_a - \tilde{p}_2)^2$	$\tilde{u} = (p_a - \tilde{p}_3)^2$	$\tilde{u} = (p_b - \tilde{p}_1)^2$

Table 5.4: "Dipole Mandelstam invariants" for six different kinematical configurations that can be distinguished for the process $\tilde{\chi}_0^1 \tilde{t}_1 \rightarrow tg$.

For the $g \rightarrow Q\bar{Q}$ dipoles $\mathcal{D}_{23,1}$ and \mathcal{D}_{23}^b in eqs. (5.169) and (5.170) the same dipole Mandelstam variables apply as for their $g \rightarrow gg$ counterparts. Since we compute a sufficiently inclusive cross section, it is not necessary to evaluate the helicity correlation for the dipoles which involve a gluon emitter explicitly. For example, the factorization

$$\mathcal{D}_{23,1} = \frac{1}{2p_2 \cdot p_3} \frac{1}{2} \langle \mathbf{V}_{g_2 g_3,1} | \mathcal{M}_2(p_b, \tilde{p}_1, \tilde{p}_{23}) |^2 \quad (5.171)$$

in terms of the averaged splitting function leads to the same results as using eq. (5.161). Compared to the Higgs in the final state, this real emission process features two identical particles in the final state. That's why each real emission diagram with two gluons in the final state carries an additional Bose symmetry factor $S_3 = \frac{1}{2}$. In order to construct the auxiliary matrix element for the virtual corrections from the dipoles, we have to count the symmetry factors for the transition from two to one gluon³. The dipoles that are related through the exchange of an emitted gluon result in the same integrated dipole. Thus, the symmetry factor S_3 gets cancelled in all cases except for the dipoles describing $g \rightarrow gg$ splitting $\mathcal{D}_{23,1}$ and \mathcal{D}_{23}^b .

³The counting of symmetry factors for the general case of going from $m+1$ to m partons is discussed extensively in [28].

Since this process furnishes double poles, another important aspect is the definition of the poles. In **DMONLO** every pole is defined with the prefactor $c_\varepsilon = (4\pi)^\varepsilon \Gamma(1+\varepsilon)$ which leads to an additional finite term in the presence of double poles through the expansion

$$\frac{1}{\Gamma(1-\varepsilon)\Gamma(1+\varepsilon)} = 1 - \frac{\pi^2 \varepsilon^2}{6} + \mathcal{O}(\varepsilon^3). \quad (5.172)$$

We are now ready to construct the auxiliary matrix element that cancels the infrared divergences of the virtual one-loop correction

$$\begin{aligned} |\mathcal{M}_{2 \rightarrow 2}^A|^2 = \frac{g_s^2}{16\pi^2} |\mathcal{M}_2|^2 & \left[C_A \left(2\mathcal{V}^{(S)}(s_{12}, m_t, 0; \varepsilon) + \mathcal{V}_g^{(\text{NS})}(s_{12}, 0, m_t; \kappa) + \mathcal{V}_t^{(\text{NS})}(s_{12}, m_t, 0) \right) \right. \\ & + \Gamma_g(\varepsilon) + \gamma_g \ln \left(\frac{\mu^2}{s_{jk}} \right) + \gamma_g + K_g + C_A \left(\frac{1}{C_F} \Gamma_t(\varepsilon) + \frac{3}{2} \ln \left(\frac{\mu^2}{s_{12}} \right) + 5 - \frac{5\pi^2}{6} \right) \\ & + \frac{g_s^2}{2\pi} |\mathcal{M}_2|^2 \left[\frac{1}{4} \left(J_{gg}^{\tilde{t}1;S}(t; \varepsilon) + J_{gg}^{\tilde{t}1;NS}(t) - \frac{C_A \pi}{12} - \frac{C_A}{12\pi} \right) + \frac{N_f}{2} \left(J_{Q\bar{Q}}^{\tilde{t}1;S} + J_{Q\bar{Q}}^{\tilde{t}1;NS} \right) \right. \\ & + \frac{C_A}{2C_F} \left(\hat{J}_g^{\tilde{t}1g;S}(t; \varepsilon) + \hat{J}_g^{\tilde{t}1g;NS}(t) \right) + \left(1 - \frac{C_A}{2C_F} \right) \left(J_{gt}^{\tilde{t}1;S}(u; \varepsilon) + J_{gt}^{\tilde{t}1;NS}(u) \right. \\ & \left. \left. + J_t^{\tilde{t}1g;S}(u; \varepsilon) + J_t^{\tilde{t}1g;NS}(u) \right) \right] \quad (5.173) \end{aligned}$$

where $s_{12} = s - m_t^2$ and s , t and u are the usual Mandelstam variables. The first part of eq. (5.173) corresponds to the case where emitter and spectator both are from the final state which is covered in [35]. The associated expanded expressions including the conventional prefactor c_ε are

$$\begin{aligned} \mathcal{V}^{(S)}(s_{12}, m_t, 0; \varepsilon) = \frac{1}{2} & \left[\frac{1}{\varepsilon^2} + \frac{1}{\varepsilon} \ln \left(\frac{\mu^2}{s_{12}} \right) + \frac{1}{2} \ln^2 \left(\frac{\mu^2}{s_{12}} \right) - \frac{\pi^2}{6} \right] + \frac{1}{2} \left[\frac{1}{\varepsilon} + \ln \left(\frac{\mu^2}{s_{12}} \right) \right] \\ & \times \ln \left(\frac{m_t^2}{s_{12}} \right) - \frac{1}{4} \ln^2 \left(\frac{m_t^2}{s_{12}} \right) - \frac{\pi^2}{12} - \frac{1}{2} \ln \left(\frac{s_{12}}{s} \right) \left[\ln \left(\frac{m_t^2}{s_{12}} \right) + \ln \left(\frac{m_t^2}{s} \right) \right] \quad (5.174) \end{aligned}$$

$$\mathcal{V}_t^{(\text{NS})}(s_{12}, m_t, 0) = \frac{3}{2} \ln \left(\frac{s_{12}}{s} \right) + \frac{\pi^2}{6} - \text{Li}_2 \left(\frac{s_{12}}{s} \right) - 2 \ln \left(\frac{s_{12}}{s} \right) - \frac{m_t^2}{s_{12}} \ln \left(\frac{m_t^2}{s} \right) \quad (5.175)$$

$$\begin{aligned} \mathcal{V}_g^{(\text{NS})}(s_{12}, 0, m_t; \kappa) = \frac{\gamma_g}{C_A} & \left(\ln \left(\frac{s_{12}}{s} \right) - 2 \ln \left(\frac{\sqrt{s} - m_t}{\sqrt{s}} \right) - \frac{2m_t}{\sqrt{s} + m_t} \right) + \frac{\pi^2}{6} \\ & - \text{Li}_2 \left(\frac{s_{12}}{s} \right) + \left(\kappa - \frac{2}{3} \right) \frac{m_t^2}{s_{12}} \left(\left(2N_f \frac{T_F}{C_A} - 1 \right) \ln \left(\frac{2m_t}{\sqrt{s} + m_t} \right) \right) \quad (5.176) \end{aligned}$$

with

$$\gamma_g = \frac{11}{6} C_A - \frac{2}{3} T_F N_f \quad (5.177)$$

$$K_g = C_A \left(\frac{67}{18} - \frac{\pi^2}{6} \right) - \frac{10}{9} T_F N_f \quad (5.178)$$

$$\Gamma_t(\varepsilon) = C_F \left(\frac{1}{\varepsilon} + \frac{1}{2} \ln \left(\frac{m_t^2}{\mu^2} \right) - 2 \right) \quad (5.179)$$

$$\Gamma_g(\varepsilon) = \frac{\gamma_g}{\varepsilon} - \frac{C_A}{6}. \quad (5.180)$$

The second part in eq. (5.173) covers final-state emission with an initial spectator and vice versa. The terms $\frac{C_A}{6}$ in eq. (5.180) and $\frac{C_A}{12\pi}$ in eq. (5.173) correspond to SUSY-restoring counterterms which transform the CDR result to DRED and are provided in [35]. For the remaining finite parts given by the different "plus"-distributions we have to distinguish between two cases. The case of a gluon acting as emitter or spectator

$$|\mathcal{M}_{\text{plus},1}^A|^2 = \frac{g_s^2}{2\pi} |\mathcal{M}_2(P^2, Q^2)|^2 \theta(x - x_0) \left(\frac{C_A}{2C_F} \left[\tilde{J}_g^{\tilde{t}_1 g}(P^2, Q^2) \right]_+ + \frac{1}{4} \left[J_{gg}^{\tilde{t}_1}(P^2, Q^2) \right]_+ + \frac{N_f}{2} \left[J_{Q\bar{Q}}^{\tilde{t}_1}(P^2, Q^2) \right]_+ \right) \quad (5.181)$$

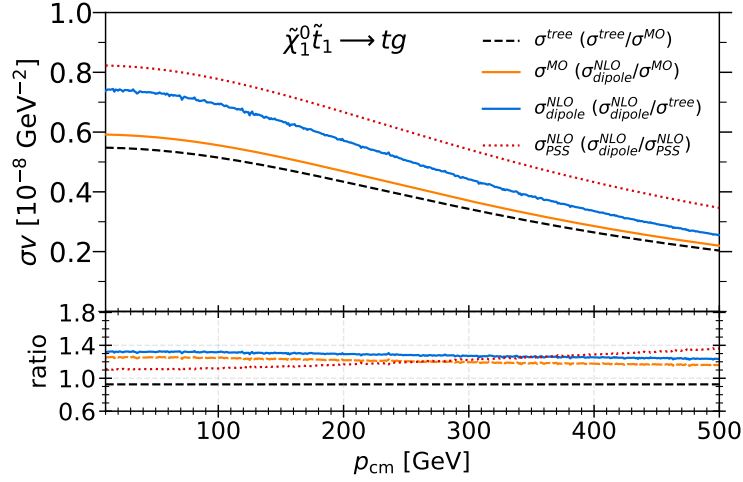
where Q^2 is related to the Mandelstam variable t and the case of the top acting as emitter or spectator

$$|\mathcal{M}_{\text{plus},2}^A|^2 = \frac{g_s^2}{2\pi} |\mathcal{M}_2(P^2, Q^2)|^2 \theta(x - x_0) \left(1 - \frac{C_A}{2C_F} \right) \left(\left[J_{gt}^{\tilde{t}_1}(P^2, Q^2) \right]_+ + \left[J_t^{\tilde{t}_1 g}(P^2, Q^2) \right]_+ \right) \quad (5.182)$$

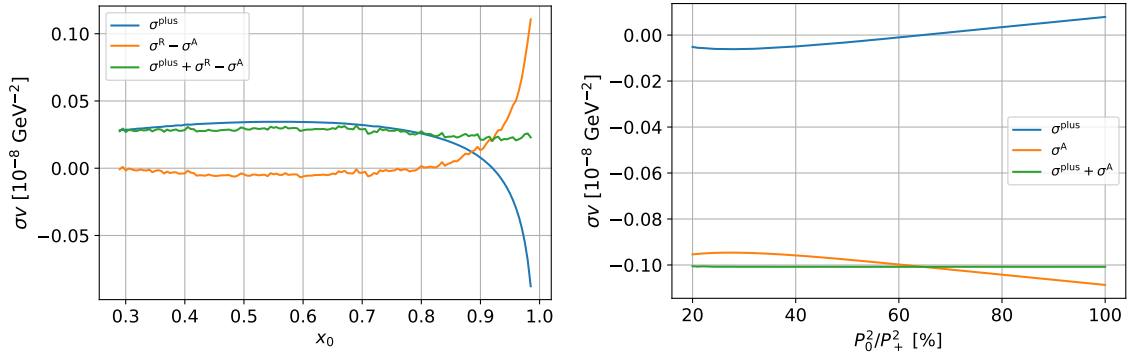
where Q^2 is related to the invariant u . In summary, the three different contributions to the total auxiliary cross section are

$$\int d\sigma^A = \frac{1}{2N_c F} \left[\int d\Phi_2(\cos \vartheta) |\mathcal{M}_{2 \rightarrow 2}^A|^2 + \int_0^{(\sqrt{s}-m_t)^2} \frac{dP^2}{2\pi} \int d\Phi_2(P^2, Q^2) |\mathcal{M}_{\text{plus},1}^A|^2 + \int_{m_t^2}^s \frac{dP^2}{2\pi} \int d\Phi_2(P^2, Q^2) |\mathcal{M}_{\text{plus},2}^A|^2 \right]. \quad (5.183)$$

Figure 5.5a shows the comparison between the dipole and the phase space slicing method. It becomes obvious that there is a large deviation between both methods. In order to ensure a correct implementation of the dipole method as well as that the integrated versions of the dipoles are correct up to additional finite terms that are independent of P_0^2 besides the non-trivial check of infrared convergence, the dependence of the result on the artificially introduced parameters x_0 and P_0^2 is examined in figs. 5.5b and 5.5c. It turns out that the result is independent of both parameters.



(a) Neutralino-stop coannihilation cross section σv with a top and a gluon in the final state for the example scenario defined in table 5.1. The leading order result is computed with `micrOMEAGs` (MO) and `DM@NLO` (tree). The fixed-order NLO results are calculated with the phase space slicing method (PSS) and the dipole method (dipole). The lower panel shows the ratio of different cross-sections indicated through the second item in the legend.



(b) Dependence of the real contribution and the "plus"-distribution on the artificial parameter x_0 . (c) Dependence of σ^A and the "plus"-distribution on the artificial parameter P_0^2 .

Figure 5.5: Comparison of the phase space slicing method with the dipole formalism for the process $\tilde{\chi}_1^0 \tilde{t}_1 \rightarrow tg$ and dependence of the results on the parameters x_0 and P_0^2 .

6 Colour bases

The non-abelian nature of (SUSY)-QCD complicates the evaluation of processes involving coloured particles. In order to make a systematic treatment of the colour factors feasible, the idea of colour bases is introduced in this chapter. As the construction of these bases is rather heavy on group and representation theory, some definitions and theorems are repeated in the first section. More information on group theory can be for example found in [36, 37, 38].

6.1 Group and representation theory essentials

Definition 6.1.1 (Group). A *group* (G, \circ) is a set G together with an operation \circ fulfilling the following axioms:

- Closure: $g_1, g_2 \in G \rightarrow g_1 \circ g_2 \in G$
- Associativity: $(g_1 \circ g_2) g_3 = g_1 (g_2 \circ g_3) \quad \forall g_1, g_2, g_3 \in G$
- Identity element: $\exists e \in G : g \circ e = e \circ g = g \quad \forall g \in G$
- Inverse element: $\forall g \in G \exists g^{-1} : g \circ g^{-1} = g^{-1} \circ g = e$

Definition 6.1.2 (Lie group). A group G which is at the same time a (smooth) manifold is called *Lie group* if the group operations

1. $G \times G \rightarrow G, (g_1, g_2) \mapsto g_1 g_2$
2. $G \rightarrow G, g \mapsto g^{-1}$

are both smooth maps.

The special properties of a Lie group allow to approximate each group element by an infinitesimal variation of its identity element. Studying this variation leads to the group's Lie algebra.

Definition 6.1.3 (Lie algebra). A *Lie algebra* is an algebra \mathfrak{g} where the bilinear product $[\cdot, \cdot]$, the *Lie bracket*, is no longer associative and obeys the following two additional requirements for all elements $T^a, T^b, T^c \in \mathfrak{g}$:

- Skew symmetry: $[T^a, T^b] = -[T^b, T^a]$
- Jacobi identity: $[T^a, [T^b, T^c]] + [T^c, [T^a, T^b]] + [T^b, [T^c, T^a]] = 0$.

The connection between Lie group and Lie algebra becomes evident through the matrix exponential

$$g = \exp(i\alpha_a T^a) . \quad (6.1)$$

Definition 6.1.4 (Representation of a group). A representation $D(g)$ of a group (G, \circ) acting on a vector space V (referred to as *representation space*) is a group homomorphism

$$D : G \rightarrow \text{GL}(V), \quad g \mapsto D(g) , \quad (6.2)$$

i.e. the function D fulfills $D(g_1 \circ g_2) = D(g_1)D(g_2)$.

Definition 6.1.5 (Representation of a Lie algebra). A representation $\pi(T^a)$ of a Lie algebra \mathfrak{g} acting on a vector space V is a Lie algebra homomorphism

$$\pi : \mathfrak{g} \rightarrow \mathfrak{gl}(V), \quad T^a \mapsto \pi(T^a), \quad (6.3)$$

i.e. π respects the Lie bracket of the Lie algebra

$$\pi \left([T^a, T^b] \right) = \left[\pi(T^a), \pi(T^b) \right] \quad \forall T^a, T^b \in \mathfrak{g}. \quad (6.4)$$

Two important representations that exist for all Lie algebras are the *fundamental* or *defining* representation where every element of the algebra is represented by itself $\pi(T^a) = T^a$ and the *adjoint representation* where the Lie algebra acts on itself.

Definition 6.1.6 (Adjoint representation). For a Lie algebra \mathfrak{g} the linear map $\text{ad}_{T^a} : \mathfrak{g} \rightarrow \mathfrak{g}$ given by

$$\text{ad}_{T^a}(T^b) = [T^a, T^b], \quad T^a, T^b \in \mathfrak{g} \quad (6.5)$$

defines the *adjoint representation* $T^a \mapsto \text{ad}_{T^a}$.

Definition 6.1.7 (Generators and structure constants). Let $\{T^a\}$ be a basis for a finite-dimensional Lie algebra \mathfrak{g} . The constants f_{abc} satisfying

$$[T^a, T^b] = if_{abc}T^c \quad (6.6)$$

are uniquely defined for the given basis and are called *structure constants*. The elements T^a are called *generators* of the corresponding group $G = \exp(\mathfrak{g})$.

With the notion of structure constants the adjoint representation can be directly read off the commutator $(\text{ad}_{T^a})_{cb} = F_{cb}^a := if_{abc}$.

Definition 6.1.8 (Invariant subspace). A subspace $W \subset V$ is an *invariant subspace* if $D(g)W \subseteq W$ for all g in a group G .

Definition 6.1.9 (Reducible and irreducible representations). A representation $D(g)$ is *reducible* if the representation space contains an invariant subspace. Otherwise the representation is *irreducible* and the associated subspace itself is called irreducible. A representation is *fully reducible* if the representation space V can be decomposed into a direct sum of irreducible subspaces $V = \bigoplus_i V_i$, where all the subspaces V_i are invariant under $D(g)$.

An irreducible representation is usually abbreviated as *irrep*.

Theorem 6.1.1 (Weyl's theorem). Let G be a compact Lie group, then every finite-dimensional representation of G is fully reducible.

Examples of compact Lie groups are $SU(N)$ and $U(N)$.

Theorem 6.1.2 (Schur's lemma).

- 1) Let D_1, D_2 be two irreducible representations of a group G on respective vector spaces V_1 and V_2 . Let $H : V_1 \rightarrow V_2$ be a linear operator such that $HD_1(g) = D_2(g)H \quad \forall g \in G$. Then either $H = 0$ or H is not singular and it holds $D_2(g) = HD_1(g)H^{-1} \quad \forall g \in G$. In the latter case, the representations D_1 and D_2 are equivalent and H is the similarity transformation.

- 2) Let $D(g)$ be an irreducible representation of a group G on a finite-dimensional vector space V . Let $H : V \rightarrow V$ be a linear operator such that $D(g)H = HD(g) \forall g \in G$, then H is a multiple of the identity element on V .

Definition 6.1.10 (Clebsch-Gordan coefficients). Let $D^{(\alpha)}(g)$ and $D^{(\beta)}(g)$ be two irreps of a group element g acting on the respective vector spaces $V^{(\alpha)}$ and $V^{(\beta)}$ with bases $\{v_1^{(\alpha)}, \dots, v_{d(\alpha)}^{(\alpha)}\}$ and $\{v_1^{(\beta)}, \dots, v_{d(\beta)}^{(\beta)}\}$. In addition, let $\{D^{(\gamma)}\}$ be a set of inequivalent irreps labelled by γ acting on the respective vector spaces $W^{(\gamma)}$ with basis $\{w_1^{(\gamma)}, \dots, w_{d(\gamma)}^{(\gamma)}\}$. For each label γ the dimension of the associated representation space is denoted by $d(\gamma)$ whereas the representation itself is referred to as \mathbf{R}_γ . The decomposition

$$D^{(\alpha)} \otimes D^{(\beta)} = \bigoplus_{\gamma} a_{\gamma}^{\alpha\beta} D^{(\gamma)}, \quad a_{\gamma}^{\alpha\beta} \in \mathbb{N} \quad (6.7)$$

of the tensor product representation into the direct sum of irreps is called *Clebsch-Gordan series*. The spaces $W^{(\gamma)}$ form a $d(\gamma)$ -dimensional subspace of $V^{(\alpha)} \otimes V^{(\beta)}$ invariant under the irrep $D^{(\gamma)}(g)$. The coefficients $a_{\gamma}^{\alpha\beta}$ give the number of times the irrep occurs in the series and are referred to as *outer multiplicity* or just *multiplicity*. This decomposition induces a basis transformation

$$v_i^{(\alpha)} \otimes v_j^{(\beta)} = \sum_{\gamma} \sum_{n_{\gamma}}^{a_{\gamma}^{\alpha\beta} d(\gamma)} \sum_{k=1}^{d(\gamma)} w_k^{(\gamma)} C_{\alpha\beta;ij}^{\gamma, n_{\gamma}; k} \quad (6.8)$$

or alternatively

$$w_k^{(\gamma)} = \sum_{i=1}^{d(\alpha)} \sum_{j=1}^{d(\beta)} C_{\alpha\beta;ij}^{\gamma, n_{\gamma}; k} v_i^{(\alpha)} \otimes v_j^{(\beta)} \quad (6.9)$$

where γ runs over all irreps contained in the decomposition and n_{γ} refers to n -th occurrence of the irrep γ . The (complex) coefficients $C_{\alpha\beta;ij}^{\gamma, k}$ are called *Clebsch-Gordan (CG) coefficients* or *CG matrices*. If the outer multiplicities take only the values $a_{\gamma}^{\alpha\beta} = 0, 1$ the group is *simply reducible*. For simplicity, every group is in general considered simply reducible such that the label n_{γ} can be omitted.

For the decomposition of a tensor product of an arbitrary number n of basis vectors

$$v_{i_1}^{\alpha_1} \otimes \dots \otimes v_{i_n}^{\alpha_n} = \sum_{\gamma} \sum_{k=1}^{d(\gamma)} w_k^{(\gamma)} C_{\{\alpha\};\{i\}}^{\gamma; k} \quad (6.10)$$

the multi-index notation $\{i\} = i_1 \dots i_n$ is suitable. Following this notation, the orthonormality relations

$$\sum_{\gamma, k} C_{\{\alpha\};\{i\}}^{\gamma; k*} C_{\{\alpha\};\{j\}}^{\gamma; k} = \delta_{i_1 j_1} \dots \delta_{i_n j_n} \quad (6.11)$$

$$\sum_{\{i\}} C_{\{\alpha\};\{i\}}^{\gamma'; k'*} C_{\{\alpha\};\{i\}}^{\gamma; k} = \delta_{\gamma \gamma'} \delta_{k k'} \quad (6.12)$$

in the case of orthonormal bases of the representation spaces appear by expressing the Kronecker symbols on the right-hand side through scalar products of the corresponding basis elements and applying eq. (6.8) and eq. (6.9) afterwards.

To derive multiplicities $a_{\gamma}^{\alpha\beta}$ a few methods have been developed such as Young tableaux or the notion of characters. A convenient alternative is the usage of a computer program such `LiE` [39]. The method that we will use in the following is the *tensor method*. As an example consider a tensor T^{ij} that transforms under a group element R of $\text{SO}(3)$

$$T^{ij} \rightarrow T'^{ij} = R^{ik} R^{jl} T^{kl}. \quad (6.13)$$

Another possibility to represent T^{ij} is to arrange all elements in a column $(T^{11} \ T^{23} \ \dots \ T^{33})^T$. This column vector then transforms under a nine dimensional representation $D(R)$ of R . To find out whether this representation is reducible or not we have to find components of T^{ij} that transform among themselves. One irreducible subspace that is easy to discover is the trace T^{kk} since

$$T^{ii} \rightarrow R^{ik} R^{il} \delta^{kl} T^{kl} = R^{ik} (R^T)^{li} T^{kl} = \delta^{kl} T^{kl} = T^{kl}. \quad (6.14)$$

This trace furnishes a one dimensional representation as there is one independent component. After taking out the trace we are left with a traceless tensor

$$S^{ij} = T^{ij} - \frac{1}{3} \delta^{ij} T^{mm}. \quad (6.15)$$

The other subspaces that can be found in S^{ij} emerge from symmetrization of the indices. Therefore, consider the antisymmetric tensor $A^{ij} = S[ij] = S^{ij} - S^{ji}$. Under $\text{SO}(3)$ the tensor A^{ij} transforms into itself

$$A^{ij} \rightarrow A'^{ij} = S'^{ij} - S'^{ji} = R^{ik} R^{jl} S^{kl} - R^{jk} R^{il} S^{kl} = R^{ik} R^{jl} S^{kl} - R^{jl} R^{ik} S^{lk} = R^{ik} R^{jl} A^{ij}. \quad (6.16)$$

The number of independent components of A^{ij} are $3^2 - 3/2 = 3$ which means that we have a three dimensional representation. After taking A^{ij} out of S^{ij} we are left with a symmetric tensor

$$S^{ij} = \frac{1}{2} (S^{ij} + S^{ji}) + \frac{1}{2} A^{ij}. \quad (6.17)$$

which is denoted by $S^{\{ij\}} = S^{ij} + S^{ji}$ and forms also an invariant subspace with $3^2 - 3 - 1 = 5$ components where the proof goes as for A^{ij} . Thus, we obtain the decomposition

$$\mathbf{3} \otimes \mathbf{3} = \mathbf{1} \oplus \mathbf{3} \oplus \mathbf{5}. \quad (6.18)$$

where the representations are denoted by their respective dimensions. If we have a complex group such as $\text{SU}(N)$, we have to distinguish between vectors ψ^i and their dual vectors $\psi^{i*} = \psi_i$, i.e. between upper and lower indices. By using this notation only traces between upper and lower indices form $\text{SU}(N)$ invariant subspaces. This short introduction to the tensor method should be sufficient for the construction of the color bases. For more information the reader is referred to [38].

6.2 Colour space

In order to lay down a clear mathematical foundation for the management of colour in (SUSY)-QCD, the notion of colour space is introduced first. Considering only the colour of particles, i.e. ignoring all other quantum numbers, squarks/quarks are elements of $V = \mathbb{C}^{N_c}$, whereas anti-squarks/quarks live in the dual space $\bar{V} = \mathbb{C}^{N_c*}$. As gluinos/gluons transform

under the adjoint representation of $SU(N_C)$ they are defined as states in $A = \mathbb{C}^{N_C^2-1}$. A SUSY-QCD amplitude is in general associated with n_g gluinos/gluons, n_q squarks/quarks and $n_{\bar{q}}$ anti-squarks/-quarks. The *colour space* associated with this amplitude is then defined through the tensor product $C = \bar{V}^{\otimes n_{\bar{q}}} \otimes V^{\otimes n_q} \otimes A^{\otimes n_g}$. An element $c \in C$ is referred to as the *colour structure* of the amplitude. A natural metric on C is induced through the scalar product

$$\langle c_1 | c_2 \rangle = \sum_{a_1, \dots, a_n} c_1^{*a_1, \dots, a_n} c_2^{a_1, \dots, a_n} \quad (6.19)$$

which is given by summing over all external color indices.

6.3 Trace bases

The simplest form of colour bases are trace bases [40, 41]. They are obtained by rewriting the structure constants f_{abc} through the generators in the fundamental representation

$$if_{abc} = \frac{1}{T_F} \text{Tr} \left([T^a, T^b] T^c \right) \quad (6.20)$$

and then "contracting" all gluon indices with the Fierz identity given in eq. (A.35). After this only linear combinations of products of traces over the indices of external gluons remain or products of the form $(T^{a_1} \dots T^{a_n})_{ij}$ with indices a_1, \dots, a_n of external gluons and i, j of external quarks/squarks.

6.4 Orthogonal multiplet bases

Trace bases have the disadvantage of being in general over-complete and non-orthogonal. By choosing an orthogonal color basis scattering amplitudes can be subdivided into smaller, separately gauge invariant pieces. Moreover, in the context of resummation it becomes necessary to associate amplitudes with irreducible subspaces in colour space invariant under $SU(3)$ since particles forming a colour octet repel each other whereas singlets are likely to form bound states.

6.4.1 Construction of the bases

The construction of orthogonal multiplet bases follows mainly the approach outlined in [42]. To start with, consider a scattering amplitude $\mathcal{M}_{\{i\},\{f\}}$ describing a process with n coloured particles in the initial state with colour indices $\{i\}$ and N coloured particles in final state with indices $\{f\}$. According to Weyl's theorem the tensor product of initial and final state representations can be decomposed into irreducible representations

$$\mathbf{R}_{\alpha_1} \otimes \dots \otimes \mathbf{R}_{\alpha_n} = \bigoplus_{\gamma} \mathbf{R}_{\gamma} \quad \mathbf{R}_{\beta_1} \otimes \dots \otimes \mathbf{R}_{\beta_N} = \bigoplus_{\Gamma} \mathbf{R}_{\Gamma}. \quad (6.21)$$

For further considerations it is useful to combine all equivalent irreducible representations that appear in both decompositions in eq. (6.21) into pairs $P_j = (\mathbf{R}_{\gamma}, \mathbf{R}_{\Gamma})$ where the index j denotes all allowed combinations.

Using the orthogonality relation in eq. (6.11) the amplitude can be decomposed into irreducible representations

$$\mathcal{M}_{\{i\},\{f\}} = \sum_{\gamma,\Gamma,k_i,k_f} \mathcal{M}_{\{i'\},\{f'\}} C_{\{\alpha\};\{i\}}^{\gamma;k_i} C_{\{\alpha\};\{i'\}}^{\gamma;k_i*} C_{\{\beta\};\{f\}}^{\Gamma;k_f} C_{\{\beta\};\{f'\}}^{\Gamma;k_f*} \quad (6.22)$$

$$= \sum_{\gamma,\Gamma,k_i,k_f} \mathcal{M}_{k_i k_f}^{\gamma\Gamma} C_{\{\alpha\};\{i\}}^{\gamma;k_i} C_{\{\beta\};\{f\}}^{\Gamma;k_f*}. \quad (6.23)$$

The coefficients $\mathcal{M}_{k_i k_f}^{\gamma\Gamma}$ are called *partial amplitudes* or *subamplitudes* and form themselves a linear map $\mathcal{M}^{\gamma\Gamma} : V^{(\Gamma)} \rightarrow V^{(\gamma)}$. Each partial amplitude must conserve colour, i.e. obey the transformation

$$\mathcal{M}^{\gamma\Gamma} = D^{(\gamma)-1} \mathcal{M}^{\gamma\Gamma} D^{(\Gamma)}. \quad (6.24)$$

Hence, according to Schur's lemma the representations \mathbf{R}_γ and \mathbf{R}_Γ are equivalent in the case of a non-zero subamplitude, i.e. initial and final state belong to one of the pairs P_j and are of the form $\mathcal{M}_{k_i k_f}^{\gamma\Gamma} = \mathcal{M}^{\gamma\Gamma} \delta_{k_i k_f}$. Therefore, the final decomposition of the amplitude reads

$$\mathcal{M}_{\{i\},\{f\}} = \sum_j \mathcal{M}^{(j)} c_{\{i\},\{f\}}^{(j)} \quad (6.25)$$

with the basis elements

$$c_{\{i\},\{f\}}^{(j)} = \sum_k C_{\{\alpha\};\{i\}}^{\gamma;k} C_{\{\beta\};\{f\}}^{\Gamma;k*}. \quad (6.26)$$

That the $c^{(j)}$ are indeed orthogonal with respect to the scalar product defined in eq. (6.19) can be verified using eq. (6.12).

6.4.2 Calculation of Clebsch-Gordan coefficients

In order to determine the Clebsch-Gordan coefficients which are relevant for the process $\tilde{q}\tilde{q}^* \rightarrow gg$, we have to decompose the product spaces of the initial and final states into irreducible representations first. This is achieved with the *tensor method* as it is only a small step from there to the CG coefficients. We start with the initial state where we have a squark and an antisquark. Therefore we have to decompose the product of a vector ψ^i and a dual vector χ_j . The only invariant subspace that we can take out is the trace $\Psi^i \chi_i$ which yields the decomposition

$$\psi^i \chi_j = \left(\psi^i \chi_j - \frac{1}{N} \psi^i \chi_i \right) + \frac{1}{N} \Psi^i \chi_i. \quad (6.27)$$

The first part furnishes an eight dimensional representation as there are eight independent components whereas the second part corresponds with one independent component to a one dimensional representation which we can write as

$$\mathbf{3} \otimes \bar{\mathbf{3}} = \mathbf{8} \oplus \mathbf{1}. \quad (6.28)$$

An alternative notation is to denote an irreducible representation (m, n) by the number of symmetric upper m and lower indices n such that eq. (6.28) corresponds to

$$(1, 0) \otimes (0, 1) = (1, 1) \oplus (0, 0). \quad (6.29)$$

A useful formula that allows to relate the dimension of a representation to the number of indices n and m is [38]

$$D(m, n) = \frac{1}{2}(m+1)(n+1)(m+n+2). \quad (6.30)$$

If we compare eq. (6.27) to eq. (6.8), we can see that we only have to rewrite the **8** part in terms of an object that carries an index that runs from one to eight. As

$$\varphi_j^i = \psi^i \chi_j - \frac{1}{N} \psi^i \chi_i \quad (6.31)$$

itself is a traceless and hermitian matrix, it can be written in terms of the generators T^a :

$$\varphi_j^i = \sum_a v_a (T^a)_j^i. \quad (6.32)$$

where v_a is a real vector with eight components. This allows to directly read of the Clebsch-Gordan coefficients

$$C_{33;ij}^1 = \delta_{ij} \quad (6.33)$$

$$C_{33;ij}^{8;a} = T_{ij}^a. \quad (6.34)$$

where upper and lower indices are not distinguished for a clearer notation. For two gluons in the final state we have to decompose the product of two tensors ψ_j^i and χ_l^k . As we usually label gluons with indices that run from 1 to $N_c^2 - 1$, it is more practical to decompose both tensors as in eq. (6.32) and turn the generators around using the trace orthonormality $\text{Tr}(T^a T^b) = \frac{1}{2} \delta^{ab}$ and write

$$v^a w^b = (T^a)_i^j (T^b)_k^l \psi_j^i \chi_l^k. \quad (6.35)$$

For the decomposition into invariant subspaces we can first take out the two traces

$$\varphi_l^i = \psi_n^i \chi_l^n - \frac{1}{N} \delta_l^i \psi_n^m \chi_m^n \quad (6.36)$$

$$\phi_j^k = \psi_j^n \chi_n^k - \frac{1}{N} \delta_j^k \psi_n^m \chi_m^n \quad (6.37)$$

which gives

$$\psi_j^i \chi_l^k = T_{jl}^{ik} + \frac{1}{N} \left(\varphi_l^i \delta_j^k + \phi_j^k \delta_l^i - \frac{2}{N} \delta_l^i \delta_j^k \psi_n^m \chi_m^n \right) \quad (6.38)$$

and leaves as remainder the traceless tensor T_{jl}^{ik} . It is possible to symmetrize $\varphi_l^i \delta_j^k$ and $\phi_j^k \delta_l^i$ further by decomposing them into a symmetric and an antisymmetric part with respect to the two "gluon" indices a and b . This symmetry becomes more obvious by noting that $(\phi_j^k)^* = \varphi_j^k$ which allows to decompose them as

$$\varphi_l^i = \sum_c (v_c + i w_c) (T^c)_l^i \quad (6.39)$$

$$\phi_j^k = \sum_c (v_c - i w_c) (T^c)_j^k \quad (6.40)$$

with two real vectors v_c and w_c . Contracting both with the generators $(T^a)_i^j (T^b)_k^l$ gives

$$\begin{aligned} (T^a)_i^j (T^b)_k^l \left(\varphi_l^i \delta_j^k + \phi_j^k \delta_l^i \right) &= \sum_c v_c \left(\text{Tr} \left(T^a T^b T^c \right) + \text{Tr} \left(T^b T^a T^c \right) \right) = \frac{1}{2} \sum_c v_c d_{abc} \quad (6.41) \\ (T^a)_i^j (T^b)_k^l \left(\varphi_l^i \delta_j^k - \phi_j^k \delta_l^i \right) &= \sum_c i w_c \left(\text{Tr} \left(T^a T^b T^c \right) - \text{Tr} \left(T^b T^a T^c \right) \right) = \frac{1}{2} \sum_c i w_c f_{abc}. \end{aligned} \quad (6.42)$$

This shows that eq. (6.41) is indeed symmetric in the indices a and b and furnishes the irreducible representation $\mathbf{8_S}$ whereas eq. (6.42) is antisymmetric in a and b and corresponds to $\mathbf{8_A}$. As a next step we can antisymmetrize T_{lj}^{ik} in its upper indices $A_{jl}^{ik} = T_{jl}^{[ik]}$. The tensor A_{jl}^{ik} is now antisymmetric in its upper indices and without any further massaging already symmetric in its lower indices. The latter part can be seen by defining $B_{mjl} = \varepsilon_{mik} A_{jl}^{ik}$. As we claim that B_{mjl} is symmetric in j and l , the contraction $B_{mjl} \varepsilon^{njl}$ must vanish. With the help of the identity

$$\varepsilon_{mik} \varepsilon^{njl} \sim \delta_m^n \delta_i^j \delta_k^l \pm \text{permutations} \quad (6.43)$$

and the fact that A_{jl}^{ik} is traceless, we get $\varepsilon_{mik} \varepsilon^{njl} A_{jl}^{ik} = 0$. Inserting three symmetric lower indices into eq. (6.30) tells us that B_{mjl} corresponds to the irreducible representation $\overline{\mathbf{10}}$. The same steps can be repeated for $\tilde{B}^{mik} = \varepsilon_{mjl} \tilde{A}_{jl}^{ik}$ with $\tilde{A}_{jl}^{ik} = T_{[jl]}^{ik}$ which show that \tilde{B}^{mik} furnishes the $\mathbf{10}$ representation. After taking A_{jl}^{ik} and \tilde{A}_{jl}^{ik} out of T_{lj}^{ik} only a symmetric tensor with two upper and lower indices remains which is the irreducible $\mathbf{27}$. Thus, we arrive at

$$\mathbf{8} \otimes \mathbf{8} = \mathbf{1} \oplus \mathbf{8_S} \oplus \mathbf{8_A} \oplus \overline{\mathbf{10}} \oplus \mathbf{10} \oplus \mathbf{27} \quad (6.44)$$

or

$$(1, 1) \otimes (1, 1) = (0, 0) \oplus (1, 1) \oplus (1, 1) \oplus (0, 3) \oplus (3, 0) \oplus (2, 2). \quad (6.45)$$

For the eight dimensional subspace we can already read of the Clebsch-Gordan coefficients from eqs. (6.41) and (6.42)

$$C_{88;ab}^{8_S;c} = d_{abc} \quad (6.46)$$

$$C_{88;ab}^{8_A;c} = i f_{abc}. \quad (6.47)$$

In order to obtain the Clebsch-Gordan coefficients for the $\mathbf{1}$ representation in eq. (6.38), we only have to compute $(T^a)_i^j (T^b)_k^l \delta_l^i \delta_j^k = \text{Tr} (T^a T^b) = \frac{1}{2} \delta_{ab}$ which gives

$$C_{88;ab}^1 = \delta_{ab}. \quad (6.48)$$

With these Clebsch-Gordan coefficients we have all we need for the construction of the bases as there are three possible combinations of equivalent initial and final state representations

$$P_i \in \{(\mathbf{1}, \mathbf{1}), (\mathbf{8}, \mathbf{8_A}), (\mathbf{8}, \mathbf{8_S})\}. \quad (6.49)$$

The corresponding orthogonal basis elements are

$$c_{st,ab}^{(\mathbf{1})} = C_{33;st}^1 C_{88;ab}^1 = \delta_{st} \delta_{ab} \quad (6.50)$$

$$c_{st,ab}^{(\mathbf{8_S})} = C_{33;st}^{8;c} C_{88;ab}^{8_S;c} = d_{abc} T_{st}^c \quad (6.51)$$

$$c_{st,ab}^{(\mathbf{8_A})} = C_{33;st}^{8;c} C_{88;ab}^{8_A;c} = i f_{abc} T_{st}^c \quad (6.52)$$

with the norms

$$\begin{aligned}
||c^{(\mathbf{1})}||^2 &= N(N^2 - 1) \\
||c^{(\mathbf{8_S})}||^2 &= C_F(N^2 - 4) \\
||c^{(\mathbf{8_A})}||^2 &= NC_A C_F.
\end{aligned} \tag{6.53}$$

The same basis elements are found in [\[42\]](#).

7 Phenomenology of squark annihilation

This thesis focusses on the case where the lightest stop is nearly mass degenerate with the lightest neutralino. There are several theoretical and phenomenological reasons why a light stop could be realized as the NLSP in nature. First, it is well studied that a light stop predicts within the MSSM the mass of the CP-even Higgs as measured at the LHC [43, 44]. Second, a light stop which is close in mass to the neutralino avoids the exclusion regions of the LHC [45]. Third, it turns out that the cross section for neutralino annihilation alone is too small to account for the whole relic density. Therefore, the annihilation rate needs to be enhanced by another mechanism which could be efficient coannihilation [46].

7.1 Squark annihilation into gluons at leading order

To prepare for the subsequent discussion of higher order corrections to squark annihilation into gluons, it is useful to get some insight into the nature of SUSY-QCD scattering amplitudes and show the computational techniques used to arrive at the tree level cross section. The Feynman diagrams for the leading order process are displayed in fig. 7.1 along with the naming convention employed for momenta and other indices relevant to the process.

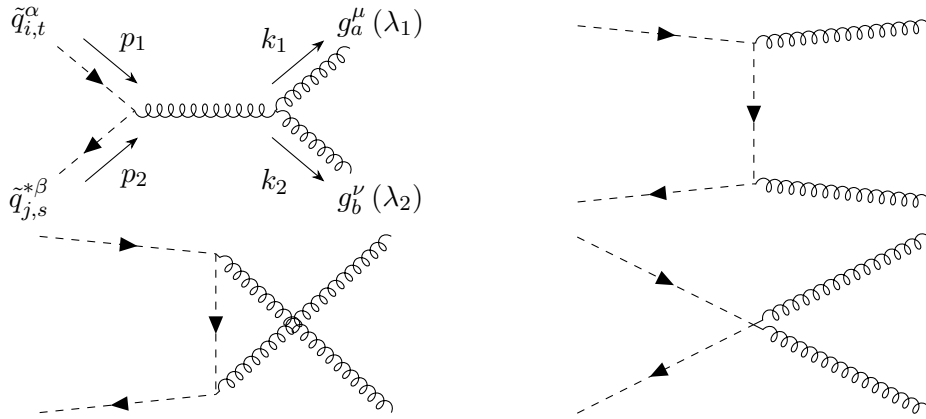


Figure 7.1: Tree level Feynman diagrams for the annihilation of a squark-antisquark pair into two gluons. Four-momenta, colours (s, t, a, b), sfermion indices (i, j), flavours (α, β) and polarizations (λ_1, λ_2) are explicitly labelled in the first diagram. The same naming convention is used for the $2 \rightarrow 2$ NLO corrections¹.

The second and third diagram are identical except for the interchange of the two gluons in the final state. Both diagrams have to be taken into account since the two gluons are indistinguishable from each other. For the same reason, an additional Bose symmetry factor

¹In the real corrections appears a third gluon $g_c^\rho(\lambda_3)$ with momentum k_3 .

$S_2 = 1/2!$ enters into the final expression for the total cross section. The different diagrams are labelled according to which of the Mandelstam variables

$$\begin{aligned} s &= (p_1 + p_2)^2 = (k_1 + k_2)^2 \\ t &= (k_1 - p_1)^2 = (k_2 - p_2)^2 \\ u &= (k_2 - p_1)^2 = (k_1 - p_2)^2 \end{aligned} \quad (7.1)$$

appears in the propagator. The last diagram is special since it has no propagator but due to its shape this kind of topology is sometimes called v -channel (or "seagull" diagram) even though there exists no corresponding kinetic invariant. Because of momentum conservation, the Mandelstam variables obey the relation $s + t + u = m_{\tilde{q}_i}^2 + m_{\tilde{q}_j}^2$ where all external particles are considered to be on their respective mass shell, i.e. $k_1^2 = k_2^2 = 0$ for the gluons and $p_1^2 = m_{\tilde{q}_i}^2$, $p_2^2 = m_{\tilde{q}_j}^2$ for the squarks. By following the Feynman rules given in appendix B and using Feynman gauge $\xi = 1$, one obtains the colour decomposed amplitudes

$$\mathcal{M}_s = c_{st,ab}^{(8_A)} \frac{-ig_s^2}{s} (p_2 - p_1)^\sigma g_{\sigma\rho} (g^{\rho\nu} (k_1 + 2k_2)^\mu - g^{\rho\mu} (2k_1 + k_2)^\nu + g^{\mu\nu} (k_1 - k_2)^\rho) \epsilon_\mu^*(\lambda_1, k_1) \epsilon_\nu^*(\lambda_2, k_2) \quad (7.2)$$

$$\mathcal{M}_t = \frac{1}{2} \left(\frac{1}{N_c} c_{st,ab}^{(1)} + c_{st,ab}^{(8_S)} - c_{st,ab}^{(8_A)} \right) \frac{ig_s^2}{t - m_{\tilde{q}_i}^2} (2p_1 - k_1)^\mu \times (2p_2 - k_2)^\nu \epsilon_\mu^*(\lambda_1, k_1) \epsilon_\nu^*(\lambda_2, k_2) \quad (7.3)$$

$$\mathcal{M}_u = \frac{1}{2} \left(\frac{1}{N_c} c_{st,ab}^{(1)} + c_{st,ab}^{(8_S)} + c_{st,ab}^{(8_A)} \right) \frac{ig_s^2}{u - m_{\tilde{q}_i}^2} (2p_2 - k_1)^\mu \times (2p_1 - k_2)^\nu \epsilon_\mu^*(\lambda_1, k_1) \epsilon_\nu^*(\lambda_2, k_2) \quad (7.4)$$

$$\mathcal{M}_v = i \left(\frac{1}{N_c} c_{st,ab}^{(1)} + c_{st,ab}^{(8_S)} \right) g_s^2 g^{\mu\nu} \epsilon_\mu^*(\lambda_1, k_1) \epsilon_\nu^*(\lambda_2, k_2) \quad (7.5)$$

for the diagrams shown in fig. 7.1. The colour decomposition into the basis elements $c_{st,ab}^{(R)}$ derived in section 6.4.2 is straightforward through the application of the $\mathfrak{su}(N_c)$ -identity given in eq. (A.42) for the t - and u -channel and eq. (A.34) for the v -channel. Since each interaction vertex that appears in the tree process preserves flavour (as one of the key assumptions of the pMSSM) and forbids the mixing of squark mass eigenstates, the associated Kronecker deltas δ_{ij} and $\delta_{\alpha\beta}$ are excluded from the amplitudes for simplicity. As these amplitudes appear within the perturbative expansion of the S -matrix following the LSZ reduction formula and as there appear no fermionic fields in the associated correlation functions which could possibly introduce relative minus signs between the individual terms, the total transition amplitude is given by the sum of all annihilation channels

$$\mathcal{M}_{\text{LO}} = \mathcal{M}_s + \mathcal{M}_t + \mathcal{M}_u + \mathcal{M}_v. \quad (7.6)$$

For the following computations it is useful to define the helicity

$$\mathcal{M}_{\text{LO}} = \mathcal{M}_{\text{LO}}^{\mu\nu} \epsilon_\mu^*(\lambda_1, k_1) \epsilon_\nu^*(\lambda_2, k_2) \quad (7.7)$$

and colour amputated amplitudes

$$\mathcal{M}_{\text{LO}} = \sum_R c_{st,ab}^{(R)} \mathcal{M}_{\text{LO}}^{(R)}. \quad (7.8)$$

As presented in chapter 4, a scattering amplitude involving a massless vector boson should be invariant under the replacement $\epsilon(\lambda, k) \rightarrow \epsilon(\lambda, k) + k$ by the principles of gauge and Lorentz invariance. That is, \mathcal{M}_{LO} should vanish if one of the polarization vectors is replaced by its associated momentum. However, if we perform the contractions of $\mathcal{M}_{\text{LO}}^{\mu\nu}$ with k_1^μ and k_2^μ and simplify the denominators to $t - m_{\tilde{q}_i^\alpha}^2 = -2p_1 \cdot k_1$ and $u - m_{\tilde{q}_i^\alpha}^2 = -2p_2 \cdot k_1$, we find that this condition is only fulfilled if the gluons lie in the physical Hilbert space and are therefore transverse

$$k_{1,\mu}\epsilon_\nu^*(\lambda_2, k_2)\mathcal{M}_{\text{LO}}^{\mu\nu} = -\frac{ig_s^2}{2s}c_{st,ab}^{(\mathbf{8}_A)}(u-t)k_2 \cdot \epsilon^*(\lambda_2, k_2) \quad (7.9)$$

$$\epsilon_\mu^*(\lambda_1, k_1)k_{2,\nu}\mathcal{M}_{\text{LO}}^{\mu\nu} = -\frac{ig_s^2}{2s}c_{st,ab}^{(\mathbf{8}_A)}(u-t)k_1 \cdot \epsilon^*(\lambda_1, k_1) \quad (7.10)$$

unlike in QED where the Ward identity $k_\mu \mathcal{M}^\mu = 0$ holds for any scattering amplitude \mathcal{M} independently of the polarization states of the other photons involved in the process described by \mathcal{M} besides $\epsilon_\mu(\lambda, k)$. The question arises whether these findings are due to the choice of the gauge fixing condition which manifests itself in this case only in the gluon propagator or due to the non-Abelian nature of the theory. To get to the bottom of this question, let us replace the gluon propagator in Feynman gauge by the one in lightcone gauge given in eq. (B.1)

$$-\frac{g^{\sigma\rho}}{s} \rightarrow \Pi_{\text{lightcone}}^{\sigma\rho}(k_1 + k_2, n) \quad (7.11)$$

which yields for eqs. (7.12) and (7.13)

$$k_{1,\mu}\epsilon_\nu^*(\lambda_2, k_2)\mathcal{M}_{\text{LO}}^{\mu\nu} = -\frac{ig_s^2}{2s}c_{st,ab}^{(\mathbf{8}_A)}\left(u-t + \frac{(p_2-p_1) \cdot n}{(p_1+p_2) \cdot n}s\right)k_2 \cdot \epsilon^*(\lambda_2, k_2) \quad (7.12)$$

$$\epsilon_\mu^*(\lambda_1, k_1)k_{2,\nu}\mathcal{M}_{\text{LO}}^{\mu\nu} = -\frac{ig_s^2}{2s}c_{st,ab}^{(\mathbf{8}_A)}\left(u-t - \frac{(p_2-p_1) \cdot n}{(p_1+p_2) \cdot n}s\right)k_1 \cdot \epsilon^*(\lambda_1, k_1) \quad (7.13)$$

where the only nonzero additional contribution comes from the $n^\sigma(k_1 + k_2)^\rho$ term whereas all other drop out through $(p_2 - p_1) \cdot (p_1 + p_2) = 0$. This shows that also in the axial gauge the amplitude with one polarization vector being substituted with its associated momentum only vanishes if the other gluon is physical.

In order to include only the physical states in the transition probability (the amplitude squared), there are two possibilities. Within both approaches \mathcal{M}_{LO} is kept in Feynman gauge. The first possibility is to explicitly sum only the transverse polarizations with the help of eq. (4.20) which holds as an algebraic relation independently of the chosen gauge fixing condition where it is useful to choose the arbitrary vector n as the respective momentum of the other gluon. Since k_1 and k_2 are lightlike, this particular choice for n corresponds to the polarization sum as obtained from the lightcone gauge fixing condition. Even though in cases where the quantization itself is done in the covariant Feynman gauge, this approach towards the determination of the squared amplitude is sometimes referred to as "working lightcone gauge".

The second possibility follows the "spirit" of BRST quantization. Thereby, all polarizations are included by using $-g^{\mu\nu}$ for the polarization sum as in QED and the cancellation of the unphysical degrees of freedom then proceeds through the inclusion of ghosts. The second option will be explained in more detail in the following. The basic approach is to derive a set of Slavnov-Taylor identities which relate the amplitude $\mathcal{M}_{\text{LO}}^{\mu\nu}$ to ghost amplitudes which are then used to replace the longitudinal polarizations $\epsilon_\mu(L, k) \sim k_\mu$ appearing in the polarization

tensor $d^{\mu\nu}(k_1, k_2)$. The first step is to derive the mentioned identities. For this, consider the four-point Green's function

$$\langle \Omega | T \{ \tilde{q}(x_1) \tilde{q}^*(x_2) \bar{c}_a(y_1) A_b^\nu(y_2) \} | \Omega \rangle = 0 \quad (7.14)$$

which vanishes because there must always appear an even number of ghosts and anti-ghosts in a scattering process by conservation of the ghost number². Application of the BRS-transformations yields

$$\begin{aligned} & \langle \Omega | T \{ (\delta_B \tilde{q}(x_1)) \tilde{q}^*(x_2) \bar{c}_a(y_1) A_b^\nu(y_2) \} | \Omega \rangle \\ & + \langle \Omega | T \{ \tilde{q}(x_1) (\delta_B \tilde{q}^*(x_2)) \bar{c}_a(y_1) A_b^\nu(y_2) \} | \Omega \rangle \\ & + \langle \Omega | T \{ \tilde{q}(x_1) \tilde{q}^*(x_2) (\delta_B \bar{c}_a(y_1)) A_b^\nu(y_2) \} | \Omega \rangle \\ & - \langle \Omega | T \{ \tilde{q}(x_1) \tilde{q}^*(x_2) \bar{c}_a(y_1) \delta_B A_b^\nu(y_2) \} | \Omega \rangle = 0. \end{aligned} \quad (7.15)$$

Let us have a closer look at the first correlation function in more detail

$$\begin{aligned} & \langle \Omega | T \{ (\delta_B \tilde{q}_t(x_1)) \tilde{q}_s^*(x_2) \bar{c}_a(y_1) A_b^\nu(y_2) \} | \Omega \rangle \\ & = i T_{tu}^a \langle \Omega | T \{ c_a(x_1) \tilde{q}_u(x_1) \tilde{q}_s^*(x_2) \bar{c}_a(y_1) A_b^\nu(y_2) \} | \Omega \rangle. \end{aligned} \quad (7.16)$$

As we wish to compute S -matrix elements from these Green's functions, they are multiplied with the inverse propagators of the external fields within the LSZ reduction formula which for $\tilde{q}_t(x_1)$ amounts to $i(m_q^2 - p_1^2)$. After the transformation there are two fields with the position x_1 which means that only the sum of the momenta of $\tilde{q}_t(x_1)$ and $c_a(x_1)$ yields the momentum p_1 . Consequently, there will not appear a propagator $\frac{i}{p_1^2 - m_q^2}$ and taking the on-shell limit $p_1^2 \rightarrow m_q^2$ will set the whole contribution from this Green's function to the scattering amplitude to zero. The same considerations apply to the second term as well as the additional field introduced through the transformation of the gluon field within the covariant derivative in eq. (4.29). A similar line of arguments can be found in [47]. After performing the remaining transformations while keeping the LSZ formula in the back of our heads, we arrive at

$$\begin{aligned} & \langle \Omega | T \{ \tilde{q}(x_1) \tilde{q}^*(x_1) \partial_{y_1, \mu} A_a^\mu(y_1) A_b^\nu(y_2) \} | \Omega \rangle \\ & = - \langle \Omega | T \{ \tilde{q} \tilde{q}^* \bar{c}_a(y_1) \partial_{y_2, \nu} c_b(y_2) \} | \Omega \rangle \\ & = \langle \Omega | T \{ \tilde{q} \tilde{q}^* \partial_{y_2, \nu} c_b(y_2) \} \bar{c}_a(y_1) | \Omega \rangle \end{aligned} \quad (7.17)$$

where the anti-ghost field was commuted to the right³ in order to ensure that all Wick contractions can be performed without introducing a new overall minus sign that would contradict the Feynman rules. The same steps apply to the four-point function

$$\langle \Omega | T \{ \tilde{q}(x_1) \tilde{q}^*(x_2) A_a^\mu(y_1) \bar{c}_b(y_2) \} | \Omega \rangle = 0 \quad (7.18)$$

such that its BRS-transformation gives

$$\begin{aligned} & \langle \Omega | T \{ \tilde{q}(x_1) \tilde{q}^*(x_2) A_a^\mu(y_1) \partial_{y_2, \nu} A_b^\nu(y_2) \} | \Omega \rangle \\ & = \langle \Omega | T \{ \tilde{q}(x_1) \tilde{q}^*(x_1) \partial_{y_1, \mu} c_a(y_1) \bar{c}_b(y_2) \} | \Omega \rangle. \end{aligned} \quad (7.19)$$

²The ghost Lagrangian is invariant under a conformal transformation $c \rightarrow e^\theta c$, $\bar{c} \rightarrow e^{-\theta} \bar{c}$ with an arbitrary real parameter θ . The resulting conserved quantum number is the ghost number which counts every ghost as +1 and every anti-ghost as -1 [24].

³Recall that fermionic fields anticommute within a time-ordered product.

As a last step we can transform both relations to momentum space via LSZ which gives us at lowest order the two Slavnov-Taylor identities

$$k_{1,\mu} \mathcal{M}_{L0}^{\mu\nu} = -k_2^\nu \mathcal{S}_1^{L0} \quad (7.20)$$

$$k_{2,\nu} \mathcal{M}_{L0}^{\mu\nu} = -k_1^\mu \mathcal{S}_2^{L0} \quad (7.21)$$

where \mathcal{S}_1^{L0} and \mathcal{S}_2^{L0} are the leading order amplitudes associated with the two different ghost processes. The corresponding diagrams are shown in fig. 7.2. The additional minus sign in eqs. (7.20) and (7.21) compared to eqs. (7.17) and (7.19) comes from the antihermiticity of the anti-ghost field.

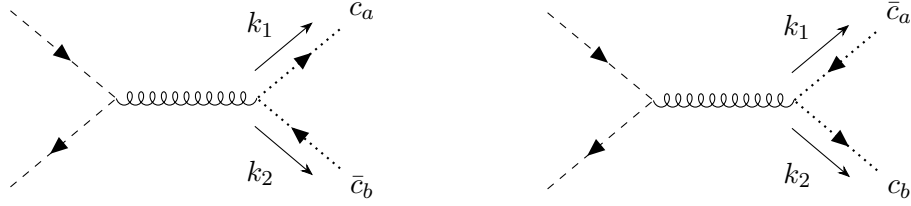


Figure 7.2: Leading order Feynman diagrams for the amplitudes \mathcal{S}_1^{L0} (left) and \mathcal{S}_2^{L0} (right).

If we now use the Feynman rules for ghosts to write down the amplitudes

$$\mathcal{S}_1^{L0} = \frac{ig_s^2}{s} c_{st,ab}^{(8_A)} k_1 \cdot (p_1 - p_2) = \frac{ig_s^2}{2s} c_{st,ab}^{(8_A)} (u - t) \quad (7.22)$$

$$\mathcal{S}_2^{L0} = \frac{-ig_s^2}{s} c_{st,ab}^{(8_A)} k_2 \cdot (p_1 - p_2) = \frac{ig_s^2}{2s} c_{st,ab}^{(8_A)} (u - t) \quad (7.23)$$

we realize that we have already verified the two Slavnov-Taylor identities by explicit computation in eq. (7.12) and eq. (7.13). These identities can now be used to replace the longitudinal polarizations within the sum over the transverse polarizations

$$\sum_{\lambda_1, \lambda_2=1}^2 \mathcal{M}_{LO}^{\mu\nu} \mathcal{M}_{LO}^{*\alpha\beta} \epsilon_\mu^*(\lambda_1, k_1) \epsilon_\nu^*(\lambda_2, k_2) \epsilon_\alpha(\lambda_1, k_1) \epsilon_\beta(\lambda_2, k_2) \quad (7.24)$$

$$= \mathcal{M}_{\mu\nu}^{LO} \mathcal{M}_{*\alpha\beta}^{LO} \left(-g^{\mu\alpha} + \frac{k_2^\mu k_1^\alpha + k_1^\mu k_2^\alpha}{k_1 \cdot k_2} \right) \left(-g^{\nu\beta} + \frac{k_1^\nu k_2^\beta + k_2^\nu k_1^\beta}{k_1 \cdot k_2} \right) \quad (7.25)$$

$$= \mathcal{M}_{LO}^{\mu\nu} \mathcal{M}_{\mu\nu}^{LO*} - \mathcal{S}_1^{LO*} \mathcal{S}_2^{LO} - \mathcal{S}_1^{LO} \mathcal{S}_2^{LO*} = \mathcal{M}_{LO}^{\mu\nu} \mathcal{M}_{\mu\nu}^{LO*} + |\mathcal{S}_1^{LO} - \mathcal{S}_2^{LO}|^2 - |\mathcal{S}_1^{LO}|^2 - |\mathcal{S}_2^{LO}|^2 \quad (7.26)$$

$$= \mathcal{M}_{LO}^{\mu\nu} \mathcal{M}_{\mu\nu}^{LO*} - |\mathcal{S}_1^{LO}|^2 - |\mathcal{S}_2^{LO}|^2 \quad (7.27)$$

where it is easy to see from eqs. (7.22) and (7.23) that the difference of the ghost amplitudes vanishes

$$\mathcal{S}_1^{L0} - \mathcal{S}_2^{L0} = 0. \quad (7.28)$$

Thus, we have finally found that the squared amplitude at leading order can also be determined by using the naive approach $-g^{\mu\nu}$ for the polarization sum, but it is therefore necessary to introduce two ghost processes whose amplitudes are squared with themselves and then subtracted. This calculation also shows that the ghost contributions receive the same normalization factor as the actual process. Now that all physical states in the helicity

space have been summed, the sum over the colours remains. For this purpose, the colour normalized amplitudes

$$|\hat{\mathcal{M}}^{(R)}|^2 = ||c^{(R)}||^2 |\mathcal{M}^{(R)}|^2 \quad (7.29)$$

are defined where the norms are given in eq. (6.53). The absolute value $|\mathcal{M}^{(R)}|^2$ is defined to also contain the sum over all Lorentz indices. In the last step it is necessary to perform the phase space integration over the scattering angle ϑ to arrive at the total cross section

$$\sigma^{(R)} = \frac{1}{F} \int |\hat{\mathcal{M}}^{(R)}|^2 d\Phi_2(k_1, k_2; p_a, p_b) \quad (7.30)$$

with the two-particle phase space in the center-of-mass frame

$$\int d\Phi_2(k_1, k_2; p_a, p_b) = \int_{-1}^1 \frac{1}{16\pi} d\cos\vartheta \quad (7.31)$$

and the flux $F = 4p_1^0 p_2^0 v = 2\sqrt{\lambda(s, m_q^2, m_q^2)}$ where v is the relative velocity between the two initial squarks

$$v = \left| \frac{\vec{p}_a}{p_a^0} - \frac{\vec{p}_b}{p_b^0} \right| = |\vec{v}_a - \vec{v}_b|. \quad (7.32)$$

In order to be able to perform the integration, the Mandelstam variables t and u are expressed through θ

$$t/u = \frac{-s}{2} + m_q^2 \pm 2\cos(\vartheta) \sqrt{\frac{s}{4} - m_q^2} \sqrt{\frac{s}{4}} \quad (7.33)$$

such that one arrives after the integration at the colour decomposed cross sections

$$\sigma^{(1)} = \frac{8\pi\alpha_s^2}{27s\beta^2} (\beta(1+\rho) + \rho(\rho-2) \operatorname{atanh}(\beta)) \quad (7.34)$$

$$\sigma^{(8_S)} = \frac{5}{2} \sigma^{(1)} \quad (7.35)$$

$$\sigma^{(8_A)} = \frac{4\pi\alpha_s^2}{9s\beta^2} (\beta(1+8\rho) - 3\rho(\rho+2) \operatorname{atanh}(\beta)) \quad (7.36)$$

with $\rho = 4m_{\tilde{q}_i^\alpha}/s$ and $\beta = \sqrt{1-\rho}$. In the context of dark matter relic abundance calculations the quantity σv is more interesting since it appears in the thermal average $\langle\sigma_{\text{eff}}v\rangle$. As we have in the CM frame

$$p_a^0 = \sqrt{p_{\text{cm}}^2 + m_q^2} = p_b^0 = \sqrt{s} \quad (7.37)$$

with the CM momentum p_{cm} the cross section weighted with velocity is simply $v\sigma = \beta/2\sigma$.

7.2 Selection of scenarios in the pMSSM

In order to select scenarios that take into account the constraints of the most important experimental searches for supersymmetry, the results of an analysis by the ATLAS collaboration performed within the pMSSM are used [48]. The collaboration started with 5×10^8 samples of the pMSSM parameter space from which 300 000 viable points remain after applying exclusion limits from ATLAS searches, requiring that the neutralino relic density is less than 0.1208 and imposing further constraints from other precision observables such as $(g-2)_\mu$ and $b \rightarrow s\gamma$.

In order to find scenarios which are in accordance with the assumption of DM@NLO that the lightest neutralino accounts for the whole dark matter content in the universe and where the annihilation of the lightest stop plays an important role, we impose two more cuts on the viable points. To fulfill the first assumption points with $0.114 \leq \Omega_{\tilde{\chi}_1^0} h^2 \leq 0.126$ are selected which corresponds to a conservative 5σ -interval of eq. (3.2). The relic density is computed with `micrOMEGAS 2.4.1` [49] which takes as input the original SUSY Les Houches Accord 2 [50] files provided by the ATLAS collaboration within which the physical mass spectrum is computed with `SoftSUSY 3.4.0` [51]. The parameter points that remain after this cut in the $m_{\tilde{t}_1} - m_{\tilde{\chi}_1^0}$ mass plane are shown in section 7.2 subdivided into bino-, higgsino- and wino-like neutralinos. The categorization into these three different types follows the definition in [48]. To ensure that the annihilation of stop makes a significant contribution to the effective cross section, the second cut excludes all parameter points which do not feature the lightest stop as NLSP. The remaining parameter points are depicted in section 7.2 where it becomes obvious that under these conditions only bino-like neutralinos remain. From these points two reference

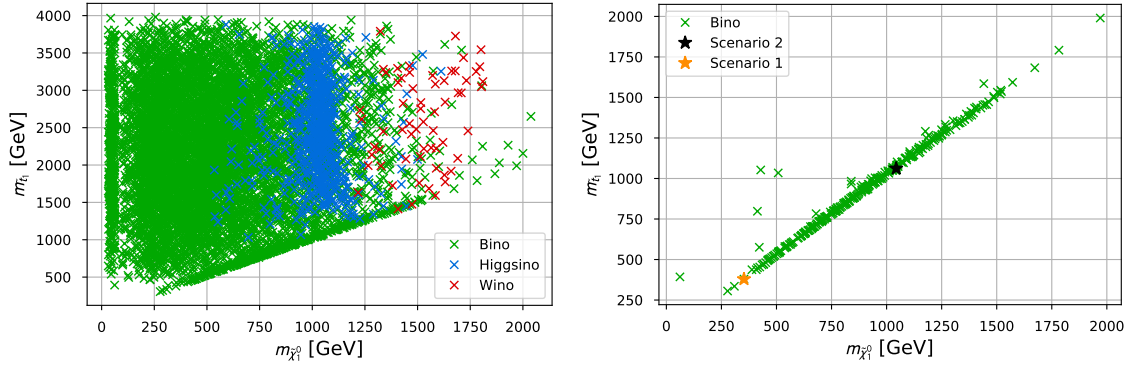


Figure 7.3: ATLAS points in the $m_{\tilde{t}_1} - m_{\tilde{\chi}_1^0}$ mass plane with the two additional constraints explained in the text.

scenarios are selected whose associated 19 pMSSM parameters defined at a scale Q_{SUSY} are given in table 7.1. The corresponding physical mass spectrum is displayed in table 7.2 for

	I	II
M_1	350.88	-1046.58
M_2	1397.86	-3942.8
M_3	2471.74	3637.32
A_t	-1946.61	3833.12
A_b	2616.21	-1492.51
A_τ	-2742.65	676.78
$M_{\tilde{t}_L}$	2976.18	3397.18
$M_{\tilde{\tau}_L}$	2019.22	3927.05
$M_{\tilde{t}_R}$	3146.26	2867.94
$M_{\tilde{\tau}_R}$	2495.18	1661.57

	I	II
$M_{\tilde{q}_L}$	3188.43	3459.34
$M_{\tilde{q}_{3L}}$	522.26	3620.61
$M_{\tilde{u}_R}$	2239.76	2375.07
$M_{\tilde{t}_R}$	1573.94	1008.22
$M_{\tilde{d}_R}$	1381.7	2845.0
$M_{\tilde{b}_R}$	1730.6	3045.87
μ	655.09	1928.59
$\tan \beta$	41.31	53.09
m_{A^0}	3877.15	2401.96
Q_{SUSY}	896.42	1909.68

Table 7.1: Reference scenarios in the pMSSM. All dimensionful quantities are given in GeV.

the spectrum generator used by the ATLAS collaboration and `SPheno 3.3.3` [9] which is

the standard spectrum generator in the DM@NLO setup. There appears a surprising difference

		$m_{\tilde{\chi}_1^0}$	$m_{\tilde{\chi}_2^0}$	$m_{\tilde{\chi}_1^\pm}$	$m_{\tilde{t}_1}$	$m_{\tilde{b}_1}$	m_{h^0}	$\Omega_{\tilde{\chi}_1^0} h^2$
I	SoftSUSY 3.4.0	352.34	657.21	658.06	379.13	405.47	124.45	0.120
	SPheno 3.3.3	352.35	657.14	657.84	344.24	373.08	123.94	-
II	SoftSUSY 3.4.0	1043.55	1937.89	1937.90	1061.97	3089.04	127.56	0.121
	SPheno 3.3.3	1043.51	1937.19	1937.17	1070.57	3095.72	127.17	0.158

Table 7.2: Physical mass spectrum for the two scenarios defined in table 7.1 computed with two spectrum generators as well the relic density from micrOMEGAS 2.4.1. All dimensionful quantities are given in GeV.

between both spectrum generators for the masses of for third-generation squarks of more than 30 GeV for scenario I and of more than 5 GeV for scenario II. For SPheno, in scenario I the mass of the stop is even below that of the neutralino, so that the neutralino is no longer a dark matter candidate and no relic density can be specified, while for scenario II the stop is already too heavy to allow efficient coannihilation, so that there occurs an overproduction of neutralinos. This shows that a set of soft-breaking parameters can lead to two completely different phenomenologies depending on the spectrum generator and that it is always necessary to specify the spectrum generator used as well as the resulting mass spectrum. This also raises the question whether model points that were discarded by the ATLAS collaboration would become viable points when using a different spectrum generator.

7.3 Numerical analysis

The contributions of different channels to $\sigma_{\text{ann}} \sim (\Omega h^2)^{-1}$ can also be computed with micrOMEGAS and are displayed for the two reference scenarios in table 7.3. For both scenarios

Contributing channel	Scenario I	Scenario II
$\tilde{t}_1 \tilde{t}_1^* \rightarrow g g$	50.5 %	61.4 %
$\tilde{t}_1 \tilde{t}_1 \rightarrow t t$	-	5.0 %
$\tilde{t}_1 \tilde{b}_1 \rightarrow t b$	2.0 %	-
$\tilde{\chi}_1^0 \tilde{t}_1 \rightarrow g t$	6.6 %	14.6 %
$\tilde{\chi}_1^0 \tilde{t}_1 \rightarrow W^+ b$	2.6 %	-
$\tilde{t}_1 \tilde{t}_1^* \rightarrow Z^0 g$	9.1 %	2.6 %
$\tilde{t}_1 \tilde{t}_1^* \rightarrow \gamma g$	6.4 %	8.7 %
$\tilde{t}_1 \tilde{t}_1^* \rightarrow h^0 h^0$	2.4 %	-
$\tilde{t}_1 \tilde{b}_1^* \rightarrow W^+ g$	5.9 %	-

Table 7.3: Dominant annihilation channels contributing to $(\Omega h^2)^{-1}$ for the mass spectrum obtained with SoftSUSY 3.4.0 and the cross sections provided by micrOMEGAS 2.4.1 where contributions below 2 % are omitted.

$\tilde{t}_1 \tilde{t}_1^* \rightarrow g g$ contributes more than 50 % and represents the most important channel. With the knowledge that stop annihilation in gluons is an important process, we can discuss aspects of

the tree level cross section. The leading order cross section as well as its singlet, symmetric

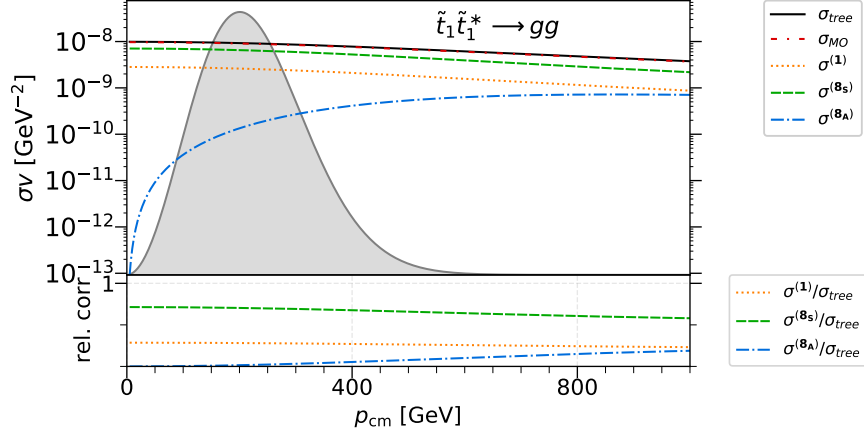


Figure 7.4: The upper panel shows the leading-order cross section σv as a function of the center-of-mass momentum p_{cm} computed with **micrOMEGAs** (MO) and **DM@NLO** (tree) as well as the subdivision into the three different colour channels. Their respective relative contribution to σ_{tree} is display in the lower panel.

octet and antisymmetric octet contributions are shown in fig. 7.4 along with the result from **micrOMEGAs**. The small deviation between the σ_{MO} and σ_{tree} results from a different precision in the strong coupling. As the cross section is invariant under the exchange of the two gluons, the partial wave of the antisymmetric octet is a p -wave which causes the dominance of the singlet and symmetric octet cross section as both contain s -wave contributions.

8 Computation of the next-to-leading order corrections

A next-to-leading order calculation consists in general of two main building blocks which are virtual and real corrections. Virtual corrections have the same initial and final states as the tree process but contain the exchange as well as creation and annihilation of virtual particles. For the process considered in this work the virtual corrections are $2 \rightarrow 2$ processes with the same kinematics and phase space as the tree process. All the different Feynman diagrams that reflect these quantum effects share divergent integrals over the undetermined virtual particle's momentum. These infinities occur at high energies (UV divergences) as well as at low energies (IR divergences). Their treatment requires the computational machinery of regularization to parametrize the divergence in the form of some artificially introduced quantity. The UV divergences are then removed through a procedure called renormalization whereas the infrared divergences in the loop integrals should cancel against those which appear through the phase space integration over the real emission matrix element squared.

8.1 Regularization and one-loop integrals

The essence behind regularization is to introduce new quantities into the theory that parameterize the divergence such that all integrals converge but the original divergence is recovered if these new quantities are set back to zero. As an example consider the correction of a fermion loop to the Higgs propagator

$$i\Sigma(p^2) = \text{---}\text{---}\text{---} \circlearrowleft \text{---}\text{---}\text{---} = (i\lambda)^2 \int \frac{d^4q}{(2\pi)^4} \frac{\text{Tr}[(\not{q} + m)(\not{q} + \not{p} + m)]}{(q^2 - m^2 + i\epsilon)((q+p)^2 - m^2 + i\epsilon)} \quad (8.1)$$

where the coupling is just denoted as λ . If we count the power of the loop momenta we get six in the numerator (including the integration measure d^4q) and four in the denominator. For high loop momenta this approximation leaves the integral

$$\int d^4q \frac{1}{q^2} \sim \infty \quad (8.2)$$

which scales quadratically with the loop momentum after the integration and is therefore called to be quadratic divergent. This idea of power counting leads to the concept of the superficial degree of divergence D defined as the difference of the number of loop momenta in the numerator and denominator

$$D = \# \text{ of momenta in the numerator} - \# \text{ of momenta in the denominator} \quad (8.3)$$

which states that an integral diverges logarithmically for $D = 0$, as a polynomial for $D > 0$ and converges if $D < 0$. However, these assignments hold only if all loop momenta diverge at the same rate and if each propagator contains at least one divergent 4-momentum. Therefore,

the superficial degree of divergence should be applied with care to decide whether a diagram is UV convergent or not.

The simplest way to apply regularization and parametrize the divergence is to impose an upper limit $\Lambda < \infty$ on the momentum of the fermion such that

$$\int_0^\Lambda dq q = \Lambda^2 \quad (8.4)$$

is finite. This method is known as the cutoff method but has the clear disadvantage of violating Lorentz invariance as the value of the cutoff depends on the frame of reference.

8.1.1 Dimensional regularization

A modern regularization procedure which respects not only Lorentz but also gauge invariance as well as unitarity and was even awarded with a Nobel Prize in 1999 is dimensional regularization invented by 't Hooft and Veltmann [52]. The key observation is that an integral as in eq. (8.1) diverges in four but not in less than four dimensions. For this reason, the dimension is used as regularization parameter and the loop integrals are analytically continued to a complex number of dimensions $D = 4 - 2\varepsilon$. The divergences manifest themselves as poles in the complex plane. In order to ensure that the mass dimension of the integrals remains unchanged, one has to introduce an artificial scale μ with mass dimension $[\mu] = 1$ so that integration measure in D dimensions reads

$$\int \frac{d^4 q}{(2\pi)^4} \rightarrow \mu^{2\varepsilon} \int \frac{d^D q}{(2\pi)^D}. \quad (8.5)$$

where the factor $\frac{1}{(2\pi)^D}$ is conventional. As we work in D dimensions, Lorentz indices take values from zero to $D - 1$ such that components of a momentum vector become

$$q^\mu = (q^0, q^1, \dots, q^{D-1}) \quad (8.6)$$

and the trace of the metric tensor evaluates to $g^\mu_\mu = D$ instead of four. The Dirac γ -matrices are kept four-dimensional by definition $\text{Tr}(\gamma^\mu \gamma^\nu) = 4g^{\mu\nu}$.

8.1.2 Scalar n -point functions and Passarino-Veltman reduction

A central method for calculating one-loop integrals is the so-called Passarino-Veltman reduction [53] which is presented in a very pedagogical way in [54]. The starting point is that a general one-loop integral

$$T_{\mu_1, \dots, \mu_M}^N(p_1, \dots, p_{N-1}, m_0, \dots, m_{N-1}) = \frac{(2\pi\mu)^{2\varepsilon}}{i\pi^2} \int d^D q \frac{q_{\mu_1} \dots q_{\mu_M}}{\mathcal{D}_0 \mathcal{D}_1 \dots \mathcal{D}_{N-1}} \quad (8.7)$$

with N propagators

$$\mathcal{D}_0 = q^2 - m_0^2 + i\epsilon \quad (8.8)$$

$$\mathcal{D}_1 = (q + p_1)^2 - m_1^2 + i\epsilon \quad (8.9)$$

$$\dots \quad (8.10)$$

$$\mathcal{D}_{N-1} = (q + p_{N-1})^2 - m_{N-1}^2 + i\epsilon \quad (8.11)$$

in the denominator and M four-momenta $q_{\mu_1}, \dots, q_{\mu_M}$ in the numerator can be reduced to four scalar integrals ($M = 0$) called A_0 , B_0 , C_0 and D_0 which just follow from the redefinitions $T^1 \rightarrow A_0$, $T^2 \rightarrow B_0$, $T^3 \rightarrow C_0$ and $T^4 \rightarrow D_0$. Their argument sets in `DM@NLO` follow the convention specified in [30]

$$A_0(m_0^2) = \int_q \frac{1}{\mathcal{D}_0} \quad (8.12)$$

$$B_0(p_1^2, m_0^2, m_1^2) = \int_q \frac{1}{\mathcal{D}_0 \mathcal{D}_1} \quad (8.13)$$

$$C_0(p_1^2, (p_1 - p_2)^2, p_2^2, m_0^2, m_1^2, m_2^2) = \int_q \frac{1}{\mathcal{D}_0 \mathcal{D}_1 \mathcal{D}_2} \quad (8.14)$$

$$D_0(p_1^2, (p_2 - p_1)^2, (p_3 - p_2)^2, p_3^2, p_2^2, (p_3 - p_1)^2, m_0^2, m_1^2, m_2^2, m_3^2) = \int_q \frac{1}{\mathcal{D}_0 \mathcal{D}_1 \mathcal{D}_2 \mathcal{D}_3} \quad (8.15)$$

where the shorthand

$$\int_q = \frac{(2\pi\mu)^{2\varepsilon}}{i\pi^2} \int d^D q \quad (8.16)$$

is employed. The decomposition of a tensor integral is performed by considering all symmetric and covariant tensor structures of rank M that can be built out of the momenta p_1, \dots, p_{N-1} and metric tensors, i.e.

$$\begin{aligned} B^\mu &= p_1^\mu B_1 \\ B^{\mu\nu} &= g^{\mu\nu} B_{00} + p_1^\mu p_1^\nu B_{11} \\ C^\mu &= p_1^\mu C_1 + p_2^\mu C_2 \\ C^{\mu\nu} &= g^{\mu\nu} C_{00} + \sum_{i,j=1}^2 p_i^\mu p_j^\nu C_{ij} \\ C^{\mu\nu\rho} &= \sum_{i=1}^2 (g^{\mu\nu} p_i^\rho + g^{\mu\rho} p_i^\nu + g^{\nu\rho} p_i^\mu) C_{00i} + \sum_{i,j,k=1}^2 p_i^\mu p_j^\nu p_k^\rho C_{ijk} \\ &\dots \end{aligned} \quad (8.17)$$

The coefficients B_1 , B_{00} , B_{11} and so on are called Passarino-Veltman coefficient functions and are computed through the following two steps:

1. Contraction of the decomposition into covariant quantities with external momenta and metric tensors where squares q^2 of the loop momentum are combined with artificially introduced masses ($q^2 = (q^2 - m^2) + m^2$) so that they cancel against the denominators.
2. Solving the linear system of equations for to the coefficient functions.

Having performed this reduction, it is still necessary to compute the scalar integrals. As an example on how to solve such an integral within dimensional regularization, we consider the simplest case

$$A_0(m^2) = \frac{(2\pi\mu)^{2\varepsilon}}{i\pi^2} \int d^D q \frac{1}{q^2 - m^2 + i\epsilon} \quad (8.18)$$

following the path outlined in [30]. The integrand of this function is complex and has poles at

$$q_0^2 = \pm \sqrt{\vec{q}^2 + m^2} \mp i\epsilon. \quad (8.19)$$

Their position in the complex plane allows to change the integration over q_0 from the real to the imaginary axis through the application of Cauchy's integral theorem. This transformation corresponds to a change from Minkowski to Euclidean space as we have $q_0 = i q_{E,0}$ and $\vec{q} = \vec{q}_E$ which changes q^2 in the denominator to

$$q^2 = q_0^2 - \vec{q}^2 = -q_{E,0}^2 - \vec{q}_E^2 = -q_E^2 \quad (8.20)$$

where q_E is the new integration variable that parametrizes the integration along the imaginary axis. After this change the integrand depends only on the absolute value of the "Euclidean" vector $q_E = (q_{E,0}, \vec{q}_E)$ which means that the integral can be greatly simplified by switching to spherical coordinates

$$\int d^D q = i \int d\Omega_D \int_0^\infty dq_E q_E^{D-1} = \frac{1}{2} \int d\Omega_D \int_0^\infty dq_E^2 (q_E^2)^{\frac{D}{2}-1} \quad (8.21)$$

with the D -dimensional solid angle [18]

$$\Omega_D = \int d\Omega_D = \frac{2\pi^{\frac{D}{2}}}{\Gamma(D/2)}. \quad (8.22)$$

The remaining integral can be related to the Eulerian β -function with the help of the substitution

$$t = \frac{-m^2 + i\epsilon}{-q_E^2 - m^2 + i\epsilon}, \quad q_E^2 = (m^2 - i\epsilon) \frac{1-t}{t} \quad (8.23)$$

which gives

$$\begin{aligned} \int dq_E^2 \frac{(-q_E^2)^{\frac{D}{2}-1}}{-q_E^2 - m^2 + i\epsilon} &= (m^2 - i\epsilon)^{\frac{D}{2}-1} \int_0^1 dt t^{-\frac{D}{2}} (1-t)^{\frac{D}{2}-1} \\ &= (m^2 - i\epsilon)^{1-2\varepsilon} \beta(\varepsilon - 1, 2 - \varepsilon). \end{aligned} \quad (8.24)$$

If we collect all terms together, we get

$$A_0(m^2) = \frac{(2\pi\mu)^{2\varepsilon}}{\pi^2} \frac{\pi^{2-\varepsilon}}{\Gamma(2-\varepsilon)} (m^2 - i\epsilon)^{1-\varepsilon} \beta(\varepsilon - 1, 2 - \varepsilon). \quad (8.25)$$

The UV pole in ε can be made visible by relating the β -function to the Gamma function $\beta(\varepsilon - 1, 2 - \varepsilon) = \Gamma(\varepsilon - 1)\Gamma(2 - \varepsilon)$ followed by the application of the recursive property of the Gamma function $\Gamma(1 + \varepsilon) = \varepsilon(\varepsilon - 1)\Gamma(\varepsilon - 1)$ giving

$$A_0(m^2) = -(m^2 - i\epsilon) (4\pi)^\varepsilon \Gamma(1 + \varepsilon) \left(\frac{m^2 - i\epsilon}{\mu^2} \right)^{-\varepsilon} \frac{1}{\varepsilon(\varepsilon - 1)}. \quad (8.26)$$

As the one-loop integrals are not multiplied with any further poles, we can safely neglect all terms of $\mathcal{O}(\varepsilon)$. This is achieved through the expansions

$$\left(\frac{m^2 - i\epsilon}{\mu^2} \right)^{-\varepsilon} = 1 - \varepsilon \ln \left(\frac{m^2 - i\epsilon}{\mu^2} \right) + \mathcal{O}(\varepsilon) \quad (8.27)$$

$$\frac{1}{\varepsilon(\varepsilon - 1)} = -\frac{1}{\varepsilon} - 1 + \mathcal{O}(\varepsilon) \quad (8.28)$$

which gives when multiplying everything out

$$A_0(m^2) = m^2 \left(\frac{c_\epsilon}{\epsilon} - \log \left(\frac{m^2}{\mu^2} \right) + 1 + \mathcal{O}(\epsilon) \right). \quad (8.29)$$

The factor

$$c_\epsilon = (4\pi)^\epsilon \Gamma(1 + \epsilon) \quad (8.30)$$

turns out to be a common prefactor for divergent loop integrals and is "defined into the pole" and not expanded any further. This convention applies to all UV and IR poles in **DM@NLO** equally. It is important to realize that the multiplication of a loop integral with D gives an extra finite part

$$(4 - D) A_0(m^2) = 2m^2. \quad (8.31)$$

These factors of D usually occur through traces of the metric tensor g^μ_μ . To obtain the finite terms, it is of course necessary to know the poles which can be found for a large number of one-loop tensor integrals in a compact form for example in [55]. As the loop library of **DM@NLO** is already quite comprehensive, it was only necessary to include the argument set $D_0(0, 0, m_3^2, m_3^2, p_2^2, (p_3 - p_1)^2, 0, 0, 0, m_3^2)$ given in [56] as new special case and to compare it with **LoopTools** [57]. However, the integrals in **LoopTools** are defined with a different prefactor $\frac{\mu^{4-D}}{i\pi^{2-\epsilon}\Gamma}$ with $r_\Gamma = \frac{\Gamma(1-\epsilon)^2\Gamma(\epsilon+1)}{\Gamma(1-2\epsilon)}$ which requires the following conversion

$$I_{\mu_1, \dots, \mu_M}^{N; \text{DM@NLO}} = c_\epsilon \frac{\Gamma(1-\epsilon)^2}{\Gamma(1-2\epsilon)} I_{\mu_1, \dots, \mu_M}^{N; \text{LoopTools}} = c_\epsilon \left(1 - \frac{\pi^2}{6} \epsilon^2 \right) I_{\mu_1, \dots, \mu_M}^{N; \text{LoopTools}} + \mathcal{O}(\epsilon) \quad (8.32)$$

where c_ϵ is effectively treated as a one.

8.1.3 Variants of dimensional regularization and dimensional reduction

Even though its many advantageous features, dimensional regularization as described in section 8.1.1 has the drawback of breaking supersymmetry as in D dimensions a vector boson has $D - 2$ degrees of freedom which are then mapped under supersymmetry to a Majorana spinor with 2 degrees of freedom. This mismatch was originally pointed out by Siegel who proposed regularization by dimensional reduction (DRED) as a variant of dimensional regularization which should preserve supersymmetry [58]. Within this regularization scheme the number of dimensions of all momenta and space time coordinates is analytically continued from four to D whereas the number of components of all other tensors, spinors and γ -matrices remains fixed.

In order to avoid potential mathematical inconsistencies within DRED that were also outlined by Siegel himself [59] and to formulate the two schemes in a consistent manner it is necessary to introduce three different spaces which are characterized by their metric tensors [60, 61, 62]. The original four-dimensional space (4S) with metric $\bar{g}^{\mu\nu}$, a quasi-four-dimensional space (Q4S) with metric tensor $g^{\mu\nu}$ for e.g. gluons in dimensional reduction and a quasi-D-dimensional space (QDS) with metric $\hat{g}^{\mu\nu}$ as a subspace of Q4S. By construction, Q4S can be decomposed into the direct sum of QDS and its $4 - D = 2\epsilon$ -dimensional complement called $Q\epsilon S$

$$\text{Q4S} = \text{QDS} \oplus \text{Q}\epsilon\text{S} \quad (8.33)$$

which induces the metric $\tilde{g}^{\mu\nu}$ with $g^{\mu\nu} = \hat{g}^{\mu\nu} + \tilde{g}^{\mu\nu}$. The dimensionality of the space becomes apparent through the traces

$$\bar{g}_{\mu\nu}\bar{g}^{\mu\nu} = g_{\mu\nu}g^{\mu\nu} = 4 \quad \hat{g}_{\mu\nu}\hat{g}^{\mu\nu} = D \quad \tilde{g}_{\mu\nu}\tilde{g}^{\mu\nu} = 2\varepsilon. \quad (8.34)$$

The projection relations

$$g_{\mu\nu}\hat{g}^\nu{}_\rho = \hat{g}_{\mu\rho} \quad \bar{g}_{\mu\nu}g^\nu{}_\rho = \bar{g}_{\mu\rho} \quad \bar{g}_{\mu\nu}\hat{g}^\nu{}_\rho = \bar{g}_{\mu\rho} \quad g_{\mu\nu}\tilde{g}^\nu{}_\rho = \tilde{g}_{\mu\rho} \quad \hat{g}_{\mu\nu}\tilde{g}^\nu{}_\rho = 0$$

show that QDS is a subspace of Q4S and that 4S is a subspace of QDS. This embedding is made possible through the fact that Q4S and QDS are actual infinite dimensional spaces whose properties resemble those of a 4 or D dimensional space. For this reason, we are talking about a *quasi*-four-dimensional space and not a four-dimensional space. Intuitively, D -dimensional quantities can be thought of as four-dimensional but whose remaining 2ε components are zero. Furthermore, this resolves the ambiguity of contracting a partial derivate with a gauge field which itself has four components in dimensional reduction but depends on D space-time coordinates. A quasi-four-dimensional vector t^μ can be projected onto the subspaces using the metrics $\hat{g}^{\mu\nu}$ and $\tilde{g}^{\mu\nu}$ as projection operators

$$t^\mu\hat{g}_\mu{}^\nu = \hat{t}^\nu \quad t^\mu\tilde{g}_\mu{}^\nu = \tilde{t}^\nu. \quad (8.35)$$

In particular, one finds

$$g^{\mu\nu}\hat{t}_\mu\hat{t}_\nu = g^{\mu\nu}\hat{g}_\mu{}^\rho\hat{t}_\rho\hat{t}_\nu = \hat{t}^{\nu\rho}\hat{t}_\rho\hat{t}_\nu = \hat{t}_\nu\hat{t}^\nu = t^2 \quad (8.36)$$

which makes it unnecessary to hat squared momenta. The spinor algebra is introduced in a similar way compared to dimensional regularization by assuming that there exist quasi-four-dimensional γ -matrices that fulfill the anti-commutation relation $\{\gamma^\mu, \gamma^\nu\} = 2g^{\mu\nu}\mathbb{1}$, where the spinor identity element must obey the trace condition $\text{Tr}\mathbb{1} = 4$. Using the projectors defined above the anti-commutation relations of the other components can be deduced:

$$\{\hat{\gamma}^\mu, \hat{\gamma}^\nu\} = 2\hat{g}^{\mu\nu}\mathbb{1} \quad \{\tilde{\gamma}^\mu, \tilde{\gamma}^\nu\} = 2\tilde{g}^{\mu\nu}\mathbb{1} \quad \{\hat{\gamma}^\mu, \tilde{\gamma}^\nu\} = 0. \quad (8.37)$$

Before moving on to the discussion of the γ^5 matrix, it is useful to recall two identities related to the fifth γ -matrix in four dimensions:

$$\{\gamma^5, \gamma^\mu\} = 0 \quad \text{Tr}(\gamma^\mu\gamma^\nu\gamma^\rho\gamma^\sigma\gamma^5) = 4i\varepsilon^{\mu\nu\rho\sigma}. \quad (8.38)$$

The treatment of γ^5 in dimensional reduction is a peculiar as in dimensional regularization due to the infinite-dimensional nature of Q4S and Q4D which makes counting impossible. The problem is that the relations given in eq. (8.38) are not compatible with each other in $D \neq 4$ -dimensions. Two approaches have developed to deal with this problem. The t'Hooft-Veltman-Breitenlohner-Maison scheme (HVBM) [63] defines γ^5 as an element of 4S $\bar{\gamma}^5 = i\gamma^1\gamma^2\gamma^3\gamma^4$ and, consequently, insists on the trace condition, whereas the naive scheme (NS) assumes γ^5 to anti-commute with all other γ -matrices

$$\{\gamma^5, \gamma^\mu\} = 0 \quad \{\gamma^5, \hat{\gamma}^\mu\} = 0 \quad \{\gamma^5, \tilde{\gamma}^\mu\} = 0 \quad (8.39)$$

causing a vanishing trace of γ^5 with any number of γ -matrices, i.e.

$$\text{Tr}\left(\gamma^5\prod_{i=0}^n\Gamma^{\mu_i}\right) = 0 \text{ with } \Gamma^\mu = \gamma^\mu, \tilde{\gamma}^\mu \text{ or } \hat{\gamma}^\mu \quad (8.40)$$

for any n . To fix this wrong result the trace can be constrained to obey the condition

$$\text{Tr}(\Gamma^\mu \Gamma^\nu \Gamma^\rho \Gamma^\sigma \gamma^5) = 4i\tilde{\varepsilon}^{\mu\nu\rho\sigma} + \mathcal{O}(\varepsilon) \quad (8.41)$$

where the tensor $\tilde{\varepsilon}^{\mu\nu\rho\sigma}$ is completely antisymmetric in all indices and gives the following result when being contracted with itself

$$\tilde{\varepsilon}^{\alpha\beta\gamma\delta}\tilde{\varepsilon}_{\rho\sigma\mu\nu} = G^{[\alpha}_{[\rho} G^\beta_{\sigma} G^\gamma_{\mu} G^{\delta]}_{\nu]} \quad (8.42)$$

to ensure that $\tilde{\varepsilon}^{\mu\nu\rho\sigma}$ converts into the four-dimensional Levi-Civita symbol in the limit $D \rightarrow 4$. The square brackets denote the usual complete antisymmetrization symbol and $G^{\mu\nu}$ stands for the metric tensor depending on the Γ^μ 's in the trace. More information on the treatment of γ^5 in the different schemes is available in [64, 61]. In connection with SUSY and DRED the HVBM-scheme has the disadvantage that supersymmetry in the case of the MSSM is already broken at one-loop level [61]. Both definitions have the property

$$\gamma_5^2 = \mathbb{1} \quad \bar{\gamma}_5^2 = \mathbb{1} \quad (8.43)$$

which guarantees the orthogonality $P_L P_R = P_R P_L = 0$ and idempotency $P_L^2 = P_L$, $P_R^2 = P_R$ of the chiral projection operators:

$$P_L = \frac{1}{2}(\mathbb{1} - \gamma^5) \quad P_R = \frac{1}{2}(\mathbb{1} + \gamma^5) . \quad (8.44)$$

The NS-scheme is mostly used in DRED and is also applied in this work¹.

With these definitions at hand it is now possible to describe the different computational rules for dimensional regularization and dimensional reduction. As the momenta are kept D -dimensional in both schemes it remains to be specified how the gluons are treated, i.e. to what space the metric tensors in the propagator, vertices and polarization sum belong. As it is not necessary to regulate all gluons, we have to introduce the notion of "internal" and "external" gluons following the definition given in [62]. Within the virtual corrections internal gluons are defined as gluons in a one-particle-irreducible diagram and within the real corrections they are defined as gluon that can become soft or collinear. All other gluons are defined as external gluons. Depending on how the external gluons are treated one can distinguish two subvariants of each scheme. Dimensional regularization has the two variants:

- Conventional dimensional regularization (CDR): Internal and external gluons are treated as D -dimensional.
- 't Hooft-Veltman scheme (HV): External gluons live in 4S whereas internal ones are D -dimensional.

The two variants of dimensional reduction are:

- original/old dimensional reduction (DRED or DR): Internal and external gluons are elements of Q4S.
- Four-dimensional helicity scheme (FDH): External gluons are strictly four-dimensional whereas internal ones are quasi-four-dimensional.

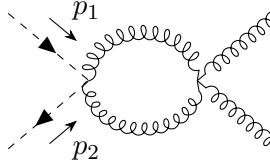
¹Traces of γ^5 with four or more γ -matrices appear within this work during the evaluation of box diagrams containing gluinos. Since the Levi-Civita symbol with four indices gets contracted with external momenta and there exist in a $2 \rightarrow 2$ processes only three linearly independent momenta, these expressions yield zero anyway.

The different metric tensors that are used within these variants are summarized in table 8.1. The analogue of the modified minimal-subtraction renormalization scheme $\overline{\text{MS}}$ in dimensional regularization is called the $\overline{\text{DR}}$ scheme in dimensional reduction.

	CDR	HV	DRED/DR	FDH
internal	$\hat{g}^{\mu\nu}$	$\hat{g}^{\mu\nu}$	$g^{\mu\nu}$	$g^{\mu\nu}$
external	$\hat{g}^{\mu\nu}$	$\bar{g}^{\mu\nu}$	$g^{\mu\nu}$	$\bar{g}^{\mu\nu}$

Table 8.1: Treatment of internal and external gluons in different regularization schemes. Table taken from [62].

In practice, the schemes differ at one-loop level only through additional finite parts coming from extra D 's which are introduced through the contractions of $\hat{g}^{\mu\nu}$'s. As an example consider the 1PI diagram²



$$= i\delta_{ij} \frac{g_s^4}{16\pi^2} \left(c_{st,ab}^{(1)} + \frac{N}{2} c_{st,ab}^{(8s)} \right) \bar{g}^{\mu\nu} \left(-3B_0 \left((p_1 + p_2)^2, 0, 0 \right) + \theta_D 2 \right) \quad (8.45)$$

where an extra finite part occurs depending on whether $\hat{g}^{\mu\nu}$ or $g^{\mu\nu}$ is used for the internal gluons which is indicated through the new parameter θ_D which takes the value one for dimensional regularization (HV) and zero for dimensional reduction (FDH). It is important to realize that also 1PI diagrams in dimensional reduction can give D -dimensional metric tensors from the Passarino-Veltman decomposition

$$\hat{B}^{\mu\nu} = \hat{g}^{\mu\nu} B_{00} + \hat{p}^\mu \hat{p}^\nu B_{11} \quad (8.46)$$

which takes place in QDS. One relation that often appears in this context is

$$g_{\mu\nu} \hat{g}^{\mu\nu} = (\hat{g}_{\mu\nu} + \tilde{g}_{\mu\nu}) \hat{g}^{\mu\nu} = D + \hat{g}^{\mu\nu} \tilde{g}_{\mu\rho} g^\rho{}_\nu = D. \quad (8.47)$$

8.2 Renormalization in DM@NLO

The concept behind renormalization is that every UV divergence can be absorbed into free parameters of a theory which could be the mass of some particle or a coupling constant. This redefinition comes at the prize that the theory loses its predictivity for those observables. Another way to think about renormalization is that the classical or "bare" Lagrangian has no connection to the quantum world, thus, the parameters in the bare Lagrangian are useless to predict quantum effects as they undergo quantum corrections themselves. A simple picture that one can keep in mind is that for example the electron is constantly surrounded by a cloud of electron-positron pairs that are created from the vacuum and therefore these effects have an impact on the charge that is measured. In this sense, the bare parameters have no connection to quantities that can be physically measured and consequently they need to be redefined/renormalized. A gentle introduction to renormalization can be found in [18] and renormalization of pure QCD is discussed in [65].

With the framework of regularization by dimensional reduction, we are now ready to discuss

²The index structure for this diagram is the same as for the tree level calculation shown in fig. 7.1.

how the UV divergences can be removed through renormalization. As only the renormalization of the gluon, squark and ghost sector as well as the renormalization of α_s is relevant for this work to achieve a UV finite result and therefore presented in the following, we refer to earlier works on DM@NLO [33, 66, 67] for other sectors.

8.2.1 Gluon sector

In multiplicative renormalization, the bare gluon field $A_{0,a}^\mu$ is related to the renormalized field A_a^μ through the field strength renormalization constant Z_g . In perturbation theory, Z_g can be expanded around the tree level value $Z_g = 1 + \delta Z_g + \mathcal{O}(g_s^4)$ where Z_g is defined at $\mathcal{O}(g_s^2)$

$$A_{0,a}^\mu = \sqrt{Z_g} A_a^\mu = \left(1 + \frac{1}{2}\delta Z_g\right) A_a^\mu. \quad (8.48)$$

Consequently, the kinetic part of the gluon in the MSSM Lagrangian including the gauge fixing term splits into a renormalized and a counterterm part that absorbs the divergence. The counterterm δZ_g appears as new interaction vertex in the Lagrangian and yields the Feynman rule

$$g_a^\mu \text{-----} \otimes \text{-----} g_b^\nu = -i\delta Z_g \delta_{ab} (p^2 g^{\mu\nu} - p^\mu p^\nu). \quad (8.49)$$

It is convenient to decompose the gluon two-point function at one-loop into a transverse Π_T and a longitudinal part Π_L

$$-i\Pi_{ab}^{\mu\nu}(p^2) = g_a^\mu \text{-----} \text{-----} g_b^\nu = -i\delta_{ab} \left[\left(g^{\mu\nu} - \frac{p^\mu p^\nu}{p^2} \right) \Pi_T(p^2) + \frac{p^\mu p^\nu}{p^2} \Pi_L(p^2) \right], \quad (8.50)$$

where we do not distinguish between $g^{\mu\nu}$, $\hat{g}^{\mu\nu}$, $\bar{g}^{\mu\nu}$ in the decomposition as we use the FDH scheme and all three give the same result when being contracted with $\bar{g}^{\mu\nu}$ from the external gluons.

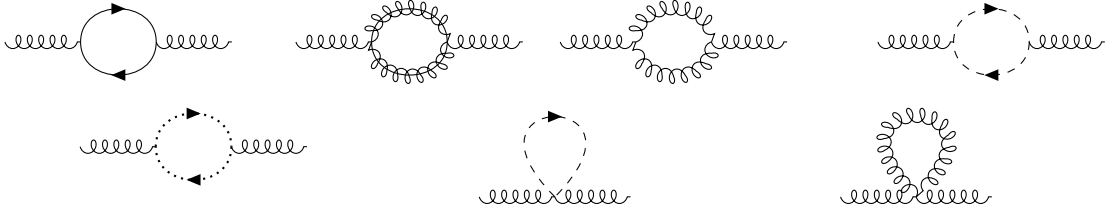


Figure 8.1: One-loop contributions to the gluon self-energy.

The individual contributions to the gluon self-energy are shown in fig. 8.1. The explicit contributions to the transverse and longitudinal part read

$$\Pi_T^{q\bar{q}} = \sum_q \frac{-g_s^2 T_F}{8\pi^2} (2A_0(m_q^2) - 4B_{00}(p^2, m_q^2, m_q^2) - p^2 B_0(p^2, m_q^2, m_q^2)) \quad (8.51)$$

$$\Pi_L^{q\bar{q}} = 0 \quad (8.52)$$

$$\Pi_T^{\tilde{g}\tilde{g}} = \frac{-g_s^2 C_A}{16\pi^2} (2A_0(m_{\tilde{g}}^2) - 4B_{00}(p^2, m_{\tilde{g}}^2, m_{\tilde{g}}^2) - p^2 B_0(p^2, m_{\tilde{g}}^2, m_{\tilde{g}}^2)) \quad (8.53)$$

$$\Pi_L^{\tilde{g}\tilde{g}} = 0 \quad (8.54)$$

$$\Pi_T^{gg} = \frac{-g_s^2 C_A}{16\pi^2} \left(2p^2 B_0(p^2, 0, 0) + 5B_{00}(p^2, 0, 0) + \theta_D \frac{p^2}{3} \right) \quad (8.55)$$

$$\Pi_L^{gg} = \frac{g_s^2 C_A}{64\pi^2} p^2 B_0(p^2, 0, 0) \quad (8.56)$$

$$\Pi_T^{\tilde{q}\tilde{q}^*} = \sum_{\alpha,k} \frac{-g_s^2 T_F}{4\pi^2} B_{00}(p^2, m_{\tilde{q}_k}^2, m_{\tilde{q}_k}^2) \quad (8.57)$$

$$\Pi_T^{\tilde{q}\tilde{q}^*} = \sum_{\alpha,k} \frac{-g_s^2 T_F}{8\pi^2} A_0(m_{\tilde{q}_k}^2) \quad (8.58)$$

$$\Pi_T^{c\bar{c}} = \frac{g_s^2 C_A}{16\pi^2} B_{00}(p^2, 0, 0) \quad (8.59)$$

$$\Pi_L^{c\bar{c}} = -\frac{g_s^2 C_A}{64\pi^2} p^2 B_0(p^2, 0, 0) \quad (8.60)$$

$$\Pi_T^{\tilde{q}} = \Pi_L^{\tilde{q}} = \sum_{\alpha,k} \frac{g_s^2 T_F}{8\pi^2} A_0(m_{\tilde{q}_k}^2) \quad (8.61)$$

$$\Pi_T^g = \Pi_L^g = 0 \quad (8.62)$$

where the superscript denotes the two virtual particles that run in the loop. It is observed that only the sum of the gluon and ghost loop as well as the sum of the squark loop and squark tadpole give a gauge invariant result, i.e. $\Pi_T(p^2) = 0$. Up to order g_s^2 the renormalized gluon two-point Green's function $G_{\mu\nu}^{ab}(p)$ reads then

$$-iG_{\mu\nu}^{ab}(p) = \text{diagram 1} + \text{diagram 2} + \text{diagram 3} + \dots \quad (8.63)$$

$$= \frac{-i\delta^{ab}}{p^2 + i\epsilon} \left(g_{\mu\nu} - \frac{p_\mu p_\nu}{p^2} \right) - \frac{-i\delta^{ac}}{p^2 + i\epsilon} \left(g_{\mu\rho} - \frac{p_\mu p_\rho}{p^2} \right) i\delta^{cd} \left[\left(g_{\rho\sigma} - \frac{p_\rho p_\sigma}{p^2} \right) \right. \quad (8.64)$$

$$\left. \times (\Pi_T(p^2) + \delta Z_g p^2) + \frac{p_\rho p_\sigma}{p^2} \Pi_L(p^2) \right] \frac{-i\delta^{db}}{p^2 + i\epsilon} \left(g_{\sigma\nu} - \frac{p_\sigma p_\nu}{p^2} \right) + \mathcal{O}(g_s^4) \quad (8.65)$$

$$= \frac{-i\delta^{ab}}{p^2 + i\epsilon} \left(g_{\mu\nu} - \frac{p_\mu p_\nu}{p^2} \right) \left(1 - \frac{\Pi_T(p^2) + \delta Z_g p^2}{p^2 + i\epsilon} \right) + \mathcal{O}(g_s^4). \quad (8.66)$$

The gluon is renormalized in the on-shell scheme, which means that the physical mass must be identical to the pole mass. This is achieved by requiring that the renormalized Green's function has a simple pole at $p^2 = -i\epsilon$ with residue 1

$$1 = \text{Res}(G, -i\epsilon) = \lim_{p^2 \rightarrow -i\epsilon} (p^2 + i\epsilon) G(p^2) = \lim_{p^2 \rightarrow -i\epsilon} \left(1 - \frac{\Pi_T(p^2) + \delta Z_g p^2}{p^2 + i\epsilon} \right) \quad (8.67)$$

which adjusts the gluon wave-function renormalization constant to

$$\delta Z_g = -\text{Re} \left(\frac{\partial}{\partial p^2} \Pi_T(p^2) \right) \Big|_{p^2=0} \quad (8.68)$$

after applying L'Hôpital's rule and setting ϵ to zero. From this on-shell condition the different contributions to δZ_g can be deduced

$$\delta Z_g^{q\bar{q}} = \sum_q \frac{-g_s^2 T_F}{12\pi^2} \left(2m_q^2 \dot{B}_0(0, m_q^2, m_q^2) + B_0(0, m_q^2, m_q^2) - \frac{1}{3} \right) \quad (8.69)$$

$$\delta Z_g^{\tilde{g}\tilde{g}} = \frac{-g_s^2 C_A}{24\pi^2} \left(2m_{\tilde{g}}^2 \dot{B}_0(0, m_{\tilde{g}}^2, m_{\tilde{g}}^2) + B_0(0, m_{\tilde{g}}^2, m_{\tilde{g}}^2) - \frac{1}{3} \right) \quad (8.70)$$

$$\delta Z_g^{gg} = \frac{g_s^2 C_A}{576 \pi^2} (57 B_0(0, 0, 0) - 67 + \theta_D 12) \quad (8.71)$$

$$\delta Z_g^{\tilde{q}\tilde{q}^*} = \sum_{\tilde{q}} \frac{-g_s^2 T_F}{48\pi^2} \left(B_0(0, m_{\tilde{q}}^2, m_{\tilde{q}}^2) - 4m_{\tilde{q}}^2 \dot{B}_0(0, m_{\tilde{q}}^2, m_{\tilde{q}}^2) + \frac{2}{3} \right) \quad (8.72)$$

$$\delta Z_g^{c\bar{c}} = \frac{g_s^2 C_A}{576\pi^2} (3B_0(0,0,0) - 1) \quad (8.73)$$

$$\delta Z_g^{\tilde{q}} = \delta Z_g^g = 0. \quad (8.74)$$

For massless particles in the loop one has to be aware of the limits

$$\lim_{p^2 \rightarrow 0} p^2 \dot{B}_0(p^2, 0, 0) = -1 \quad \lim_{m^2 \rightarrow 0} m^2 \dot{B}(0, m^2, m^2) = \frac{1}{6} \quad (8.75)$$

which can be found in [30]. The renormalization constant δZ_g is ultraviolet and infrared divergent. Both parts can be extracted from the Passarino-Veltman functions and yield

$$\delta Z_g^{\text{UV}} = \frac{g_s^2}{16\pi^2 \varepsilon_{\text{UV}}} (C_A - 2T_F n_q) \quad (8.76)$$

$$\delta Z_g^{\text{IR}} = \frac{g_s^2}{48\pi^2 \varepsilon_{IR}} (4N_f T_F - 5C_A) \quad (8.77)$$

where n_q gives the number of quarks included in the loops and N_f the number of quark flavours that are treated as effectively massless.

8.2.2 Squark sector

Having discussed the renormalization of the gluon, we can move on to the squark sector where we have to account for mixing effects. Therefore, the squark wave-function renormalization constant Z_{ij}^q carries indices i, j related to the two squark mass eigenstates of squarks. As squarks are massive we also have to introduce a mass counterterm $\delta m_{q_i}^2$

$$\tilde{q}_{0,i} = \sqrt{Z_{ij}^{\tilde{q}}} \tilde{q}_j = \left(\delta_{ij} + \frac{1}{2} \delta Z_{ij}^{\tilde{q}} \right) \tilde{q}_j \quad (8.78)$$

$$m_{0,\tilde{a}_i}^2 = m_{\tilde{a}_i}^2 + \delta m_{\tilde{a}_i}^2. \quad (8.79)$$

Then we can define the squark two-point function as

$$i\Pi_{i,st}^{\tilde{q},\alpha\beta}(p^2) = \tilde{q}_{i,s}^{\alpha*} \text{---}\overrightarrow{\text{---}}\overbrace{\hspace{1cm}}^p \text{---}\overrightarrow{\text{---}} \text{---}\overrightarrow{\text{---}}\overbrace{\hspace{1cm}}^p \text{---}\overrightarrow{\text{---}} \tilde{q}_{i,t}^{\beta} = i\delta_{st}\delta^{\alpha\beta}\Pi_{ij}(p^2). \quad (8.80)$$

where α, β are flavour, s, t colour and i, j sfermion mass eigenstate indices.



Figure 8.2: Contributions to the squark self-energy at one-loop.

Note that the squark propagator at one loop is symmetric in the sfermion indices i and j . The contributions to the squark self-energy shown in fig. 8.2 read explicitly

$$\Pi_{ij}^{\tilde{g}q}(p^2) = \frac{-g_s^2 C_F}{8\pi^2} \left(\delta_{ij} (A_0(m_{\tilde{g}}^2) + A_0(m_{q^\alpha}^2)) + B_0(p^2, m_{\tilde{g}}^2, m_{q^\alpha}^2) \right. \\ \left. \times (\delta_{ij} (m_{q^\alpha}^2 + m_{\tilde{g}}^2 - p^2) - 2m_{\tilde{g}}m_{q^\alpha} (R_{i1}^\alpha R_{j2}^\alpha + R_{j1}^\alpha R_{i2}^\alpha)) \right) \quad (8.81)$$

$$\Pi_{ij}^{g\tilde{q}}(p^2) = \frac{g_s^2 C_F \delta_{ij}}{16\pi^2} \left(A_0(m_{\tilde{q}_i^\alpha}^2) - 2B_0(p^2, 0, m_{\tilde{q}_i^\alpha}^2) (m_{\tilde{q}_i^\alpha}^2 + p^2) \right) \quad (8.82)$$

$$\Pi_{ij}^{\tilde{q}}(p^2) = \sum_{k=1}^2 \frac{g_s^2 C_F}{16\pi^2} A_{ik}^\alpha A_{jk}^\alpha A_0(m_{\tilde{q}_k^\alpha}^2) \quad (8.83)$$

$$\Pi_{ij}^g(p^2) = 0. \quad (8.84)$$

From there we can define the renormalized two-point function as

$$\hat{\Pi}_{ij} = \Pi_{ij}(p^2) + \frac{1}{2} (p^2 - m_{\tilde{q}_i}^2) \delta Z_{ij}^{\tilde{q}} + \frac{1}{2} (p^2 - m_{\tilde{q}_j}^2) \delta Z_{ji}^{\tilde{q}*} - \delta_{ij} \delta m_{\tilde{q}_i}^2 \quad (8.85)$$

In order to work out the on-shell renormalization conditions for the squark sector, we can look at the one-loop corrected Green's function for squarks

$$iG_{ij}^{\tilde{q}}(p^2) = \frac{i}{p^2 - m_{\tilde{q}_i}^2 + i\epsilon} \left(\delta_{ij} - \frac{\hat{\Pi}_{ij}(p^2)}{p^2 - m_{\tilde{q}_j}^2 + i\epsilon} \right) + \mathcal{O}(g_s^4). \quad (8.86)$$

The requirement that the pole of the propagator is located at the physical mass is equal to setting the residue to 1 for $i = j$

$$1 = \text{Res}(G_{ii}^{\tilde{q}}, m_{\tilde{q}_i}^2 - i\epsilon) = \lim_{p^2 \rightarrow m_{\tilde{q}_i}^2 - i\epsilon} (p^2 - m_{\tilde{q}_i}^2 + i\epsilon) G_{ii}^{\tilde{q}}(p^2). \quad (8.87)$$

Applying L'Hôpital's rule as well as setting ϵ to zero gives the squark field strength counterterm

$$Z_{ii}^{\tilde{q}} = -\text{Re} \left(\frac{\partial}{\partial p^2} \Pi_{ii}(p^2) \right) \Big|_{p^2=m_{\tilde{q}_i}^2}, \quad i = j. \quad (8.88)$$

The next condition

$$0 = \left((p^2 - m_{\tilde{q}_j}^2) G_{ij}^{\tilde{q}}(p^2) \right) \Big|_{p^2=m_{\tilde{q}_j}^2}, \quad i \neq j \quad (8.89)$$

forbids an on-shell squark to change its mass eigenstate while propagating freely and adjusts the counterterm in this case to

$$\delta Z_{ij}^{\tilde{q}} = \frac{2 \text{Re} \Pi_{ji}(m_{\tilde{q}_i}^2)}{m_{\tilde{q}_j}^2 - m_{\tilde{q}_i}^2}, \quad i \neq j. \quad (8.90)$$

The last condition

$$\hat{\Pi}_{ij}(m_{\tilde{q}_i}^2) = 0 \quad (8.91)$$

ensures that any mass correction to a physical squark vanishes and defines the squark mass counterterm to be

$$\delta m_{\tilde{q}_i}^2 = \text{Re} \Pi_{ii}(m_{\tilde{q}_i}^2). \quad (8.92)$$

For the case of identical sfermion mass eigenstates the two contributions to $\delta Z_{ii}^{\tilde{q}}$ are

$$\delta Z_{ii}^{\tilde{q}, \tilde{g}q} = \frac{g_s^2 C_F}{8\pi^2} \left(\dot{B}_0(m_{\tilde{q}_i}^2, m_{\tilde{g}}^2, m_q^2) (m_q^2 + m_{\tilde{g}}^2 - m_{\tilde{q}_i}^2 - 4m_{\tilde{g}}m_q R_{i1}R_{i2}) - B_0(m_{\tilde{q}_i}^2, m_{\tilde{g}}^2, m_q^2) \right) \quad (8.93)$$

$$\delta Z_{ii}^{\tilde{q}, g\tilde{q}} = \frac{g_s^2 C_F}{8\pi^2} \left(2m_{\tilde{q}_i}^2 \dot{B}_0(m_{\tilde{q}_i}^2, 0, m_{\tilde{q}_i}^2) + B_0(m_{\tilde{q}_i}^2, 0, m_{\tilde{q}_i}^2) \right) \quad (8.94)$$

and the squark renormalization constant is ultraviolet finite

$$\delta Z_{ii}^{\tilde{q}; \text{UV}} = 0 \quad (8.95)$$

whereas it may contain UV divergent pieces for different sfermion indices depending on the mixing matrices in eqs. (8.81) and (8.83). It is the other way round for the infrared divergent parts

$$\delta Z_{ij}^{\tilde{q}; \text{IR}} = \begin{cases} -\frac{g_s^2 C_F}{8\pi^2 \varepsilon_{\text{IR}}}, & i = j \\ 0, & i \neq j \end{cases} \quad (8.96)$$

Since the correction to the squark propagator does not contain any infrared divergent pieces, the squark mass renormalization constant is infrared finite as well $\left(\delta m_{\tilde{q}_i}^2\right)^{\text{IR}} = 0$.

8.2.3 Ghost sector

As we renormalize the n -particle irreducible Green's function and not the complete NLO process as a whole, the ghost fields must also be renormalized. As ghost and anti-ghost share



Figure 8.3: One-loop contributions to the ghost self-energy.

the same self-energy they can be renormalized with the same wave function renormalization constant δZ_c . The renormalized fields are then defined as

$$\bar{c}_a^0 = \sqrt{Z_c} \bar{c}_a^R \quad (8.97)$$

$$c_a^0 = \sqrt{Z_c} c_a^R \quad (8.98)$$

where we need δZ_c only up to $\mathcal{O}(g_s^2)$ which leads to the expansion

$$Z_c = 1 + \delta Z_c. \quad (8.99)$$

Since the gluon is renormalized in the on-shell scheme, the same scheme is chosen for the ghost. That is, the ghost renormalization constant is obtained by requiring that the ghost Green's function at one-loop level has a unit residue

$$\delta Z_c = -\text{Re} \left(\frac{\partial}{\partial p^2} \Pi^c(p^2) \right) \Big|_{p^2=0}. \quad (8.100)$$

The ghost two-point function takes the general form

$$i\Pi_{ab}^c(p^2) = c_a \cdots \xrightarrow{p} \text{blob} \cdots \xrightarrow{p} \bar{c}_b = i\delta_{ab}\Pi^c(p^2) \quad (8.101)$$

and there exists only one contribution which is depicted in fig. 8.3 and gives

$$\Pi^c(p^2) = -\frac{g_s^2 C_A}{32\pi^2} p^2 B_0(p^2, 0, 0). \quad (8.102)$$

The QCD derivative of the ghost self-energy is then

$$\frac{\partial}{\partial p^2} \Pi^c(p^2) = -\frac{g_s^2 C_A}{32\pi^2} (B_0(p^2, 0, 0) - 1). \quad (8.103)$$

As the gluon renormalization constant is both ultraviolet and infrared divergent, the same is expected for the ghost renormalization constant. The UV and IR divergent parts read explicitly

$$\delta Z_c^{\text{UV}} = \frac{g_s^2 C_A}{32\pi^2 \varepsilon_{\text{UV}}} \quad (8.104)$$

$$\delta Z_c^{\text{IR}} = -\frac{g_s^2 C_A}{32\pi^2 \varepsilon_{\text{IR}}}. \quad (8.105)$$

8.2.4 Renormalization of α_s

The renormalization of the strong coupling $\alpha_s = \frac{g_s^2}{4\pi}$ is already discussed in detail in an earlier work [33]. For that reason only the value of the associated renormalization constant

$$\frac{\delta g_s}{g_s} = \frac{g_s^2}{32\pi^2 \varepsilon_{\text{UV}}} (n_q - 3C_A) \quad (8.106)$$

that emerges from the perturbative expansion of the bare coupling $g_{s,0}$

$$g_{s,0} = Z_s g_s = g_s + \delta g_s \quad (8.107)$$

is repeated.

8.3 The virtual corrections

The computation of the virtual corrections is performed by identifying all one-particle irreducible subgraphs which represent a correction of $\mathcal{O}(\alpha_s)$ with respect to the tree level amplitude. These subgraphs then correspond to corrections to the propagators and vertices and are shown as blobs in fig. 8.4. The advantage of focusing on the computation of Green's functions rather than the overall S -matrix element is that the 1PI graphs can be renormalized individually and are process independent. Thus, they can be calculated once and for all and then be embedded in any other process or diagram making an efficient and clear computation of a large number of diagrams feasible.

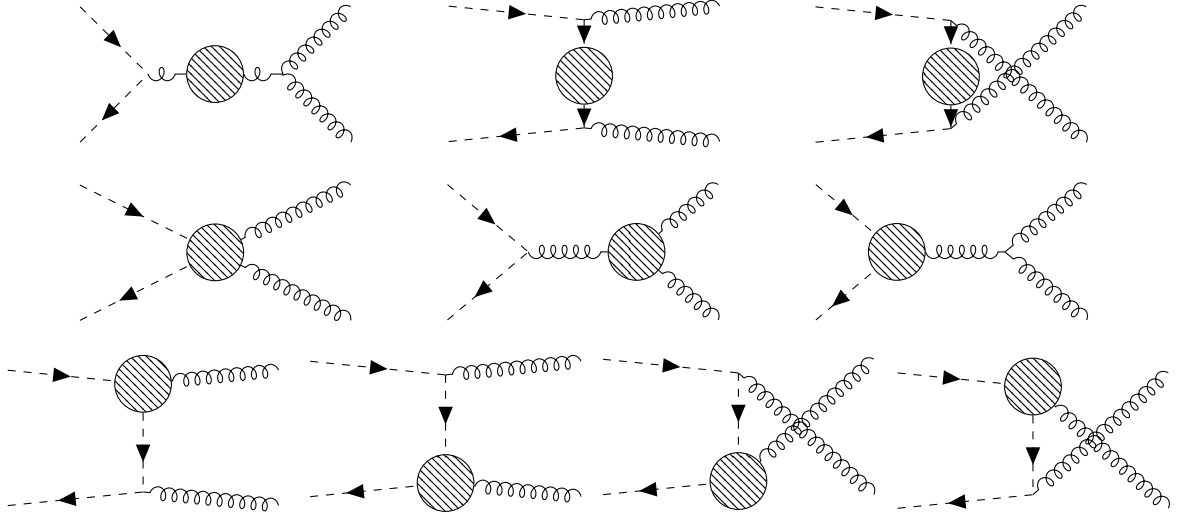


Figure 8.4: Irreducible subgraphs that can be embedded into the overall $2 \rightarrow 2$ process.

The amplitude for the virtual corrections is grouped further into propagator corrections, the three different vertex corrections and counterterms that render the amplitude UV finite

$$\mathcal{M}^V = \mathcal{M}^{\text{prop}} + \mathcal{M}_4^{\text{vertex}} + \mathcal{M}_{3g}^{\text{vertex}} + \mathcal{M}_{2\bar{q}g}^{\text{vertex}} + \mathcal{M}^{\text{counter}}. \quad (8.108)$$

For the evaluation of the Feynman diagrams the same naming conventions for momenta and indices as for the tree level process shown in fig. 7.1 are used. The cross section for the virtual part averaged/summed over initial/final state colours and polarizations is then computed as

$$\sigma^V = \frac{1}{2FN_c^2} \int d\Phi_2(k_1, k_2) \sum_{s,t,a,b} \sum_{\lambda_1, \lambda_2} 2 \text{Re} \mathcal{M}_{\text{LO}}^* \mathcal{M}^V \quad (8.109)$$

where only the transverse polarizations are summed, which is why the tensor $d^{\mu\nu}(k_1, k_2)$ introduced in eq. (4.20) is used for the polarization sums. The alternative possibility to use ghosts for the subtraction of the unphysical polarizations as well as the corresponding virtual corrections are discussed separately in section 8.3.3.

The virtual corrections are computed in the FDH scheme which has the advantage that it is in practice not necessary to distinguish between four- and D -dimensional metric tensors that occur within the Passarino-Veltman decomposition as both give the same result when being contracted with an external strictly four dimensional metric $\bar{g}^{\mu\nu}$. To convert the squared matrix element from FDH to DRED one can use the transition rules provided in [62]. The individual contributions in eq. (8.108) are presented in the following in more detail.

8.3.1 The propagator corrections

We begin with the propagator corrections $\mathcal{M}_s^{\text{prop}}$, $\mathcal{M}_t^{\text{prop}}$ and $\mathcal{M}_u^{\text{prop}}$ which sum up to

$$\mathcal{M}^{\text{prop}} = \mathcal{M}_s^{\text{prop}} + \mathcal{M}_t^{\text{prop}} + \mathcal{M}_u^{\text{prop}} \quad (8.110)$$

of eq. (8.108). These are obtained by inserting the squark self-energies in fig. 8.1 and the gluon self-energies in fig. 8.2 into the blobs shown the first row of fig. 8.4. As the squark is a scalar, the propagator corrections completely factorize from the tree level amplitude. The transverse part of the gluon self-energy factorizes as well even though the gluon is a vector

particle. This is because all terms proportional to $p_1^\mu + p_2^\mu$ in $\Pi_{ab}^{\mu\nu}(s)$ cancel out when inserting them into the s -channel amplitude in eq. (7.2) through the relation $(p_2 - p_1) \cdot (p_1 + p_2) = 0$. Thus, the corresponding corrections are achieved through the replacements

$$\mathcal{M}_s \rightarrow \frac{-\Pi_T^g(s)}{s} \mathcal{M}_s = \mathcal{M}_s^{\text{prop}} \quad (8.111)$$

$$\mathcal{M}_t \rightarrow \frac{-\Pi_{ij}^{\tilde{q}}(t)}{t - m_{\tilde{q}_i}^2} \mathcal{M}_t = \mathcal{M}_t^{\text{prop}} \quad (8.112)$$

$$\mathcal{M}_u \rightarrow \frac{-\Pi_{ij}^{\tilde{q}}(u)}{u - m_{\tilde{q}_i}^2} \mathcal{M}_u = \mathcal{M}_u^{\text{prop}}. \quad (8.113)$$

It is important to realize that the one-loop corrected squark propagator allows in principle the annihilation of different squark mass eigenstates. However, since all NLO matrix elements are combined with the tree level amplitude to arrive at the NLO cross section, this process is forbidden at NLO as well.

In the context of the propagator corrections the question may arise as to why external lines are not corrected but internal ones are. This is because in the renormalized LSZ theorem only Green's functions of renormalized fields are considered. For the derivation of the LSZ, however, one had to assume that the external fields are free for asymptotic times $t \rightarrow \pm\infty$, but the renormalized fields result precisely from the free fields by including the series of 1PI insertions onto the corresponding propagator. In our case these are the squark and gluon self-energies that shift the bare masses to the pole masses and define the wave function renormalization constants. Thus, loop corrections of the external legs are already taken into account by using the on-shell scheme while this does not apply to the internal propagators.

8.3.2 The vertex corrections

In the case of all three vertices, the computation of the corrections follows the same scheme of choosing a certain parametrization for each vertex that captures all possible structures of a correction. For the calculations themselves, aside to manual calculations a dedicated **Mathematica** [68] function was developed for each vertex that reduces the amplitude to Passarino-Veltmann functions. These functions are build upon **FeynCalc** 9.3.1 [69] which provides the necessary **Mathematica** [68] objects for four-momenta and metric tensors and handles the contraction of Lorentz indices as well as the expansion of scalar products. The package **Tracer** 1.1 [70] takes on the evaluation of Dirac traces as it allows to define an anticommuting γ^5 -matrix in D -dimensions within the naive scheme. The Levi-Civita symbols that occur then through traces of γ^5 with four or more γ -matrices during the evaluation of diagrams with fermions as virtual particles are directly set to zero since they vanish anyway when being contracted with external momenta. The code for each vertex is available in appendix C.6. As a further computational support, **FeynArts** 3.11 [71] was used for the verification of all Feynman diagrams that were found based on graph theory. In the following, the chosen parametrizations are explained in more detail.

8.3.2.1 The four-gluon-squark vertex correction

The most general form of the four-gluon-squark vertex is constructed by considering all Lorentz structures of rank two build upon metric tensors as well as incoming and outgoing momenta. Then, the linear coefficients still depend on the colour structure but can be decomposed in

terms of the colour basis elements found in section 6.4.2. The only remaining dependence is on the squark mass eigenstates i and j which cannot be separated further due to the possibility of mixing effects. A special feature of this vertex is that the external particles already correspond to those of the target process. For this reason, the momenta and other indices follow the same convention as defined in fig. 7.1. The final parametrization takes the form

$$\delta^{\alpha\beta}\Gamma_{st,ab}^{\mu\nu;ij}(p_1, p_2, k_1, k_2) = \text{diagram} = i\delta^{\alpha\beta} \sum_R c_{st,ab}^{(R)} \left(g^{\mu\nu} A_g^{(R);ij} + \sum_{m,n=1}^2 \left(k_m^\mu k_n^\nu A_{mn}^{(R);ij} + p_m^\mu p_n^\nu A_{m+2\ n+2}^{(R);ij} + k_m^\mu p_n^\nu A_{m\ n+2}^{(R);ij} + p_m^\mu k_n^\nu A_{m+2\ n}^{(R);ij} \right) \right). \quad (8.114)$$

During the computation the external squarks and gluons are already taken to be on-shell since the corrected vertex cannot be embedded into another diagram without increasing the loop order. Because of the large number of Feynman diagrams that contribute to this corrections, they are further subdivided into bubbles, triangles and boxes according to their topology and are shown in figs. 8.5 to 8.7 respectively. One might be lead to the wrong assumption that the boxes are convergent on their own, however, they turn out to be badly UV divergent and that's why they subsume under this correction and can not be treated separately . The form

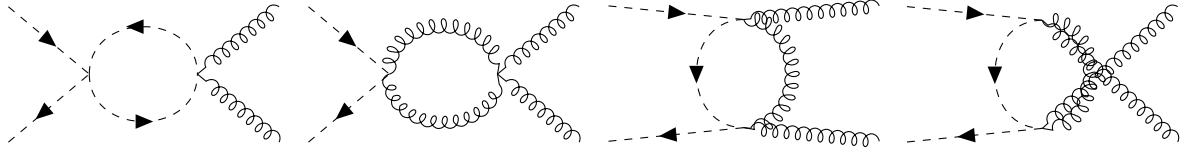


Figure 8.5: Bubble contributions to the four-gluon-squark vertex correction at one-loop.

factors A_g and A_{nm} for the bubbles and triangles are given in terms of Passarino-Veltman functions in appendix C.1 for each diagram. This is no longer reasonable for the boxes due to the large number of terms arising from the tensor reduction. Nevertheless, to ensure the reproducibility of the results, the associated amplitudes are given in appendix C.1 along with the `Mathematica` code in appendix C.6. Even though the u -channel contributions are related to the t -channel ones by crossing symmetry through the exchanges $t \leftrightarrow u$, $\mu \leftrightarrow \nu$, $a \leftrightarrow b$ and $k_1 \leftrightarrow k_2$ the corresponding results are still given in appendix C.1 for completeness. The final contribution of this vertex correction in eq. (8.108) is

$$\mathcal{M}_4^{\text{vertex}} = \Gamma_{st,ab}^{\mu\nu;ij} \epsilon_\mu^*(\lambda_1, k_1) \epsilon_\nu^*(\lambda_2, k_2). \quad (8.115)$$

8.3.2.2 The triple-gluon vertex correction

The three-gluon vertex correction can be decomposed by considering all Lorentz structures of rank three build out of the momenta k_1 , k_2 and k_3 and as well as metric tensors. Just based on the available colour indices the corrections can only be proportional to f_{cde} or d_{cde} . However, as all interactions that lead to the corrections are non-chiral and therefore anomaly

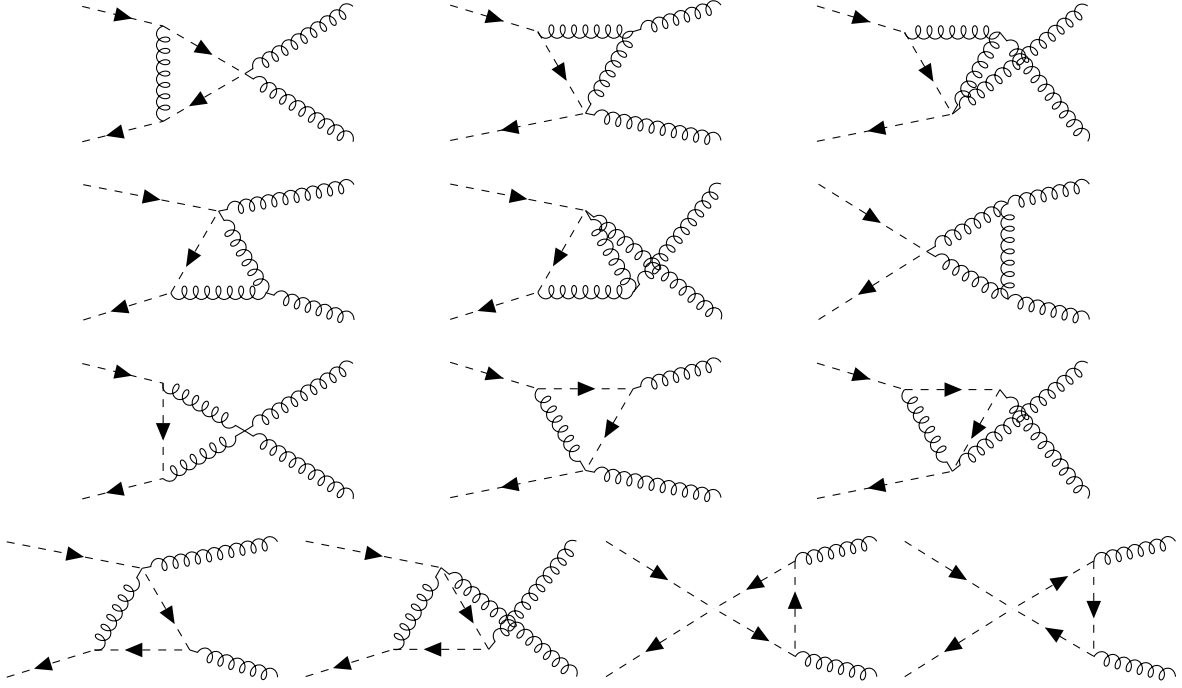


Figure 8.6: Triangle contributions to the four-gluon-squark vertex correction at one-loop.

free, the anomaly coefficient³ is zero and therefore only f_{cde} can contribute. The correction of this vertex is then parametrized as

$$\begin{aligned}
 if_{cde}\Gamma_{3g}^{\rho\sigma\tau}(k_1, k_2, k_3) &= g_d^\sigma \text{ (diagram) } = i(if_{cde}) \sum_{m=1}^3 \left(\sum_{n,o=1}^3 k_m^\rho k_n^\sigma k_o^\tau A_{mno} \right. \\
 &\quad \left. + g^{\rho\sigma} k_m^\tau A_{g1,m} + g^{\rho\tau} k_m^\sigma A_{g2,m} + g^{\sigma\tau} k_m^\rho A_{g3,m} \right) \quad (8.116)
 \end{aligned}$$

where all gluons are assumed to be in general off their mass shell. All Feynman diagrams that contribute are shown in fig. 8.8 and their decomposed amplitudes are given in appendix C.2. The `Mathematica` code is provided in appendix C.6.2. Note that within the quark triangles the first two quark generations are considered as massless. The matrix element $\mathcal{M}_{3g}^{\text{vertex}}$ in eq. (8.108) is obtained by inserting the $\mathcal{O}(\alpha_s)$ correction into the s -channel amplitude

$$\begin{aligned}
 \mathcal{M}_{3g}^{\text{vertex}} &= \text{ (diagram) } = \delta_{ij} c_{st,ab}^{(8_A)} \frac{-g_s}{s} (p_1 - p_2)_\sigma \Gamma_{3g}^{\nu\sigma\mu}(-k_2, p_1 + p_2, k_1) \\
 &\quad \times \epsilon_\mu^*(\lambda_1, k_1) \epsilon_\nu^*(\lambda_2, k_2). \quad (8.117)
 \end{aligned}$$

³For a discussion of (gauge) anomalies and the anomaly coefficient $A(R)$ see [18, chap. 30].

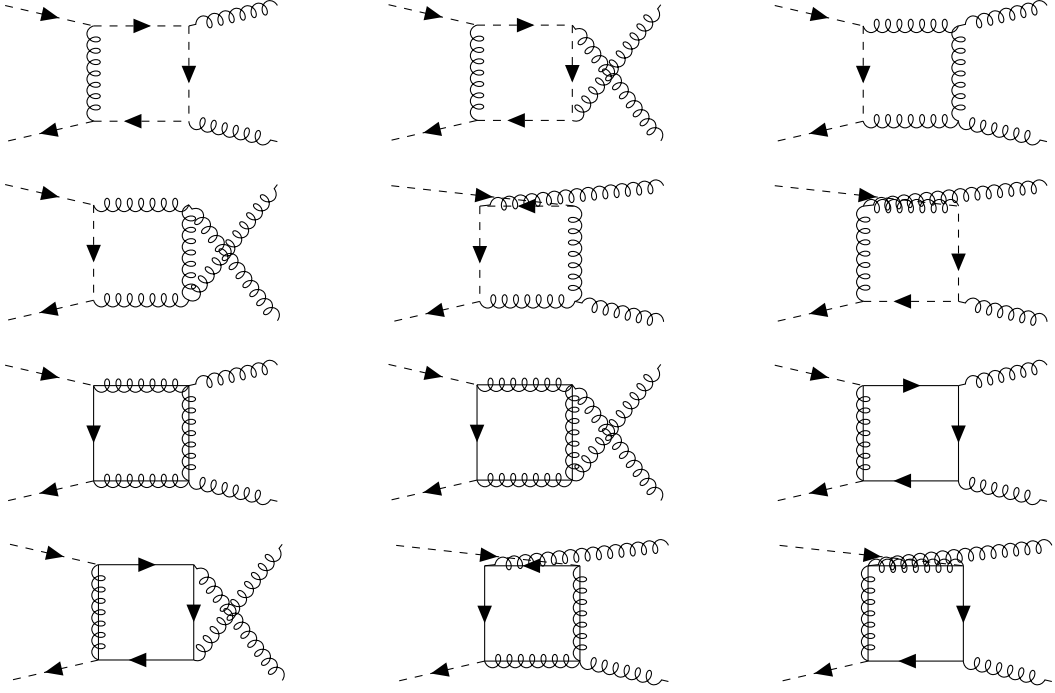


Figure 8.7: Box contributions to the four-gluon-squark vertex correction at one-loop.

8.3.2.3 The squark-gluon vertex correction

In contrast to the previous two vertex corrections, the Lorentz basis for the squark-gluon vertex is chosen to be minimal in the sense that momentum conservation is already used from the beginning to eliminate the momentum of the gluon. The vertex correction is then parametrized as

$$\delta^{\alpha\beta} T_{ur}^c \Gamma_{2\tilde{q}g}^{\sigma;lk}(p_1, p_2) = \begin{array}{c} \tilde{q}_{k,r}^\alpha \\ \swarrow \\ p_1 \\ \searrow \\ \tilde{q}_{l,u}^{\beta*} \end{array} \begin{array}{c} p_1 + p_2 \\ \longrightarrow \\ \text{loop} \end{array} g_c^\sigma = i\delta^{\alpha\beta} T_{ur}^c \left(A_+^{lk} (p_1^\sigma + p_2^\sigma) + A_-^{lk} (p_1^\sigma - p_2^\sigma) \right) \quad (8.118)$$

so that it is easy to read off the part proportional to the tree level vertex which is A_-^{lk} . Just based on the available colour indices one can deduce that this vertex can only be proportional to the colour basis element T_{ur}^c . This vertex correction was already computed within **DM@NLO** in [67] for the process $\tilde{q}\tilde{q}^* \rightarrow Q\bar{Q}$ under use of the same parametrization. However, there it was sufficient to consider only on-shell squarks. In order to be able to embed the vertex correction also in the amplitudes \mathcal{M}_t and \mathcal{M}_u , it is necessary to compute the correction again but this time for all external fields taken to be off-shell. All diagrams that contribute to this vertex correction are shown in fig. 8.9 and the corresponding form factors A_+^{lk} and A_-^{lk} are provided for each diagram in appendix C.3 along with the **Mathematica** code for the Passarino-Veltmann reduction in appendix C.6.3. The matrix element

$$\mathcal{M}_{2\tilde{q}g}^{\text{vertex}} = \mathcal{M}_s^{\text{squark}} + \mathcal{M}_{t,\text{upper}}^{\text{squark}} + \mathcal{M}_{t,\text{lower}}^{\text{squark}} + \mathcal{M}_{u,\text{upper}}^{\text{squark}} + \mathcal{M}_{u,\text{lower}}^{\text{squark}} \quad (8.119)$$

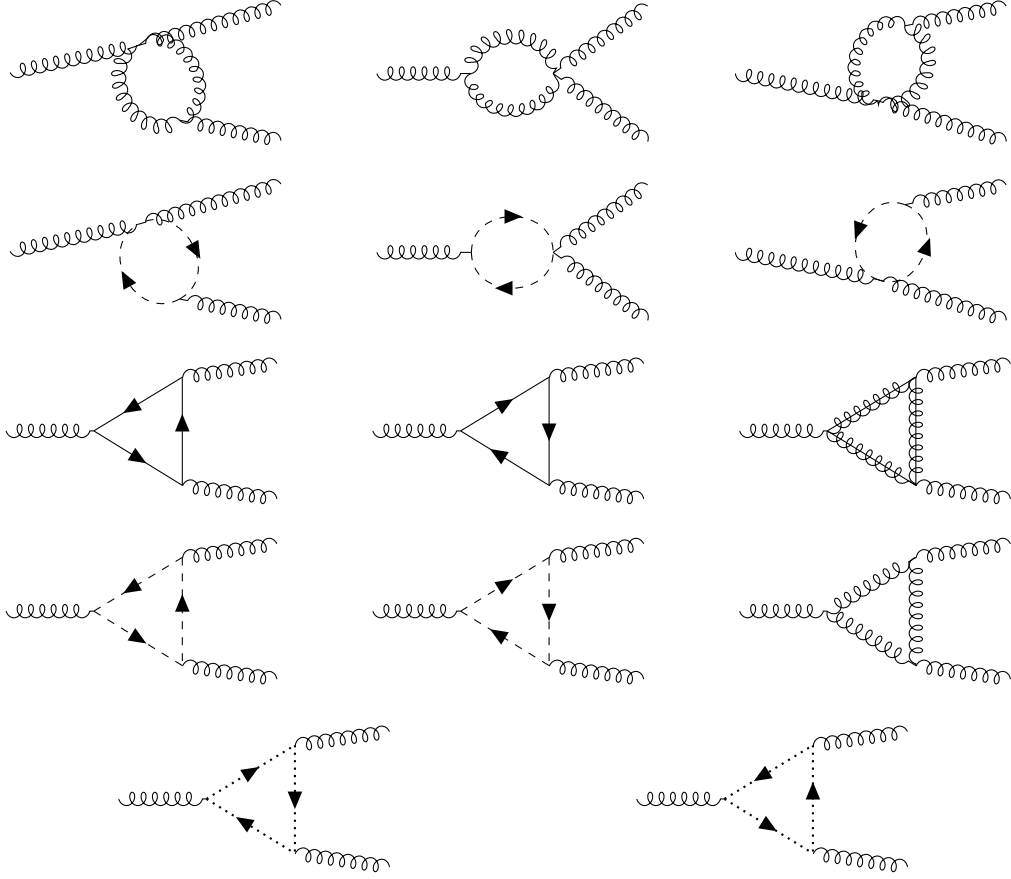


Figure 8.8: One-loop contributions to the triple-gluon vertex.

of eq. (8.108) consists of the following five insertions into the tree amplitude

$$\begin{aligned}
 \mathcal{M}_s^{\text{squark}} = & \text{Diagram: A vertex (shaded circle) with two incoming dashed lines labeled p_1 and p_2, and two outgoing curly lines.} \\
 = & c_{st,ab}^{(8_A)} \frac{-g_s}{s} \Gamma_{2\bar{q}g}^{\rho;ji}(p_1, p_2) \left(g_\rho{}^\nu (k_1 + 2k_2)^\mu - g_\rho{}^\mu (2k_1 + k_2)^\nu \right. \\
 & \left. + g^{\mu\nu} (k_1 - k_2)_\rho \right) \epsilon_\mu^*(\lambda_1, k_1) \epsilon_\nu^*(\lambda_2, k_2)
 \end{aligned} \tag{8.120}$$

$$\begin{aligned}
 \mathcal{M}_{t,\text{upper}}^{\text{squark}} = & \text{Diagram: A vertex (shaded circle) with one incoming dashed line labeled p_1, one outgoing dashed line, and two curly lines. An internal dashed line connects the vertex to a lower vertex, labeled $k_1 - p_1$ with an arrow pointing up.} \\
 = & \frac{1}{2} \left(\frac{1}{N} c_{st,ab}^{(1)} + c_{st,ab}^{(8_S)} - c_{st,ab}^{(8_A)} \right) \frac{g_s}{t - m_{q_j^\alpha}^2} \\
 & \times \Gamma_{2\bar{q}g}^{\mu;ji}(p_1, k_1 - p_1) (k_2 - 2p_2)^\nu \epsilon_\mu^*(\lambda_1, k_1) \epsilon_\nu^*(\lambda_2, k_2)
 \end{aligned} \tag{8.121}$$

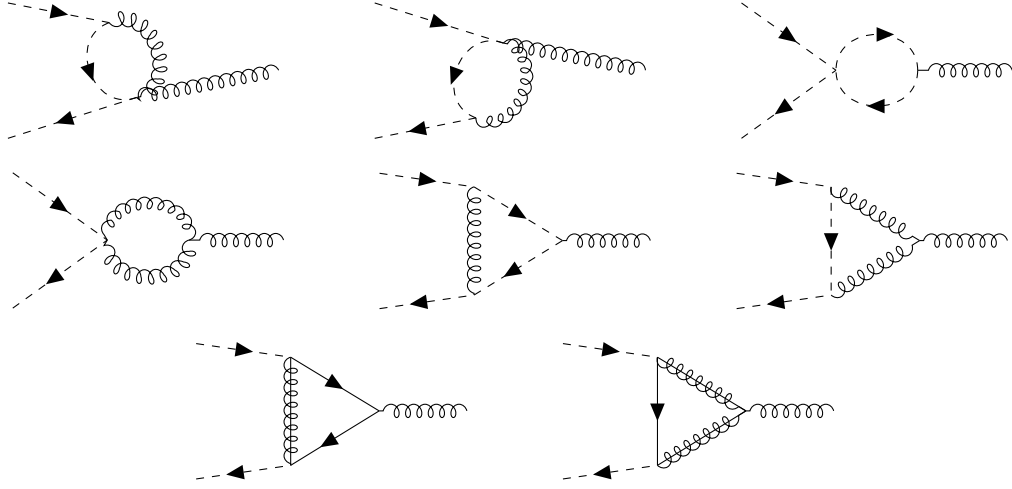


Figure 8.9: One-loop contributions to the squark-gluon vertex.

$$\begin{aligned}
 \mathcal{M}_{t,\text{lower}}^{\text{squark}} &= \begin{array}{c} \text{Diagram: A gluon line (wavy) enters from the top, a ghost line (dashed) enters from the left, and a squark line (solid) enters from the bottom. They meet at a vertex, and a gluon line (wavy) exits to the right. The vertex is a shaded circle. The momentum of the incoming gluon is $k_2 - p_2$, the incoming ghost is p_2, and the outgoing gluon is p_2. \end{array} \\
 &= \frac{1}{2} \left(\frac{1}{N} c_{st,ab}^{(\mathbf{1})} + c_{st,ab}^{(\mathbf{8_S})} - c_{st,ab}^{(\mathbf{8_A})} \right) \frac{g_s}{t - m_{q_i}^2} \\
 &\quad \times \Gamma_{2\bar{q}g}^{\nu,ji}(k_2 - p_2, p_2) (2p_1 - k_1)^\mu \epsilon_\mu^*(\lambda_1, k_1) \epsilon_\nu^*(\lambda_2, k_2)
 \end{aligned} \tag{8.122}$$

$$\begin{aligned}
 \mathcal{M}_{u,\text{upper}}^{\text{squark}} &= \begin{array}{c} \text{Diagram: A gluon line (wavy) enters from the top, a ghost line (dashed) enters from the left, and a squark line (solid) enters from the bottom. They meet at a vertex, and a gluon line (wavy) exits to the right. The vertex is a shaded circle. The momentum of the incoming gluon is p_1, the incoming ghost is $k_2 - p_1$, and the outgoing gluon is $k_2 - p_1$. \end{array} \\
 &= \frac{1}{2} \left(\frac{1}{N} c_{st,ab}^{(\mathbf{1})} + c_{st,ab}^{(\mathbf{8_S})} + c_{st,ab}^{(\mathbf{8_A})} \right) \frac{g_s}{u - m_{q_j}^2} \\
 &\quad \times \Gamma_{2\bar{q}g}^{\nu,ji}(p_1, k_2 - p_1) (k_1 - 2p_2)^\mu \epsilon_\mu^*(\lambda_1, k_1) \epsilon_\nu^*(\lambda_2, k_2)
 \end{aligned} \tag{8.123}$$

$$\begin{aligned}
 \mathcal{M}_{u,\text{lower}}^{\text{squark}} &= \begin{array}{c} \text{Diagram: A gluon line (wavy) enters from the top, a ghost line (dashed) enters from the left, and a squark line (solid) enters from the bottom. They meet at a vertex, and a gluon line (wavy) exits to the right. The vertex is a shaded circle. The momentum of the incoming gluon is $k_1 - p_2$, the incoming ghost is p_2, and the outgoing gluon is p_2. \end{array} \\
 &= \frac{1}{2} \left(\frac{1}{N} c_{st,ab}^{(\mathbf{1})} + c_{st,ab}^{(\mathbf{8_S})} + c_{st,ab}^{(\mathbf{8_A})} \right) \frac{g_s}{u - m_{q_i}^2} \\
 &\quad \times \Gamma_{2\bar{q}g}^{\mu,ji}(k_1 - p_2, p_2) (2p_1 - k_2)^\nu \epsilon_\mu^*(\lambda_1, k_1) \epsilon_\nu^*(\lambda_2, k_2)
 \end{aligned} \tag{8.124}$$

8.3.3 Ghost corrections

For the construction of the ghosts at NLO we can follow the same considerations as for the tree level. The two Slavnov-Taylor identities in eqs. (7.17) and (7.19) are valid non-perturbatively for all orders and can therefore be expanded to the next higher order, so that we get in momentum space the identities

$$k_{1,\mu} \mathcal{M}_V^{\mu\nu} = -k_2^\nu \mathcal{S}_1^{\text{NLO}} \tag{8.125}$$

$$k_{2,\nu} \mathcal{M}_V^{\mu\nu} = -k_1^\mu \mathcal{S}_2^{\text{NLO}} \quad (8.126)$$

where $\mathcal{S}_i^{\text{NLO}}$ is the NLO analogue to $\mathcal{S}_i^{\text{LO}}$. The different irreducible subgraphs that can be embedded into the tree ghost processes and yield the NLO corrections are shown in fig. 8.10.

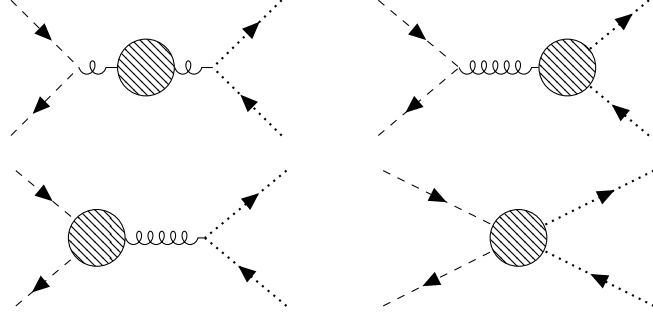


Figure 8.10: Irreducible subgraphs that can be embedded into the two $2 \rightarrow 2$ ghost processes where only the diagrams for $\mathcal{S}_1^{\text{NLO}}$ are shown. The diagrams for $\mathcal{S}_2^{\text{NLO}}$ can be obtained by reversing the ghost flow.

There is the correction of gluon propagator which factorizes as discussed in section 8.3.1

$$S_i^{\text{LO}} \rightarrow \frac{-\Pi_T(s)}{s} S_i^{\text{LO}} = S_i^{\text{prop}}. \quad (8.127)$$



Figure 8.11: One-loop contributions to the ghost-gluon vertex.

Next we have the correction of the ghost-gluon vertex which is parametrized as

$$if_{cde} \Gamma_{\bar{c}cg}^\sigma(k_1, k_2) = g_d^\sigma \text{ (diagram) } = i (if_{cde}) (A_1 k_1^\sigma + A_2 k_2^\sigma) \quad (8.128)$$

(The diagram in the equation is a shaded circle with a wavy line entering from the left labeled $k_2 - k_1$, a dashed line with an arrow entering from the bottom right labeled c_c , a dashed line with an arrow exiting to the top right labeled \bar{c}_e , and a dashed line with an arrow exiting to the top left labeled k_2 .)

and whose two contributions are shown in fig. 8.11. The values of their associated amplitudes split into the form factors A_1 and A_2 which are provided in appendix C.4. This vertex correction can be embedded into the $2 \rightarrow 2$ process to give

$$\mathcal{S}_1^{\text{ghost}} = \text{(diagram)} = \delta^{\alpha\beta} \delta_{ij} c_{st,ab}^{(8_A)} (p_1 - p_2)_\sigma \frac{-g_s}{s} \Gamma_{\bar{c}cg}^\sigma(-k_2, k_1) \quad (8.129)$$

(The diagram in the equation is a shaded circle with a wavy line entering from the left, and two dashed lines with arrows exiting to the right, labeled k_1 and k_2 .)

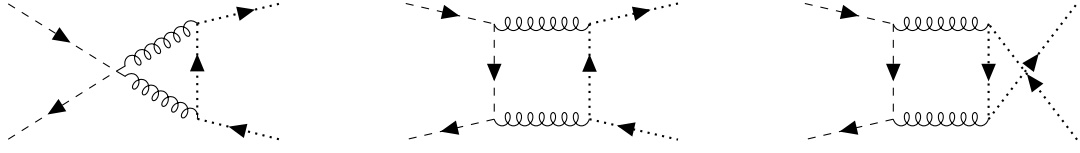


Figure 8.12: Triangle and box corrections to the ghost process $\mathcal{S}_1^{\text{NLO}}$ which do not have a tree level analogue. The diagrams for $\mathcal{S}_2^{\text{NLO}}$ can be obtained by reversing the ghost flow

and similarly for $\mathcal{S}_2^{\text{ghost}}$. The squark-gluon vertex correction is embedded into the tree diagram as in the case of $\mathcal{M}_s^{\text{squark}}$ to yield $\mathcal{S}_i^{\text{squark}}$. Lastly, there are the box corrections with amplitudes $\mathcal{S}_i^{\text{box}}$ which do not have a direct tree analogue and are shown in fig. 8.12. Their amplitudes are given for both directions of the ghost flow in appendix C.5. The total amplitude is then the sum of these four corrections and the counterterms $\mathcal{S}_i^{\text{counter}}$ additionally

$$\mathcal{S}_i^{\text{NLO}} = \mathcal{S}_i^{\text{prop}} + \mathcal{S}_i^{\text{ghost}} + \mathcal{S}_i^{\text{squark}} + \mathcal{S}_i^{\text{box}} + \mathcal{S}_i^{\text{counter}}. \quad (8.130)$$

The construction of the amplitude squared proceeds as in the tree level case as well by inserting the Slavnov-Taylor identities given in eqs. (8.125) and (8.126) into the full polarization sum

$$\sum_{\lambda_1, \lambda_2=1}^2 2 \text{Re} \left[\mathcal{M}_{\text{LO}}^{\mu\nu} \mathcal{M}_V^{*\alpha\beta} \epsilon_\mu^*(\lambda_1, k_1) \epsilon_\nu^*(\lambda_2, k_2) \epsilon_\alpha(\lambda_1, k_1) \epsilon_\beta(\lambda_2, k_2) \right] \quad (8.131)$$

$$= 2 \text{Re} \left[\mathcal{M}_{\text{LO}}^{\mu\nu*} \mathcal{M}_{\mu\nu}^{\text{NLO}} - \mathcal{S}_1^{\text{LO}*} \mathcal{S}_1^{\text{V}} - \mathcal{S}_2^{\text{LO}*} \mathcal{S}_2^{\text{NLO}} \right]. \quad (8.132)$$

It was checked numerically that the NLO amplitudes obey $\mathcal{S}_1^{\text{NLO}} - \mathcal{S}_2^{\text{NLO}} = 0$ similar to the tree level. However, note that the construction of the amplitude squared is independent of this identity.

8.3.4 The counterterms

With all necessary renormalization constants for masses, wave functions and the strong coupling at hand, we are now able to construct the counterterms for all corrected vertices. As an example, we can derive the counterterm for the four-squark-gluon vertex with the bare Lagrangian density

$$\mathcal{L} = \frac{1}{2} g_{s,0}^2 \left(\frac{1}{N} \delta_{st} \delta_{ab} + d_{abc} T_{st}^c \right) A_{0,\mu}^a A_0^{\mu,b} \tilde{q}_{0,i,s}^* \tilde{q}_{0,i,t}. \quad (8.133)$$

If all bare quantities are now substituted with their renormalized analogues and the associated renormalization constants are expanded around the tree level value up to order g_s^2 , the term

$$\delta_{jk}^4 = 2 \frac{\delta g_s}{g_s} \delta_{jk} + \delta Z_g \delta_{jk} + \frac{1}{2} \delta Z_{jk}^{\tilde{q}} + \frac{1}{2} \left[\delta Z_{kj}^{\tilde{q}} \right]^* \quad (8.134)$$

appears as new constant in the interaction vertex. As a non trivial check whether this counterterm makes sense, we can verify that the dependence of the number of squark and quark flavours present in δg_s and Z_g drops out since there appear no UV divergent diagrams

within the vertex correction itself that carry this dependence. A short calculation shows that this is true

$$\delta_{ii}^{4,\text{UV}} = 2 \frac{\delta g_s^{\text{UV}}}{g_s} + \delta Z_g^{\text{UV}} = \frac{-g_s^2 C_A}{8\pi^2 \epsilon_{\text{UV}}} \quad (8.135)$$

where we looked only at the case of identical sfermion indices relevant for us. The derivation of the other counterterms proceeds in the same way and they are all provided as additional Feynman rules in appendix B.3. The matrix elements $\mathcal{M}^{\text{counter}}$ and $\mathcal{S}_i^{\text{counter}}$ of eq. (8.108) and eq. (8.130) respectively are then obtained by inserting the counterterms instead of the vertex corrections.

8.4 The real corrections

In this section, the real corrections are addressed which are another kind of $\mathcal{O}(\alpha_s)$ corrections and feature the emission of massless particles. The inclusion of these real emission processes should ultimately cancel the infrared divergences that one encounters within the virtual corrections. For the calculation of the cross section, it is of course not possible to use the usual two-particle phase space, so a parametrization of the three-particle phase space has to be found. In order to ensure the unitarity of the real emission matrix element, it is again necessary to include ghosts as asymptotic states. How this must be done exactly is deduced with the tool of BRS-symmetry. As the integration is performed numerically, the infrared divergences that emerge from the phase-space integration have to be somehow transferred to the virtual corrections which is achieved through the dipole subtraction method. Lastly, the long standing question is answered on whether the processes `stsT2gg` and `stsT2QQbar` have to be combined - the answer is yes - and how this has to be done.

8.4.1 Kinematics and phase space integration

We begin with a brief discussion of the parametrization of the three-particle phase space and of the associated final state momenta. Following [30, 67] the three-particle phase space

$$\begin{aligned} \int d\Phi_3 = \int \frac{d^4 k_1}{(2\pi)^4} \frac{d^4 k_2}{(2\pi)^4} \frac{d^4 k_3}{(2\pi)^4} & (2\pi) \delta_+(k_1^2 - m_1^2) (2\pi) \delta_+(k_2^2 - m_2^2) \\ & \times (2\pi) \delta_+(k_3^2 - m_3^2) \delta^{(4)}(k_1 + k_2 + k_3 - p_a - p_b) \end{aligned} \quad (8.136)$$

with external momenta k_1, k_2, k_3 and p_a, p_b can be parametrized through three angles η, θ, ϕ and two energies k_1^0, k_3^0 . For real emission processes it is common to use the dimensionless quantities

$$x_i = \frac{2k_i^0}{\sqrt{s}}, \quad i = 1, 2, 3 \quad \mu_i = \frac{m_i}{\sqrt{s}}, \quad i = 1, 2, 3, a, b \quad (8.137)$$

instead of energies and masses directly. In these new quantities energy conservation can be written as

$$x_1 + x_2 + x_3 = 2 \quad (8.138)$$

and integrating out the Dirac distributions yields the phase space

$$\int d\Phi_3 = \frac{s}{32} \frac{1}{(2\pi)^5} \int dx_1 d\eta dx_3 d\cos\theta d\phi \quad (8.139)$$

with the integration limits

$$\eta \in (0, 2\pi), \quad \phi \in (0, 2\pi), \quad \theta \in (0, \pi) \quad (8.140)$$

$$x_3^{\min} = 2\mu_3, \quad x_3^{\max} = 1 - \mu_+^2 + \mu_3^2 \quad (8.141)$$

$$(x_1)_{\min}^{\max} = \frac{1}{2\tau} \left[\sigma(\tau + \mu_+ \mu_-) \pm \sqrt{x_3^2 - 4\mu_3^2} \sqrt{(\tau - \mu_+^2)(\tau - \mu_-^2)} \right]. \quad (8.142)$$

The shorthands σ , τ and m_{\pm} are defined as

$$\sigma = 2 - x_3, \quad \tau = 1 - x_3 + \mu_3^2, \quad \mu_{\pm} = \mu_1 \pm \mu_2. \quad (8.143)$$

The derivation of this parametrization was performed in the center-of-mass frame of the initial momenta p_a and p_b which are taken to be aligned along the z -axis

$$p_a^{\mu} = \frac{\sqrt{s}}{2} \left(1 + \mu_a^2 - \mu_b^2, 0, 0, \sqrt{(1 - \mu_a^2 - \mu_b^2)^2 - 4\mu_a^2 \mu_b^2} \right) \quad (8.144)$$

$$p_b^{\mu} = \frac{\sqrt{s}}{2} \left(1 - \mu_a^2 + \mu_b^2, 0, 0, -\sqrt{(1 - \mu_a^2 - \mu_b^2)^2 - 4\mu_a^2 \mu_b^2} \right). \quad (8.145)$$

From there it follows that the final state momenta take the form

$$\vec{k}_1 = \frac{\sqrt{s}}{2} \sqrt{x_1^2 - 4\mu_1^2} \begin{pmatrix} \cos(\eta) \cos(\theta) \sin(\xi) + \sin(\theta) \cos(\xi) \\ \sin(\eta) \sin(\xi) \\ \cos(\theta) \cos(\xi) - \cos(\eta) \sin(\theta) \sin(\xi) \end{pmatrix} \quad (8.146)$$

$$\vec{k}_3 = \frac{\sqrt{s}}{2} \sqrt{x_3^2 - 4\mu_3^2} \begin{pmatrix} \sin(\theta) \\ 0 \\ \cos(\theta) \end{pmatrix} \quad (8.147)$$

where \vec{k}_2 follows from momentum conservation $\vec{k}_2 = -\vec{k}_1 - \vec{k}_3$ and the respective temporal components form the energy-momentum relation $(k_i^0)^2 = \vec{k}_i^2 + m_i^2$. The auxiliary angle ξ is

$$\cos \xi = \frac{(2 - x_1 - x_3)^2 + 4\mu_1^2 + 4\mu_3^2 - 4\mu_2^2 - x_1^2 - x_3^2}{2\sqrt{x_1^2 - \mu_1^2} \sqrt{x_3^2 - \mu_3^2}}. \quad (8.148)$$

The integration within DM@NLO itself is performed numerically using the Vegas algorithm from the CUBA library [72]. In order to ensure the correct implementation of the three-particle phase space, the phase space volume $\Phi_3(m_1, m_2, m_3)$ was computed analytically for different mass configurations and compared to the numerical result. The analytic results are

$$\Phi_3(0, 0, 0) = \frac{s}{256\pi^3} \quad (8.149)$$

$$\Phi_3(m_1, 0, 0) = \frac{2m_1^2 s \ln\left(\frac{m_1^2}{s}\right) - m_1^4 + s^2}{256\pi^3 s} \quad (8.150)$$

$$\begin{aligned} \Phi_3(m_1, m_2, 0) = \frac{1}{1024\pi^3} & \left(s \left(2i(\mu_-^4 - 2\mu_-^2(\mu_+^2 + 2) + (\mu_+^2 - 4)\mu_+^2) \arcsin\left(\sqrt{\frac{\mu_-^2 - 1}{\mu_-^2 - \mu_+^2}}\right) \right. \right. \\ & \left. \left. - i\pi\mu_-^4 + 2\mu_-^2 \sqrt{(\mu_-^2 - 1)(\mu_+^2 - 1)} + 2i\pi\mu_-^2 \mu_+^2 + 2\mu_+^2 \sqrt{(\mu_-^2 - 1)(\mu_+^2 - 1)} \right) \right) \end{aligned}$$

$$\begin{aligned}
& +4\sqrt{(\mu_-^2 - 1)(\mu_+^2 - 1)} - 8\sqrt{\mu_-^2 \mu_+^2} \ln \left(\sqrt{\frac{(\mu_-^2 - 1)\mu_+^2}{\mu_-^2(\mu_+^2 - 1)}} - 1 \right) \\
& +8\sqrt{\mu_-^2 \mu_+^2} \ln \left(\sqrt{\frac{(\mu_-^2 - 1)\mu_+^2}{\mu_-^2(\mu_+^2 - 1)}} + 1 \right) + 4i\pi\mu_-^2 - i\pi\mu_+^4 + 4i\pi\mu_+^2 \Bigg) \Bigg). \quad (8.151)
\end{aligned}$$

As $\Phi_3(m_1, m_2, m_3)$ is symmetric with respect to the interchange of masses, the results for other mass configurations with the same number of massless and massive particles are identical to those given here. For the fully massive case no analytic result could be found.

8.4.2 Real emission processes

As postulated in the Kinoshita-Lee-Nauenberg theorem [27], it is necessary to include real emission processes to cancel the infrared divergences that appear within the virtual corrections. At first sight, in our case this is the process

$$\tilde{q}_{i,t}(p_1) + \tilde{q}_{j,s}^*(p_2) \longrightarrow g_a^\mu(k_1) + g_b^\nu(k_2) + g_c^\rho(k_3) \quad (8.152)$$

whose corresponding diagrams are depicted in fig. 8.13 where the momenta of the gluons are read from top to bottom starting with k_1 .

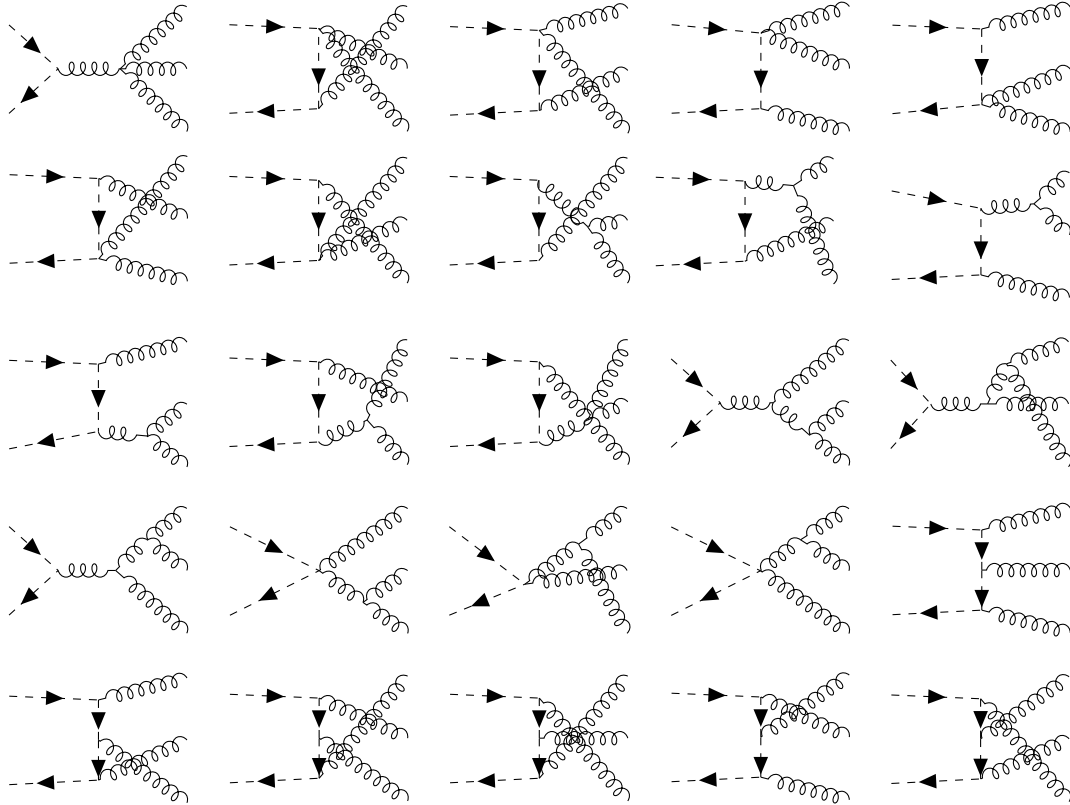


Figure 8.13: Real gluon emission diagrams contributing at next-to-leading order to squark annihilation into two gluons.

However, there can also occur infrared divergences through massless quarks which in turn depend on the number N_f of quarks whose masses are neglected. In the following, we want

to track this dependence within the virtual corrections to find out whether it is necessary to include real emission diagrams with massless quarks as final states. We perform the discussion in the "lightcone" gauge first and then again with ghosts. The only potential source for infrared divergences within the vertex corrections (not the counterterms) that depend on N_f is the quark triangle diagram. These double poles cancel each other out within the vertex correction itself when considering both directions of the fermion flow. Furthermore, the N_f dependent simple poles also disappear when the vertex correction is contracted with $\mathcal{M}^{(8_A)}$ under usage of the full polarization sum. The only other source is the gluon renormalization constant that enters through the counterterms in many places. The easiest way to track this dependence is to explicitly write down all contributions with the help of the colour decomposition

$$\begin{aligned}
& \underbrace{\frac{1}{2}\delta Z_g \left[\mathcal{M}_s^{(8_A)} \mathcal{M}_{\text{LO}}^{*(8_A)} + 2\mathcal{M}_t^{(8_A)} \mathcal{M}_{\text{LO}}^{*(8_A)} + 2\mathcal{M}_u^{(8_A)} \mathcal{M}_{\text{LO}}^{*(8_A)} \right]}_{\tilde{q}^* \tilde{q} g} + \underbrace{\frac{3}{2}\delta Z_g \mathcal{M}_s^{(8_A)} \mathcal{M}_{\text{LO}}^{*(8_A)}}_{3g} \\
& \underbrace{-\delta Z_g \mathcal{M}_s^{(8_A)} \mathcal{M}_{\text{LO}}^{*(8_A)}}_{\text{propagator}} + \sum_{R=1,8_S} \left(\underbrace{\delta Z_g \mathcal{M}_v^{(R)} \mathcal{M}_{\text{LO}}^{*(R)}}_{4\text{-vertex}} + \underbrace{\frac{1}{2}\delta Z_g \left[2\mathcal{M}_t^{(R)} \mathcal{M}_{\text{LO}}^{*(R)} + 2\mathcal{M}_u^{(R)} \mathcal{M}_{\text{LO}}^{*(R)} \right]}_{\tilde{q}^* \tilde{q} g} \right) \\
& = \delta Z_g \sum_R |\mathcal{M}_{\text{LO}}^{(R)}|^2 \tag{8.153}
\end{aligned}$$

which means that we are left with $g_s^2 T_F N_f / 12\pi^2 \varepsilon_{\text{IR}} |\mathcal{M}_{\text{LO}}|^2$ after including the normalization factor from the colour basis elements and cancelling the Bose symmetry factor S_2 with the global factor two from $2\mathcal{M}_{\text{NLO}}\mathcal{M}_{\text{LO}}^*$ ⁴.

We can now focus on the case where the polarization sum is performed by means of the ghosts. In that case the N_f dependent simple poles from the two quark triangles do not drop out by "themselves" but are precisely cancelled by the infrared dependence of the gluon renormalization constant entering through the propagator correction of the ghost diagrams. In addition, we receive in total a term $-\delta Z_g (|\mathcal{S}_1|^2 + |\mathcal{S}_2|^2)$ from the squark-gluon and ghost-gluon counterterm within the ghost corrections. So, we obtain the same N_f dependence for both methods. This contribution to the infrared divergences can only be compensated by including the process

$$\tilde{q}\tilde{q}^* \longrightarrow q_r(k_1) + \bar{q}_u(k_2) + g_a^\mu(k_3).$$

The corresponding diagrams are shown in fig. 8.14. However, it turns out that only a subset of the diagrams shown are needed for the process **stsT2gg**. These are the four which contain the splitting of a gluon into a massless quark-antiquark pair which becomes obvious by constructing the singular parts of the associated dipoles

$$\langle \tilde{q}, \tilde{q}^*, g, g | \frac{g_s^2 N_f}{2\pi} \left(J_{Q\bar{Q},g}^S \frac{\mathbf{T}_3 \mathbf{T}_4}{\mathbf{T}_3^2} + J_{\tilde{q}\bar{Q}}^S \frac{\mathbf{T}_1 \mathbf{T}_3}{\mathbf{T}_3^2} + J_{Q\bar{Q}}^{\tilde{q}^* S} \frac{\mathbf{T}_2 \mathbf{T}_3}{\mathbf{T}_3^2} \right) | \tilde{q}, \tilde{q}^*, g, g \rangle = -\frac{g_s^2 T_F N_f}{12\pi^2 \varepsilon_{\text{IR}}} |\mathcal{M}_{\text{LO}}|^2 \tag{8.154}$$

where colour conservation $\mathbf{T}_1 + \mathbf{T}_2 + \mathbf{T}_4 = -\mathbf{T}_3$ with $\mathbf{T}_1 = \mathbf{T}_{\tilde{q}}$, $\mathbf{T}_2 = \mathbf{T}_{\tilde{q}^*}$, $\mathbf{T}_3 = \mathbf{T}_q$ and $\mathbf{T}_4 = \mathbf{T}_{\bar{q}}$ was used to combine the different integrated dipoles⁵. But since only all six diagrams taken together reflect the correct probability of this process, we cannot consider only the

⁴This factor two is not included in eq. (8.153).

⁵The dipole for emitter and spectator both from the final state $J_{Q\bar{Q},g}^S$ computed by Catani and Seymour was converted from their notation and convention in [28] to the one used in chapter 5.

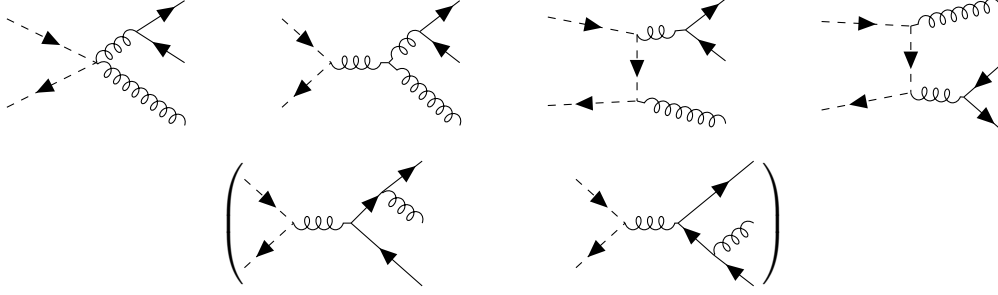


Figure 8.14: Real emission diagrams with light quarks as final states that contribute to squark annihilation into two gluons at next-to-leading order. The infrared divergences from the two diagrams in brackets are found in `stsT2QQbar`.

relevant four diagrams. The IR poles from the other two diagrams occurring for massless quarks must also be found somewhere. Since the same diagrams show up as real emissions for the process $\tilde{q}\tilde{q}^* \rightarrow Q\bar{Q}$ which is already available for massive quarks in `DM@NLO` as `stsT2QQbar`, the poles are expected to be found there. Furthermore, Cutkosky's cutting rules tell us also where these poles are to be found. These double poles can only be located in the correction of the quark-gluon vertex. *These findings then indicate that `stsT2QQbar` must inevitably be extended to support massless quarks and combined with `stsT2gg` to obtain a well defined and infrared finite cross section.*

Another source of additional processes which have to be considered is gauge invariance. As in the case of the $2 \rightarrow 2$ process, we face the issue that we want to include only the two physical polarizations within the polarization sum. The first option is again to use the full polarization sum from eq. (4.20). However, it is not simply possible to use the momentum of another gluon as reference vector n as any gluon can potentially become collinear to any other gluon which would violate the condition $n \cdot k \neq 0$. An easy way out is to use the parity transformed vectors \bar{k}_i which can be obtained from the parametrization introduced in section 8.4.1 such that the polarization sum for each gluon becomes

$$\sum_{\lambda=1,2} \epsilon^{\mu*}(\lambda, k_i) \epsilon^{\nu}(\lambda, k_i) = -g^{\mu\nu} + \frac{k_i^{\mu} \bar{k}_i^{\nu} + k_i^{\nu} \bar{k}_i^{\mu}}{\bar{k}_i \cdot k_i} \quad (8.155)$$

where the denominator is always nonzero by construction. The second option is to use ghost. In order to find out what processes with ghosts as asymptotic states have to be included and how, we can resort to Slavnov-Taylor identities. For their derivation, let us have a look at the Green's functions

$$\langle \Omega | T \{ \tilde{q}\tilde{q}^* \bar{c}_a(y_1) A_b^{\nu}(y_2) A_c^{\rho}(y_3) \} | \Omega \rangle = 0 \quad (8.156)$$

$$\langle \Omega | T \{ \tilde{q}\tilde{q}^* A_a^{\mu}(y_1) \bar{c}_b(y_2) A_c^{\rho}(y_3) \} | \Omega \rangle = 0 \quad (8.157)$$

$$\langle \Omega | T \{ \tilde{q}\tilde{q}^* A_a^{\mu}(y_1) A_b^{\nu}(y_2) \bar{c}_c(y_3) \} | \Omega \rangle = 0. \quad (8.158)$$

Applying the BRS-transformation δ_B to the first one yields

$$0 = \langle \Omega | T \{ \tilde{q}\tilde{q}^* (\delta_B \bar{c}_a(y_1)) A^{\nu}(y_2)_b A_c^{\mu}(y_3) \} | \Omega \rangle - \langle \Omega | T \{ \tilde{q}\tilde{q}^* \bar{c}_a(y_1) (\delta_B A_b^{\nu}(y_2)) A_c^{\mu}(y_3) \} | \Omega \rangle \\ - \langle \Omega | T \{ \tilde{q}\tilde{q}^* \bar{c}_a(y_1) A_b^{\nu}(y_2) (\delta_B A_c^{\mu}(y_3)) \} | \Omega \rangle \quad (8.159)$$

and in more detail

$$\langle \Omega | T \{ \tilde{q} \tilde{q}^* \partial_\mu^{y_1} A_a^\mu(y_1) A_b^\nu(y_2) A_c^\rho(y_3) \} | \Omega \rangle = - \langle \Omega | T \{ \tilde{q} \tilde{q}^* \bar{c}_a(y_1) \partial_{y_2}^\nu c_b(y_2) A_c^\rho(y_3) \} | \Omega \rangle \quad (8.160)$$

$$- \langle \Omega | T \{ \tilde{q} \tilde{q}^* \bar{c}_a(x_1) A_b^\nu(x_2) \partial_{x_3}^\rho c_c(x_3) \} | \Omega \rangle \quad (8.161)$$

where the contribution from the transformations that are nonlinear in the fields are already neglected for the same reasons discussed in section 7.1. The same steps can be repeated for the other two Green's functions so that we arrive at in total six ghost processes

$$S_1 : \tilde{q}_{i,t}(p_1) + \tilde{q}_{j,s}^*(p_2) \longrightarrow \bar{c}_a(k_1) + c_b(k_2) + g_c^\mu(k_3) \quad (8.162)$$

$$S_2 : \tilde{q}_{i,t}(p_1) + \tilde{q}_{j,s}^*(p_2) \longrightarrow c_a(k_1) + \bar{c}_b(k_2) + g_c^\mu(k_3) \quad (8.163)$$

$$S_3 : \tilde{q}_{i,t}(p_1) + \tilde{q}_{j,s}^*(p_2) \longrightarrow \bar{c}_a(k_1) + g_b^\mu(k_2) + c_c(k_3) \quad (8.164)$$

$$S_4 : \tilde{q}_{i,t}(p_1) + \tilde{q}_{j,s}^*(p_2) \longrightarrow c_a(k_1) + g_b^\mu(k_2) + \bar{c}_c(k_3) \quad (8.165)$$

$$S_5 : \tilde{q}_{i,t}(p_1) + \tilde{q}_{j,s}^*(p_2) \longrightarrow g_a^\mu(k_1) + c_b(k_2) + \bar{c}_c(k_3) \quad (8.166)$$

$$S_6 : \tilde{q}_{i,t}(p_1) + \tilde{q}_{j,s}^*(p_2) \longrightarrow g_a^\mu(k_1) + \bar{c}_b(k_2) + c_c(k_3) \quad (8.167)$$

with amplitudes S_1 to S_6 which are simultaneously used as labels for the different processes. Applying the LSZ formula with the assignments $y_{1,2,3} \rightarrow k_{1,2,3}$ yields the generalized Ward-Takahashi identities

$$\begin{aligned} k_{1,\mu} \mathcal{M}_3^{\mu\nu\rho} &= -k_2^\nu \mathcal{S}_1^\rho - k_3^\rho \mathcal{S}_3^\nu \\ k_{2,\nu} \mathcal{M}_3^{\mu\nu\rho} &= -k_1^\mu \mathcal{S}_2^\rho - k_3^\rho \mathcal{S}_6^\mu \\ k_{3,\rho} \mathcal{M}_3^{\mu\nu\rho} &= -k_1^\mu \mathcal{S}_4^\nu - k_2^\nu \mathcal{S}_5^\mu, \end{aligned} \quad (8.168)$$

whereby one has to commute all anti-ghost fields to the right and to include the additional minus sign from the antihermiticity of the anti-ghost field to obtain the correct relative sign. The BRS-transformation of the five-point functions

$$\langle \Omega | T \{ \tilde{q} \tilde{q}^* c_a(y_1) \bar{c}_b(y_2) \bar{c}_c(y_3) \} | \Omega \rangle = 0 \quad (8.169)$$

$$\langle \Omega | T \{ \tilde{q} \tilde{q}^* \bar{c}_a(y_1) c_b(y_2) \bar{c}_c(y_3) \} | \Omega \rangle = 0 \quad (8.170)$$

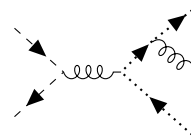
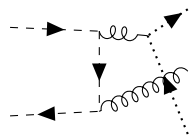
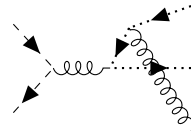
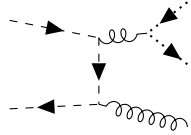
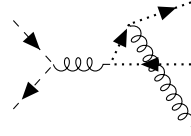
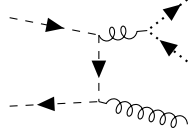
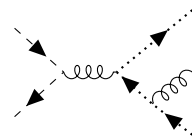
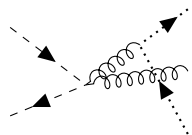
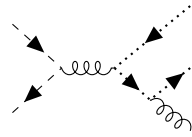
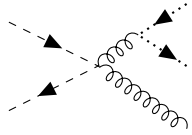
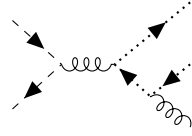
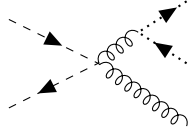
$$\langle \Omega | T \{ \tilde{q} \tilde{q}^* \bar{c}_a(y_1) \bar{c}_b(y_2) c_c(y_3) \} | \Omega \rangle = 0 \quad (8.171)$$

allow us to relate the different correlation functions associated with the ghost amplitudes to each other

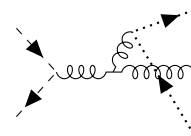
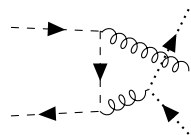
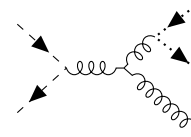
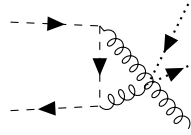
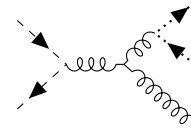
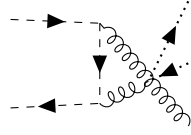
$$\begin{aligned} 0 &= \langle \Omega | T \{ \tilde{q} \tilde{q}^* c_a(y_1) \partial_\nu^{y_2} A_b^\nu(y_2) \bar{c}_c(y_3) \} | \Omega \rangle - \langle \Omega | T \{ \tilde{q} \tilde{q}^* c_a(y_1) \bar{c}_b(y_2) \partial_\rho^{y_3} A_c^\rho(y_3) \} | \Omega \rangle \\ 0 &= - \langle \Omega | T \{ \tilde{q} \tilde{q}^* \partial_\mu^{y_1} A_a^\mu(y_1) c_b(y_2) \bar{c}_c(y_3) \} | \Omega \rangle - \langle \Omega | T \{ \tilde{q} \tilde{q}^* \bar{c}_a(y_1) c_b(y_2) \partial_\rho^{y_3} A_c^\rho(y_3) \} | \Omega \rangle \\ 0 &= - \langle \Omega | T \{ \tilde{q} \tilde{q}^* \partial_\mu^{y_1} A_a^\mu(y_1) \bar{c}_b(y_2) c_c(y_3) \} | \Omega \rangle + \langle \Omega | T \{ \tilde{q} \tilde{q}^* \bar{c}_a(y_1) \partial_\nu^{y_2} A_b^\nu(y_2) c_c(y_3) \} | \Omega \rangle \end{aligned} \quad (8.172)$$

which read in momentum space

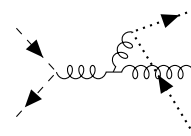
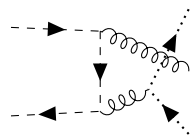
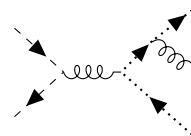
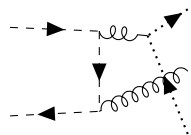
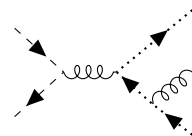
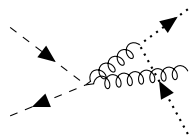
$$\begin{aligned} k_{2,\nu} \mathcal{S}_4^\nu &= k_{3,\rho} \mathcal{S}_2^\rho \\ k_{1,\mu} \mathcal{S}_5^\mu &= k_{3,\rho} \mathcal{S}_1^\rho \\ k_{1,\mu} \mathcal{S}_6^\mu &= k_{2,\nu} \mathcal{S}_3^\nu. \end{aligned} \quad (8.173)$$



(a) Process \mathcal{S}_1 .



(b) Process \mathcal{S}_2 .



(c) Process \mathcal{S}_3 .

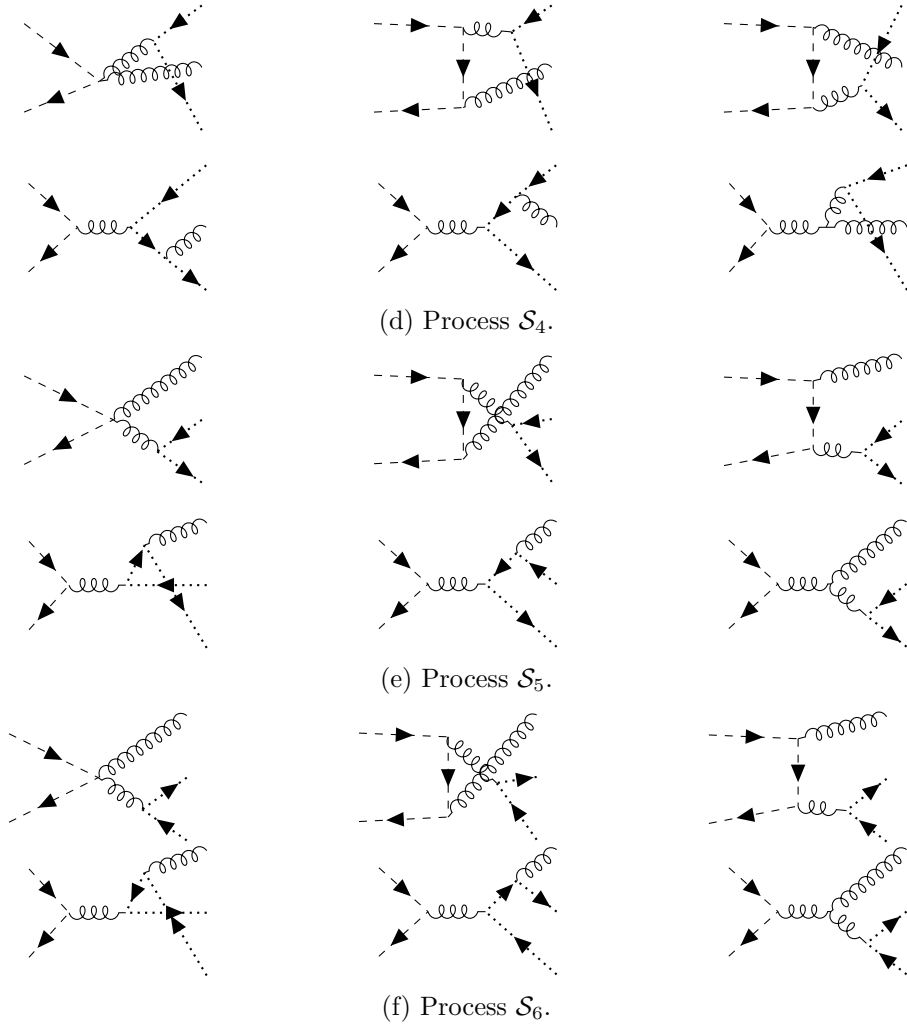


Figure 8.15: Ghost diagrams that contribute to squark annihilation at next-to-leading order.

With these two sets of Ward identities at hand, we are now ready to replace the unphysical modes through ghost

$$\sum_{\lambda_1, \lambda_2, \lambda_3=1}^2 \mathcal{M}^{\mu\nu\rho} \mathcal{M}_{\alpha\beta\gamma}^* \epsilon_\mu^*(\lambda_1, k_1) \epsilon_\nu^*(\lambda_2, k_2) \epsilon_\rho^*(\lambda_3, k_3) \epsilon^\alpha(\lambda_1, k_1) \epsilon^\beta(\lambda_2, k_2) \epsilon^\gamma(\lambda_3, k_3) \quad (8.174)$$

$$= \mathcal{M}_{\mu\nu\rho} \mathcal{M}_{\alpha\beta\gamma}^* \left(-g^{\mu\alpha} + \frac{\bar{k}_1^\mu k_1^\alpha + k_1^\mu \bar{k}_1^\alpha}{k_1 \cdot \bar{k}_1} \right) \left(-g^{\nu\beta} + \frac{\bar{k}_2^\nu k_2^\beta + k_2^\nu \bar{k}_2^\beta}{k_2 \cdot \bar{k}_2} \right) \left(-g^{\rho\gamma} + \frac{\bar{k}_3^\rho k_3^\gamma + k_3^\rho \bar{k}_3^\gamma}{k_3 \cdot \bar{k}_3} \right) \quad (8.175)$$

$$= -\mathcal{M}^{\mu\nu\rho} \mathcal{M}_{\mu\nu\rho}^* + \mathcal{S}_1 \cdot \mathcal{S}_2^* + \mathcal{S}_2 \cdot \mathcal{S}_1^* + \mathcal{S}_3 \cdot \mathcal{S}_4^* + \mathcal{S}_4 \cdot \mathcal{S}_3^* + \mathcal{S}_5 \cdot \mathcal{S}_6^* + \mathcal{S}_6 \cdot \mathcal{S}_5^* \quad (8.176)$$

$$+ \frac{\bar{k}_2 \cdot \mathcal{S}_4}{\bar{k}_2 \cdot k_2} (k_1 \cdot \mathcal{S}_6^* - k_2 \cdot \mathcal{S}_3^*) + \frac{\bar{k}_3 \cdot \mathcal{S}_2}{\bar{k}_3 \cdot k_3} (k_1 \cdot \mathcal{S}_5^* - k_3 \cdot \mathcal{S}_1^*) \quad (8.177)$$

$$+ \frac{\bar{k}_3 \cdot \mathcal{S}_1}{\bar{k}_3 \cdot k_3} (k_2 \cdot \mathcal{S}_4^* - k_3 \cdot \mathcal{S}_2^*) \quad (8.178)$$

$$= -\mathcal{M}^{\mu\nu\rho} \mathcal{M}_{\mu\nu\rho}^* + \mathcal{S}_1 \cdot \mathcal{S}_2^* + \mathcal{S}_2 \cdot \mathcal{S}_1^* + \mathcal{S}_3 \cdot \mathcal{S}_4^* + \mathcal{S}_4 \cdot \mathcal{S}_3^* + \mathcal{S}_5 \cdot \mathcal{S}_6^* + \mathcal{S}_6 \cdot \mathcal{S}_5^* \quad (8.179)$$

$$= -\mathcal{M}^{\mu\nu\rho} \mathcal{M}_{\mu\nu\rho}^* + \sum_{i=1}^6 \mathcal{S}_i^\mu \mathcal{S}_{i,\mu}^*. \quad (8.180)$$

The first step corresponds to the replacement of the transverse polarizations with the polarization sum in eq. (8.155). Then the identities in eq. (8.168) are used to replace the momenta in the polarization sum. In the following step, the relations in eq. (8.173) between the ghost amplitudes themselves are used to eliminate the differences of the ghost amplitudes. For the last step we need further identities between the ghost amplitudes, which result from the explicit evaluation of the amplitudes with the help of Feynman rules

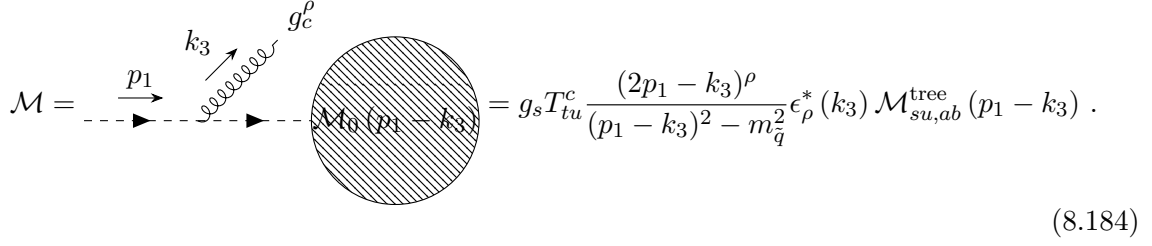
$$(\mathcal{S}_1 - \mathcal{S}_2)^* \cdot (\mathcal{S}_1 - \mathcal{S}_2) = (\mathcal{S}_3 - \mathcal{S}_4)^* \cdot (\mathcal{S}_3 - \mathcal{S}_4) = (\mathcal{S}_5 - \mathcal{S}_6)^* \cdot (\mathcal{S}_5 - \mathcal{S}_6) = 0. \quad (8.181)$$

Inserting these gives a similar picture as in the $2 \rightarrow 2$ calculation. The ghost processes are only squared with themselves and then subtracted from the matrix element squared of the actual process.

After all processes that have to be included are found, we can proceed with the calculation of the squared matrix elements. After the manual construction of all amplitudes, the contraction of all Lorentz indices is performed with **FeynCalc 9.3** which also handles the summation of all colour indices. The matrix element describing the production of the three gluons is equipped with a Bose symmetry factor $1/3!$ to account for the fact that we have three identical particles in the final state. The additional Dirac traces which occur for the process with quarks in the final state are calculated with **Tracer 1.1**. In that case, the summation over all final spin states is achieved through the common completeness relations

$$\sum_s u^{(s)}(p) \bar{u}^{(s)}(p) = \not{p} + m \quad (8.182)$$

$$\sum_s v^{(s)}(p) \bar{v}^{(s)}(p) = \not{p} - m. \quad (8.183)$$



$$\mathcal{M} = \dots = g_s T_{tu}^c \frac{(2p_1 - k_3)^\rho}{(p_1 - k_3)^2 - m_{\tilde{q}}^2} \epsilon_\rho^*(k_3) \mathcal{M}_{su,ab}^{\text{tree}}(p_1 - k_3) . \quad (8.184)$$

8.4.3 Treatment of soft and collinear divergences

To make the integration over the three-particle phase space numerically accessible, we rely on the results for the dipole subtraction method from chapter 5. As there are already two detailed examples provided for the application of the dipole method in the mentioned chapter, only the required dipoles are discussed briefly and a special feature which occurs in processes with more than three coloured particles is described. To simplify the notation, the initial momenta are labelled as $p_a = p_1$ and $p_b = p_2$ in this section.

8.4.3.1 Three gluons in the final state

For the tree process with three gluons in the final state, all four possibilities to form emitter and spectator pairs occur. The dipole formula results in a total of 27 dipoles which have to be considered:

- FE-FS: $\mathcal{D}_{12,3}, \mathcal{D}_{13,2}, \mathcal{D}_{23,1}$
- IE-IS: $\mathcal{D}^{a1,b}, \mathcal{D}^{a2,b}, \mathcal{D}^{a3,b}, \mathcal{D}^{b1,a}, \mathcal{D}^{b2,a}, \mathcal{D}^{b3,a}$
- IE-FS: $\mathcal{D}_1^{a2}, \mathcal{D}_1^{a3}, \mathcal{D}_2^{a1}, \mathcal{D}_2^{a3}, \mathcal{D}_3^{a2}, \mathcal{D}_3^{a1}, \mathcal{D}_1^{b2}, \mathcal{D}_1^{b3}, \mathcal{D}_2^{b1}, \mathcal{D}_2^{b3}, \mathcal{D}_3^{b2}, \mathcal{D}_3^{b1}$
- FE-IS: $\mathcal{D}_{12}^a, \mathcal{D}_{23}^a, \mathcal{D}_{13}^a, \mathcal{D}_{12}^b, \mathcal{D}_{13}^b, \mathcal{D}_{23}^b$.

For a tree matrix element involving four coloured particles it is no longer possible to factorize the colour charge algebra. It follows from colour conservation, that four of the six colour charge operators $\mathbf{T}_i \mathbf{T}_j$ with $i \neq j$ can be expressed through the quadratic Casimir invariants and $\mathbf{T}_1 \mathbf{T}_2, \mathbf{T}_1 \mathbf{T}_3$ giving [28]

$$\mathbf{T}_3 \mathbf{T}_4 |1, 2, 3, 4\rangle = \left[\frac{1}{2} (C_1 + C_2 - C_3 - C_4) + \mathbf{T}_1 \mathbf{T}_2 \right] |1, 2, 3, 4\rangle \quad (8.185)$$

$$\mathbf{T}_2 \mathbf{T}_4 |1, 2, 3, 4\rangle = \left[\frac{1}{2} (C_1 + C_3 - C_2 - C_4) + \mathbf{T}_1 \mathbf{T}_3 \right] |1, 2, 3, 4\rangle \quad (8.186)$$

$$\mathbf{T}_2 \mathbf{T}_3 |1, 2, 3, 4\rangle = \left[\frac{1}{2} (C_4 - C_1 - C_2 - C_3) - \mathbf{T}_1 \mathbf{T}_2 - \mathbf{T}_1 \mathbf{T}_3 \right] |1, 2, 3, 4\rangle \quad (8.187)$$

$$\mathbf{T}_1 \mathbf{T}_4 |1, 2, 3, 4\rangle = - (C_1 + \mathbf{T}_1 \mathbf{T}_2 + \mathbf{T}_1 \mathbf{T}_3) |1, 2, 3, 4\rangle . \quad (8.188)$$

The four colour charge operators are associated with the particles in our process as follows:

$$\mathbf{T}_1 = \mathbf{T}_{\tilde{q}}, \quad \mathbf{T}_2 = \mathbf{T}_{\tilde{q}^*}, \quad \mathbf{T}_3 = \mathbf{T}_{g_a} \text{ and } \mathbf{T}_4 = \mathbf{T}_{g_b}. \quad (8.189)$$

For the remaining two operators the colour correlations have to be evaluated explicitly. For $\mathbf{T}_1\mathbf{T}_2$ the colour correlated matrix element splits into the three known colour channels

$$\langle 1, 2, 3, 4 | \mathbf{T}_1\mathbf{T}_2 | 1, 2, 3, 4 \rangle = \left[\mathcal{M}_{\text{LO}}^{st,ab}(p_a, p_b, k_1, k_2) \right]^* (-t_{vt}^c) t_{su}^c \mathcal{M}_{\text{LO}}^{uv,ab}(p_a, p_b, k_1, k_2) \quad (8.190)$$

$$= -C_F |\hat{\mathcal{M}}_{\text{LO}}^{(1)}|^2 + \frac{1}{2N} |\hat{\mathcal{M}}_{\text{LO}}^{(8_S)}|^2 + \frac{1}{2N} |\hat{\mathcal{M}}_{\text{LO}}^{(8_A)}|^2 \quad (8.191)$$

whereas $\mathbf{T}_1\mathbf{T}_3$ mixes them

$$\langle 1, 2, 3, 4 | \mathbf{T}_1\mathbf{T}_3 | 1, 2, 3, 4 \rangle = \left[\mathcal{M}_2^{st,ab}(p_a, p_b, k_1, k_2) \right]^* (-t_{vt}^c) i f_{acd} \mathcal{M}_2^{sv,db}(p_a, p_b, k_1, k_2). \quad (8.192)$$

Recall that s denotes here the colour of the anti-squark and t the colour of the squark. This means that \mathbf{T}_1 acts on t and \mathbf{T}_2 on s . As an additional cross-check we can compare the relations from colour conservation above with the explicit computation of the colour correlation, for example

$$\begin{aligned} \langle 1, 2, 3, 4 | \mathbf{T}_3\mathbf{T}_4 | 1, 2, 3, 4 \rangle &= \left[\mathcal{M}_{gg}^{st,eb}(p_a, p_b, k_1, k_2) \right]^* (-i f_{eca}) i f_{dcb} \mathcal{M}_{gg}^{st,ad}(p_a, p_b, k_1, k_2) \\ &= -C_A |\mathcal{M}_{gg}^{(1)}|^2 - \frac{N}{2} |\mathcal{M}_{gg}^{(8_S)}|^2 - \frac{N}{2} |\mathcal{M}_{gg}^{(8_A)}|^2 = \langle 1, 2, 3, 4 | C_F - C_A + \mathbf{T}_1\mathbf{T}_2 | 1, 2, 3, 4 \rangle. \end{aligned} \quad (8.193)$$

The large number of different dipoles, which have to be considered on the real side, are reduced to a few on the virtual side since two dipoles, that are related through the exchange of gluon, give the same results after integrating out the emitted gluon

- FE-FS: $3I_{gg,g}$
- IE-IS: $3I_{\tilde{q}g,\tilde{q}^*}, 3I_{\tilde{q}^*g,\tilde{q}}$
- IE-FS: $6I_{\tilde{q}g}^{\tilde{q}g}, 6I_{\tilde{q}g}^{\tilde{q}^*g}$
- FE-IS: $3I_{gg}^{\tilde{q}}, 3I_{gg}^{\tilde{q}^*}$.

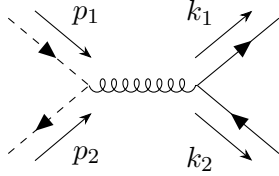
8.4.3.2 A quark-antiquark pair in the final state

For the process with a quark-antiquark pair in the final state a total of 15 dipoles are needed to ensure an infrared finite result:

- IE-IS: $\mathcal{D}^{a3,b}, \mathcal{D}^{b3,a}$
- IE-FS: $\mathcal{D}_1^{a3}, \mathcal{D}_2^{a3}, \mathcal{D}_1^{b3}, \mathcal{D}_2^{b3}$
- FE-FS: $\mathcal{D}_{12,3}, \mathcal{D}_{13,2}, \mathcal{D}_{23,1}$
- FE-IS: $\mathcal{D}_{12}^a, \mathcal{D}_{12}^b, \mathcal{D}_{31}^a, \mathcal{D}_{32}^a, \mathcal{D}_{31}^b, \mathcal{D}_{32}^b$.

It is important to recognize that in the singular limit, the Feynman diagrams in parentheses from fig. 8.14 are reduced to the process $\tilde{q}\tilde{q}^* \rightarrow Q\bar{Q}$, while the remaining diagrams transition to $\tilde{q}\tilde{q}^* \rightarrow gg$. For this reason, two different tree matrix elements occur in the dipoles. For

the latter process the already known amplitude \mathcal{M}_{LO} applies and for the other one the new amplitude



$$\mathcal{M}_{q\bar{q}} = \delta_{ij} T_{st}^a T_{ru}^a \frac{ig_s^2}{s} (p_1 - p_2)_\sigma \bar{u}^{(s)}(k_1) \gamma^\sigma v^{(s)}(k_2) \quad (8.194)$$

which gives the squared and summed matrix element

$$|\mathcal{M}_{q\bar{q}}|^2 = \frac{g_s^4}{s^2} N C_F \left(s^2 - 4m_{\tilde{q}_i}^2 s - (t - u)^2 \right) \quad (8.195)$$

has to be used. The colour correlated matrix elements factorize into $|\mathcal{M}_{q\bar{q}}|^2$ and a colour factor

$$\langle 1, 2, 3, 4 | \mathbf{T}_1 \mathbf{T}_2 | 1, 2, 3, 4 \rangle = \frac{1}{2N} |\mathcal{M}_{q\bar{q}}|^2 \langle 1, 2, 3, 4 | \mathbf{T}_1 \mathbf{T}_3 | 1, 2, 3, 4 \rangle = \frac{2 - N^2}{2N} |\mathcal{M}_{q\bar{q}}|^2. \quad (8.196)$$

8.5 Preliminary results and discussion

To check the consistency of the result for the corrected cross section $\Delta\sigma^{\text{NLO}}$ both the virtual and real corrections are with the methods of ghosts and also by using the lightcone gauge (full polarization sum). As the ghosts emerge from Slavnov-Taylor identities that the amplitudes must fulfill, this effectively probes the gauge invariance of the cross section. However, since the discrepancy between the dipole and the phase-space slicing method for the process $\tilde{\chi}_1^0 \tilde{t}_1 \rightarrow tg$ could not be resolved until the thesis was to be finished and thus the correctness of the finite parts of the integrated dipoles could not be finally confirmed, we refrain from giving a result for the entire NLO correction. However, by applying the newly developed integrated dipoles to the mentioned process, the correctness of the singular parts for the cases of a final emitter with an initial spectator and vice versa could be confirmed which legitimises their application to this process. Through extensive checks the infrared and ultraviolet convergence could then be verified which provides a non-trivial check for the virtual cross section. In addition, this confirms the correctness of the singular parts of the integrated dipole involving $\tilde{q} \rightarrow \tilde{q}g$ splitting for emitter and spectator both from the initial state which have not been probed yet by another process. The results for the virtual corrections in both gauges where the infrared poles are discarded are shown in table 8.2. Both gauges for different center-of-mass momenta agree within two or three digits. Due to the lack of reference results in the literature, it is not possible to determine whether this difference is of pure numerical nature or whether there might still be an error in the calculation. However, it should be noted that this uncertainty is smaller than the errors arising in connection with methods such as the phase-space slicing approach as discussed in section 5.6.2 or [29].

p_{cm} [GeV]	$v\sigma^{\text{LO}}$	$v\sigma_{\text{finite}}^{\text{V}}$ (FDH)	
		lightcone	ghost
100	9.735215	4.857407	4.856361
200	9.276764	2.934100	2.931544
300	8.595282	2.192852	2.188095
400	7.785973	1.741655	1.734365
500	6.94020	1.414466	1.404658

Table 8.2: Leading order cross section $v\sigma^{\text{LO}}$ and the IR finite parts of the virtual cross section $v\sigma_{\text{finite}}^{\text{V}}$ in the FDH scheme for different center-of-mass momenta p_{cm} and for the two different gauges. All cross sections times velocity $v\sigma$ are given in 10^{-9}GeV^{-2} and are obtained for the pMSSM scenario II defined in table 7.1.

9 Conclusion and outlook

In this thesis, the virtual corrections to squark-antisquark annihilation into two gluons were computed within the **DM@NLO** project where an infrared and ultraviolet finite result was achieved. As an additional cross check the calculation was performed by employing the full polarization sum ("lightcone gauge") for the matrix element squared as well as by including ghosts to subtract the unphysical polarizations of the gluon. However, the agreement of both methods on the level of the cross section is limited to three digits which might point towards an inconsistency within the calculation or implementation. In order to arrive at this result orthogonal multiplet bases were introduced as an efficient method to deal with colour in (loop) calculations as well Slavnov-Taylor identities that emerge from BRS-symmetry and allow to derive how ghost processes have to be included in order to ensure a gauge invariant cross section.

Building on [1] the dipole subtraction method for massive initial states was brought to the point where all integrated dipoles relevant for this process are present. To check the correctness of the results, the dipole method was implemented as an alternative for two processes which are already available in **DM@NLO** and for which the phase-space slicing method was used. For the first process $\tilde{\chi}_1^0 \tilde{t}_1 \rightarrow th^0/H$ where only soft divergences appear both methods agree within the expected uncertainties whereas for the second process $\tilde{\chi}_1^0 \tilde{t}_1 \rightarrow tg$ where in addition collinear and soft-collinear divergences are present, a large deviation between both approaches is observed. However, the correctness of the singular parts of the integrated dipoles was confirmed which allowed to render the process of this thesis $\tilde{q}\tilde{q}^* \rightarrow gg$ (**stsT2gg**) infrared finite in the first place. Related to the real corrections it turned out that the process $\tilde{q}\tilde{q}^* \rightarrow Q\bar{Q}$ (**stSt2QQbar**) needs to be extended to support massless quarks in the final state and that this process then has to be combined with **stsT2gg** in order to ensure a well-defined cross section. However, as long as the discrepancy between the dipole and the phase-space slicing method remains unsolved no final result for $\tilde{q}\tilde{q}^* \rightarrow gg$ can be given which prevents this process from being finished. In addition, it is reasonable to compare the dipole method against the phase-space slicing approach for other processes available in **DM@NLO**. Suitable examples would be $\tilde{q}\tilde{q} \rightarrow QQ$ and $\tilde{q}\tilde{q}^* \rightarrow Q\bar{Q}$ as these also cover the integrated dipole for an emitter and spectator both from the initial state whose corresponding finite parts have not been checked so far.

A Useful formula and relations

A.1 Useful functions within dimensional regularization

This section lists some special functions and relations which turn out to be helpful for calculations in dimensional regularization and can be found in the many standard mathematical handbooks such as [73, 74]. In addition, expansions for two different argument sets of the Gaussian hypergeometric function are derived in detail starting from the hypergeometric equation in appendix A.1.3.

A.1.1 Gamma and Beta function

For complex numbers z with a positive real part, the Gamma function $\Gamma(z)$ can be defined as the improper integral

$$\Gamma(z) = \int_0^\infty dt t^{z-1} e^{-t}, \quad \text{Re } z > 0. \quad (\text{A.1})$$

It obeys the recursion relation $\Gamma(z+1) = z\Gamma(z)$ and has the expansions

$$\Gamma(z) = \frac{1}{z} - \gamma_E + \frac{1}{2} \left(\gamma_E^2 + \frac{\pi^2}{6} \right) z - \frac{1}{6} \left(\gamma_E^3 + \gamma_E \frac{\pi^2}{2} + 2\zeta(3) \right) z^2 + \mathcal{O}(z^3) \quad (\text{A.2})$$

$$\frac{1}{\Gamma(z)} = z + \gamma_E z^2 + \frac{1}{2} \left(\gamma_E^2 - \frac{\pi^2}{6} \right) z^3 + \mathcal{O}(z^4) \quad (\text{A.3})$$

where γ_E is the Euler-Mascheroni constant and $\zeta(z)$ the Riemann zeta function. The Euler β -function (or Eulerian integral of the first kind)

$$\beta(a, b) = \int_0^1 dt (1-t)^{a-1} t^{b-1} = \frac{\Gamma(a)\Gamma(b)}{\Gamma(a+b)} \quad (\text{A.4})$$

often makes an expansion of an integral in some small parameter ε accessible through the Gamma function. Two of these expansions needed within this work are

$$\beta(1-\varepsilon, 1-\varepsilon) = 1 + 2\varepsilon + \left(4 - \frac{\pi^2}{6} \right) \varepsilon^2 + \mathcal{O}(\varepsilon^3) \quad (\text{A.5})$$

$$\beta(2-\varepsilon, 2-\varepsilon) = \frac{1}{6} + \frac{5}{18} \varepsilon + \mathcal{O}(\varepsilon^2). \quad (\text{A.6})$$

A.1.2 Spence function

The Spence function or dilogarithm is defined as

$$\text{Li}_2(z) = - \int_0^1 dt \frac{\ln(1-zt)}{t} = - \int_0^z dt \frac{\ln(1-t)}{t}. \quad (\text{A.7})$$

A.1.3 Gaussian hypergeometric function

The Gaussian or just ordinary hypergeometric function $u = {}_2F_1(a, b; c; z)$ is in general a solution of the hypergeometric equation

$$z(1-z)u''(z) + (c - (a+b+1)z)u'(z) - ab u(z) = 0 \quad (\text{A.8})$$

with the initial condition $u(0) = 1$. A solution of this homogenous second-order linear ODE is given by the integral

$${}_2F_1(a, b; c; z) = \frac{\Gamma(c)}{\Gamma(b)\Gamma(c-b)} \int_0^1 dt \frac{t^{b-1}(1-t)^{c-b-1}}{(1-zt)^a}. \quad (\text{A.9})$$

The identity

$$\int_0^\infty dt t^{\alpha-1} {}_2F_1(a, b; c; -t) = \frac{\Gamma(\alpha)\Gamma(c)\Gamma(a-\alpha)\Gamma(b-\alpha)}{\Gamma(a)\Gamma(b)\Gamma(c-\alpha)}, \quad 0 < \text{Re}(\alpha) < \min(\text{Re}(a), \text{Re}(b)) \quad (\text{A.10})$$

allows to integrate over a hypergeometric function[75]. The Pfaff transformation

$${}_2F_1(a, b; c; z) = (1-z)^{-a} {}_2F_1\left(a, c-b; c; \frac{z}{z-1}\right) \quad (\text{A.11})$$

relates different argument sets.

It is often very useful to expand the argument set of the hypergeometric function for an infinitesimal parameter ε . The expansion can be obtained by inserting the ansatz

$$u(z) = r(z) + \varepsilon s(z) + \mathcal{O}(\varepsilon^2) \quad (\text{A.12})$$

into the differential equation in eq. (A.8) and solving the resulting system of equations order by order while enforcing the boundary conditions $r(0) = 1$ and $s(0) = 0$. This method is illustrated by the argument set ${}_2F_1(1, 1-\varepsilon, 2-2\varepsilon; z)$ leading to

$$\mathcal{O}(\varepsilon^0) : (1-z)zr''(z) + (2-3z)r'(z) - r(z) = 0 \quad (\text{A.13})$$

$$\mathcal{O}(\varepsilon^1) : (1-z)zs''(z) + (z-2)r'(z) + (2-3z)s'(z) - s(z) + r(z) = 0. \quad (\text{A.14})$$

This system of ODEs can be solved by applying the product rule for differentiation "inversely" giving

$$\mathcal{O}(\varepsilon^0) : \frac{d}{dz} \left[(1-z) \frac{d}{dz} zr(z) \right] = 0 \quad (\text{A.15})$$

$$\mathcal{O}(\varepsilon^1) : \frac{d}{dz} \left[(1-z) \frac{d}{dz} zs(z) + zr(z) - 2r(z) \right] = 0 \quad (\text{A.16})$$

such that one obtains after two subsequent integrations

$$r(z) = C_1 \frac{\ln(1-z)}{z} + \frac{C_2}{z} \quad (\text{A.17})$$

$$s(z) = \frac{1}{z} \left(C_3 \ln(1-z) + 2 \text{Li}_2(z) + \frac{1}{2} \ln^2(1-z) \right) + \frac{C_4}{z} \quad (\text{A.18})$$

where the C_i are constants of integration. These take the values $C_1 = -1$, $C_2 = 0$, $C_3 = 2$ and $C_4 = 0$ after using L'Hôpital's rule to ensure the limits $r(0) = 1$ and $s(0) = 0$. The complete result reads

$${}_2F_1(1, 1 - \varepsilon, 2 - 2\varepsilon; z) = -\frac{\ln(1 - z)}{z} + \frac{\varepsilon}{z} \left(2\text{Li}_2(z) + \frac{1}{2}\ln^2(1 - z) + 2\ln(1 - z) \right) + \mathcal{O}(\varepsilon^2). \quad (\text{A.19})$$

The same steps can be repeated to obtain the expansion

$${}_2F_1(2, 1 - \varepsilon, 2 - 2\varepsilon; z) = \frac{1}{1 - z} + \frac{\varepsilon}{z(z - 1)} (2z + \ln(1 - z)(2 - z)) + \mathcal{O}(\varepsilon^2). \quad (\text{A.20})$$

A.1.4 Integrals related to the dipole subtraction method

The following integral is needed up to order $\mathcal{O}(\varepsilon)$

$$\mathcal{I}_1(y_0; \varepsilon) = \int_0^{y_0} dy \frac{1}{y^{1+\varepsilon}} I_1 \left(-\frac{1}{y}; \varepsilon \right). \quad (\text{A.21})$$

The integral can be separated into a part giving the divergences for $y \rightarrow 0$ and a finite part

$$\begin{aligned} \mathcal{I}_1(y_0; \varepsilon) = \beta(1 - \varepsilon, 1 - \varepsilon) & \left(\frac{1}{y_0^{1+\varepsilon}} \int_0^1 dt t^\varepsilon {}_2F_1 \left(1, 1 - \varepsilon; 2 - 2\varepsilon; -\frac{t}{y_0} \right) \right. \\ & \left. - \int_0^\infty dt t^\varepsilon {}_2F_1(1, 1 - \varepsilon; 2 - 2\varepsilon; -t) \right). \quad (\text{A.22}) \end{aligned}$$

The last integral contains the divergent piece and is evaluated using eq. (A.10)

$$\int_0^\infty dt t^\varepsilon {}_2F_1(1, 1 - \varepsilon, 2 - 2\varepsilon; -t) = \frac{\Gamma(2 - 2\varepsilon)\Gamma(-2\varepsilon)\Gamma(-\varepsilon)\Gamma(1 + \varepsilon)}{\Gamma(1 - 3\varepsilon)\Gamma(1 - \varepsilon)} = \frac{1}{2\varepsilon^2} - \frac{1}{\varepsilon} + \mathcal{O}(\varepsilon). \quad (\text{A.23})$$

The other integral is finite and can be evaluated for $\varepsilon = 0$ where the hypergeometric function takes the form of the zeroth order term in eq. (A.19) giving a dilogarithm

$$\int_0^1 dt t^\varepsilon {}_2F_1 \left(1, 1 - \varepsilon; 2 - 2\varepsilon; -\frac{t}{y_0} \right) = -y_0 \text{Li}_2 \left(-\frac{1}{y_0} \right) + \mathcal{O}(\varepsilon). \quad (\text{A.24})$$

After expanding everything up to order $\mathcal{O}(\varepsilon)$ one obtains

$$\mathcal{I}_1(y_0; \varepsilon) = -\frac{1}{2\varepsilon^2} + \frac{\pi^2}{12} - \text{Li}_2 \left(-\frac{1}{y_0} \right) + \mathcal{O}(\varepsilon). \quad (\text{A.25})$$

The same steps can be repeated for the integral

$$\mathcal{I}_2(y_0; \varepsilon) = \int_0^{y_0} dy \frac{1}{y^{1+\varepsilon}} I_2 \left(-\frac{1}{y}; \varepsilon \right) = \frac{1}{2\varepsilon} + \ln \left(1 + \frac{1}{y_0} \right) + \mathcal{O}(\varepsilon) \quad (\text{A.26})$$

which are

$$\int_0^\infty dt t^\varepsilon {}_2F_1(2, 1 - \varepsilon, 2 - 2\varepsilon; -t) = \frac{\Gamma(2 - 2\varepsilon)\Gamma(-2\varepsilon)\Gamma(\varepsilon + 1)}{\Gamma(1 - 3\varepsilon)} = -\frac{1}{2\varepsilon} + 1 + \mathcal{O}(\varepsilon) \quad (\text{A.27})$$

$$\int_0^1 dt t^\varepsilon {}_2F_1\left(2, 1 - \varepsilon; 2 - 2\varepsilon; -\frac{t}{y_0}\right) = y_0 \int_0^1 dt \frac{1}{t + y_0} + \mathcal{O}(\varepsilon) = y_0 \ln\left(1 + \frac{1}{y_0}\right) + \mathcal{O}(\varepsilon). \quad (\text{A.28})$$

A.2 Useful relations for the $\text{SU}(N_c)$ generators

These relations can be found in [76] but are given here in a more modern notation. It is convenient to introduce a matrix notation for the f - and d -symbol

$$(F^a)_{bc} = \text{i} f_{bac} \quad (\text{A.29})$$

$$(D^a)_{bc} = d_{bac}. \quad (\text{A.30})$$

The (anti)commutators are defined through

$$[T^a, T^b] = \text{i} f_{abc} T^c \quad (\text{A.31})$$

$$[F^a, F^b] = \text{i} f_{abc} F^c \quad (\text{A.32})$$

$$[F^a, D^b] = \text{i} f_{abc} D^c \quad (\text{A.33})$$

$$\{T^a, T^b\} = \frac{1}{N} \delta_{ab} \mathbb{1} + d_{abc} T^c. \quad (\text{A.34})$$

The Fierz identity

$$T_{ij}^a T_{kl}^a = \frac{1}{2} \left(\delta_{il} \delta_{jk} - \frac{1}{N} \delta_{ij} \delta_{kl} \right) \quad (\text{A.35})$$

allows to contract indices that belong to the adjoint representation. The quadratic Casimirs take the following values

$$T^a T^a = C_F \mathbb{1}, \quad C_F = \frac{N^2 - 1}{2N} \quad (\text{A.36})$$

$$F^a F^a = C_A \mathbb{1}, \quad C_A = N \quad (\text{A.37})$$

$$D^a D^a = \frac{N^2 - 4}{N} \mathbb{1}. \quad (\text{A.38})$$

The Dynkin indices define the normalization of a representation and are given by

$$\text{Tr}(T^a T^b) = T_F \delta_{ab}, \quad T_F = \frac{1}{2} \quad (\text{A.39})$$

$$\text{Tr}(F^a F^b) = N \delta_{ab} \quad (\text{A.40})$$

$$\text{Tr}(D^a D^b) = \frac{N^2 - 4}{N} \delta_{ab}. \quad (\text{A.41})$$

Other useful relations that can be derived from the definitions above are

$$T^a T^b = \frac{1}{2} \left[\frac{1}{N} \delta_{ab} \mathbb{1} + (d_{abc} + \text{i} f_{abc}) T^c \right] \quad (\text{A.42})$$

$$\mathrm{Tr} \left(F^a F^b F^c \right) = \frac{i}{2} N f_{abc} \tag{A.43}$$

$$T^a T^b T^a = -\frac{1}{2N} T^b . \tag{A.44}$$

B Feynman rules

B.1 Propagators

The momentum p in the fermionic propagators points for internal lines in the direction of the fermion flow.

$$\mu, a \text{ } \text{-----} \text{ } \nu, b = \begin{cases} i\delta_{ab}\Pi_{R\xi}^{\mu\nu}(p) = i\delta_{ab}\frac{-g^{\mu\nu} + (1-\xi)\frac{p^\mu p^\nu}{p^2}}{p^2 + i\epsilon} \\ i\delta_{ab}\Pi_{\text{lightcone}}^{\mu\nu}(p, n) = \delta_{ab}\frac{i}{p^2 + i\epsilon} \left(-g^{\mu\nu} + \frac{n^\mu p^\nu + n^\nu p^\mu}{n \cdot p} \right) \end{cases} \quad (\text{B.1})$$

$$\alpha, s \text{ } \text{-----} \text{ } \beta, t = \delta_{st}\delta^{\alpha\beta} \frac{i(\not{p} + m_{q^\alpha})}{p^2 - m_{q^\alpha}^2 + i\epsilon} \quad (\text{B.2})$$

$$a \text{ } \text{-----} \text{ } b = \delta_{ab} \frac{i(\not{p} + m_{\tilde{g}})}{p^2 - m_{\tilde{g}}^2 + i\epsilon} \quad (\text{B.3})$$

$$\alpha, i, r \text{ } \text{-----} \text{ } \beta, j, s = \frac{i\delta_{ij}\delta_{st}\delta^{\alpha\beta}}{p^2 - m_{q_i^\alpha}^2 + i\epsilon} \quad (\text{B.4})$$

$$a \text{ } \text{-----} \text{ } b = \frac{i\delta_{ab}}{p^2 + i\epsilon} \quad (\text{B.5})$$

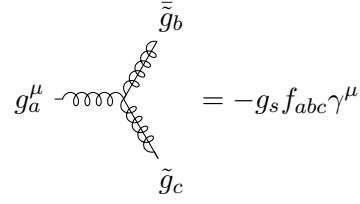
B.2 Couplings

All couplings relevant for stop annihilation into gluons are listed below. These are taken from [5] and compared to those in [77]. In order to arrive at the Feynman rules given in [77] starting from [5], the quark gauge eigenstates have to be redefined via the replacements $U^{u_R}, U^{d_R}, U^{u_L} \rightarrow \mathbb{1}$ and $U^{d_L} \rightarrow V^{q_L}$. In addition, the squark mixing matrices $W^{\tilde{f}}$ have to be flavour diagonal reducing them to the $L - R$ -mixing matrices $R^{\tilde{f}}$ in accordance with the assumptions of the pMSSM.

2-quark-gluon vertex

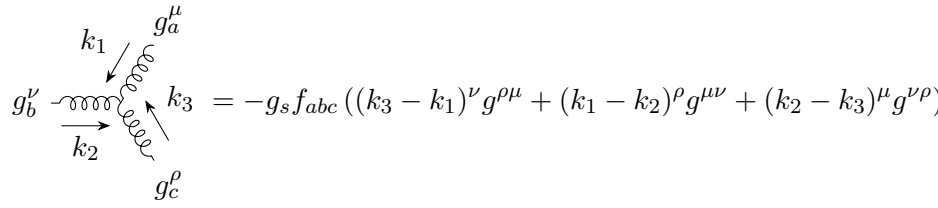
$$g_a^\mu \text{ } \text{-----} \text{ } \begin{array}{c} q_r^\alpha \\ \swarrow \\ \searrow \\ \bar{q}_s^\beta \end{array} = -ig_s T_{sr}^a \delta^{\alpha\beta} \gamma^\mu \quad (\text{B.6})$$

2-gluino-gluon vertex



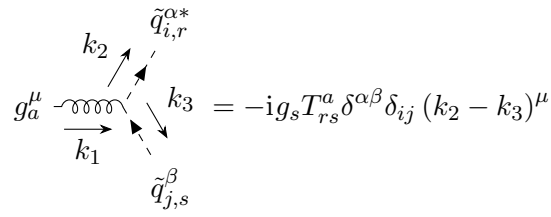
$$g_a^\mu \text{---} \text{---} \text{---} \begin{array}{l} \nearrow \bar{g}_b \\ \searrow \tilde{g}_c \end{array} = -g_s f_{abc} \gamma^\mu \quad (\text{B.7})$$

Triple-gluon vertex



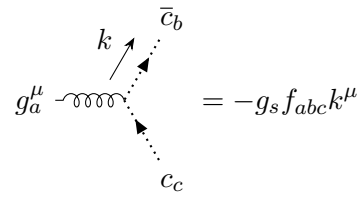
$$\begin{array}{c} g_a^\mu \\ \nearrow k_1 \\ g_b^\nu \text{---} \text{---} \text{---} k_2 \text{---} \text{---} \text{---} k_3 \searrow \\ g_c^\rho \end{array} = -g_s f_{abc} ((k_3 - k_1)^\nu g^{\rho\mu} + (k_1 - k_2)^\rho g^{\mu\nu} + (k_2 - k_3)^\mu g^{\nu\rho}) \quad (\text{B.8})$$

2-squark-gluon vertex



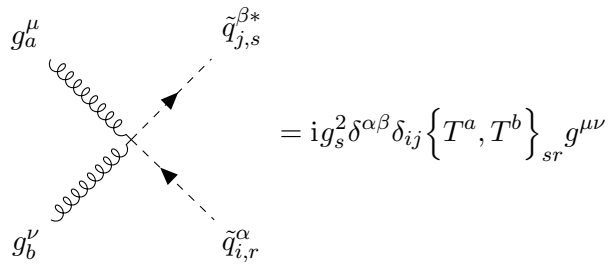
$$g_a^\mu \text{---} \text{---} \text{---} \begin{array}{l} \nearrow \tilde{q}_{i,r}^{\alpha*} \\ \searrow \tilde{q}_{j,s}^\beta \end{array} = -i g_s T_{rs}^a \delta^{\alpha\beta} \delta_{ij} (k_2 - k_3)^\mu \quad (\text{B.9})$$

Gluon-ghost vertex



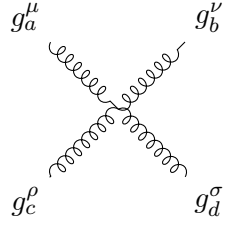
$$g_a^\mu \text{---} \text{---} \text{---} \begin{array}{l} \nearrow \bar{c}_b \\ \searrow c_c \end{array} = -g_s f_{abc} k^\mu \quad (\text{B.10})$$

Four-gluon-squark vertex



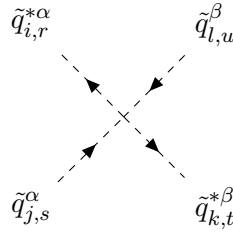
$$\begin{array}{c} g_a^\mu \\ \nearrow \\ g_b^\nu \end{array} \text{---} \text{---} \text{---} \begin{array}{l} \nearrow \tilde{q}_{j,s}^{\beta*} \\ \searrow \tilde{q}_{i,r}^\alpha \end{array} = i g_s^2 \delta^{\alpha\beta} \delta_{ij} \{T^a, T^b\}_{sr} g^{\mu\nu} \quad (\text{B.11})$$

Four-gluon vertex



$$\begin{aligned}
 &= -ig_s^2 (f_{abe}f_{cde} (g^{\mu\rho}g^{\nu\sigma} - g^{\mu\sigma}g^{\nu\rho}) \\
 &\quad + f_{ace}f_{bde} (g^{\mu\nu}g^{\rho\sigma} - g^{\mu\sigma}g^{\nu\rho}) \\
 &\quad + f_{ade}f_{bce} (g^{\mu\nu}g^{\sigma\rho} - g^{\mu\rho}g^{\nu\sigma})) \\
 &\quad (B.12)
 \end{aligned}$$

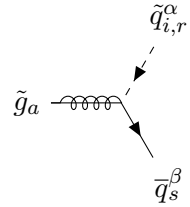
Four-squark vertex



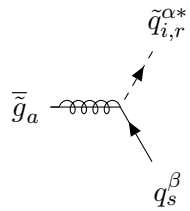
$$= -ig_s^2 \left(T_{rs}^a T_{tu}^a A_{ij}^\alpha A_{kl}^\beta + \delta^{\alpha\beta} T_{ru}^a T_{ts}^a A_{il}^\alpha A_{kj}^\alpha \right) \quad (B.13)$$

$$\text{with } A_{ij}^\alpha := R_{i1}^\alpha R_{j1}^\alpha - R_{i2}^\alpha R_{j2}^\alpha \quad (B.14)$$

Quark-squark-gluino vertex

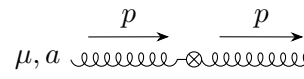


$$= -i\sqrt{2}g_s T_{sr}^a \delta^{\alpha\beta} (R_{i1}^\alpha P_R - R_{i2}^\alpha P_L) \quad (B.15)$$

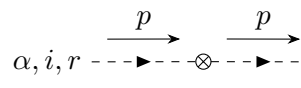


$$= -i\sqrt{2}g_s T_{rs}^a \delta^{\alpha\beta} (R_{i1}^\alpha P_L - R_{i2}^\alpha P_R) \quad (B.16)$$

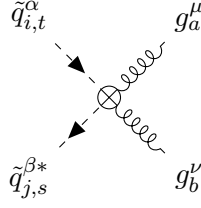
B.3 Counterterms



$$\mu, a \xrightarrow{p} \nu, b = -i\delta_{ab} (p^2 g^{\mu\nu} - p^\mu p^\nu) \delta Z_g \quad (B.17)$$

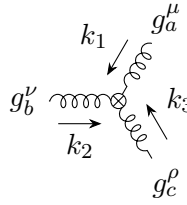


$$\alpha, i, r \xrightarrow{p} \beta, j, s = i\delta^{\alpha\beta} \delta_{rs} \left((p^2 - m_{\tilde{q}_i^\alpha}^2) \delta Z_{ji}^{\tilde{q}_i^\alpha} - \delta_{ij} \delta m_{\tilde{q}_i^\alpha}^2 \right) \quad (B.18)$$



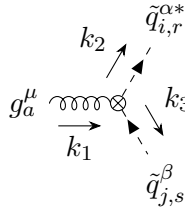
$$= i g_s^2 g^{\mu\nu} \{T^a, T^b\}_{st} \delta^{\alpha\beta} \delta_{ji}^{4,\alpha} \quad (\text{B.19})$$

$$\text{with } \delta_{ji}^{4,\alpha} = 2 \frac{\delta g_s}{g_s} \delta_{ji} + \delta Z_g \delta_{ji} + \frac{1}{2} \delta Z_{ji}^{\bar{q}^\alpha} + \frac{1}{2} [\delta Z_{ij}^{\bar{q}^\alpha}]^* \quad (\text{B.20})$$



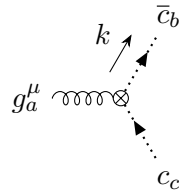
$$= -g_s f_{abc} ((k_3 - k_1)^\nu g^{\rho\mu} + (k_1 - k_2)^\rho g^{\mu\nu} + (k_2 - k_3)^\mu g^{\nu\rho}) \delta_{3g} \quad (\text{B.21})$$

$$\text{with } \delta_{3g} = \frac{3}{2} \delta Z_g + \frac{\delta g_s}{g_s} \quad (\text{B.22})$$



$$= -i g_s T_{rs}^a \delta^{\alpha\beta} (k_2 - k_3)^\mu \delta_{ij}^{2\bar{q}g,\alpha} \quad (\text{B.23})$$

$$\text{with } \delta_{ij}^{2\bar{q}g,\alpha} = \left(\frac{\delta g_s}{g_s} + \frac{1}{2} \delta Z_g \right) \delta_{ij} + \frac{1}{2} [\delta Z_{ji}^{\bar{q}^\alpha}]^* + \frac{1}{2} \delta Z_{ij}^{\bar{q}^\alpha} \quad (\text{B.24})$$



$$= -g_s f_{abc} k^\mu \delta_{2cg} \quad (\text{B.25})$$

$$\text{with } \delta_{2cg} = \frac{\delta g_s}{g_s} + \delta Z_c + \frac{1}{2} \delta Z_g \quad (\text{B.26})$$

C Vertex corrections

The vertex corrections in this chapter are computed in the HV and FDH schemes simultaneously. The parameter θ_D takes the value zero for the dimensional reduction and one for the dimensional regularization scheme. The shorthand \int_q is used for

$$\int \frac{d^D q}{(2\pi)^D} \frac{\mu^{2\varepsilon} g_s^m}{\mathcal{D}_0 \dots \mathcal{D}_n} \quad (\text{C.1})$$

where to correct number of appearances m of the strong coupling g_s and number of propagators $n + 1$ have to be inserted depending on the underlying Feynman diagram. Each vertex is decomposed into partial amplitudes that are defined in the respective section in section 8.3. The colour structure for each vertex has already been simplified so that only the colour basis elements remain where each basis vector is accompanied by a real number as prefactor which is referred to as colour factor and written directly in front of the basis element. The partial amplitudes listed here are given without the colour factor. Of course, the final expression for a whole vertex correction is obtained by combing the colour factors and form factors listed in this section. In some cases additional mixing matrices appear which are kept outside the form factors. In other cases, there arise colour structures that do not factorize with the rest of the amplitude as in eq. (C.3) or eq. (C.73). In those few cases the relation between the partial amplitudes and the rest of the amplitude is explicitly written out. The relationship between colour factors and partial amplitudes is illustrated by some further examples such as eq. (C.7) or eq. (C.89). Furthermore, the form factors listed for each vertex correction are defined *without* the imaginary unit i that comes from the definition of the general n -point integral in eq. (8.7). The subamplitudes that are not listed for a given diagram are zero.

C.1 Four-gluon-squark vertex

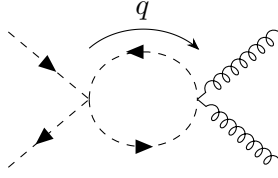
The momentum and index convention for the correction of the four-squark-gluon vertex as well as its parametrization in terms of the form factors A_g and A_{mn} is shown in eq. (8.114). As the external fields of this vertex coincide with the ones of the whole $2 \rightarrow 2$ process, the same indices and momentum labels are used.

C.1.1 Bubbles

Squark bubble

The matrices A^γ related to the mixing matrices R^γ for the squark sector with flavour γ are defined in eq. (B.14).

$$B_0 \left(s, m_{\tilde{q}_k}^2, m_{\tilde{q}_k}^2 \right) \quad (\text{C.2})$$



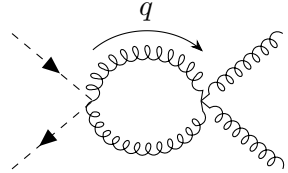
$$= i \sum_{\gamma, k} \left(\frac{1}{2} c_{st,ab}^{(8_S)} A_{ji}^\alpha A_{kk}^\gamma + \delta^{\alpha\gamma} \left(\frac{C_F}{N} c_{st,ab}^{(1)} - \frac{1}{2N} c_{st,ab}^{(8_S)} \right) A_{jk}^\alpha A_{ki}^\gamma \right) g^{\mu\nu} A_g \quad (C.3)$$

$$A_g = \frac{-g_s^4}{16\pi^2} B_0 \quad (C.4)$$

$$\mathcal{D}_0 = q^2 - m_{\tilde{q}_k}^2 + i\epsilon \quad \mathcal{D}_1 = (q - k_1 - k_2)^2 - m_{\tilde{q}_k}^2 + i\epsilon \quad (C.5)$$

Gluon bubble

$$B_0(s, 0, 0) \quad (C.6)$$



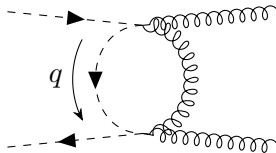
$$= i \delta_{ij} \left(c_{st,ab}^{(1)} + \frac{N}{2} c_{st,ab}^{(8_S)} \right) g^{\mu\nu} A_g \quad (C.7)$$

$$A_g = \frac{g_s^4}{16\pi^2} (-3B_0 + \theta_D 2) \quad (C.8)$$

$$\mathcal{D}_0 = q^2 - m_{\tilde{q}_i^\alpha}^2 + i\epsilon \quad \mathcal{D}_1 = (q - k_1 - k_2)^2 - m_{\tilde{q}_i^\alpha}^2 + i\epsilon \quad (C.9)$$

Squark-gluon bubble t

$$B_0(t, 0, m_{\tilde{q}_i^\alpha}^2) \quad (C.10)$$



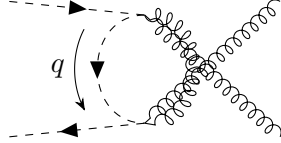
$$= i \delta_{ij} \left(\frac{N^2 - 2}{2N^2} c_{st,ab}^{(1)} + \frac{N^2 - 4}{4N} c_{st,ab}^{(8_S)} - \frac{N^2 - 4}{4N} c_{st,ab}^{(8_A)} \right) g^{\mu\nu} A_g \quad (C.11)$$

$$A_g = \frac{-g_s^4}{16\pi^2} B_0 \quad (C.12)$$

$$\mathcal{D}_0 = q^2 - m_{\tilde{q}_i^\alpha}^2 + i\epsilon \quad \mathcal{D}_1 = (q + p_2 - k_2)^2 + i\epsilon \quad (C.13)$$

Squark-gluon bubble u

$$B_0(u, 0, m_{\tilde{q}_i^\alpha}^2) \quad (\text{C.14})$$



$$= i\delta_{ij} \left(\frac{N^2 - 2}{2N^2} c_{st,ab}^{(1)} + \frac{N^2 - 4}{4N} c_{st,ab}^{(8_S)} + \frac{N^2 - 4}{4N} c_{st,ab}^{(8_A)} \right) g^{\mu\nu} A_g \quad (\text{C.15})$$

$$A_g = \frac{-g_s^4}{16\pi^2} B_0 \quad (\text{C.16})$$

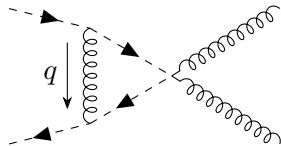
$$\mathcal{D}_0 = q^2 - m_{\tilde{q}_i^\alpha}^2 + i\epsilon \quad \mathcal{D}_1 = (q - k_1 + p_2)^2 + i\epsilon \quad (\text{C.17})$$

C.1.2 Triangles

Gluon exchange left

$$C_0(m_{\tilde{q}_i^\alpha}^2, s, m_{\tilde{q}_i^\alpha}^2, 0, m_{\tilde{q}_i^\alpha}^2, m_{\tilde{q}_i^\alpha}^2) \quad (\text{C.18})$$

$$B_0(s, m_{\tilde{q}_i^\alpha}^2, m_{\tilde{q}_i^\alpha}^2) \quad (\text{C.19})$$



$$= \delta_{ij} \left(\frac{C_F}{N} c_{st,ab}^{(1)} - \frac{1}{2N} c_{st,ab}^{(8_S)} \right) g^{\mu\nu} \int_q (2p_1 - q) \cdot (-2p_2 - q) \quad (\text{C.20})$$

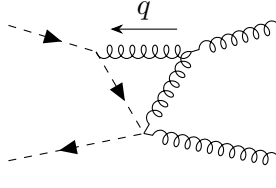
$$A_g = \frac{g_s^4}{16\pi^2} (B_0 + (4m_{\tilde{q}_i^\alpha}^2 - s)C_0 + 2(4m_{\tilde{q}_i^\alpha}^2 - s)C_1) \quad (\text{C.21})$$

$$\mathcal{D}_0 = q^2 + i\epsilon \quad \mathcal{D}_1 = (q + p_2)^2 - m_{\tilde{q}_i^\alpha}^2 + i\epsilon \quad \mathcal{D}_2 = (q - 2p_1)^2 - m_{\tilde{q}_i^\alpha}^2 + i\epsilon \quad (\text{C.22})$$

Gluon exchange above

$$C_0(m_{\tilde{q}_i^\alpha}^2, t, 0, 0, m_{\tilde{q}_i^\alpha}^2, 0) \quad (\text{C.23})$$

$$B_0(t, m_{\tilde{q}_i^\alpha}^2, 0) \quad (\text{C.24})$$



$$= \delta_{ij} \frac{N}{4} \left(c_{st,ab}^{(\mathbf{8}_A)} - c_{st,ab}^{(\mathbf{8}_S)} \right) \int_q -(2p_1 + q)_\sigma \quad (\text{C.25})$$

$$\times (g^{\mu\nu}(2k_1 + q)^\sigma + g^{\mu\sigma}(q - k_1)^\nu - g^{\nu\sigma}(k_1 + 2q)^\mu)$$

$$A_g = -\frac{g_s^4}{16\pi^2} (m_{\tilde{q}_i^\alpha}^2 (2C_0 + 3C_1 + C_2) - 2tC_0 - tC_1 - tC_2 + B_0 - C_{00}) \quad (\text{C.26})$$

$$A_{11} = \frac{g_s^4}{16\pi^2} (2C_2 + C_{22}) \quad (\text{C.27})$$

$$A_{33} = \frac{g_s^4}{16\pi^2} (2C_1 + C_{11}) \quad (\text{C.28})$$

$$A_{13} = \frac{g_s^4}{16\pi^2} (2C_0 + C_1 + C_{12} + 4C_2) \quad (\text{C.29})$$

$$A_{31} = \frac{g_s^4}{16\pi^2} (2C_0 + C_1 + C_{12} - 2C_2) \quad (\text{C.30})$$

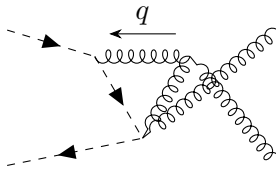
$$(\text{C.31})$$

$$\mathcal{D}_0 = q^2 + i\epsilon \quad \mathcal{D}_1 = (q + p_1)^2 - m_{\tilde{q}_i^\alpha}^2 + i\epsilon \quad \mathcal{D}_2 = (q + k_1)^2 + i\epsilon \quad (\text{C.32})$$

Gluon exchange above u

$$C_0 \left(m_{\tilde{q}_i^\alpha}^2, u, 0, 0, m_{\tilde{q}_i^\alpha}^2, 0 \right) \quad (\text{C.33})$$

$$B_0 \left(u, m_{\tilde{q}_i^\alpha}^2, 0 \right) \quad (\text{C.34})$$



$$= \delta_{ij} \frac{-N}{4} \left(c_{st,ab}^{(\mathbf{8}_A)} + c_{st,ab}^{(\mathbf{8}_S)} \right) \int_q -(2p_1 + q)_\sigma \quad (\text{C.35})$$

$$\times (g^{\mu\nu}(2k_2 + q)^\sigma - g^{\mu\sigma}(k_2 + 2q)^\nu + g^{\nu\sigma}(q - k_2)^\mu)$$

$$A_g = -\frac{g_s^4}{16\pi^2} (M_2(2C_0 + 3C_1 + C_2) - 2uC_0 - uC_1 - uC_2 + B_0 - C_{00}) \quad (\text{C.36})$$

$$A_{22} = \frac{g_s^4}{16\pi^2} (2C_2 + C_{22}) \quad (\text{C.37})$$

$$A_{33} = \frac{g_s^4}{16\pi^2} (2C_1 + C_{11}) \quad (\text{C.38})$$

$$A_{23} = \frac{g_s^4}{16\pi^2} (2C_0 + C_1 + C_{12} - 2C_2) \quad (\text{C.39})$$

$$A_{32} = \frac{g_s^4}{16\pi^2} (2C_0 + C_1 + C_{12} + 4C_2) \quad (\text{C.40})$$

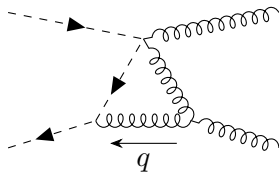
$$(C.41)$$

$$\mathcal{D}_0 = q^2 + i\epsilon \quad \mathcal{D}_1 = (q + p_1)^2 - m_{\tilde{q}_i^\alpha}^2 + i\epsilon \quad \mathcal{D}_2 = (q + k_2)^2 + i\epsilon \quad (C.42)$$

Gluon exchange below

$$C_0 \left(m_{\tilde{q}_i^\alpha}^2, t, 0, 0, m_{\tilde{q}_i^\alpha}^2, 0 \right) \quad (C.43)$$

$$B_0 \left(t, m_{\tilde{q}_i^\alpha}^2, 0 \right) \quad (C.44)$$



$$= \delta_{ij} \frac{N}{4} \left(c_{st,ab}^{(8_S)} - c_{st,ab}^{(8_A)} \right) \int_q (-2p_2 - q)_\sigma \times (g^{\mu\nu} (-(2k_2 + q)^\sigma) + g^{\mu\sigma} (k_2 + 2q)^\nu + g^{\nu\sigma} (k_2 - q)^\mu) \quad (C.45)$$

$$A_g = \frac{g_s^4}{16\pi^2} (m_{\tilde{q}_i^\alpha}^2 (2C_0 + 3C_1 + C_2) - 2tC_0 - tC_1 - tC_2 + B_0 - C_{00}) \quad (C.46)$$

$$A_{22} = -\frac{g_s^4}{16\pi^2} (2C_2 + C_{22}) \quad (C.47)$$

$$A_{44} = -\frac{g_s^4}{16\pi^2} (2C_1 + C_{11}) \quad (C.48)$$

$$A_{24} = -\frac{g_s^4}{16\pi^2} (2C_0 + C_1 + C_{12} - 2C_2) \quad (C.49)$$

$$A_{42} = -\frac{g_s^4}{16\pi^2} (2C_0 + C_1 + C_{12} + 4C_2) \quad (C.50)$$

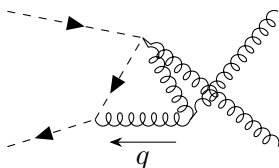
$$(C.51)$$

$$\mathcal{D}_0 = q^2 + i\epsilon \quad \mathcal{D}_1 = (q + p_2)^2 - m_{\tilde{q}_i^\alpha}^2 + i\epsilon \quad \mathcal{D}_2 = (q + k_2)^2 + i\epsilon \quad (C.52)$$

Gluon exchange below u

$$C_0 \left(m_{\tilde{q}_i^\alpha}^2, u, 0, 0, m_{\tilde{q}_i^\alpha}^2, 0 \right) \quad (C.53)$$

$$B_0 \left(u, m_{\tilde{q}_i^\alpha}^2, 0 \right) \quad (C.54)$$



$$= \delta_{ij} \frac{N}{4} \left(c_{st,ab}^{(8_A)} + c_{st,ab}^{(8_S)} \right) \int_q (-2p_2 - q)_\sigma \times (g^{\mu\nu} (-(2k_1 + q)^\sigma) + g^{\mu\sigma} (k_1 - q)^\nu + g^{\nu\sigma} (k_1 + 2q)^\mu) \quad (C.55)$$

$$A_g = \frac{g_s^4}{16\pi^2} (m_{\tilde{q}_i^\alpha}^2 (2C_0 + 3C_1 + C_2) - 2uC_0 - uC_1 - uC_2 + B_0 - C_{00}) \quad (\text{C.56})$$

$$A_{11} = -\frac{g_s^4}{16\pi^2} (2C_2 + C_{22}) \quad (\text{C.57})$$

$$A_{44} = -\frac{g_s^4}{16\pi^2} (2C_1 + C_{11}) \quad (\text{C.58})$$

$$A_{14} = -\frac{g_s^4}{16\pi^2} (2C_0 + C_1 + C_{12} + 4C_2) \quad (\text{C.59})$$

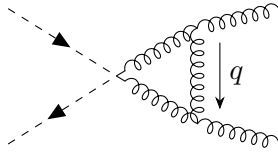
$$A_{41} = -\frac{g_s^4}{16\pi^2} (2C_0 + C_1 + C_{12} - 2C_2) \quad (\text{C.60})$$

$$\mathcal{D}_0 = q^2 + i\epsilon \quad \mathcal{D}_1 = (q + p_2)^2 - m_{\tilde{q}_i^\alpha}^2 + i\epsilon \quad \mathcal{D}_2 = (q + k_1)^2 + i\epsilon \quad (\text{C.61})$$

Gluon exchange right

$$C_0(0, s, 0, 0, 0, 0) \quad (\text{C.62})$$

$$B_0(s, 0, 0) \quad (\text{C.63})$$



$$= \delta_{ij} \left(c_{st,ab}^{(1)} + \frac{N}{2} c_{st,ab}^{(8_S)} \right) \int_q (g^\mu{}_\rho (-2k_1 - q)_\sigma + g^\mu{}_\sigma (k_1 - q)_\rho + g_{\rho\sigma} (k_1 + 2q)^\mu) (g^{\nu\rho} (2k_2 - q)^\sigma - g^{\nu\sigma} (k_2 + q)^\rho + g^{\rho\sigma} (2q - k_2)^\nu) \quad (\text{C.64})$$

$$A_g = \frac{g_s^4}{16\pi^2} \left(2B_0 - \frac{5}{2} sC_0 + 10C_{00} - sC_1 - 2\theta_D \right) \quad (\text{C.65})$$

$$A_{11} = \frac{g_s^4}{16\pi^2} (5C_1 + 10C_{11}) \quad (\text{C.66})$$

$$A_{22} = \frac{g_s^4}{16\pi^2} (5C_1 + 10C_{11}) \quad (\text{C.67})$$

$$A_{12} = \frac{-g_s^4}{8\pi^2} (C_0 + 4C_1 + 5C_{12}) \quad (\text{C.68})$$

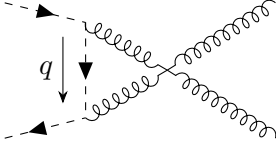
$$A_{21} = \frac{g_s^4}{8\pi^2} (2C_0 - C_1 - 5C_{12}) \quad (\text{C.69})$$

$$\mathcal{D}_0 = q^2 + i\epsilon \quad \mathcal{D}_1 = (q - k_2)^2 + i\epsilon \quad \mathcal{D}_2 = (q + k_1)^2 + i\epsilon \quad (\text{C.70})$$

Squark exchange left

$$C_0 \left(m_{\tilde{q}_i^\alpha}^2, s, m_{\tilde{q}_i^\alpha}^2, m_{\tilde{q}_i^\alpha}^2, 0, 0 \right) \quad (\text{C.71})$$

$$B_0(s, 0, 0) \quad (C.72)$$



$$= i\delta_{ij} \left[\left(c_{st,ab}^{(1)} + \frac{N}{2} c_{st,ab}^{(8S)} \right) (g^{\mu\nu} A_g + p_1^\mu p_1^\nu A_{33} + p_2^\mu p_2^\nu A_{44}) \right. \\ \left. + \sum_R c_{st,ab}^{(R)} \left(p_1^\mu p_2^\nu A_{34}^{(R)} + p_2^\mu p_1^\nu A_{43}^{(R)} \right) \right] \quad (C.73)$$

$$A_g = \frac{g_s^4}{32\pi^2} (2B_0 + (4m_{\tilde{q}_i}^2 - s) C_0 - 2C_{00} + 2(s - 4m_{\tilde{q}_i}^2) C_1) \quad (C.74)$$

$$A_{33} = A_{44} = \frac{g_s^4}{16\pi^2} (C_1 - C_{11}) \quad (C.75)$$

$$A_{34}^{(1)} = A_{43}^{(1)} = \frac{g_s^4}{32\pi^2} (C_0 - 2C_1 + 2C_{12}) \quad (C.76)$$

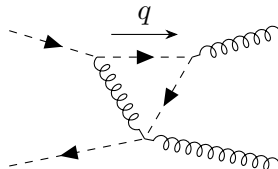
$$A_{34}^{(8S)} = A_{43}^{(8S)} = \frac{N}{2} \frac{g_s^4}{32\pi^2} (C_0 - 2C_1 + 2C_{12}) \quad (C.77)$$

$$A_{34}^{(8A)} = -A_{43}^{(8A)} = 3N \frac{g_s^4}{64\pi^2} (C_0 - 2C_1) \quad (C.78)$$

$$\mathcal{D}_0 = q^2 - m_{\tilde{q}_i^\alpha}^2 + i\epsilon \quad \mathcal{D}_1 = (q + p_2)^2 + i\epsilon \quad \mathcal{D}_2 = (q - p_1)^2 + i\epsilon \quad (C.79)$$

Squark exchange above

$$C_0(0, t, m_{\tilde{q}_i^\alpha}^2, m_{\tilde{q}_i^\alpha}^2, m_{\tilde{q}_i}^2, 0) \quad (C.80)$$



$$= i\delta_{ij} \frac{1}{2N} \left(\frac{N^2 - 2}{2N} c_{st,ab}^{(1)} - c_{st,ab}^{(8S)} + c_{st,ab}^{(8A)} \right) \int_q (2q - k_1)^\mu (p_1 + q)^\nu \quad (C.81)$$

$$A_g = \frac{g_s^4}{8\pi^2} C_{00} \quad (C.82)$$

$$A_{11} = \frac{g_s^4}{16\pi^2} (C_1 + 2C_{11}) \quad (C.83)$$

$$A_{33} = \frac{-g_s^4}{8\pi^2} (C_2 - C_{22}) \quad (C.84)$$

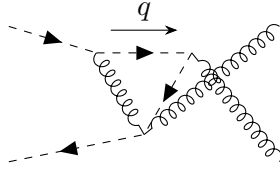
$$A_{13} = \frac{-g_s^4}{16\pi^2} (C_0 + 2C_1 - 2C_{12} - C_2) \quad (C.85)$$

$$A_{31} = \frac{g_s^4}{8\pi^2} C_{12} \quad (\text{C.86})$$

$$\mathcal{D}_0 = q^2 - m_{\tilde{q}_i^\alpha}^2 + i\epsilon \quad \mathcal{D}_1 = (q - k_1)^2 - m_{\tilde{q}_i^\alpha}^2 + i\epsilon \quad \mathcal{D}_2 = (q - p_1)^2 + i\epsilon \quad (\text{C.87})$$

Squark exchange above u

$$C_0 \left(0, u, m_{\tilde{q}_i^\alpha}^2, m_{\tilde{q}_i^\alpha}^2, m_{\tilde{q}_i^\alpha}^2, 0 \right) \quad (\text{C.88})$$



$$= i\delta_{ij} \frac{1}{2N} \left(\frac{N^2 - 2}{2N} c_{st,ab}^{(1)} - c_{st,ab}^{(\mathbf{8}_S)} - c_{st,ab}^{(\mathbf{8}_A)} \right) \times (g^{\mu\nu} A_g + k_2^\mu k_2^\nu A_{22} + p_1^\mu p_1^\nu A_{33} + k_2^\mu p_1^\nu A_{23} + p_1^\mu k_2^\nu A_{32}) \quad (\text{C.89})$$

$$A_g = \frac{g_s^4}{8\pi^2} C_{00} \quad (\text{C.90})$$

$$A_{22} = \frac{g_s^4}{16\pi^2} (C_1 + 2C_{11}) \quad (\text{C.91})$$

$$A_{33} = \frac{-g_s^4}{8\pi^2} (C_2 - C_{22}) \quad (\text{C.92})$$

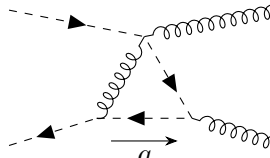
$$A_{23} = \frac{g_s^4}{8\pi^2} C_{12} \quad (\text{C.93})$$

$$A_{32} = \frac{-g_s^4}{16\pi^2} (C_0 + 2C_1 - 2C_{12} - C_2) \quad (\text{C.94})$$

$$\mathcal{D}_0 = q^2 - m_{\tilde{q}_i^\alpha}^2 + i\epsilon \quad \mathcal{D}_1 = (q - k_2)^2 - m_{\tilde{q}_i^\alpha}^2 + i\epsilon \quad \mathcal{D}_2 = (q - p_1)^2 + i\epsilon \quad (\text{C.95})$$

Squark exchange below

$$C_0 \left(0, t, m_{\tilde{q}_i^\alpha}^2, m_{\tilde{q}_i^\alpha}^2, m_{\tilde{q}_i^\alpha}^2, 0 \right) \quad (\text{C.96})$$



$$= i\delta_{ij} \frac{1}{2N} \left(\frac{N^2 - 2}{2N} c_{st,ab}^{(1)} - c_{st,ab}^{(\mathbf{8}_S)} + c_{st,ab}^{(\mathbf{8}_A)} \right) \int_q (k_2 - 2q)^\nu (-p_2 - q)^\mu \quad (\text{C.97})$$

$$A_g = \frac{g_s^4}{8\pi^2} C_{00} \quad (\text{C.98})$$

$$A_{22} = \frac{g_s^4}{16\pi^2} (C_1 + 2C_{11}) \quad (\text{C.99})$$

$$A_{44} = \frac{-g_s^4}{8\pi^2} (C_2 - C_{22}) \quad (\text{C.100})$$

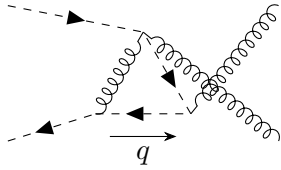
$$A_{24} = \frac{g_s^4}{8\pi^2} C_{12} \quad (\text{C.101})$$

$$A_{42} = \frac{-g_s^4}{16\pi^2} (C_0 + 2C_1 - 2C_{12} - C_2) \quad (\text{C.102})$$

$$\mathcal{D}_0 = q^2 - m_{\tilde{q}_i^\alpha}^2 + i\epsilon \quad \mathcal{D}_1 = (q - k_2)^2 - m_{\tilde{q}_i^\alpha}^2 + i\epsilon \quad \mathcal{D}_2 = (q - p_2)^2 + i\epsilon \quad (\text{C.103})$$

Squark exchange below u

$$C_0(0, u, m_{\tilde{q}_i}^2, m_{\tilde{q}_i}^2, m_{\tilde{q}_i}^2, 0) \quad (\text{C.104})$$



$$= i\delta_{ij} \frac{1}{2N} \left(\frac{N^2 - 2}{2N} c_{st,ab}^{(1)} - c_{st,ab}^{(\mathbf{8}_S)} - c_{st,ab}^{(\mathbf{8}_A)} \right) \times (g^{\mu\nu} A_g + k_1^\mu k_1^\nu A_{11} + p_2^\mu p_2^\nu A_{44} + k_1^\mu p_2^\nu A_{14} + p_2^\mu k_1^\nu A_{41}) \quad (\text{C.105})$$

$$A_g = \frac{g_s^4}{8\pi^2} C_{00} \quad (\text{C.106})$$

$$A_{11} = \frac{g_s^4}{16\pi^2} (C_1 + 2C_{11}) \quad (\text{C.107})$$

$$A_{44} = \frac{-g_s^4}{8\pi^2} (C_2 - C_{22}) \quad (\text{C.108})$$

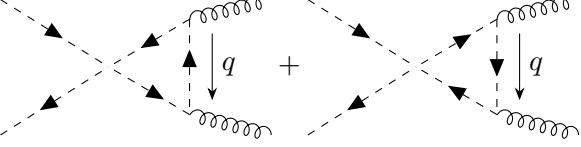
$$A_{14} = \frac{-g_s^4}{16\pi^2} (C_0 + 2C_1 - 2C_{12} - C_2) \quad (\text{C.109})$$

$$A_{41} = \frac{g_s^4}{8\pi^2} C_{12} \quad (\text{C.110})$$

$$\mathcal{D}_0 = q^2 - m_{\tilde{q}_i^\alpha}^2 + i\epsilon \quad \mathcal{D}_1 = (q - k_1)^2 - m_{\tilde{q}_i^\alpha}^2 + i\epsilon \quad \mathcal{D}_2 = (q - p_2)^2 + i\epsilon \quad (\text{C.111})$$

Squark exchange right

$$C_0(0, s, 0, m_{\tilde{q}_k}^2, m_{\tilde{q}_k}^2, m_{\tilde{q}_k}^2) \quad (\text{C.112})$$



$$= i \sum_{\gamma, k} \left(\frac{1}{4} c_{st,ab}^{(8_S)} A_{ji}^\alpha A_{kk}^\gamma + \delta^{\alpha\gamma} \left(\frac{C_F}{2N} c_{st,ab}^{(1)} - \frac{1}{4N} c_{st,ab}^{(8_S)} \right) A_{jk}^\alpha A_{ki}^\gamma \right) \\ \times (g^{\mu\nu} A_g + k_1^\mu k_1^\nu A_{11} + k_2^\mu k_2^\nu A_{22} + k_1^\mu k_2^\nu A_{12} + k_2^\mu k_1^\nu A_{21})$$

$$A_g = \frac{g_s^4}{2\pi^2} C_{00} \quad (C.113)$$

$$A_{11} = A_{22} = \frac{g_s^4}{4\pi^2} (C_1 + 2C_{11}) \quad (C.114)$$

$$A_{12} = \frac{-g_s^4}{8\pi^2} (C_0 + 4(C_1 + C_{12})) \quad (C.115)$$

$$A_{21} = \frac{-g_s^4}{2\pi^2} C_{12} \quad (C.116)$$

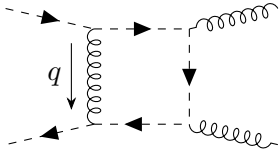
$$\mathcal{D}_0 = q^2 - m_{\tilde{q}_k^\gamma}^2 + i\epsilon \quad \mathcal{D}_1 = (q - k_2)^2 - m_{\tilde{q}_k^\gamma}^2 + i\epsilon \quad \mathcal{D}_2 = (q + k_1)^2 - m_{\tilde{q}_k^\gamma}^2 + i\epsilon \quad (C.117)$$

C.1.3 Boxes

Box 1

$$D_0 \left(m_{\tilde{q}_i^\alpha}^2, 0, 0, m_{\tilde{q}_i^\alpha}^2, t, s, 0, m_{\tilde{q}_i^\alpha}^2, m_{\tilde{q}_i^\alpha}^2, m_{\tilde{q}_i^\alpha}^2 \right) \quad (C.118)$$

$$C_0 \left(0, 0, s, m_{\tilde{q}_i^\alpha}^2, m_{\tilde{q}_i^\alpha}^2, m_{\tilde{q}_i^\alpha}^2 \right) \quad (C.119)$$



$$= \delta_{ij} \left(\frac{C_F}{2N} c_{st,ab}^{(1)} - \frac{1}{4N} c_{st,ab}^{(8_S)} + \frac{1}{4N} c_{st,ab}^{(8_A)} \right) \int_q (k_2 + p_1 - p_2 - 2q)^\mu \\ \times (-2q - 2p_2 + k_2)^\nu (2p_1 - q) \cdot (q + 2p_2) \quad (C.120)$$

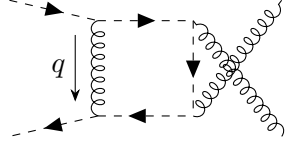
$$\mathcal{D}_0 = q^2 \quad \mathcal{D}_1 = (q + p_2)^2 - m_{\tilde{q}_i^\alpha}^2 \quad (C.121)$$

$$\mathcal{D}_2 = (q - k_2 + p_2)^2 - m_{\tilde{q}_i^\alpha}^2 \quad \mathcal{D}_3 = (q - p_1)^2 - m_{\tilde{q}_i^\alpha}^2 \quad (C.122)$$

Box 1 u (18)

$$D_0 \left(m_{\tilde{q}_i^\alpha}^2, 0, 0, m_{\tilde{q}_i^\alpha}^2, u, s, 0, m_{\tilde{q}_i^\alpha}^2, m_{\tilde{q}_i^\alpha}^2, m_{\tilde{q}_i^\alpha}^2 \right) \quad (C.123)$$

$$C_0 \left(0, 0, s, m_{\tilde{q}_i^\alpha}^2, m_{\tilde{q}_i^\alpha}^2, m_{\tilde{q}_i^\alpha}^2 \right) \quad (\text{C.124})$$



$$= \delta_{ij} \left(\frac{C_F}{2N} c_{st,ab}^{(1)} - \frac{1}{4N} c_{st,ab}^{(8_S)} - \frac{1}{4N} c_{st,ab}^{(8_A)} \right) \int_q (k_1 - 2p_2 - 2q)^\mu \quad (\text{C.125})$$

$$\times (p_1 - p_2 + k_1 - 2q)^\nu (2p_1 - q) \cdot (q + 2p_2)$$

$$\mathcal{D}_0 = q^2 \quad \mathcal{D}_1 = (q + p_2)^2 - m_{\tilde{q}_i^\alpha}^2 \quad (\text{C.126})$$

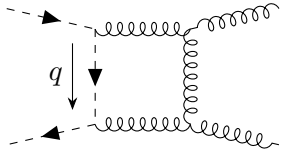
$$\mathcal{D}_2 = (q + p_2 - k_1)^2 - m_{\tilde{q}_i^\alpha}^2 \quad \mathcal{D}_3 = (q - p_1)^2 - m_{\tilde{q}_i^\alpha}^2 \quad (\text{C.127})$$

Box 2

$$D_0 \left(m_{\tilde{q}_i^\alpha}^2, 0, 0, m_{\tilde{q}_i^\alpha}^2, t, s, m_{\tilde{q}_i^\alpha}^2, 0, 0, 0 \right) \quad (\text{C.128})$$

$$C_0(0, 0, s, 0, 0, 0) \quad (\text{C.129})$$

$$B_0(0, 0, 0) \quad (\text{C.130})$$



$$= \delta_{ij} \left(\frac{1}{2} c_{st,ab}^{(1)} + \frac{N}{4} c_{st,ab}^{(8_S)} - \frac{N}{4} c_{st,ab}^{(8_A)} \right) \int_q (q + p_1)_\sigma (p_2 - q)_\rho$$

$$\times \left((q - 2k_2 + p_2)^\rho g^{\nu\beta} + (k_2 - 2p_2 - 2q)^\nu g^{\beta\rho} + (q + p_2 + k_2)^\beta g^{\nu\rho} \right)$$

$$\times \left((q - 2k_2 + 2p_2 + p_1)^\sigma g_\beta{}^\mu (q - 2p_1 - p_2 + k_2)_\beta g^{\sigma\mu} + (p_1 - 2q + k_2 - p_2)^\mu g^\sigma{}_\beta \right) \quad (\text{C.131})$$

$$\mathcal{D}_0 = q^2 - m_{\tilde{q}_i^\alpha}^2 \quad \mathcal{D}_1 = (q + p_2)^2 \quad (\text{C.132})$$

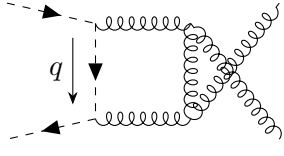
$$\mathcal{D}_2 = (q + p_2 - k_2)^2 \quad \mathcal{D}_3 = (q - p_1)^2 \quad (\text{C.133})$$

Box 2 u

$$D_0 \left(m_{\tilde{q}_i^\alpha}^2, 0, 0, m_{\tilde{q}_i^\alpha}^2, u, s, m_{\tilde{q}_i^\alpha}^2, 0, 0, 0 \right) \quad (\text{C.134})$$

$$C_0(0, 0, s, 0, 0, 0) \quad (\text{C.135})$$

$$B_0(0, 0, 0) \quad (\text{C.136})$$



$$\begin{aligned}
&= \delta_{ij} \left(\frac{1}{2} c_{st,ab}^{(1)} + \frac{N}{4} c_{st,ab}^{(\mathbf{8_S})} + \frac{N}{4} c_{st,ab}^{(\mathbf{8_A})} \right) \int_q (q + p_1)_\sigma (p_2 - q)_\rho \\
&\quad \times \left((q - 2k_1 + p_2)^\rho g^{\mu\beta} + (k_1 - 2p_2 - 2q)^\mu g^{\beta\rho} + (q + p_2 + k_1)^\beta g^{\mu\rho} \right) \\
&\quad \times \left((q - 2k_1 + 2p_2 + p_1)^\sigma g_\beta{}^\nu + (q - 2p_1 - p_2 + k_1)_\beta g^{\sigma\nu} + (p_1 - 2q + k_1 - p_2)^\nu g^\sigma{}_\beta \right)
\end{aligned} \tag{C.137}$$

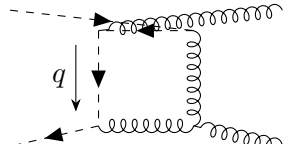
$$\mathcal{D}_0 = q^2 - m_{\tilde{q}_i^\alpha}^2 \quad \mathcal{D}_1 = (q + p_2)^2 \tag{C.138}$$

$$\mathcal{D}_2 = (q + p_2 - k_1)^2 \quad \mathcal{D}_3 = (q - p_1)^2 \tag{C.139}$$

Box 3.1

$$D_0 \left(m_{\tilde{q}_i^\alpha}^2, 0, m_{\tilde{q}_i^\alpha}^2, 0, t, u, m_{\tilde{q}_i^\alpha}^2, 0, 0, m_{\tilde{q}_i^\alpha}^2 \right) \tag{C.140}$$

$$C_0 \left(0, m_{\tilde{q}_i^\alpha}^2, u, 0, 0, m_{\tilde{q}_i^\alpha}^2 \right) \tag{C.141}$$



$$\begin{aligned}
&= \delta_{ij} \frac{1}{4} c_{st,ab}^{(1)} \int_q (2q + k_1)^\mu (q + 2k_1 + k_2 - p_2)_\rho (q - p_2)_\beta \\
&\quad \times \left((q - 2k_2 + p_2)^\beta g^{\nu\rho} + (k_2 - 2q - 2p_2)^\nu g^{\beta\rho} + (q + p_2 + k_2)^\rho g^{\beta\nu} \right)
\end{aligned} \tag{C.142}$$

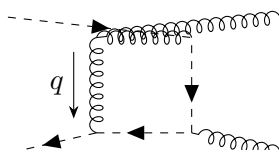
$$\mathcal{D}_0 = q^2 - m_{\tilde{q}_i^\alpha}^2 \quad \mathcal{D}_1 = (q + p_2)^2 \tag{C.143}$$

$$\mathcal{D}_2 = (q - k_2 + p_2)^2 \quad \mathcal{D}_3 = (q + k_1)^2 - m_{\tilde{q}_i^\alpha}^2 \tag{C.144}$$

Box 3.2

$$D_0 \left(m_{\tilde{q}_i^\alpha}^2, 0, m_{\tilde{q}_i^\alpha}^2, 0, t, u, 0, m_{\tilde{q}_i^\alpha}^2, m_{\tilde{q}_i^\alpha}^2, 0 \right) \tag{C.145}$$

$$C_0 \left(0, m_{\tilde{q}_i^\alpha}^2, u, m_{\tilde{q}_i^\alpha}^2, m_{\tilde{q}_i^\alpha}^2, 0 \right) \tag{C.146}$$



$$\begin{aligned}
&= \delta_{ij} \frac{1}{4} c_{st,ab}^{(1)} \int_q (2p_2 + q)^\alpha (k_2 - 2p_2 - 2q)^\nu (k_1 + 2k_2 - 2p_2 - q)^\rho \\
&\quad \times \left((q - k_1)^\rho g^{\alpha\mu} + (-k_1 - 2q)^\mu g^{\alpha\rho} + (2k_1 + q)^\alpha g^{\mu\rho} \right)
\end{aligned} \tag{C.147}$$

$$\mathcal{D}_0 = q^2 \quad \mathcal{D}_1 = (q + p_2)^2 - m_{\tilde{q}_i^\alpha}^2 \quad (\text{C.148})$$

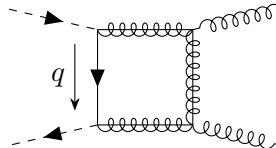
$$\mathcal{D}_2 = (q - k_2 + p_2)^2 - m_{\tilde{q}_i^\alpha}^2 \quad \mathcal{D}_3 = (q + k_1)^2 \quad (\text{C.149})$$

Box 4

$$D_0 \left(m_{\tilde{q}_j^\alpha}^2, 0, 0, m_{\tilde{q}_i^\alpha}^2, t, s, m_{q^\alpha}^2, m_{\tilde{g}}^2, m_{\tilde{g}}^2, m_{\tilde{g}}^2 \right) \quad (\text{C.150})$$

$$C_0 \left(0, 0, s, m_{\tilde{g}}^2, m_{\tilde{g}}^2, m_{\tilde{g}}^2 \right) \quad (\text{C.151})$$

$$B_0 \left(0, m_{\tilde{g}}^2, m_{\tilde{g}}^2 \right) \quad (\text{C.152})$$



$$= \left(\frac{1}{2} c_{st,ab}^{(\mathbf{1})} + \frac{N}{4} c_{st,ab}^{(\mathbf{8_S})} - \frac{N}{4} c_{st,ab}^{(\mathbf{8_A})} \right) \int_q \text{Tr} [(R_{i1}^\alpha P_R - R_{i2}^\alpha P_L) \quad (\text{C.153})$$

$$\times (\not{q} - \not{p}_1 + m_{\tilde{g}}) \gamma^\mu (\not{q} - \not{k}_2 + \not{p}_2 + m_{\tilde{g}}) \gamma^\nu$$

$$\times (\not{q} + \not{p}_2 + m_{\tilde{g}}) (R_{j1}^\alpha P_L - R_{j2}^\alpha P_R) (\not{q} + m_{q^\alpha})]$$

$$\mathcal{D}_0 = q^2 - m_{q^\alpha}^2 \quad \mathcal{D}_1 = (q + p_2)^2 - m_{\tilde{g}}^2 \quad (\text{C.154})$$

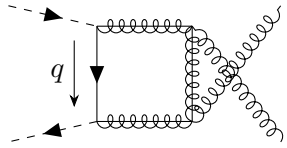
$$\mathcal{D}_2 = (q - k_2 + p_2)^2 - m_{\tilde{g}}^2 \quad \mathcal{D}_3 = (q - p_1)^2 - m_{\tilde{g}}^2 \quad (\text{C.155})$$

Box 4 u

$$D_0 \left(m_{\tilde{q}_j^\alpha}^2, 0, 0, m_{\tilde{q}_i^\alpha}^2, u, s, m_{q^\alpha}^2, m_{\tilde{g}}^2, m_{\tilde{g}}^2, m_{\tilde{g}}^2 \right) \quad (\text{C.156})$$

$$C_0 \left(0, 0, s, m_{\tilde{g}}^2, m_{\tilde{g}}^2, m_{\tilde{g}}^2 \right) \quad (\text{C.157})$$

$$B_0 \left(0, m_{\tilde{g}}^2, m_{\tilde{g}}^2 \right) \quad (\text{C.158})$$



$$= \left(\frac{1}{2} c_{st,ab}^{(\mathbf{1})} + \frac{N}{4} c_{st,ab}^{(\mathbf{8_S})} + \frac{N}{4} c_{st,ab}^{(\mathbf{8_A})} \right) \int_q -2 \text{Tr} [(R_{i1}^\alpha P_R - R_{i2}^\alpha P_L) \quad (\text{C.159})$$

$$\times (\not{q} - \not{p}_1 + m_{\tilde{g}}) \gamma^\nu (\not{q} - \not{k}_1 + \not{p}_2 + m_{\tilde{g}}) \gamma^\mu$$

$$\times (\not{q} + \not{p}_2 + m_{\tilde{g}}) (R_{j1}^\alpha P_L - R_{j2}^\alpha P_R) (\not{q} + m_{q^\alpha})]$$

$$\mathcal{D}_0 = q^2 - m_{q^\alpha}^2 \quad \mathcal{D}_1 = (q + p_2)^2 - m_{\tilde{g}}^2 \quad (\text{C.160})$$

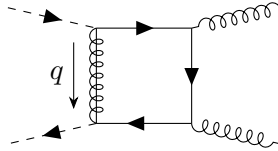
$$\mathcal{D}_2 = (q - k_1 + p_2)^2 - m_{\tilde{g}}^2 \quad \mathcal{D}_3 = (q - p_1)^2 - m_{\tilde{g}}^2 \quad (\text{C.161})$$

Box 5

$$D_0 \left(m_{\tilde{q}_j^\alpha}^2, 0, 0, m_{\tilde{q}_i^\alpha}^2, t, s, m_{\tilde{g}}^2, m_{q^\alpha}^2, m_{q^\alpha}^2, m_{q^\alpha}^2 \right) \quad (\text{C.162})$$

$$C_0 \left(0, 0, s, m_{q^\alpha}^2, m_{q^\alpha}^2, m_{q^\alpha}^2 \right) \quad (\text{C.163})$$

$$B_0 \left(0, m_{q^\alpha}^2, m_{q^\alpha}^2 \right) \quad (\text{C.164})$$



$$= \left(\frac{C_F}{2N} c_{st,ab}^{(1)} - \frac{1}{4N} c_{st,ab}^{(8_S)} + \frac{1}{4N} c_{st,ab}^{(8_A)} \right) \int_q -2 \text{Tr} [(R_{i1}^\alpha P_R - R_{i2}^\alpha P_L) \\ \times (-\not{q} + m_{\tilde{g}}) (R_{j1}^\alpha P_L - R_{j2}^\alpha P_R) (-\not{q} - \not{p}_2 + m_{q^\alpha}) \gamma^\nu \\ \times (-\not{q} - \not{p}_2 + \not{k}_2 + m_{q^\alpha}) \gamma^\mu (-\not{q} + \not{p}_1 + m_{q^\alpha})] \quad (\text{C.165})$$

$$\mathcal{D}_0 = q^2 - m_{\tilde{g}}^2 \quad \mathcal{D}_1 = (q + p_2)^2 - m_{q^\alpha}^2 \quad (\text{C.166})$$

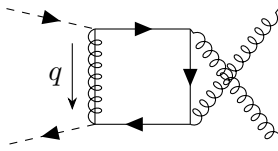
$$\mathcal{D}_2 = (q + p_2 - k_2)^2 - m_{q^\alpha}^2 \quad \mathcal{D}_3 = (q - p_1)^2 - m_{q^\alpha}^2 \quad (\text{C.167})$$

Box 5 u

$$D_0 \left(m_{\tilde{q}_j^\alpha}^2, 0, 0, m_{\tilde{q}_i^\alpha}^2, u, s, m_{\tilde{g}}^2, m_{q^\alpha}^2, m_{q^\alpha}^2, m_{q^\alpha}^2 \right) \quad (\text{C.168})$$

$$C_0 \left(0, 0, s, m_{q^\alpha}^2, m_{q^\alpha}^2, m_{q^\alpha}^2 \right) \quad (\text{C.169})$$

$$B_0 \left(0, m_{q^\alpha}^2, m_{q^\alpha}^2 \right) \quad (\text{C.170})$$



$$= \left(\frac{C_F}{2N} c_{st,ab}^{(1)} - \frac{1}{4N} c_{st,ab}^{(8_S)} - \frac{1}{4N} c_{st,ab}^{(8_A)} \right) \int_q -2 \text{Tr} [(R_{i1}^\alpha P_R - R_{i2}^\alpha P_L) \\ \times (-\not{q} + m_{\tilde{g}}) (R_{j1}^\alpha P_L - R_{j2}^\alpha P_R) (-\not{q} - \not{p}_2 + m_{q^\alpha}) \gamma^\mu \\ \times (-\not{q} - \not{p}_2 + \not{k}_1 + m_{q^\alpha}) \gamma^\nu (-\not{q} + \not{p}_1 + m_{q^\alpha})] \quad (\text{C.171})$$

$$\mathcal{D}_0 = q^2 - m_{\tilde{g}}^2 \quad \mathcal{D}_1 = (q + p_2)^2 - m_{q^\alpha}^2 \quad (\text{C.172})$$

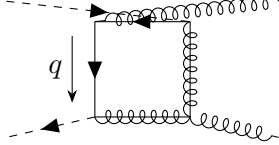
$$\mathcal{D}_2 = (q + p_2 - k_1)^2 - m_{q^\alpha}^2 \quad \mathcal{D}_3 = (q - p_1)^2 - m_{q^\alpha}^2 \quad (\text{C.173})$$

Box 6.1

$$D_0 \left(m_{\tilde{q}_j^\alpha}^2, 0, m_{\tilde{q}_i^\alpha}^2, 0, t, u, m_{q^\alpha}^2, m_{\tilde{g}}^2, m_{\tilde{g}}^2, m_{q^\alpha}^2 \right) \quad (\text{C.174})$$

$$C_0 \left(0, m_{\tilde{q}_i^\alpha}^2, u, m_{\tilde{g}}^2, m_{\tilde{g}}^2, m_{q^\alpha}^2 \right) \quad (\text{C.175})$$

$$B_0 \left(m_{\tilde{q}_i^\alpha}^2, m_{\tilde{g}}^2, m_{q^\alpha}^2 \right) \quad (\text{C.176})$$



$$= \frac{1}{4} c_{st,ab}^{(1)} \int_q -2 \text{Tr} \left[(\not{q} + \not{k}_1 + m_{q^\alpha}) (R_{i1}^\alpha P_R - R_{i2}^\alpha P_L) (\not{q} - \not{k}_2 + \not{p}_2 + m_{\tilde{g}}) \right. \\ \left. \times \gamma^\nu (\not{q} + \not{p}_2 + m_{\tilde{g}}) (R_{j1}^\alpha P_L - R_{j2}^\alpha P_R) (\not{q} + m_{q^\alpha}) \gamma^\mu \right] \quad (\text{C.177})$$

$$\mathcal{D}_0 = q^2 - m_{q^\alpha}^2 \quad \mathcal{D}_1 = (q + p_2)^2 - m_{\tilde{g}}^2 \quad (\text{C.178})$$

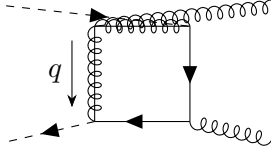
$$\mathcal{D}_2 = (q + p_2 - k_2)^2 - m_{\tilde{g}}^2 \quad \mathcal{D}_3 = (q + k_1)^2 - m_{q^\alpha}^2 \quad (\text{C.179})$$

Box 6.2

$$D_0 \left(m_{\tilde{q}_j^\alpha}^2, 0, m_{\tilde{q}_i^\alpha}^2, 0, t, u, m_{\tilde{g}}^2, m_{q^\alpha}^2, m_{q^\alpha}^2, m_{\tilde{g}}^2 \right) \quad (\text{C.180})$$

$$C_0 \left(0, m_{\tilde{q}_i^\alpha}^2, u, m_{q^\alpha}^2, m_{q^\alpha}^2, m_{\tilde{g}}^2 \right) \quad (\text{C.181})$$

$$B_0 \left(m_{\tilde{q}_i^\alpha}^2, m_{q^\alpha}^2, m_{\tilde{g}}^2 \right) \quad (\text{C.182})$$



$$= \frac{1}{4} c_{st,ab}^{(1)} \int_q -2 \text{Tr} \left[\gamma^\mu (-\not{q} + m_{\tilde{g}}) (R_{j1}^\alpha P_L - R_{j2}^\alpha P_R) (-\not{q} - \not{p}_2 + m_{q^\alpha}) \right. \\ \left. \times \gamma^\nu (-\not{q} - \not{p}_2 + \not{k}_2 + m_{q^\alpha}) (R_{i1}^\alpha P_R - R_{i2}^\alpha P_L) (-\not{q} - \not{k}_1 + m_{\tilde{g}}) \right] \quad (\text{C.183})$$

$$\mathcal{D}_0 = q^2 - m_{\tilde{g}}^2 \quad \mathcal{D}_1 = (q + p_2)^2 - m_{q^\alpha}^2 \quad (\text{C.184})$$

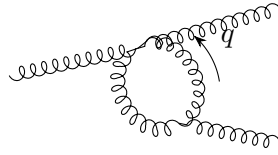
$$\mathcal{D}_2 = (q + p_2 - k_2)^2 - m_{q^\alpha}^2 \quad \mathcal{D}_3 = (q + k_1)^2 - m_{\tilde{g}}^2 \quad (\text{C.185})$$

C.2 Triple-gluon vertex

The naming and momentum conventions for the triple-gluon vertex correction as well as its parametrization in terms of the partial amplitudes A_{mno} , $A_{g1,m}$, $A_{g2,m}$ and $A_{g3,m}$ are shown in eq. (8.116).

Gluon bubble k1

$$B_0 (k_1^2, 0, 0) \quad (\text{C.186})$$



$$= \frac{N}{2} i f_{cde} \Gamma^{\rho\sigma\tau} = i \frac{N}{2} i f_{cde} (g^{\rho\sigma} k_1^\tau A_{g1,1} + g^{\rho\tau} k_1^\sigma A_{g2,1}) \quad (\text{C.187})$$

$$\Gamma^{\rho\sigma\tau} = -\frac{1}{2} \int_q g_{\alpha\mu} g_{\beta\nu} \left(g^{\alpha\tau} g^{\beta\sigma} - g^{\alpha\sigma} g^{\beta\tau} - 2 \left(g^{\alpha\sigma} g^{\beta\tau} - g^{\alpha\tau} g^{\beta\sigma} \right) \right) \\ \times (g^{\mu\nu} (k_1 - 2q)^\rho + g^{\mu\rho} (q - 2k_1)^\nu + g^{\nu\rho} (k_1 + q)^\mu) \quad (\text{C.188})$$

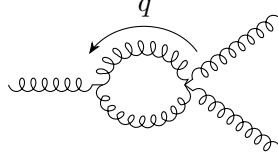
$$A_{g1,1} = -\frac{9g_s^3}{32\pi^2} B_0 \quad (\text{C.189})$$

$$A_{g2,1} = \frac{9g_s^3}{32\pi^2} B_0 \quad (\text{C.190})$$

$$\mathcal{D}_0 = q^2 + i\epsilon \quad \mathcal{D}_1 = (q - k_1)^2 + i\epsilon \quad (\text{C.191})$$

Gluon bubble k2

$$B_0(k_2^2, 0, 0) \quad (\text{C.192})$$



$$= \frac{N}{2} i f_{cde} \Gamma^{\rho\sigma\tau} = i \frac{N}{2} i f_{cde} (g^{\rho\sigma} k_2^\tau A_{g1,2} + g^{\sigma\tau} k_2^\rho A_{g3,2}) \quad (\text{C.193})$$

$$\Gamma^{\rho\sigma\tau} = -\frac{1}{2} \int_q g_{\alpha\beta} g_{\mu\nu} \left(-g^{\beta\tau} g^{\nu\rho} + g^{\beta\rho} g^{\nu\tau} - 2 \left(g^{\beta\tau} g^{\nu\rho} - g^{\beta\rho} g^{\nu\tau} \right) \right) \\ \times (g^{\alpha\mu} (2q - k_2)^\sigma + g^{\alpha\sigma} (-k_2 - q)^\mu + g^{\mu\sigma} (2k_2 - q)^\alpha) \quad (\text{C.194})$$

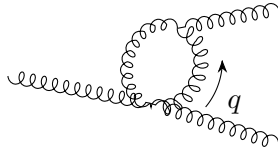
$$A_{g1,2} = \frac{9g_s^3}{32\pi^2} B_0 \quad (\text{C.195})$$

$$A_{g3,2} = -\frac{9g_s^3}{32\pi^2} B_0 \quad (\text{C.196})$$

$$\mathcal{D}_0 = q^2 + i\epsilon \quad \mathcal{D}_1 = (q - k_2)^2 + i\epsilon \quad (\text{C.197})$$

Gluon bubble k3

$$B_0(k_3^2, 0, 0) \quad (\text{C.198})$$



$$= \frac{N}{2} i f_{cde} \Gamma^{\rho\sigma\tau} = i \frac{N}{2} i f_{cde} (g^{\rho\tau} k_3^\sigma A_{g2,3} + g^{\sigma\tau} k_3^\rho A_{g3,3}) \quad (\text{C.199})$$

$$\Gamma^{\rho\sigma\tau} = -\frac{1}{2} \int_q g_{\alpha\mu} g_{\beta\nu} (-g^{\mu\sigma} g^{\nu\rho} + g^{\mu\rho} g^{\nu\sigma} - 2(g^{\mu\sigma} g^{\nu\rho} - g^{\mu\rho} g^{\nu\sigma})) \times (g^{\alpha\beta} (k_3 - 2q)^\tau + g^{\alpha\tau} (q - 2k_3)^\beta + g^{\beta\tau} (k_3 + q)^\alpha) \quad (\text{C.200})$$

$$A_{g2,3} = \frac{9g_s^3}{32\pi^2} B_0 \quad (\text{C.201})$$

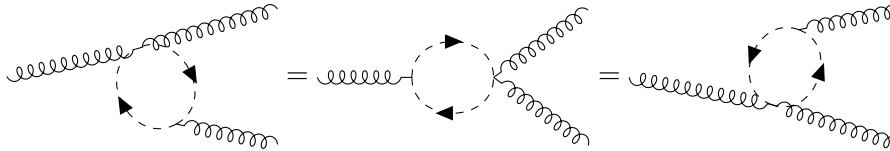
$$A_{g3,3} = -\frac{9g_s^3}{32\pi^2} B_0 \quad (\text{C.202})$$

$$\mathcal{D}_0 = q^2 + i\epsilon \quad \mathcal{D}_1 = (q - k_3)^2 + i\epsilon \quad (\text{C.203})$$

Squark bubbles

All three squark bubbles vanish through the application of the identity

$$B_1(p^2, m^2, m^2) = -\frac{1}{2} B_0(p^2, m^2, m^2). \quad (\text{C.204})$$



$$= 0 \quad (\text{C.205})$$

Quark and gluino triangles

The quark triangle where the fermion flow is in the clockwise direction gives a colour structure $\text{Tr}(T^d T^c T^e) = \frac{1}{4} (d_{cde} - i f_{cde})$ and a fermionic trace

$$\mathcal{T}_1^{\rho\sigma\tau}(m) = \text{Tr}(\gamma^\sigma (-\not{q} + \not{k}_1 + m) \gamma^\rho (-\not{q} + m) \gamma^\tau (-\not{q} + \not{k}_3 + m)) \quad (\text{C.206})$$

whereas the other quark triangle with the flow in the counter-clockwise direction gives a colour structure $\text{Tr}(T^c T^d T^e) = \frac{1}{4} (d_{cde} + i f_{cde})$ and a fermionic trace

$$\mathcal{T}_2^{\rho\sigma\tau}(m) = \text{Tr}(\gamma^\sigma (\not{q} - \not{k}_3 + m) \gamma^\tau (\not{q} + m) \gamma^\rho (\not{q} - \not{k}_1 + m)) . \quad (\text{C.207})$$

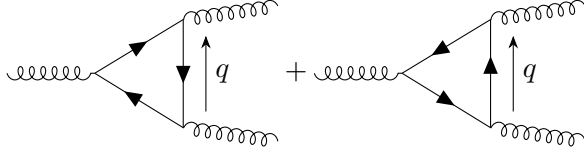
It can be shown by explicit computation that the sum of both traces vanishes $\mathcal{T}_1^{\rho\sigma\tau} + \mathcal{T}_2^{\rho\sigma\tau} = 0$ so that only the antisymmetric part with respect to the colour indices survives.

The direction of the fermion flow for the gluino triangle is chosen to be counter-clockwise such that its trace coincides with $\mathcal{T}_2^{\rho\sigma\tau}$ and the only difference lies in the colour factor. Consequently, the quark and gluino triangles yield the same form factors in terms of Passarino-Veltmann functions just evaluated for different argument sets. The form factors given below are the

ones for the *sum* of both quark diagrams corresponding to $-2\mathcal{T}_2^{\rho\sigma\tau}$. In order to arrive at the partial amplitudes for the gluino, the form factors below have to be divided by two.

$$C_0(k_1^2, k_2^2, k_3^2, m_{q\gamma}^2, m_{q\gamma}^2, m_{q\gamma}^2) \quad (\text{C.208})$$

$$B_0(k_2^2, m_{q\gamma}^2, m_{q\gamma}^2) \quad (\text{C.209})$$

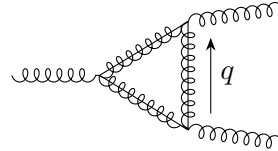


$$= \frac{1}{4} i f_{cde} \sum_{\gamma} \int_q -(\mathcal{T}_2^{\rho\sigma\tau}(m_{q\gamma}) - \mathcal{T}_1^{\rho\sigma\tau}(m_{q\gamma})) \quad (\text{C.210})$$

$$\mathcal{D}_0 = q^2 - m_{q\gamma}^2 + i\epsilon \quad \mathcal{D}_1 = (q - k_1)^2 - m_{q\gamma}^2 + i\epsilon \quad \mathcal{D}_2 = (q - k_3)^2 - m_{q\gamma}^2 + i\epsilon \quad (\text{C.211})$$

$$C_0(k_1^2, k_2^2, k_3^2, m_{\tilde{g}}^2, m_{\tilde{g}}^2, m_{\tilde{g}}^2) \quad (\text{C.212})$$

$$B_0(k_2^2, m_{\tilde{g}}^2, m_{\tilde{g}}^2) \quad (\text{C.213})$$



$$= \frac{N}{2} i f_{cde} \int_q -\mathcal{T}_2^{\rho\sigma\tau}(m_{\tilde{g}}) \quad (\text{C.214})$$

$$\mathcal{D}_0 = q^2 - m_{\tilde{g}}^2 + i\epsilon \quad \mathcal{D}_1 = (q - k_1)^2 - m_{\tilde{g}}^2 + i\epsilon \quad \mathcal{D}_2 = (q - k_3)^2 - m_{\tilde{g}}^2 + i\epsilon \quad (\text{C.215})$$

$$A_{g1,1} = \frac{g_s^3}{2\pi^2} (-2C_{12}(k_1 \cdot k_3) - 2k_1^2 C_{11} + k_3^2 C_2 + 2B_0 + B_1 - 2C_{00} + 4C_{001}) \quad (\text{C.216})$$

$$A_{g1,3} = -\frac{g_s^3}{2\pi^2} (2(C_2 + C_{22})(k_1 \cdot k_3) + k_1^2(C_1 + 2C_{12}) + B_0 + B_1 - 2C_{00} - 4C_{002}) \quad (\text{C.217})$$

$$A_{g2,1} = \frac{g_s^3}{2\pi^2} (-k_3^2 C_2 + B_1 + 2C_{00} + 4C_{001}) \quad (\text{C.218})$$

$$A_{g2,3} = -\frac{g_s^3}{2\pi^2} (k_1^2 C_1 + B_0 + B_1 - 2C_{00} - 4C_{002}) \quad (\text{C.219})$$

$$A_{g3,1} = \frac{g_s^3}{2\pi^2} (-2(C_1 + C_{11})(k_1 \cdot k_3) - k_3^2(2C_{12} + C_2) + B_1 + 2C_{00} + 4C_{001}) \quad (\text{C.220})$$

$$A_{g3,3} = \frac{g_s^3}{2\pi^2} (-2C_{12}(k_1 \cdot k_3) + k_1^2 C_1 - 2k_3^2 C_{22} + B_0 - B_1 - 2C_{00} + 4C_{002}) \quad (\text{C.221})$$

$$A_{111} = \frac{2g_s^3}{\pi^2} (C_{11} + C_{111}) \quad (\text{C.222})$$

$$A_{311} = \frac{g_s^3}{\pi^2}(2C_{112} + C_{12}) \quad (\text{C.223})$$

$$A_{113} = \frac{g_s^3}{\pi^2}(C_{11} + 2(C_{112} + C_{12})) \quad (\text{C.224})$$

$$A_{313} = \frac{g_s^3}{\pi^2}(C_{12} + 2C_{122} + C_{22}) \quad (\text{C.225})$$

$$A_{131} = \frac{g_s^3}{\pi^2}(C_{11} + 2C_{112} + C_{12}) \quad (\text{C.226})$$

$$A_{331} = \frac{g_s^3}{\pi^2}(C_{12} + 2C_{122}) \quad (\text{C.227})$$

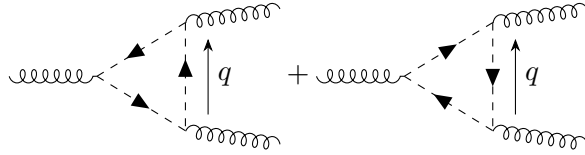
$$A_{133} = \frac{g_s^3}{\pi^2}(2C_{12} + 2C_{122} + C_{22}) \quad (\text{C.228})$$

$$A_{333} = \frac{2g_s^3}{\pi^2}(C_{22} + C_{222}) \quad (\text{C.229})$$

Squark triangles

When taking into account both directions of the charge flow, the symmetric colour part d_{cde} of the squark triangles vanishes, as for the quark triangles in appendix C.2. The form factors given below are only valid for the sum of both diagrams.

$$C_0(k_1^2, k_2^2, k_3^2, m_{q_k}^2, m_{q_k}^2, m_{q_k}^2) \quad (\text{C.230})$$



$$= \frac{1}{4} i f_{cde} \sum_{\gamma, k} \int_q 2(2q - k_1 - k_3)^\sigma \times (2q - k_1)^\rho (2q - k_3)^\tau \quad (\text{C.231})$$

$$\mathcal{D}_0 = q^2 - m_{q_k}^2 + i\epsilon \quad \mathcal{D}_1 = (q - k_1)^2 - m_{q_k}^2 + i\epsilon \quad \mathcal{D}_2 = (q - k_3)^2 - m_{q_k}^2 + i\epsilon \quad (\text{C.232})$$

$$A_{g1,1} = -\frac{g_s^3}{\pi^2} C_{001} \quad (\text{C.233})$$

$$A_{g1,3} = -\frac{g_s^3}{2\pi^2} (C_{00} + 2C_{002}) \quad (\text{C.234})$$

$$A_{g2,1} = -\frac{g_s^3}{2\pi^2} (C_{00} + 2C_{001}) \quad (\text{C.235})$$

$$A_{g2,3} = -\frac{g_s^3}{2\pi^2} (C_{00} + 2C_{002}) \quad (\text{C.236})$$

$$A_{g3,1} = -\frac{g_s^3}{2\pi^2} (C_{00} + 2C_{001}) \quad (\text{C.237})$$

$$A_{g3,3} = -\frac{g_s^3}{\pi^2} C_{002} \quad (\text{C.238})$$

$$A_{111} = -\frac{g_s^3}{4\pi^2} (C_1 + 4(C_{11} + C_{111})) \quad (\text{C.239})$$

$$A_{311} = -\frac{g_s^3}{2\pi^2}(2C_{112} + C_{12}) \quad (\text{C.240})$$

$$A_{113} = -\frac{g_s^3}{8\pi^2}(C_0 + 4C_1 + 4C_{11} + 8C_{112} + 8C_{12} + 2C_2) \quad (\text{C.241})$$

$$A_{313} = -\frac{g_s^3}{4\pi^2}(2C_{12} + 4C_{122} + C_2 + 2C_{22}) \quad (\text{C.242})$$

$$A_{131} = -\frac{g_s^3}{4\pi^2}(C_1 + 2(C_{11} + 2C_{112} + C_{12})) \quad (\text{C.243})$$

$$A_{331} = -\frac{g_s^3}{2\pi^2}(C_{12} + 2C_{122}) \quad (\text{C.244})$$

$$A_{133} = -\frac{g_s^3}{8\pi^2}(C_0 + 2C_1 + 4(2C_{12} + 2C_{122} + C_2 + C_{22})) \quad (\text{C.245})$$

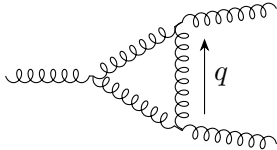
$$A_{333} = -\frac{g_s^3}{4\pi^2}(C_2 + 4(C_{22} + C_{222})) \quad (\text{C.246})$$

Gluon triangle

The gluon triangle is the only correction to the triple gluon vertex where the dimensional regularization and the dimensional reduction schemes differ.

$$C_0(k_1^2, k_2^2, k_3^2, 0, 0, 0) \quad (\text{C.247})$$

$$B_0(k_2^2, 0, 0) \quad (\text{C.248})$$



$$= \frac{N}{2} i f_{cde} \Gamma^{\rho\sigma\tau} \quad (\text{C.249})$$

$$\begin{aligned} \Gamma^{\rho\sigma\tau} = & - \int_q \left(g^{\beta\nu}(k_1 - 2q)^\rho + g^{\beta\rho}(k_1 + q)^\nu + g^{\nu\rho}(q - 2k_1)^\beta \right) \\ & \times (g_{\beta\mu}(k_3 - 2q)^\tau + g_\beta{}^\tau(k_3 + q)_\mu + g_\mu{}^\tau(q - 2k_3)_\beta) \\ & \times (g^\mu{}_\nu(k_1 + k_3 - 2q)^\sigma + g^{\mu\sigma}(k_1 - 2k_3 + q)_\nu + g_\nu{}^\sigma(-2k_1 + k_3 + q)^\mu) \end{aligned} \quad (\text{C.250})$$

$$\mathcal{D}_0 = q^2 + i\epsilon \quad \mathcal{D}_1 = (q - k_1)^2 + i\epsilon \quad \mathcal{D}_2 = (q - k_3)^2 + i\epsilon \quad (\text{C.251})$$

$$\begin{aligned} A_{g1,1} = & \frac{g_s^3}{16\pi^2} \left(-32C_{001} - \frac{4}{3}\theta_D + 2(k_1 \cdot k_3)(2C_0 + 5C_1 - C_{11} + 4C_2) - 2k_1^2 C_1 + 2k_3^2 C_0 \right. \\ & \left. + k_3^2 C_1 - 2k_3^2 C_{12} + 6B_0 + 2B_1 + 14C_{001} \right) \end{aligned} \quad (\text{C.252})$$

$$\begin{aligned} A_{g1,3} = & -\frac{g_s^3}{16\pi^2} \left(16C_{00} + 32C_{002} - \frac{2}{3}\theta_D + (k_1 \cdot k_3)(3C_1 + 2C_{12} - 6C_2) \right. \\ & \left. + k_1^2(5C_0 + 4C_1 + 10C_2) + 2k_3^2 C_2 + 2k_3^2 C_{22} + 3B_0 + 2B_1 - 5C_{00} - 14C_{002} \right) \end{aligned} \quad (\text{C.253})$$

$$A_{g2,1} = -\frac{g_s^3}{16\pi^2} \left(16C_{00} + 32C_{001} - \frac{2}{3}\theta_D + (k_1 \cdot k_3)(3C_0 + 13C_1 + 2C_{11} + 2C_{12} + 3C_2) \right. \\ \left. + 2k_1^2(C_1 + C_{11}) + k_3^2C_0 - k_3^2C_1 + 2k_3^2C_{12} - k_3^2C_2 + B_0 - 2B_1 - 5C_{00} - 14C_{001} \right) \quad (\text{C.254})$$

$$A_{g2,3} = -\frac{g_s^3}{16\pi^2} \left(16C_{00} + 32C_{002} - \frac{2}{3}\theta_D + (k_1 \cdot k_3)(3C_0 + 3C_1 + 2C_{12} + 13C_2 + 2C_{22}) \right. \\ \left. + k_1^2(C_0 - C_1 + 2C_{12} - C_2) + 2k_3^2C_2 + 2k_3^2C_{22} + 3B_0 + 2B_1 - 5C_{00} - 14C_{002} \right) \quad (\text{C.255})$$

$$A_{g3,1} = -\frac{g_s^3}{16\pi^2} \left(16C_{00} + 32C_{001} - \frac{2}{3}\theta_D + (k_1 \cdot k_3)(-6C_1 + 2C_{12} + 3C_2) \right. \\ \left. + 2k_1^2(C_1 + C_{11}) + 5k_3^2C_0 + 10k_3^2C_1 + 4k_3^2C_2 + B_0 - 2B_1 - 5C_{00} - 14C_{001} \right) \quad (\text{C.256})$$

$$A_{g3,3} = -\frac{g_s^3}{16\pi^2} \left(-32C_{002} - \frac{4}{3}\theta_D + 2(k_1 \cdot k_3)(2C_0 + 4C_1 + 5C_2 - C_{22}) \right. \\ \left. + k_1^2(2C_0 - 2C_{12} + C_2) - 2k_3^2C_2 + 4B_0 - 2B_1 + 14C_{002} \right) \quad (\text{C.257})$$

$$A_{111} = -\frac{9g_s^3}{8\pi^2}(C_{11} + C_{111}) \quad (\text{C.258})$$

$$A_{311} = -\frac{g_s^3}{16\pi^2}(3C_1 - 18C_{112} - 9C_{12} - 3C_2) \quad (\text{C.259})$$

$$A_{113} = -\frac{g_s^3}{16\pi^2}(-3C_0 + 6C_1 + 9C_{11} + 18C_{112} + 18C_{12} - 6C_2) \quad (\text{C.260})$$

$$A_{313} = -\frac{g_s^3}{16\pi^2}(3C_0 + 3C_1 + 9C_{12} + 18C_{122} + 15C_2 + 9C_{22}) \quad (\text{C.261})$$

$$A_{131} = -\frac{g_s^3}{16\pi^2}(3C_0 + 15C_1 + 9C_{11} + 18C_{112} + 9C_{12} + 3C_2) \quad (\text{C.262})$$

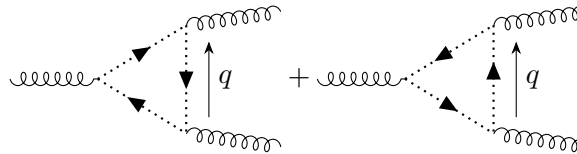
$$A_{331} = -\frac{g_s^3}{16\pi^2}(3C_1 + 9C_{12} + 18C_{122} - 3C_2) \quad (\text{C.263})$$

$$A_{133} = -\frac{g_s^3}{16\pi^2}(-3C_0 - 6C_1 + 18C_{12} + 18C_{122} + 6C_2 + 9C_{22}) \quad (\text{C.264})$$

$$A_{333} = -\frac{9g_s^3}{8\pi^2}(C_{22} + C_{222}) \quad (\text{C.265})$$

Ghost triangles

$$C_0(k_1^2, k_2^2, k_3^2, 0, 0, 0) \quad (\text{C.266})$$



$$= \frac{N}{2} i f_{cde} \int_q (q^\tau (q - k_1)^\rho (k_3 - q)^\sigma + q^\rho \\ \times (k_1 - q)^\sigma (q - k_3)^\tau) \quad (\text{C.267})$$

$$\mathcal{D}_0 = q^2 + i\epsilon \quad \mathcal{D}_1 = (q - k_1)^2 + i\epsilon \quad \mathcal{D}_2 = (q - k_3)^2 + i\epsilon \quad (\text{C.268})$$

$$A_{g1,1} = \frac{g_s^3}{8\pi^2} C_{001} \quad (\text{C.269})$$

$$A_{g1,3} = \frac{g_s^3}{16\pi^2} (C_{00} + 2C_{002}) \quad (\text{C.270})$$

$$A_{g2,1} = \frac{g_s^3}{16\pi^2} (C_{00} + 2C_{001}) \quad (\text{C.271})$$

$$A_{g2,3} = \frac{g_s^3}{16\pi^2} (C_{00} + 2C_{002}) \quad (\text{C.272})$$

$$A_{g3,1} = \frac{g_s^3}{16\pi^2} (C_{00} + 2C_{001}) \quad (\text{C.273})$$

$$A_{g3,3} = \frac{g_s^3}{8\pi^2} C_{002} \quad (\text{C.274})$$

$$A_{111} = \frac{g_s^3}{8\pi^2} (C_{11} + C_{111}) \quad (\text{C.275})$$

$$A_{311} = \frac{g_s^3}{16\pi^2} (2C_{112} + C_{12}) \quad (\text{C.276})$$

$$A_{113} = \frac{g_s^3}{16\pi^2} (C_1 + C_{11} + 2(C_{112} + C_{12})) \quad (\text{C.277})$$

$$A_{313} = \frac{g_s^3}{16\pi^2} (C_{12} + 2C_{122} + C_2 + C_{22}) \quad (\text{C.278})$$

$$A_{131} = \frac{g_s^3}{16\pi^2} (C_1 + C_{11} + 2C_{112} + C_{12}) \quad (\text{C.279})$$

$$A_{331} = \frac{g_s^3}{16\pi^2} (C_{12} + 2C_{122}) \quad (\text{C.280})$$

$$A_{133} = \frac{g_s^3}{16\pi^2} (2C_{12} + 2C_{122} + C_2 + C_{22}) \quad (\text{C.281})$$

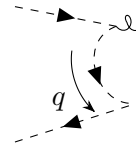
$$A_{333} = \frac{g_s^3}{8\pi^2} (C_{22} + C_{222}) \quad (\text{C.282})$$

C.3 Squark-gluon vertex

The momentum and index convention for the correction of the squark-squark-gluon vertex is given in eq. (8.118). The form factors A_-^{lk} and A_+^{lk} for this vertex are uniquely determined in terms of their numerical value in contrast to the two vertex corrections before.

Gluon-squark bubble at p1

$$B_0(p_1^2, m_{\tilde{q}_k^\alpha}^2, 0) \quad (\text{C.283})$$



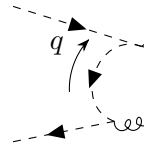
$$= \frac{N^2 - 2}{2N} T_{ur}^c \int_q (q + p_1)^\rho \quad (\text{C.284})$$

$$A_+^{lk} = A_-^{lk} = \delta_{kl} \frac{g_s^3}{32\pi^2} (B_0 - B_1) \quad (\text{C.285})$$

$$\mathcal{D}_0 = q^2 - m_{\tilde{q}_k^\alpha}^2 + i\epsilon \quad \mathcal{D}_1 = (q - p_1)^2 + i\epsilon \quad (\text{C.286})$$

Gluon-squark bubble at p2

$$B_0(p_2^2, m_{\tilde{q}_k^\alpha}^2, 0) \quad (\text{C.287})$$



$$= \frac{N^2 - 2}{2N} T_{ur}^c \int_q (-q - p_2)^\sigma \quad (\text{C.288})$$

$$A_+^{lk} = -A_-^{lk} = \delta_{kl} \frac{g_s^3}{32\pi^2} (B_1 - B_0) \quad (\text{C.289})$$

$$\mathcal{D}_0 = q^2 - m_{\tilde{q}_k^\alpha}^2 + i\epsilon \quad \mathcal{D}_1 = (q - p_1)^2 + i\epsilon \quad (\text{C.290})$$

Squark bubble

The squark bubble vanishes through $B_0(p^2, m^2, m^2) - 2B_1(p^2, m^2, m^2) = 0$.



$$= 0 \quad (\text{C.291})$$

Gluon bubble

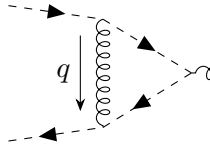


$$= 0 \quad (\text{C.292})$$

Gluon exchange

$$C_0 \left(p_1^2, (p_1 + p_2)^2, p_2^2, 0, m_{\tilde{q}_k^\alpha}^2, m_{\tilde{q}_k^\alpha}^2 \right) \quad (\text{C.293})$$

$$B_0 \left((p_1 + p_2)^2, m_{\tilde{q}_k^\alpha}^2, m_{\tilde{q}_k^\alpha}^2 \right) \quad (\text{C.294})$$



$$= -\frac{1}{2N} T_{ur}^c \int_q (2p_1 - q) \cdot (q + 2p_2) (p_1 - p_2 - 2q)^\sigma \quad (\text{C.295})$$

$$A_+^{lk} = \delta_{kl} \frac{g_s^3}{16\pi^2} (B_0 + 2B_1 - 2p_1^2(C_{11} - C_{12}) + 2p_2^2(C_{22} - C_{12}) + 2p_1 \cdot p_2(2C_1 + C_{11} - 2C_2 - C_{22})) \quad (\text{C.296})$$

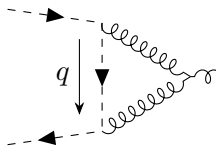
$$A_-^{lk} = -\delta_{kl} \frac{g_s^3}{8\pi^2} (2C_{00} + p_2^2(C_{12} + C_2 + C_{22}) + p_1^2(C_1 + C_{11} + C_{12}) - p_1 \cdot p_2(2C_0 + 3C_1 + C_{11} + 2C_{12} + 3C_2 + C_{22})) \quad (\text{C.297})$$

$$\mathcal{D}_0 = q^2 + i\epsilon \quad \mathcal{D}_1 = (q - p_1)^2 - m_{\tilde{q}_k^\alpha}^2 + i\epsilon \quad \mathcal{D}_2 = (q + p_2)^2 - m_{\tilde{q}_k^\alpha}^2 + i\epsilon \quad (\text{C.298})$$

Squark exchange

$$C_0 \left(p_1^2, (p_1 + p_2)^2, p_2^2, m_{\tilde{q}_k^\alpha}^2, 0, 0 \right) \quad (\text{C.299})$$

$$B_0 \left((p_1 + p_2)^2, 0, 0 \right) \quad (\text{C.300})$$



$$= \frac{N}{2} T_{ur}^c \int_q -[(2p_2 + q + p_1) \cdot (q + p_1) (q - p_2)^\sigma + (q - p_2 - 2p_1) \cdot (q - p_2)(q + p_1)^\sigma + (q - p_2)(q + p_1) \cdot (p_1 - p_2 - 2q)^\sigma]$$

$$\mathcal{A} = \int_q -[(2p_2 + q + p_1) \cdot (q + p_1) (q - p_2)^\sigma + (q - p_2 - 2p_1) \cdot (q - p_2)(q + p_1)^\sigma + (q - p_2)(q + p_1) \cdot (p_1 - p_2 - 2q)^\sigma] \quad (\text{C.301})$$

$$A_+^{lk} = \delta_{kl} \frac{g_s^3}{32\pi^2} (p_1^2(C_0 - 3C_1 + 2C_{11} - 2C_{12} - C_2) + p_2^2(-C_0 + C_1 + 2C_{12} + 3C_2 - 2C_{22}) + 2p_1 \cdot p_2(C_1 - C_{11} - C_2 + C_{22})) \quad (\text{C.302})$$

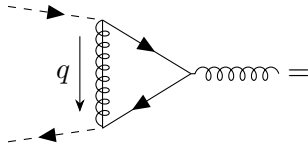
$$A_-^{lk} = \delta_{kl} \frac{g_s^3}{32\pi^2} (-4B_0 + 4C_{00} + p_2^2(-C_0 + C_1 + 2C_{12} + 3C_2 + 2C_{22}) + p_1^2(-C_0 + 3C_1 + 2C_{11} + 2C_{12} + C_2) - 2p_1 \cdot p_2(C_0 - 2C_1 + C_{11} + 2C_{12} - 2C_2 + C_{22}) - 4C_0 m_{\tilde{q}_k^\alpha}^2) \quad (\text{C.303})$$

$$\mathcal{D}_0 = q^2 - m_{\tilde{q}_k^\alpha}^2 + i\epsilon \quad \mathcal{D}_1 = (q - p_1)^2 + i\epsilon \quad \mathcal{D}_2 = (q + p_2)^2 + i\epsilon \quad (\text{C.304})$$

Gluiino exchange

$$C_0(p_1^2, (p_1 + p_2)^2, p_2^2, m_{\tilde{g}}^2, m_{q^\alpha}^2, m_{q^\alpha}^2) \quad (\text{C.305})$$

$$B_0((p_1 + p_2)^2, m_{q^\alpha}^2, m_{q^\alpha}^2) \quad (\text{C.306})$$



$$= -\frac{1}{2N} T_{ur}^c \int_q -2 \text{Tr} [(R_{k1}^\alpha P_R - R_{k2}^\alpha P_L) (m_{\tilde{g}} - \not{q}) \times (R_{l1}^\alpha P_L - R_{l2}^\alpha P_R) (m_{q^\alpha} - \not{q} - \not{p}_2) \gamma^\sigma (m_{q^\alpha} - \not{q} + \not{p}_1)] \quad (\text{C.307})$$

$$A_+^{lk} = \frac{g_s^3}{8\pi^2} (2m_{\tilde{g}} m_{q^\alpha} (R_{k2} R_{l1} + R_{k1} R_{l2}) (C_1 - C_2) + (B_0 + 2B_1 - m_{\tilde{g}}^2 C_1 - m_{q^\alpha}^2 C_1 + p_1^2 C_1 + m_{\tilde{g}}^2 C_2 + m_{q^\alpha}^2 C_2 - p_2^2 C_2) \delta_{kl}) \quad (\text{C.308})$$

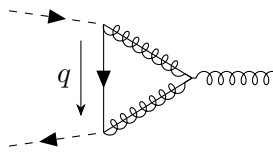
$$A_-^{lk} = \frac{g_s^3}{8\pi^2} (-2m_{\tilde{g}} m_{q^\alpha} (R_{k2} R_{l1} + R_{k1} R_{l2}) (C_0 + C_1 + C_2) + (B_0 + 2m_{\tilde{g}}^2 C_0 + m_{\tilde{g}}^2 C_1 + m_{q^\alpha}^2 C_1 + p_1^2 C_1 + m_{\tilde{g}}^2 C_2 + m_{q^\alpha}^2 C_2 + p_2^2 C_2) \delta_{kl}) \quad (\text{C.309})$$

$$\mathcal{D}_0 = q^2 - m_{\tilde{g}}^2 + i\epsilon \quad \mathcal{D}_1 = (q - p_1)^2 - m_{q^\alpha}^2 + i\epsilon \quad \mathcal{D}_2 = (q + p_2)^2 - m_{q^\alpha}^2 + i\epsilon \quad (\text{C.310})$$

Quark exchange

$$C_0(p_1^2, (p_1 + p_2)^2, p_2^2, m_{q^\alpha}^2, m_{\tilde{g}}^2, m_{q^\alpha}^2) \quad (\text{C.311})$$

$$B_0((p_1 + p_2)^2, m_{\tilde{g}}^2, m_{\tilde{g}}^2) \quad (\text{C.312})$$



$$= \frac{N}{2} T_{ur}^c \int_q 2 \text{Tr} [(R_{k1}^\alpha P_R - R_{k2}^\alpha P_L) (m_{\tilde{g}} + \not{q} - \not{p}_1) \gamma^\sigma \times (m_{\tilde{g}} + \not{q} + \not{p}_2) (R_{l1}^\alpha P_L - R_{l2}^\alpha P_R) (m_{q^\alpha} + \not{q})] \quad (\text{C.313})$$

$$A_+^{lk} = \frac{g_s^3}{8\pi^2} (2m_{\tilde{g}}m_{q^\alpha} (R_{k2}R_{l1} + R_{k1}R_{l2}) (C_1 - C_2) + (B_0 + 2B_1 - m_{\tilde{g}}^2C_1 - m_{q^\alpha}^2C_1 + p_1^2C_1 + m_{\tilde{g}}^2C_2 + m_{q^\alpha}^2C_2 - p_2^2C_2)\delta_{kl}) \quad (\text{C.314})$$

$$A_-^{lk} = \frac{g_s^3}{8\pi^2} (-2m_{\tilde{g}}m_{q^\alpha} (R_{k2}R_{l1} + R_{k1}R_{l2}) (C_0 + C_1 + C_2) + (B_0 + 2m_{q^\alpha}^2C_0 + m_{\tilde{g}}^2C_1 + m_{q^\alpha}^2C_1 + p_1^2C_1 + m_{\tilde{g}}^2C_2 + m_{q^\alpha}^2C_2 + p_2^2C_2)\delta_{kl}) \quad (\text{C.315})$$

$$\mathcal{D}_0 = q^2 - m_{q^\alpha}^2 + i\epsilon \quad \mathcal{D}_1 = (q - p_1)^2 - m_{\tilde{g}}^2 + i\epsilon \quad \mathcal{D}_2 = (q + p_2)^2 - m_{\tilde{g}}^2 + i\epsilon \quad (\text{C.316})$$

C.4 Ghost-gluon vertex

The momentum and index convention as well as the definition of the partial amplitudes A_1 and A_2 for the corrected ghost-gluon vertex are shown in eq. (8.128). For both Feynman diagrams that contribute to this correction applies the same argument set

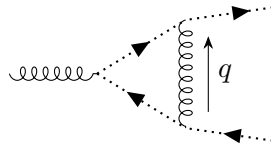
$$C_0 \left(k_2^2, (k_2 - k_1)^2, k_1^2, 0, 0, 0 \right) \quad (\text{C.317})$$

$$B_0 \left((k_2 - k_1)^2, 0, 0 \right) \quad (\text{C.318})$$

with the denominators

$$\mathcal{D}_0 = q^2 + i\epsilon \quad \mathcal{D}_1 = (q - k_2)^2 + i\epsilon \quad \mathcal{D}_2 = (q - k_1)^2 + i\epsilon. \quad (\text{C.319})$$

Gluon exchange

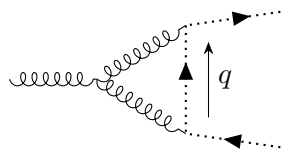


$$= \frac{N}{2} i f_{cde} \int_q -k_2 \cdot (k_1 - q)(k_2 - q)^\sigma = i \frac{N}{2} i f_{cde} (A_1 k_1^\sigma + A_2 k_2^\sigma) \quad (\text{C.320})$$

$$A_1 = -\frac{g_s^3}{16\pi^2} ((C_2 + C_{22})(k_1 \cdot k_2) + k_2^2 C_{12}) \quad (\text{C.321})$$

$$A_2 = -\frac{g_s^3}{16\pi^2} ((k_1 \cdot k_2)(C_0 + C_1 + C_{12} + C_2) + k_2^2(C_1 + C_{11}) + C_{00}) \quad (\text{C.322})$$

Ghost exchange



$$= \frac{N}{2} i f_{cde} \int_q -((k_2 + k_1 - 2q)^\sigma k_2 \cdot q + k_2^\sigma (q - 2k_2 + k_1) \cdot q + q^\sigma (q + k_2 - 2k_1) \cdot k_2) = i \frac{N}{2} i f_{cde} (A_1 k_1^\sigma + A_2 k_2^\sigma) \quad (\text{C.323})$$

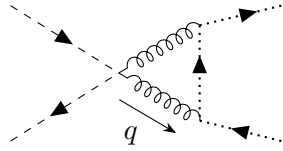
$$A_1 = \frac{g_s^3}{16\pi^2} ((-C_2 + C_{22})k_1 \cdot k_2 + (C_1 + C_{12} + C_2)k_2^2) \quad (\text{C.324})$$

$$A_2 = \frac{g_s^3}{16\pi^2} (-B_0 + C_{00} + C_2 k_1^2 - (C_1 - C_{12} + C_2)k_1 \cdot k_2 + C_{11}k_2^2) \quad (\text{C.325})$$

C.5 Further ghost boxes and triangles

Ghost exchange right 1

$$C_0(0, 0, s, 0, 0, 0) \quad (\text{C.326})$$

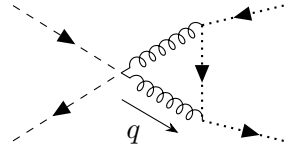


$$= -\frac{ig_s^4}{32\pi^2} \delta_{ij} \left(c_{st,ab}^{(1)} + \frac{N}{2} c_{st,ab}^{(8_S)} \right) s (C_0 + C_1 + C_2) \quad (\text{C.327})$$

$$\mathcal{D}_0 = q^2 + i\epsilon \quad \mathcal{D}_1 = (q - k_2)^2 + i\epsilon \quad \mathcal{D}_2 = (q - k_1 - k_2)^2 + i\epsilon \quad (\text{C.328})$$

Ghost exchange right 2

$$C_0(0, 0, s, 0, 0, 0) \quad (\text{C.329})$$



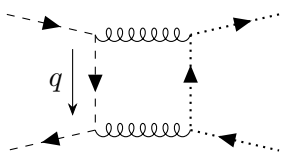
$$= -\frac{ig_s^4}{32\pi^2} \delta_{ij} \left(c_{st,ab}^{(1)} + \frac{N}{2} c_{st,ab}^{(8_S)} \right) s C_2 \quad (\text{C.330})$$

$$\mathcal{D}_0 = q^2 + i\epsilon \quad \mathcal{D}_1 = (q - k_2)^2 + i\epsilon \quad \mathcal{D}_2 = (q - k_1 - k_2)^2 + i\epsilon \quad (\text{C.331})$$

Ghost box 1

$$C_0(0, 0, s, 0, 0, 0) \quad (\text{C.332})$$

$$D_0(m_{\tilde{q}_i^\alpha}^2, 0, 0, m_{\tilde{q}_i^\alpha}^2, t, s, m_{\tilde{q}_i^\alpha}^2, 0, 0, 0) \quad (\text{C.333})$$



$$= \delta_{ij} \left(\frac{1}{2} c_{st,ab}^{(1)} + \frac{N}{4} c_{st,ab}^{(8_S)} - \frac{N}{4} c_{st,ab}^{(8_A)} \right) \times \int_q -(q - p_2) \cdot (q - k_2 + p_2) k_1 \cdot (q + p_1) \quad (\text{C.334})$$

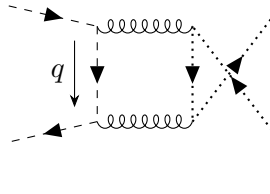
$$\mathcal{D}_0 = q^2 - m_{\tilde{q}_i^\alpha}^2 + i\epsilon \quad \mathcal{D}_1 = (q + p_2)^2 + i\epsilon \quad (\text{C.335})$$

$$\mathcal{D}_2 = (q + p_2 - k_2)^2 + i\epsilon \quad \mathcal{D}_3 = (q - p_1)^2 + i\epsilon \quad (\text{C.336})$$

Ghost box 1 u

$$D_0 \left(m_{\tilde{q}_i^\alpha}^2, 0, 0, m_{\tilde{q}_i^\alpha}^2, u, s, m_{\tilde{q}_i^\alpha}^2, 0, 0, 0 \right) \quad (\text{C.337})$$

$$C_0 (0, 0, s, 0, 0, 0) \quad (\text{C.338})$$



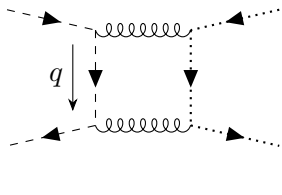
$$= \delta_{ij} \left(\frac{1}{2} c_{st,ab}^{(1)} + \frac{N}{4} c_{st,ab}^{(\mathbf{8}_S)} - \frac{N}{4} c_{st,ab}^{(\mathbf{8}_A)} \right) \times \int_q (q - p_2) \cdot k_1 (q + p_1) \cdot (k_1 - q - p_2) \quad (\text{C.339})$$

$$\mathcal{D}_0 = q^2 - m_{\tilde{q}_i^\alpha}^2 + i\epsilon \quad \mathcal{D}_1 = (q + p_2)^2 + i\epsilon \quad (\text{C.340})$$

$$\mathcal{D}_2 = (q + p_2 - k_1)^2 + i\epsilon \quad \mathcal{D}_3 = (q - p_1)^2 + i\epsilon \quad (\text{C.341})$$

Ghost box 2

$$D_0 \left(m_{\tilde{q}_i^\alpha}^2, 0, 0, m_{\tilde{q}_i^\alpha}^2, t, s, m_{\tilde{q}_i^\alpha}^2, 0, 0, 0 \right) \quad C_0 (0, 0, s, 0, 0, 0) \quad (\text{C.342})$$



$$= \delta_{ij} \left(\frac{1}{2} c_{st,ab}^{(1)} + \frac{N}{4} c_{st,ab}^{(\mathbf{8}_S)} - \frac{N}{4} c_{st,ab}^{(\mathbf{8}_A)} \right) \times \int_q - (q - p_2) \cdot k_2 (k_2 - p_2 - q) \cdot (q + p_1) \quad (\text{C.343})$$

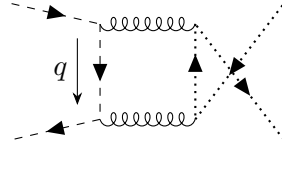
$$\mathcal{D}_0 = q^2 - m_{\tilde{q}_i^\alpha}^2 + i\epsilon \quad \mathcal{D}_1 = (q + p_2)^2 + i\epsilon \quad (\text{C.344})$$

$$\mathcal{D}_2 = (q + p_2 - k_2)^2 + i\epsilon \quad \mathcal{D}_3 = (q - p_1)^2 + i\epsilon \quad (\text{C.345})$$

Ghost box 2 u

$$D_0 \left(m_{\tilde{q}_i^\alpha}^2, 0, 0, m_{\tilde{q}_i^\alpha}^2, u, s, m_{\tilde{q}_i^\alpha}^2, 0, 0, 0 \right) \quad (\text{C.346})$$

$$C_0 (0, 0, s, 0, 0, 0) \quad (\text{C.347})$$



$$= \delta_{ij} \left(\frac{1}{2} c_{st,ab}^{(1)} + \frac{N}{4} c_{st,ab}^{(8_S)} - \frac{N}{4} c_{st,ab}^{(8_A)} \right) \times \int_q (q - p_2) \cdot (q - k_1 + p_2) k_2 \cdot (q + p_1) \quad (\text{C.348})$$

$$\mathcal{D}_0 = q^2 - m_{\tilde{q}_i^{\alpha}}^2 + i\epsilon \quad \mathcal{D}_1 = (q + p_2)^2 + i\epsilon \quad (\text{C.349})$$

$$\mathcal{D}_2 = (q + p_2 - k_1)^2 + i\epsilon \quad \mathcal{D}_3 = (q - p_1)^2 + i\epsilon \quad (\text{C.350})$$

C.6 Mathematica codes for the Passarino-Veltman reduction

For each vertex a dedicated `Mathematica` routine was developed built on top of `FeynCalc 9.3` that performs the reduction of an amplitude to Passarino-Veltman functions. The `Mathematica` functions `CMu`, `DMu`, `DMuNu`, ... correspond to the decompositions in eq. (8.17).

C.6.1 Boxes

The `Mathematica` function `ToPaVeBoxes` performs the Passarino-Veltmann reduction for the Boxes. It takes the `numerator` of a Box amplitude as input as well as the Lorentz indices `mu` and `nu` of the two vector bosons. The list `ExtP` is required to contain all external momenta which in our case are p_1, p_2, k_1 and k_2 . The variable `q` defines the loop momentum. The momenta `p1`, `p2` and `p3` as well as masses `m0` and `m1` are the ones that appear in denominator as defined in the general n -point function in eq. (8.7).

```

1 ToPaVeBoxes[numerator_, mu_, nu_, q_, ExtP_, p1_, p2_, p3_, m0_, m1_]
2 := Module[{sigma, rho, temp, ExtP2, ExtP3},
3   temp = FCE[numerator // ExpandScalarProduct // ExpandAll // Contract];
4   ExtP2 = Tuples[{ExtP, ExtP}];
5   ExtP3 = Tuples[{ExtP, ExtP, ExtP}];
6   temp/.Flatten[{
7     MTD[mu, nu] SPD[q, q]^2 -> MTD[mu, nu] (m0^4 xd0 + (m0^2 + m1^2
8       + SPD[p1, p1]) xc0 - 2 FVD[p1, sigma]
9       CMu[sigma, p2 - p1, p3 - p1] + xb0),
10    MTD[mu, nu] SPD[#1, q] SPD[#2, q] -> MTD[mu, nu] FVD[#1, sigma]
11    FVD[#2, rho] DMuNu[sigma, rho, p1, p2, p3] & @@@ ExtP2,
12    MTD[mu, nu] SPD[#, q] SPD[q, q] -> MTD[mu, nu] (FVD[#, sigma]
13    CMu[sigma, p2 - p1, p3 - p1] - SPD[#, p1] xc0 + m0^2 FVD[#, sigma]
14    DMu[sigma, p1, p2, p3]) & /@ ExtP,
15    MTD[mu, nu] SPD[#, q] -> MTD[mu, nu] FVD[#, sigma]
16    DMu[sigma, p1, p2, p3] & /@ ExtP,
17    MTD[mu, nu] SPD[q, q] -> MTD[mu, nu] (xc0 + m0^2 xd0),
18    MTD[mu, nu] -> MTD[mu, nu] xd0,
19    SPD[q, q] FVD[q, mu] FVD[q, nu] -> m0^2 DMuNu[mu, nu, p1, p2, p3]
20    + CMuNu[mu, nu, p2 - p1, p3 - p1] + FVD[p1, mu] FVD[p1, nu] xc0
21    - FVD[p1, mu] CMu[nu, p2 - p1, p3 - p1]

```

```

22      - FVD[p1, nu] CMu[mu, p2 - p1, p3 - p1],
23 SPD[q, q] FVD[q, mu] FVD[#, nu] -> m0^2 DMu[mu, p1, p2, p3] FVD[#, nu]
24 + FVD[#, nu] CMu[mu, p2 - p1, p3 - p1]
25      - FVD[#, nu] FVD[p1, mu] xc0 & /@ ExtP,
26 SPD[q, q] FVD[q, nu] FVD[#, mu] -> m0^2 DMu[nu, p1, p2, p3] FVD[#, mu]
27 + FVD[#, mu] CMu[nu, p2 - p1, p3 - p1]
28      - FVD[#, mu] FVD[p1, nu] xc0 & /@ ExtP,
29 SPD[q, q] FVD[#1, nu] FVD[#2, mu] -> FVD[#1, nu] FVD[#2, mu] xc0
30 + FVD[#1, nu] FVD[#2, mu] m0^2 xd0 & @@@ ExtP2,
31 SPD[q, #] FVD[q, mu] FVD[q, nu] -> FVD[#, sigma]
32 DMuNuRho[sigma, mu, nu, p1, p2, p3] & /@ ExtP,
33 SPD[q, #1] FVD[q, mu] FVD[#2, nu] -> FVD[#1, sigma] FVD[#2, nu]
34 DMuNu[sigma, mu, p1, p2, p3] & @@@ ExtP2,
35 SPD[q, #1] FVD[q, nu] FVD[#2, mu] -> FVD[#1, sigma] FVD[#2, mu]
36 DMuNu[sigma, nu, p1, p2, p3] & @@@ ExtP2,
37 SPD[q, #1] FVD[#2, nu] FVD[#3, mu] -> FVD[#1, sigma] FVD[#2, nu]
38 FVD[#3, mu] DMu[sigma, p1, p2, p3] & @@@ ExtP3,
39 FVD[#1, mu] FVD[#2, nu] -> FVD[#1, mu] FVD[#2, nu] xd0 & @@@ ExtP2,
40 FVD[q, nu] FVD[#, mu] -> DMu[nu, p1, p2, p3] FVD[#, mu] & /@ ExtP,
41 FVD[q, mu] FVD[#, nu] -> DMu[mu, p1, p2, p3] FVD[#, nu] & /@ ExtP,
42 FVD[q, mu] FVD[q, nu] -> DMuNu[mu, nu, p1, p2, p3]}} // Contract];

```

As an example consider the first box whose numerator

$$M = I \frac{GS^4}{(16 \sqrt{p_i}^2)} SPD[2 \, p_1 - q, 2 \, p_2 + q] FVD[k_2 + p_1 - p_2 - 2 \, q, \sqrt{[Mu]}] FVD[-2 \, q - 2 \, p_2 + k_2, \sqrt{[Nu]}];$$

is given in eq. (C.120). The command

`ToPaVeBoxes[M, \[Mu], \[Nu], q, {p1, p2, k1, k2}, p2, -k2 + p2, -p1, 0, mi]`

yields the reduced amplitude. Notice that the factor $i/(4\pi)^2$ from the loop functions is already defined into M since `ToPaVeBoxes` does not perform the corresponding replacement.

C.6.2 Triple-gluon vertex

```

1 ToPaVe3g[numerator_, q_, ExtP_, p1_, p2_, m0_] :=
2 Module[{alpha, temp, ExtP2, ExtP3},
3 temp = FCE[numerator // ExpandScalarProduct // ExpandAll // Contract];
4 ExtP2 = Tuples[{ExtP, ExtP}];
5 ExtP3 = Tuples[{ExtP, ExtP, ExtP}];
6 temp/.Flatten[{
7 MTD[a_, b_] FVD[q, c_] SPD[q, q] -> MTD[a, b] (BMu[c, p2 - p1]
8 - FVD[p1, c] xb0 + m0^2 CMu[c, p1, p2]),
9 MTD[a_, b_] FVD[#, c_] SPD[q, q] -> MTD[a, b] FVD[#, c]
10 (xb0 + m0^2 xc0) & /@ ExtP,
11 MTD[a_, b_] FVD[q, c_] SPD[#, q] -> MTD[a, b] FVD[#, alpha]
12 CMuNu[alpha, c, p1, p2] & /@ ExtP,
13 MTD[a_, b_] FVD[#1, c_] SPD[#2, q] -> MTD[a, b] FVD[#1, c]
14 FVD[#2, alpha] CMu[alpha, p1, p2] & @@@ ExtP2,

```

```

15 MTD[a_, b_] FVD[q, c_] SPD[#1, #2] ->
16 MTD[a, b] SPD[#1, #2] CMu[c, p1, p2] & @@@ ExtP2,
17 MTD[a_, b_] FVD[q, c_] -> MTD[a, b] CMu[c, p1, p2],
18 MTD[a_, b_] FVD[#1, c_] -> MTD[a, b] FVD[#1, c] xc0 & /@ ExtP,
19 FVD[q, a_] FVD[q, b_] FVD[q, c_] -> CMuNuRho[a, b, c, p1, p2],
20 FVD[q, a_] FVD[q, b_] FVD[#, c_] -> FVD[#, c]
21 CMuNu[a, b, p1, p2] & /@ ExtP,
22 FVD[q, a_] FVD[#1, b_] FVD[#2, c_] -> FVD[#1, b] FVD[#2, c]
23 CMu[a, p1, p2] & @@@ ExtP2,
24 FVD[#1, a_] FVD[#2, b_] FVD[#3, c_] -> FVD[#1, a] FVD[#2, b]
25 FVD[#3, c] xc0 & @@@ ExtP3}] // Contract];

```

C.6.3 Squark-gluon vertex

```

1 ToPaVe2SqG[numerator_, mu_, q_, ExtP_, p1_, p2_, m0_] :=
2 Module[{alpha, temp, ExtP2, ExtP3},
3 temp = FCE[numerator // ExpandScalarProduct // ExpandAll // Expand //
4 Contract];
5 ExtP2 = Tuples[{ExtP, ExtP}];
6 ExtP3 = Tuples[{ExtP, ExtP, ExtP}];
7 temp /. Flatten[{
8 SPD[q, q] FVD[q, mu] -> BMu[mu, p2 - p1] - FVD[p1, mu] xb0
9 + m0^2 CMu[mu, p1, p2],
10 SPD[q, q] FVD[#, mu] -> FVD[#, mu] (xb0 + m0^2 xc0) & /@ ExtP,
11 SPD[q, #] FVD[q, mu] ->
12 FVD[#, alpha] CMuNu[mu, alpha, p1, p2] & /@ ExtP,
13 SPD[q, #1] FVD[#2, mu] -> FVD[#2, mu] FVD[#1, alpha]
14 CMu[alpha, p1, p2] & @@@ ExtP2,
15 SPD[#1, #2] FVD[q, mu] -> SPD[#1, #2] CMu[mu, p1, p2] & @@@ ExtP2,
16 SPD[#1, #2] FVD[#3, mu] -> SPD[#1, #2] FVD[#3, mu] xc0 & @@@ ExtP3,
17 FVD[q, mu] -> CMu[mu, p1, p2],
18 FVD[#, mu] -> FVD[#, mu] xc0 & /@ ExtP }] // Contract];

```


Bibliography

- [1] Mohamed Younes Sassi. “The Catani-Seymour Dipole Subtraction Method with Massive Initial States in the Context of the Dark Matter Relic Abundance Calculations”. Master’s Thesis. Technical University of Munich, 2021.
- [2] Sidney R. Coleman and J. Mandula. “All Possible Symmetries of the S Matrix”. In: *Phys. Rev.* 159 (1967). Ed. by A. Zichichi, pp. 1251–1256.
- [3] J. Wess and B. Zumino. “Supergauge Transformations in Four-Dimensions”. In: *Nucl. Phys. B* 70 (1974). Ed. by A. Salam and E. Sezgin, pp. 39–50.
- [4] Rudolf Haag, Jan T. Lopuszanski, and Martin Sohnius. “All Possible Generators of Supersymmetries of the s Matrix”. In: *Nucl. Phys. B* 88 (1975), p. 257.
- [5] M. Drees, R. Godbole, and P. Roy. *Theory And Phenomenology Of Sparticles: An Account Of Four-dimensional N=1 Supersymmetry In High Energy Physics*. World Scientific Publishing Company, 2005. ISBN: 9789814495349.
- [6] Stephen P. Martin. “A Supersymmetry primer”. In: *Adv. Ser. Direct. High Energy Phys.* 18 (1998). Ed. by Gordon L. Kane, pp. 1–98. arXiv: [hep-ph/9709356](#).
- [7] Martin Ammon and Johanna Erdmenger. *Gauge/gravity duality: Foundations and applications*. Cambridge: Cambridge University Press, Apr. 2015. ISBN: 978-1-107-01034-5, 978-1-316-23594-2.
- [8] Juan Antonio Aguilar-Saavedra et al. “Supersymmetry parameter analysis: SPA convention and project”. In: *Eur. Phys. J. C* 46 (2006), pp. 43–60. arXiv: [hep-ph/0511344](#).
- [9] Werner Porod. “SPHeno, a program for calculating supersymmetric spectra, SUSY particle decays and SUSY particle production at e+ e- colliders”. In: *Comput. Phys. Commun.* 153 (2003), pp. 275–315. arXiv: [hep-ph/0301101](#).
- [10] A. Djouadi et al. “The Minimal supersymmetric standard model: Group summary report”. In: *GDR (Groupement De Recherche) - Supersymetrie*. Dec. 1998. arXiv: [hep-ph/9901246](#).
- [11] F. Zwicky. “Die Rotverschiebung von extragalaktischen Nebeln”. In: *Helv. Phys. Acta* 6 (1933), pp. 110–127.
- [12] Vera C. Rubin and W. Kent Ford Jr. “Rotation of the Andromeda Nebula from a Spectroscopic Survey of Emission Regions”. In: *Astrophys. J.* 159 (1970), pp. 379–403.
- [13] Ernesto Lopez Fune, Paolo Salucci, and Edvige Corbelli. “Radial dependence of the dark matter distribution in M33”. In: *Mon. Not. Roy. Astron. Soc.* 468.1 (2017), pp. 147–153. arXiv: [1611.01409 \[astro-ph.GA\]](#).
- [14] Arno A. Penzias and Robert Woodrow Wilson. “A Measurement of excess antenna temperature at 4080-Mc/s”. In: *Astrophys. J.* 142 (1965), pp. 419–421.
- [15] Planck Collaboration et al. *Planck 2018 results. VI. Cosmological parameters*. 2020. arXiv: [1807.06209 \[astro-ph.CO\]](#).
- [16] Joakim Edsjo and Paolo Gondolo. “Neutralino relic density including coannihilations”. In: *Phys. Rev. D* 56 (1997), pp. 1879–1894. arXiv: [hep-ph/9704361](#).

- [17] E. Kolb and M. Turner. *The Early Universe*. Frontiers in physics. Avalon Publishing, 1994. ISBN: 9780813346458.
- [18] Matthew D. Schwartz. *Quantum Field Theory and the Standard Model*. Cambridge University Press, Mar. 2014. ISBN: 978-1-107-03473-0, 978-1-107-03473-0.
- [19] M.E. Peskin and D.V. Schroeder. *An Introduction To Quantum Field Theory*. Frontiers in Physics. Avalon Publishing, 1995. ISBN: 9780813345437.
- [20] Steven Weinberg. *The Quantum theory of fields. Vol. 1: Foundations*. Cambridge University Press, June 2005. ISBN: 978-0-521-67053-1, 978-0-511-25204-4.
- [21] M. K. Gümüş and M. Boz. “Gauge fixing problem and the constrained quantization”. In: (Jan. 2017). arXiv: [1701.09035 \[hep-th\]](#).
- [22] L. D. Faddeev and V. N. Popov. “Feynman Diagrams for the Yang-Mills Field”. In: *Phys. Lett. B* 25 (1967). Ed. by Jong-Ping Hsu and D. Fine, pp. 29–30.
- [23] C. Becchi, A. Rouet, and R. Stora. “The abelian Higgs Kibble model, unitarity of the S-operator”. In: *Physics Letters B* 52.3 (1974), pp. 344–346. ISSN: 0370-2693.
- [24] Taichiro Kugo and Izumi Ojima. “Manifestly Covariant Canonical Formulation of Yang-Mills Field Theories. 1. The Case of Yang-Mills Fields of Higgs-Kibble Type in Landau Gauge”. In: *Prog. Theor. Phys.* 60 (1978), p. 1869.
- [25] Taichiro Kugo. *Eichtheorie*. Berlin, Heidelberg: Springer Berlin Heidelberg, 1997. ISBN: 978-3-642-59128-0.
- [26] Stefano Catani et al. “The Dipole formalism for next-to-leading order QCD calculations with massive partons”. In: *Nucl. Phys. B* 627 (2002), pp. 189–265. arXiv: [hep-ph/0201036](#).
- [27] Toichiro Kinoshita. “Mass Singularities of Feynman Amplitudes”. In: *Journal of Mathematical Physics* 3.4 (1962), pp. 650–677.
- [28] S. Catani and M. H. Seymour. “A General algorithm for calculating jet cross-sections in NLO QCD”. In: *Nucl. Phys. B* 485 (1997). [Erratum: Nucl.Phys.B 510, 503–504 (1998)], pp. 291–419. arXiv: [hep-ph/9605323](#).
- [29] Stefan Dittmaier. “A General approach to photon radiation off fermions”. In: *Nucl. Phys. B* 565 (2000), pp. 69–122. arXiv: [hep-ph/9904440](#).
- [30] Karol Kovařík. *Hitchhiker’s Guide To Renormalization*. (Not yet published). 2020.
- [31] Eero. Byckling and K. Kajantie. *Particle kinematics*. English. Wiley London, New York, 1973, ix, 319 p. ISBN: 0471128856.
- [32] Piotr Kotko. “General Mass Scheme for Jet Production in QCD (revised version)”. PhD thesis. Jagiellonian U. (main), 2012.
- [33] Julia Harz. “Supersymmetric QCD Corrections and Phenomenological Studies in Relation to Coannihilation of Dark Matter”. PhD thesis. Hamburg U., 2013.
- [34] J. Harz et al. “One-loop corrections to neutralino-stop coannihilation revisited”. In: *Phys. Rev. D* 91.3 (2015), p. 034028. arXiv: [1409.2898 \[hep-ph\]](#).
- [35] Stefano Catani, Stefan Dittmaier, and Zoltan Trocsanyi. “One loop singular behavior of QCD and SUSY QCD amplitudes with massive partons”. In: *Phys. Lett. B* 500 (2001), pp. 149–160. arXiv: [hep-ph/0011222](#).
- [36] Brian C. Hall. “Lie Groups, Lie Algebras, and Representations”. In: New York, NY: Springer New York, 2013. ISBN: 978-1-4614-7116-5.

- [37] Nicolas Borghini. *Symmetries in Physics*. 2018. URL: <https://www.physik.uni-bielefeld.de/~borghini/Teaching/Symmetries17/>.
- [38] A. Zee. *Group Theory in a Nutshell for Physicists*. USA: Princeton University Press, 2016. ISBN: 978-0-691-16269-0, 978-0-691-16269-0, 978-1-4008-8118-5.
- [39] B. Lisser M. A. A. van Leeuwen A. M. Cohen. “LiE, A Package for Lie Group Computations”. In: *Computer Algebra Nederland* (1992).
- [40] Stefan Keppeler and Malin Sjödal. “Orthogonal multiplet bases in $SU(N_c)$ color space”. In: *JHEP* 09 (2012), p. 124. arXiv: [1207.0609 \[hep-ph\]](#).
- [41] Malin Sjödal and Stefan Keppeler. “Tools for calculations in color space”. In: *PoS DIS2013* (2013). Ed. by E. Kajfasz, p. 166. arXiv: [1307.1319 \[hep-ph\]](#).
- [42] M. Beneke, P. Falgari, and C. Schwinn. “All-Order Colour Structure and Two-Loop Anomalous Dimension of soft Radiation in Heavy-Particle Pair Production at the LHC”. In: *PoS RADCOR2009* (2010), p. 011. arXiv: [1001.4621 \[hep-ph\]](#).
- [43] Ali Çiçi, Zerrin Kırca, and Cem Salih Ün. “Light Stops and Fine-Tuning in MSSM”. In: *Eur. Phys. J. C* 78.1 (2018), p. 60. arXiv: [1611.05270 \[hep-ph\]](#).
- [44] Howard E. Haber, Ralf Hempfling, and Andre H. Hoang. “Approximating the radiatively corrected Higgs mass in the minimal supersymmetric model”. In: *Z. Phys. C* 75 (1997), pp. 539–554. arXiv: [hep-ph/9609331](#).
- [45] Zhao-Huan Yu et al. “Detecting light stop pairs in coannihilation scenarios at the LHC”. In: *Phys. Rev. D* 87.5 (2013), p. 055007. arXiv: [1211.2997 \[hep-ph\]](#).
- [46] John R. Ellis, Keith A. Olive, and Yudi Santoso. “Calculations of neutralino stop coannihilation in the CMSSM”. In: *Astropart. Phys.* 18 (2003), pp. 395–432. arXiv: [hep-ph/0112113](#).
- [47] T. P. Cheng and L. F. Li. *Gauge theory of elementary particle physics*. Oxford, UK: Oxford University Press, 1984. ISBN: 978-0-19-851961-4, 978-0-19-851961-4.
- [48] Georges Aad et al. “Summary of the ATLAS experiment’s sensitivity to supersymmetry after LHC Run 1 — interpreted in the phenomenological MSSM”. In: *JHEP* 10 (2015), p. 134. arXiv: [1508.06608 \[hep-ex\]](#).
- [49] G. Belanger et al. “MicrOMEGAs: A Program for calculating the relic density in the MSSM”. In: *Comput. Phys. Commun.* 149 (2002), pp. 103–120. arXiv: [hep-ph/0112278](#).
- [50] B. C. Allanach et al. “SUSY Les Houches Accord 2”. In: *Comput. Phys. Commun.* 180 (2009), pp. 8–25. arXiv: [0801.0045 \[hep-ph\]](#).
- [51] B. C. Allanach. “SOFTSUSY: a program for calculating supersymmetric spectra”. In: *Comput. Phys. Commun.* 143 (2002), pp. 305–331. arXiv: [hep-ph/0104145](#).
- [52] Gerard ’t Hooft and M. J. G. Veltman. “Regularization and Renormalization of Gauge Fields”. In: *Nucl. Phys. B* 44 (1972), pp. 189–213.
- [53] G. Passarino and M. J. G. Veltman. “One Loop Corrections for e^+e^- Annihilation Into $\mu^+\mu^-$ in the Weinberg Model”. In: *Nucl. Phys. B* 160 (1979), pp. 151–207.
- [54] Wolfgang Kilian. *Übungen zu Strahlungskorrekturen in Eichtheorien*. Maria Laach, 2001.
- [55] Georg Sulyok. “A closed expression for the UV-divergent parts of one-loop tensor integrals in dimensional regularization”. In: *Phys. Part. Nucl. Lett.* 14.4 (2017), pp. 631–643. arXiv: [hep-ph/0609282](#).
- [56] A. Denner and S. Dittmaier. “Scalar one-loop 4-point integrals”. In: *Nucl. Phys. B* 844 (2011), pp. 199–242. arXiv: [1005.2076 \[hep-ph\]](#).

- [57] T. Hahn and M. Perez-Victoria. “Automatized one loop calculations in four-dimensions and D-dimensions”. In: *Comput. Phys. Commun.* 118 (1999), pp. 153–165. arXiv: [hep-ph/9807565](#).
- [58] W. Siegel. “Supersymmetric Dimensional Regularization via Dimensional Reduction”. In: *Phys. Lett. B* 84 (1979), pp. 193–196.
- [59] W. Siegel. “Inconsistency of Supersymmetric Dimensional Regularization”. In: *Phys. Lett. B* 94 (1980), pp. 37–40.
- [60] Dominik Stockinger. “Regularization by dimensional reduction: consistency, quantum action principle, and supersymmetry”. In: *JHEP* 03 (2005), p. 076. arXiv: [hep-ph/0503129](#).
- [61] L. Mihaila. “Precision Calculations in Supersymmetric Theories”. In: *Adv. High Energy Phys.* 2013 (2013), p. 607807. arXiv: [1310.6178 \[hep-ph\]](#).
- [62] Adrian Signer and Dominik Stockinger. “Using Dimensional Reduction for Hadronic Collisions”. In: *Nucl. Phys. B* 808 (2009), pp. 88–120. arXiv: [0807.4424 \[hep-ph\]](#).
- [63] P. Breitenlohner and D. Maison. “Dimensional Renormalization and the Action Principle”. In: *Commun. Math. Phys.* 52 (1977), pp. 11–38.
- [64] F. Jegerlehner. “Facts of life with gamma(5)”. In: *Eur. Phys. J. C* 18 (2001), pp. 673–679. arXiv: [hep-th/0005255](#).
- [65] Taizo Muta. *Foundations of Quantum Chromodynamics: An Introduction to Perturbative Methods in Gauge Theories, (3rd ed.)* 3rd. Vol. 78. World scientific Lecture Notes in Physics. Hackensack, N.J.: World Scientific, 2010. ISBN: 978-981-279-353-9.
- [66] Moritz Meinecke. “SUSY-QCD Corrections to the (Co)Annihilation of Neutralino Dark Matter within the MSSM”. PhD thesis. University of Münster, 2015.
- [67] S. Schmiemann. “Squark Annihilation Contributions to Neutralino Dark Matter in NLO SUSY-QCD”. PhD thesis. Munster U., ITP, 2019.
- [68] Wolfram Research, Inc. *Mathematica, Version 12.3.1*. Champaign, IL, 2021. URL: <https://www.wolfram.com/mathematica>.
- [69] Vladyslav Shtabovenko, Rolf Mertig, and Frederik Orellana. “FeynCalc 9.3: New features and improvements”. In: *Computer Physics Communications* 256 (2020), p. 107478. ISSN: 0010-4655.
- [70] Matthias Jamin and Markus E. Lautenbacher. “TRACER: Version 1.1: A Mathematica package for gamma algebra in arbitrary dimensions”. In: *Comput. Phys. Commun.* 74 (1993), pp. 265–288.
- [71] Thomas Hahn. “Generating Feynman diagrams and amplitudes with FeynArts 3”. In: *Comput. Phys. Commun.* 140 (2001), pp. 418–431. arXiv: [hep-ph/0012260](#).
- [72] T. Hahn. “CUBA: A Library for multidimensional numerical integration”. In: *Comput. Phys. Commun.* 168 (2005), pp. 78–95. arXiv: [hep-ph/0404043](#).
- [73] Milton Abramowitz and Irene A. Stegun. *Handbook of Mathematical Functions with Formulas, Graphs, and Mathematical Tables*. New York: Dover, 1964.
- [74] N.N. Lebedev and R.A. Silverman. *Special Functions and Their Applications*. Dover Books on Mathematics. Dover Publications, 1972. ISBN: 9780486606248.
- [75] Inc. Wolfram Research. *Gauss hypergeometric function ${}_2F_1$. Definite integration (formula 07.23.21.0014.01)*. Visited on 03/08/2021. URL: <http://functions.wolfram.com/07.23.21.0014.01>.

- [76] A. J. MacFarlane, Anthony Sudbery, and P. H. Weisz. “On Gell-Mann’s lambda-matrices, d- and f-tensors, octets, and parametrizations of $SU(3)$ ”. In: *Commun. Math. Phys.* 11 (1968), pp. 77–90.
- [77] Johannes Branahl. “QCD Corrections to SUSY Dark Matter Coannihilation Processes”. Master’s Thesis. University of Münster, 2019.
- [78] J. D. Hunter. “Matplotlib: A 2D graphics environment”. In: *Computing in Science & Engineering* 9.3 (2007), pp. 90–95.
- [79] Joshua Ellis. “TikZ-Feynman: Feynman diagrams with TikZ”. In: *Comput. Phys. Commun.* 210 (2017), pp. 103–123. arXiv: [1601.05437 \[hep-ph\]](#).

D Acknowledgments

In the first place, I would like to thank *Prof. Dr. Michael Klasen* for the possibility to work on this diverse and rich topic. In addition, I was pleased to be given the opportunity to participate in the annual GRK retreat. I would also like to thank *PD Dr. Karol Kovařík* for the many helpful conversations and his ability to open up completely new perspectives with just a few words. Moreover, I am grateful to *Alexander Neuwirth* for his company during our master's studies and to *my parents* for their constant support.

The figures and Feynman diagrams presented in this thesis have been generated using `Matplotlib` [78] and `TikZ-Feynman` [79].

Declaration of Academic Integrity

I, *Luca Paolo Wiggering*, hereby confirm that this thesis on "*Squark Annihilation into a Pair of Gluons in the MSSM*" is solely my own work and that I have used no sources or aids other than the ones stated. All passages in my thesis for which other sources, including electronic media, have been used, be it direct quotes or content references, have been acknowledged as such and the sources cited.

(date)

(signature of student)

I, *Luca Paolo Wiggering*, agree to have my thesis checked in order to rule out potential similarities with other works and to have my thesis stored in a database for this purpose.

(date)

(signature of student)